



HAL
open science

Characterization of Histone H3 Lysine 18 deacetylation during infection with *Listeria monocytogenes*

Haig Alexander Eskandarian

► To cite this version:

Haig Alexander Eskandarian. Characterization of Histone H3 Lysine 18 deacetylation during infection with *Listeria monocytogenes*. Agricultural sciences. Université René Descartes - Paris V, 2013. English. NNT : 2013PA05T012 . tel-00844134

HAL Id: tel-00844134

<https://theses.hal.science/tel-00844134>

Submitted on 12 Jul 2013

HAL is a multi-disciplinary open access archive for the deposit and dissemination of scientific research documents, whether they are published or not. The documents may come from teaching and research institutions in France or abroad, or from public or private research centers.

L'archive ouverte pluridisciplinaire **HAL**, est destinée au dépôt et à la diffusion de documents scientifiques de niveau recherche, publiés ou non, émanant des établissements d'enseignement et de recherche français ou étrangers, des laboratoires publics ou privés.

Doctoral Thesis of Philosophy

Université de Paris V: René Descartes

Ecole Doctorale

N°474, Interdisciplinaire Européenne Frontières du Vivant

Doctorat en Biologie

Auteur

Haig Alexander Eskandarian

**Characterization of Histone H3 Lysine 18 deacetylation during
infection with *Listeria monocytogenes***

Thèse dirigée par
Dr. Mélanie Hamon
Prof. Pascale Cossart

Jury
Prof. Wolf Hervé Fridmann
Dr. Geneviève Almouzni
Dr. Guillaume Duménil
Prof. David Holden

Acknowledgements

This work was conducted at Institut Pasteur in the Unité des Interactions Bactéries-Cellules, headed by Pascale Cossart. I am very thankful for her welcoming me into her lab and providing me the opportunity to work at the frontier of current knowledge. I equally thank Mélanie Hamon who has directed my thesis work on a daily basis. Her patients, willingness to listen and offer advice has been very helpful. Furthermore, her systematic and scientific approach to addressing the questions that we encounter in biology is paramount to her success. Finally, I would like to thank both Mélanie and Pascale for their demonstrated professionalism, as this is a quality, which I promise to demonstrate more of in the future.

I would also like to acknowledge my lab members (past and present) of the UIBC and elsewhere at Institut Pasteur. I thank Francis Impens for his very fruitful and enriching collaboration in the last few months of my thesis work. I would also like to thank Marie-Anne Nahori, Mélanie Hamon, Cristel Archambaud, Olivier Dussurget, and Lilliana Radoshevic for their effort in aiding me collect critical *in vivo* results. I also stand to thank Guillaume Soubigou, Christophe Bécavin, and Robin Friedman for their help in collecting, analyzing, and representing the transcriptome experiments. Furthermore, I would thank Tham To Nam, Javier Pizarro-Cerdá, Edith Gouin, Ascel Samba-Louaka, Fabrizia Stavru, J.R. Mellin, Serge Mostowy, Hélène Biérne, Alice Lebreton, Goran Lakisic, Andreas Kühbacher, Andrzej Prokop, David Ribet, Nina Sesto, Alix Rousseau, Matteo Bonazzi, Véronique Villiers, Laurence Maranghi, and Hana Jilani for their kindhearted help and contribution of materials, scientific discussion, feedback, and moral support. I would also thank the UIBC secretary, Marie-Thérèse Vicente, who has always been helpful in facilitating the administrative burdens that I have endured.

I would like to equally thank my doctoral school, Frontières du Vivant for their active drive to provide a dynamic, interdisciplinary and exciting science education. François Taddei, Samuel Bottani, and Ariel Lindner as well as the secretaries, Laura Ciriani and Céline Garrigues for their support and generosity in funding my travel to Armenia in order to teach a course on host-pathogens interactions. Without the financial support of my doctoral school, I would not have experienced the opportunity to teach with my friends and colleagues, Sarkis Mazmanian (CalTech), Bana Jabri (University of Chicago), and Raffi Aroian (UCSD).

To the members of my thesis advisory committee and members of my thesis defense jury, I am thankful that they kindly accepted to take precious time to judge my work. I thank therefore, my *rapporteurs*, Mme. Geneviève Almouzni and Professor David Holden, my *examineurs* M. Guillaume Duménil, Mesdames Professor Pascale Cossart, and Mélanie Hamon, as well as the president of the jury, Professor Wolf-Hervé Fridman.

Finally, I especially thank my friends Assaf Amitai, François Vromman, my girlfriend Laetitia Aymeric, my roommate Robin Friedman, and the American community at Institut Pasteur with whom I have had countless enriching scientific discussions. Lastly, I thank my family for their support throughout my life and in imparting me a drive to succeed. *Carpe diem!*

Table of Contents

List of Abbreviations	5
List of Figures and Tables	7
Abstract	10
Preamble	11
Introduction	15
• Section 1.	
1.1 Uncovering the basis for gene regulation	15
1.2 Eukaryotic chromatin and its two majors states	18
1.3 Histones: a crucial part of the nucleosome	22
1.4 Nucleosome assembly: an essential process for chromatin organization	25
1.5 Nucleosome positioning	28
1.6 Histone Post-Translational modifications	33
1.7 Histone modifying enzymes	39
1.8 Biological impact of histone modifications	39
1.9 Impact of histone acetylation	41
1.10 Classification and targeting of acetyltransferases	44
1.11 Classification and targeting of histone deacetylases	46
• Section 2.	
2.1 Host-Microbe Interactions	49
2.2 Pathogenesis governing host-pathogen interactions	51
2.3 Histone modifications induced by bacterial infection	58
2.4 Direct histone modification by virulence factors	59
2.5 Histone modifiers regulated by virulence factors	61
2.6 Histone modifications resulting from infection-induced signaling	64
• Section 3.	
3.1 <i>Listeria monocytogenes</i> pathogenesis	65
3.2 Host chromatin modifications induced by <i>Listeria monocytogenes</i>	66
• Section 4.	
Thesis Objectives	70
Summary of Thesis	70

Results	71
Overview	72
• Section 1. A role for SIRT2-dependent histone H3K18 deacetylation in bacterial infection_	77
• Section 2. CBP/p300 does not antagonize H3K18 deacetylation during infection with <i>Listeria monocytogenes</i> _____	104
• Section 3. SIRT2 N-terminal dephosphorylation causes nuclear localization_____	107
• Section 4. Generalizing Histone H3K18 deacetylation to other bacterial pathogens_____	116
Discussion	119
Manipulating host histone acetylation_____	119
<i>L. monocytogenes</i> imposes a histone code_____	120
<i>L. monocytogenes</i> induces SIRT2-dependent transcriptional repression_____	124
Impact of SIRT2-dependent gene regulation_____	124
Perspectives	
A nuclear function for SIRT2 during <i>L. monocytogenes</i> infection_____	127
Conclusion	130
Annexes	132
Materials and Methods_____	133
Microarray Transcriptome_____	143
References_____	159

List of Abbreviations

Nucleic acids:

DNA	deoxyribonucleic acid
RNA	ribonucleic acid
Mb	megabase

Histones:

H1	Histone H1
H2A/B	Histones H2A and H2B
H2A.Z	Histone H2A variant Z, encoded by H2AFZ
γ -H2A.X	phosphorylated (serine 139) H2AFX, gene encoding H2A protein
H3	Histone H3
H3.1/2/3	Histone H3 variants 1, 2, and 3
H4	Histone H4

Histone modifications:

PTM	Post-translational modification
ADP	Adenosine diphosphate
ATP	Adenosine triphosphate

Proteins, protein families, protein domains:

C-terminal	Carboxy-terminal
N-terminal	Amino-terminal
K	Lysine
S	Serine
Pol II	Polymerase II
HEAT domain	Huntingtin, elongation factor 3, protein phosphatase 2A, yeast kinase TOR1
WD40 repeat	tryptophan-aspartic acid (also known as beta-transducin)
BIR domain	Baculovirus inhibitor of apoptosis protein repeat domain
BRCT domain	BRCA1 C-Terminal domain
PHD fingers	Plant Homeo Domain
GNAT	Gcn5 N-acetyltransferase
MYST	Morf, Ybf2, Sas2, Tip60
SAGA	Spt-Ada-Gcn5-acetyltransferase
Ank	Ankyrin repeat containing protein
FAK	Focal adhesion kinase
PI3K	Phosphatidylinositide 3-kinase
Akt	Protein kinase B
EGF	Epidermal Growth Factor
HGF	Hepatocyte Growth Factor
FLAG	FLAG octapeptide sequence (N-DYKDDDDK-C) tag
GFP	Green Fluorescent Protein

Chaperones:

CAF1	chromatin assembly factor 1
HIRA	HIR histone cell cycle regulation defective homolog A

PCNA proliferating cell nuclear antigen
Asf1 Anti-silencing function protein 1

Genes, elements, genome:

TSS Transcriptional start site
poly-(dA:dT) poly(deoxyadenylic-deoxythymidylic) acid
TATA box DNA sequence (5'-TATAAA-3') cis-regulatory element of promoters
TBP TATA-binding protein
TAF TATA-binding protein associated factor
TFIID Transcription Factor II D
HML Hidden MAT left
Alu element *Arthrobacter luteus* restriction endonuclease sensitive transposable
 element
HMR Hidden MAT right
MAT Yeast mating type locus
UTR untranslated region

Host-Microbe Interactions:

MAMP Microbial-associated molecular pattern
PAMP Pathogen-associated molecular pattern
PRR Pattern-recognition receptor
TTSS Type III Secretion System
SCV *Salmonella*-containing vacuole
LLO Listeriolysin O (pore forming toxin from *Listeria monocytogenes*)
PFO Perfringolysin O (pore forming toxin from *Clostridium perfringens*)
PLY Pneumolysin (pore forming toxin from *Streptococcus pneumoniae*)
LT Lethal toxin (from *Bacillus anthracis*)
PGN Peptidoglycan
NAD⁺ Nicotinamide Adenine Dinucleotide coenzyme
NUE Nuclear Effector
IFN Interferon
ISG Interferon-stimulated gene
Inv Invasin (from *Yersinia pseudotuberculosis*; [\(Isberg and Falkow, 1985\)](#))
M90T *Shigella flexneri* wildtype serotype 5 strain ([\(Sansonetti et al., 1982\)](#))

List of Figures and Tables

Introduction:

Section 1.1

Figure 1. Bacterial gene regulation_____16

Figure 2. Transcriptional states in prokaryotes and eukaryotes_____17

Section 1.2

Figure 3. Arrangement of the nucleosome_____20

Figure 4. “Beads on a string” view of calf thymus histones associated to Adenovirus-2 DNA_____20

Figure 5. Hierarchical folding and plasticity of higher order chromatin structures_____21

Figure 6. Cartoon model of the five principal chromatin types_____21

Section 1.3

Figure 7. Left-handed protein superhelix structure of the histone octamer__23

Table 1. Classification of histone genes_____24

Section 1.4

Figure 8. Nucleosome assembly_____27

Section 1.5

Table 2. Conservation and distribution of histone variants_____31

Figure 9. DNA translocation model for nucleosome remodeling_____32

Figure 10. Lateral cross-transfer model for nucleosome remodeling_____32

Section 1.6

Figure 11. Histone modifications_____36

Figure 12. A toolkit for modifying the chromatin template_____37

Figure 13. Mechanisms of histone-recognition modules_____37

Table 3. Chromatin-binding domains_____38

Section 1.9

Figure 14. Unfolding of the nucleosome core particle by histone acetylation_43

Section 1.10

Table 4. Characteristics of HAT families_____45

Section 1.11

Table 5. Classification of mammalian HDACs_____47

Figure 15. The NAD⁺ -dependent deacetylation reaction catalyzed by Sir2p__48

Section 2.2

Figure 16. Mechanisms used by bacteria to enter cells_____55

Section 2.4

Figure 17. Bacterial nucleomodulins targeting chromatin_____60

Section 2.5

Figure 18. Bacterial signaling to histones and transcriptional response____63

Section 3.2

Figure 19. *L. monocytogenes*-induced host chromatin modifications_____69

Results:

Section 1

Figure 1. Infection induces deacetylation of H3K18	84
Figure 2. SIRT2 deacetylates H3K18 and is relocalized to the nucleus upon infection	85
Figure 3. SIRT2 regulates genes during infection	86
Figure 4. SIRT2 is necessary for infection	87
Figure S1. <i>L. monocytogenes</i> induces H3K18 deacetylation	90
Figure S2. Quantification of H3K18 deacetylation levels by mass spectrometry	91
Figure S3. The catalytic activity of SIRT2 is necessary for H3K18 deacetylation	93
Figure S4. SIRT2 is relocalized to the nuclear and chromatin fractions upon infection	94
Figure S5. Nuclear localization of SIRT2 is not sufficient for inducing H3K18 deacetylation	95
Figure S6. H3K18 deacetylation is induced through activation of the PI3K/AKT pathway	96
Figure S7. Validation of microarray analysis	97
Figure S8. InlB and HGF are sufficient to modulate SIRT2-dependent genes	98
Figure S9. H3K18 deacetylation does not occur at exon 2	99
Figure S10. Deacetylation at TSS is specific to K18	100
Figure S11. AGK2 does not affect the cell cycle	101
Figure S12. SIRT2 is essential for a listerial infection <i>in vivo</i>	102

Section 2

Figure 1. p300 activity regulates basal H3K18 acetyl levels, but does not antagonize H3K18 deacetylation during infection	105
Figure 2. p300 activation increases basal H3K18 acetyl levels at 3 hours, but does not inhibit H3K18 deacetylation during infection	106

Section 3

Figure 1. SIRT2 S368 phospho status does not dictate sub-cellular localization	111
Figure 2. Sub-nuclear localization of SIRT2-GFP S368 mutants	112
Figure 3. SIRT2 phosphorylation status of N- and C- terminal phospho sites	113
Figure 4. SIRT2 S27 phosphorylation regulates SIRT2 nuclear recruitment	114
Table 1. Mass spectrometric quantification of PPM1B peptides	114
Figure 5. PPM1B is necessary for H3K18 deacetylation during infection	115

Section 4

Figure 1. Invasin expressing <i>E. coli</i> causes H3K18 deacetylation and SIRT2 nuclear relocalization, like <i>L. monocytogenes</i>	117
---	-----

Discussion:

Figure 1. LLO causes a reduction in host nuclear size	122
Figure 2. H3K18/H4K16 acetylation dictates state of chromatin and transcription	123
Figure 3. Model of <i>L. monocytogenes</i> -induced SIRT2-dependent H3K18 deacetylation	130

Abstract

Bacterial pathogens dramatically affect host cell transcription programs for their own profit, however the underlying mechanisms in most cases remain elusive. While investigating the effects of *Listeria monocytogenes* on histone modifications, we discovered a new transcription regulatory mechanism by which the expression of genes is repressed, during infection. Upon infection by *L. monocytogenes*, the secreted virulence factor, InlB, binds the c-Met receptor and activates signaling through PI3K/Akt. This signaling platform is necessary for causing the relocalization of the histone deacetylase, SIRT2, to the nucleus and associating to chromatin.

In characterizing the mechanism governing SIRT2 nuclear relocalization during infection, our results have demonstrated that SIRT2 undergoes a post-translational modification. SIRT2 undergoes dephosphorylation at a novel N-terminal phospho-site. SIRT2 is recruited to the transcription start sites of genes repressed during infection leading to H3K18 deacetylation and transcriptional repression.

Finally, my results demonstrate that SIRT2 is hijacked by *L. monocytogenes* and promotes an increase in intracellular bacteria. Together, these data uncover a key role for SIRT2 mediated H3K18 deacetylation during infection and characterize a novel mechanism imposed by a pathogenic bacterium to reprogram the host cell.

Résumé

De nombreuses bactéries pathogènes sont capables d'affecter les programmes transcriptionnels de la cellule hôte pendant l'infection. Cependant, les mécanismes contrôlant ce processus restent largement inconnus. En investiguant les effets de *Listeria monocytogenes* sur les modifications des histones de l'hôte, nous avons mis en évidence un nouveau mécanisme de régulation de transcription nécessaire pour la répression de l'expression de certains gènes, pendant l'infection. Lors de l'infection par *L. monocytogenes*, le facteur de virulence sécrété, InlB, se lie au récepteur c-Met et active la signalisation par les intermédiaires PI3K et Akt. Cette plateforme de signalisation est nécessaire pour la relocalisation de la déacetylase d'histone, SIRT2, au noyau et l'association à la chromatine.

En caractérisant le mécanisme gouvernant la relocalisation nucléaire de SIRT2 lors de l'infection, nous avons démontrés que SIRT2 subit une modification post-traductionnelle. SIRT2 est déphosphorylée à un nouveau site de phosphorylation localisé à la partie N-terminale de la protéine. SIRT2 est recrutée aux sites de démarrage de la transcription des gènes réprimés lors de l'infection menant à la deacetylation de H3K18 et la répression transcriptionnelle.

Nous avons mis en évidence que SIRT2 est détournée par *L. monocytogenes* et provoque une croissance des bactéries intracellulaires. Ces résultats démontrent un rôle clef de SIRT2 en provoquant la deacetylation de H3K18 lors de l'infection et dévoilent un nouveau mécanisme imposé par les bactéries pathogènes dans le but de reprogrammer la cellule hôte.

Preamble

Since the first description of the operon model detailing the basic principles governing the regulation of gene expression in prokaryotes by François Jacob, Jacques Monod and their colleagues ([Jacob and Monod, 1961](#)), many studies have sought to determine whether similar mechanisms operate in eukaryotes. Jacques Monod's famed quote, "all that is true for *Colibacillus* is true for the elephant," has been scrutinized with the hopes of determining whether indeed the operon model is sufficient to describe the regulation of gene expression in eukaryotes. While some basic principles are true for both prokaryotes and eukaryotes, the operon model is arguably not sufficient to describe the complexity of eukaryotic gene regulation. Unlike in prokaryotes, in which repressors act to repress gene expression, eukaryotic genes are transcriptionally silent unless an activation mechanism is put in place ([Struhl, 1999](#)). The description of mechanisms by which eukaryotes undertake to activate or silence genes is a dynamic field of research. How the various structural components of eukaryotic chromatin function to control gene expression will be essential to uncovering the principles that distinguish the regulation of gene expression in eukaryotes from that in prokaryotes.

Chromatin is composed of essential repeating units of nucleosomes, which are made of 147 base pairs of DNA and a hetero-octamer of histone proteins for a core particle and 20 – 50 base pairs of DNA acting as a linker to the neighboring nucleosome ([Kornberg and Lorch, 1999](#)). In higher eukaryotes, an accessory histone can compact nucleosomes into a tighter configuration than exhibited in lower eukaryotes like yeast ([Grunstein, 1990](#)). Histones of the core particle contain N-terminal tails, which protrude out from the core and can be post-translationally modified. Interestingly, these histone modifications have been correlated with changes in gene expression ([Allfrey et al., 1964](#)). It was initially believed that histone modifications resulted in regulated the compaction of chromatin, which could promote or inhibit access of transcriptional machinery to DNA ([Shahbazian and Grunstein, 2007](#)). However, a more recent hypothesis suggests that transcription factors and machinery can still access DNA even at compacted chromatin ([van Steensel, 2011](#)). Therefore, histone modifications might be a reflection of the types of proteins complexing with nucleosomes, forming enhanceosomes or repressosomes, to regulate the access of transcriptional machinery to DNA ([Carey, 1998](#)). Nevertheless, histone modifications play a major role in eukaryotic gene regulation and therefore,

uncovering the various mechanisms that cooperatively modify gene expression is essential ([Gardner et al., 2011](#); [Strahl and Allis, 2000](#)).

Histones are modified in both the cytosol and in the nucleus. Modifications in the cytosol play an important role in stocking histones or directing their import into the nucleus for assembly into chromatin. At the chromatin level, histone modifications play an important role in the maintenance of chromatin integrity, DNA repair, and importantly transcriptional control. One such histone modification, which has an essential role in regulating transcription, is histone lysine acetylation and deacetylation. However, the mechanisms by which histone acetylation and deacetylation occur are not fully understood, nor have the conditions under which histone acetylation is modified thoroughly described.

The field of host-microbes interactions has emerged as a field interested in both uncovering the mechanisms by which pathogens control host gene expression and describing how host health is impacted. In eukaryotes, post-translational modifications (PTMs) to histones play an important role in regulating transcription. The modulation of acetylation at the N-terminal tail of histone H3 has been identified and characterized as a major determinant of the state of transcription. The modulation of host gene expression by modifying host chromatin has emerged as an important aspect of host-pathogen interactions. Among the various pathogens, which cause host histone modifications is *Listeria monocytogenes*. This Gram-positive, facultative-intracellular pathogen has been demonstrated to cause various histone modifications on histones H3 and H4. Listerial virulence factors are essential for inducing histone modifications one of which is listeriolysin O (LLO), which causes global modifications such as: H3 dephosphorylation and H4 deacetylation. *Listeria* has been observed to cause H3 deacetylation in a LLO-independent manner, a modification previously undescribed during bacterial infection.

My thesis work has aimed to characterize this modification, uncover the condition(s) under which it occurs, the host machinery catalyzing H3 deacetylation, and the impact it has on infection. We observed that histone H3 lysine 18 underwent deacetylation during infection. We report that the virulence factor conferring bacterial entry, InlB, induces the PI3K/Akt signaling cascade, which causes the NAD⁺-dependent deacetylase, SIRT2, to relocate to the nucleus and catalyze H3K18 deacetylation. We further demonstrate that SIRT2 recruitment and H3K18 deacetylation to the

transcriptional start sites of host genes repressed during infection in a SIRT2-dependent manner. Further study demonstrates that SIRT2 is a major host factor promoting virulence in both tissue culture and *in vivo*. This work describes a role for H3K18 deacetylation, a newly discovered function for SIRT2 in transcriptional regulation, and a virulence mechanism previously undescribed.

Introduction

Section 1:

1.1 Uncovering the basis for gene regulation

The operon model described the basic principles of gene regulation, were established in the operon model. The operon model provided a basis for understanding the control of gene expression in bacteria (Fig. 1) ([Jacob and Monod, 1961](#)). They described three types of DNA sequences, which act as fundamental units of gene regulation: promoters, operators, and positive control elements. Promoters determine the maximal potential level of gene expression and are recognized by RNA polymerase for transcriptional initiation. Operators are recognized by repressor proteins acting to inhibit transcription. Finally, positive control elements are recognized by activator proteins, which stimulate transcription from the promoter. These basic units of gene regulation describe gene expression control in prokaryotes. Unless a repressor actively blocks transcription, bacteria exhibit a relatively unrestricted state of active transcription (Fig. 2). Eukaryotes do not depend on repressors for maintaining transcriptional silencing (Fig. 2) ([Struhl, 1999](#)). In contrast to prokaryotes, a strong core promoter is essentially inactive in eukaryotic cells. Underlying the distinct logical program of gene regulation in eukaryotes is the inherent difference from prokaryotes in the structural organization of the genomes, *in vivo*. In order to understand how eukaryotic and prokaryotic gene regulation differ it is important to describe the structural components of the genome.

In prokaryotes, genomic DNA is assembled with proteins into a structure called the nucleoid. However, this semi-compacted structure created by scaffold proteins does not globally inhibit transcription, such that prokaryotic promoters are readily accessible for binding. The ease in accessibility of prokaryotic promoters to binding by transcriptional machinery describes an unrestrictive transcriptional ground state, which is the inherent activity of promoters in the absence of regulatory elements ([Struhl, 1999](#)). In prokaryotes, repressors function to block the activity of RNA polymerase on DNA by occlusion of binding to the promoter ([Geanakopoulos et al., 1999](#); [Hochschild and Dove, 1998](#)). Repressors are required to keep gene activity at a low level, except for promoters exhibiting weak RNA polymerase binding.

Transcription in eukaryotes requires that multiple activators synergistically bind to DNA at regions that enhance transcriptional factor binding and together this protein-DNA complex is termed the enhanceosome ([Carey, 1998](#)). As a result, transcriptional activation in eukaryotes is combinatorial. Each of the large number of possible combinations of regulatory and activating factors is biologically distinct and an individual core promoter may be regulated with diversity and precision. The general principles of transcriptional control in eukaryotes goes beyond those described in the operon model by François Jacob and Jacques Monod. The structure of the eukaryotic genome plays a major role in controlling transcription through the regulation of DNA compaction or by steric hindrance of transcriptional machinery from associating to DNA.

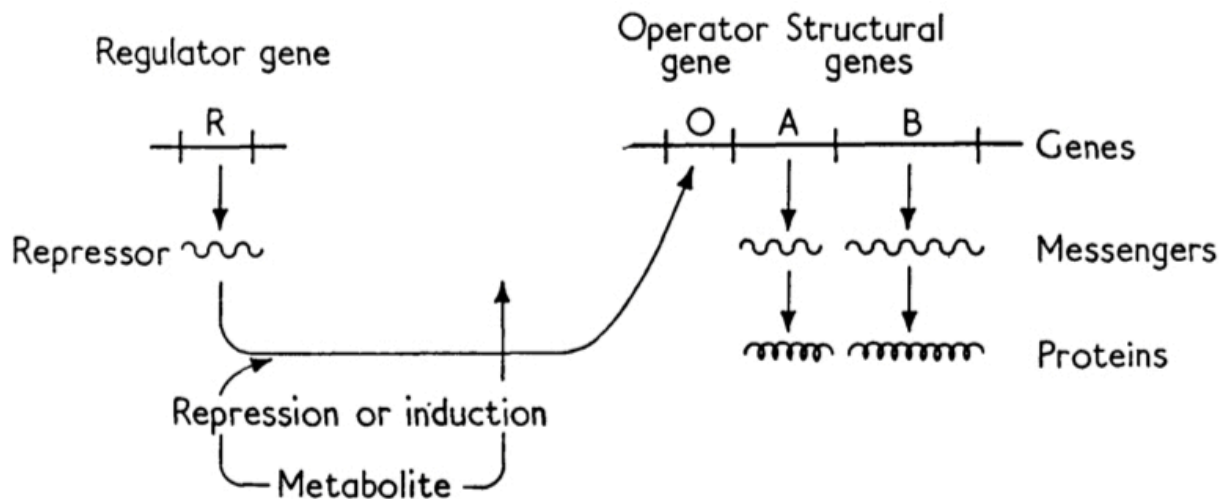


Figure 1. Bacterial gene regulation depends on repressor binding to a target operator and blocking transcriptional machinery from accessing the genes ([Jacob and Monod, 1961](#)).

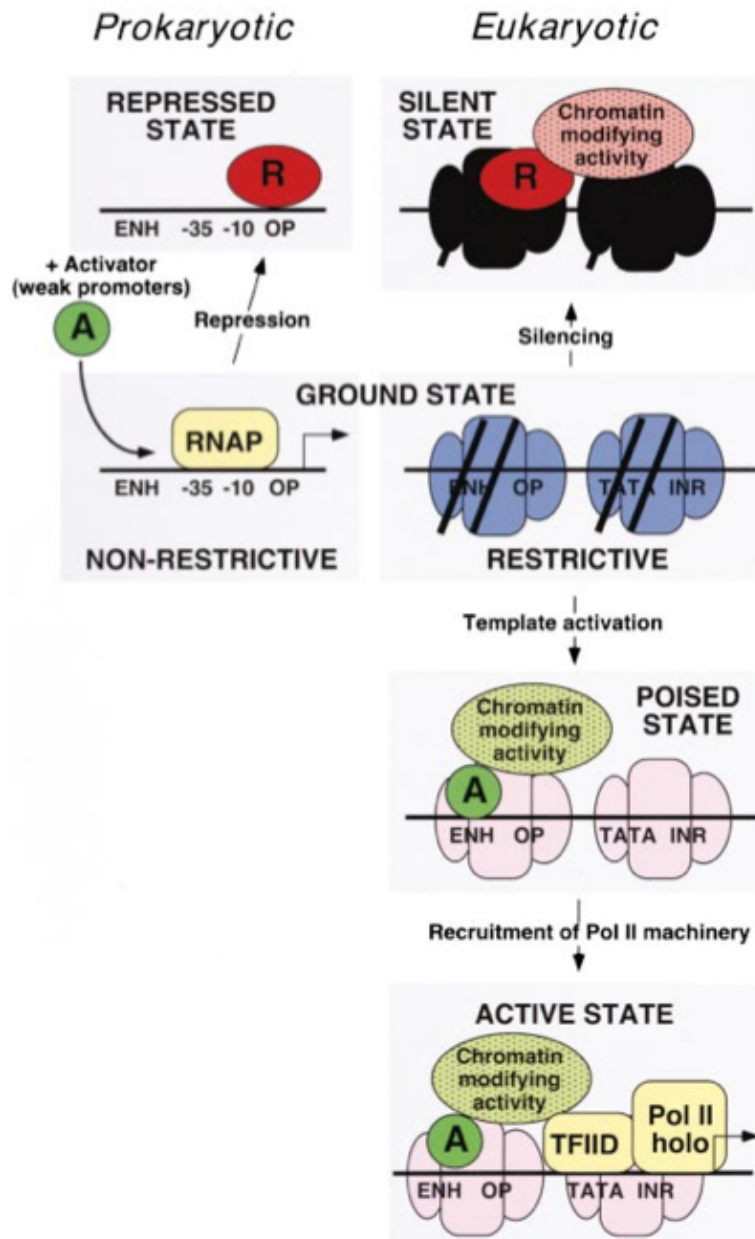


Figure 2. Transcriptional States in Prokaryotes and Eukaryotes.

Activators (A) and repressors (R) interact respectively with enhancer (ENH) or operator (OP) sequences and affect transcription by prokaryotic RNA polymerase (RNAP) or the eukaryotic Pol II machinery (TFIID + Pol II holoenzyme). In eukaryotes, recruitment of chromatin modifying activities by activators or repressors leads to altered chromatin structure (depicted by color or DNA within nucleosomes) ([Struhl, 1999](#)).

1.2 Eukaryotic chromatin and its two major states

Eukaryotic genomes of fungi, plants and mammals are composed of billions of base pairs, for which compaction is achieved by the winding of DNA around associated proteins into a structure called chromatin. Approximately 147 base pairs of DNA are wrapped around a set of proteins called histones forming the core particle of a structure known as the nucleosome. Each nucleosome is linked to the next by a DNA segment of variable length (Fig. 3 & 6). The variation in the length of linker DNA ([Spadafora et al., 1976](#)) is important for the diversity of gene regulation. Despite the variety in length of the linker, nucleosomes can still coil in a regular manner into a chromatin fiber. The loose association of DNA to core histone proteins has been characterized as a “beads on a string” conformation, based on electron microscopy imagery (Fig. 4) ([Oudet et al., 1975](#)). The *open* state of chromatin is called euchromatin. The impact on transcriptional regulation of this configuration facilitates the binding of transcriptional machinery and initiation of transcription. Chelation of magnesium ion from the “beads on a string” configuration of chromatin causes an intermediate state of nucleosomes zig-zagging (Fig. 5) ([Li and Reinberg, 2011](#)). Further adding the accessory histone H1 represents an additional organizational switch to a more compacted solenoid structure that measures 30nm in diameter (Fig. 5). The compacted state of the 30nm fiber is transcriptionally silent, as the access to DNA of transcriptional machinery is limited. Chromatin exists in these various configurations in non-mitotic cells. However, during mitosis, chromatin undergoes a super-coiling of the 30nm fiber in order to ultimately compact DNA into discrete chromosomes.

Traditionally, chromatin has been described to exist in two major states, based on the morphological differences observed by electron microscopy, whereby one state of chromatin is dark and the other light ([Kornberg and Lorch, 1999](#)). The *open* euchromatin is transcriptionally active and contrasts with the transcriptionally silent heterochromatin. More recent studies have revisited whether the classical model describing a dichotomy in chromatin states is an oversimplification of the complexity in structure and function of chromatin states ([van Steensel, 2011](#)). Indeed a carefully controlled study in *Saccharomyces cerevisiae* found that chromatin-remodeling factors are capable to access both heterochromatin and euchromatin ([Chen and Widom, 2005](#)). Further studies have revealed that DNA-interacting proteins are also found to have normal access to repressive

chromatin ([Filion et al.](#)) and transcription factors to associate to mitotic chromosomes ([Chen and Widom, 2005](#)), suggesting that the morphologically described state of chromatin compaction is not so accurate to predict biological outcome. One proposed model for redefining chromatin types is by describing where DNA- and chromatin-associating factors localize along the genome ([Filion et al.](#)). The numerous chromatin proteins and possible interactions among them suggest that distinct and unique combinations of proteins can associate along the entire genome. This 'combinatorial code' was proposed for one aspect of chromatin structure, the post-translational modification of its constituent parts ([Strahl and Allis, 2000](#)). Curiously, based on the association of over 50 proteins with DNA whose possible combinations of association are innumerable, only five major types of chromatin can generally be distinguished, which are schematically represented in figure 6 as green, blue, yellow, black and red chromatin types ([Filion et al.; van Steensel, 2011](#)). Black chromatin most highly correlates with silent transcription. Red chromatin has the highest overall protein occupancy and along with yellow chromatin correlate with what is generally considered euchromatin. Blue and green chromatin, correspond to what is considered heterochromatin. Together, these chromatin types do not adhere to the dogma that euchromatin correlates with "open," transcriptional active DNA regions and heterochromatin corresponding with the opposite. These studies repartitioning chromatin into five types based on the combination of proteins associating to DNA at distinct regions may provide the possibility to uncover new principles about eukaryotic nuclear organization and how it impacts biological outcome.

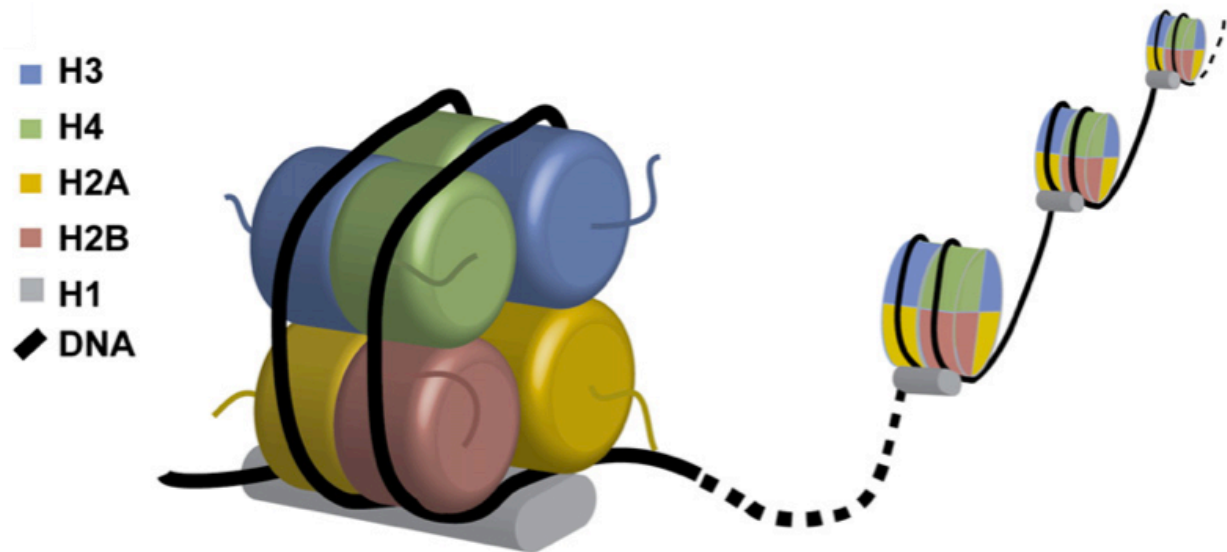


Figure 3. Arrangement of the nucleosome

The arrangement of the eight-histone proteins in the nucleosome core is shown schematically. 147 base pairs of DNA are wrapped around the histone core. Histone H1 associates on the outer groove of DNA, conferring nucleosome compaction and separating each nucleosomal unit from one another. ([Hamon and Cossart, 2008](#))

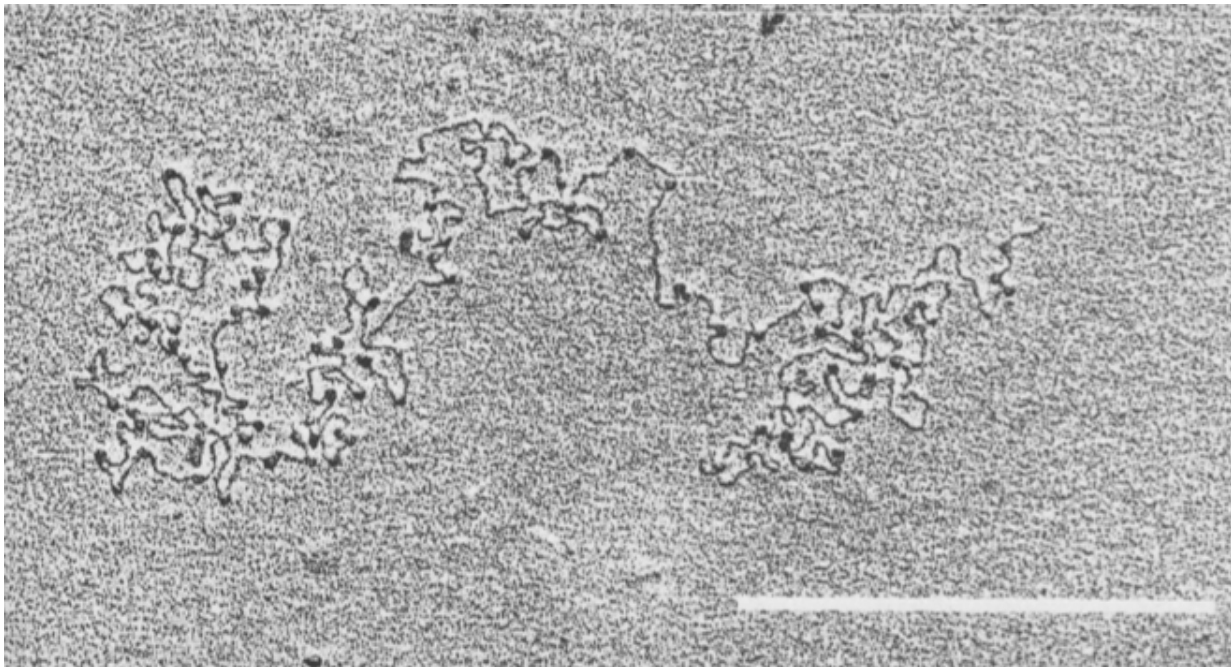


Figure 4. "Beads on a string" view of calf thymus histones associated to Adenovirus-2 DNA

The 10nm fibre of DNA and four histones associated at a ratio of 1.0 histone/DNA ratio. Scale bar indicates 0.5 μm . ([Oudet et al., 1975](#))

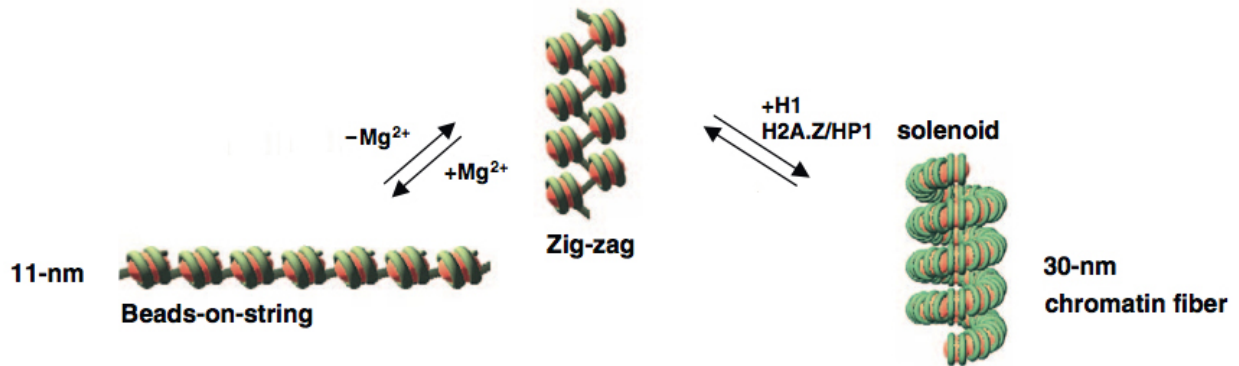


Figure 5. Hierarchical folding and plasticity of higher order chromatin structures.

A general scheme represents the folding of chromatin from 11 nm nucleosomal arrays (beads on a string) to a higher order chromatin structure, namely 10 nm chromatin fiber. The addition of magnesium ions contributes to the decompaction of chromatin from a “zig-zag” configuration to a beads on a string configuration. The compacted form of chromatin is a right-handed solenoid 30 nm fiber, which is dependent on the association of histone H1, H2A.Z and heterochromatin protein 1 (HP1) proteins. Figure adapted from ([Li and Reinberg, 2011](#)).

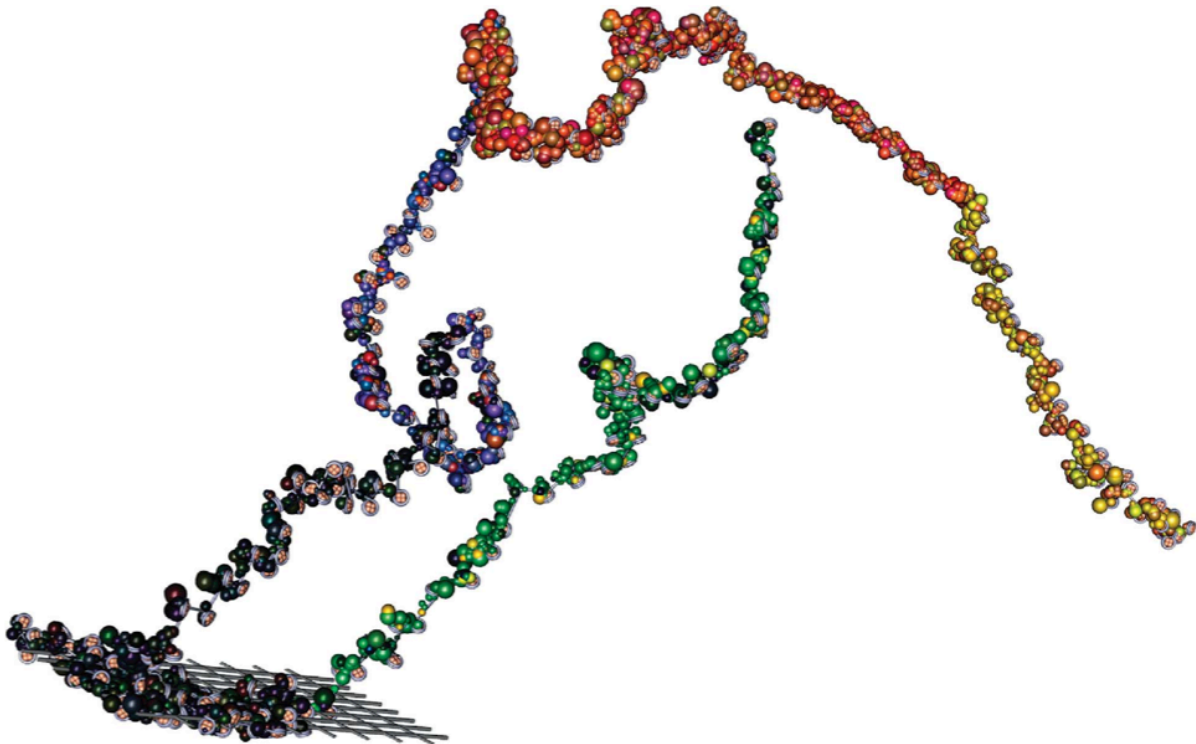


Figure 6. Cartoon model of the five principal chromatin types as identified in *Drosophila melanogaster* cells. Some proteins are shared between two or more chromatin types. BLACK chromatin has a preference to be in contact with the nuclear lamina (grey lattice, bottom left). RED chromatin has the highest overall protein occupancy. ([van Steensel, 2011](#))

1.3 Histones: a crucial component of the nucleosome

The nucleosome is composed of three parts in higher eukaryotes: 1) a core particle, which is a hetero-octamer of histone proteins around which DNA is wrapped, 2) linker DNA, which goes between two nucleosomes, and 3) one accessory histone H1 (Fig. 3). The nucleosome core is formed of two pairs of histone types H2A, H2B, H3 and H4 (Fig. 7). Histone H1 is an accessory protein associating to the outer groove of the nucleosome. H1 is only present in higher eukaryotes and has been hypothesized to promote a greater level of chromatin compaction and restrictive transcriptional activation across the human genome as compared to the yeast, *Saccharomyces cerevisiae* ([Grunstein, 1990](#); [Hereford and Rosbash, 1977](#); [Lohr and Hereford, 1979](#)).

Histones are encoded by many genes in humans and show a high level of redundancy in their sequence. These histone genes are grouped into three main clusters of genes, which are differentially expressed during the cell cycle and have a major role in maintaining chromatin integrity during DNA replication or repair. Most of the replication-dependent histone genes are found in two clusters: a major histone gene cluster, located on chromosome 6 ([Albig and Doenecke, 1997](#); [Albig et al., 1997](#)), termed *HIST1* and a minor cluster *HIST2* on chromosome 1 (Table 1) ([Marzluff et al., 2002](#)). Locus *HIST1* is comprised of accessory and core histone types and the majority of these genes are not distributed uniformly across the cluster. In contrast, the *HIST2* gene locus on chromosome 1 is comprised solely of genes encoding core histone proteins, which are distributed evenly across the cluster ([Marzluff et al., 2002](#)). *HIST1* histones are denoted Hx.1 whereas *HIST2* clustered histones are denoted Hx.2 (“x” represents the number denoting the histone type). At a distance of approximately 87 mega-bases (Mb) from the *HIST2* gene cluster, there exists a third gene locus termed the *HIST3* cluster encoding a unique H3 gene, as well as H2A and H2B core histone genes. The *HIST3* cluster is expressed primarily in testes ([Witt et al., 1996](#)).

Differences in sequence of histone genes play an important role in controlling various biological processes like transcription, DNA damage repair, and the maintenance of chromatin integrity. For example, H2AX, encoded by the H2AFX gene plays a critical role in the recruitment of repair factors following DNA damage ([Paull et al., 2000](#)). Indeed, many histone variants have been described to localize to specific genomic loci under conditions of cellular stress or during cell cycling (Table 2). Histone variants are

implicated in more than just maintaining chromatin integrity during DNA synthesis; they provide the ability to specifically control biological functions.

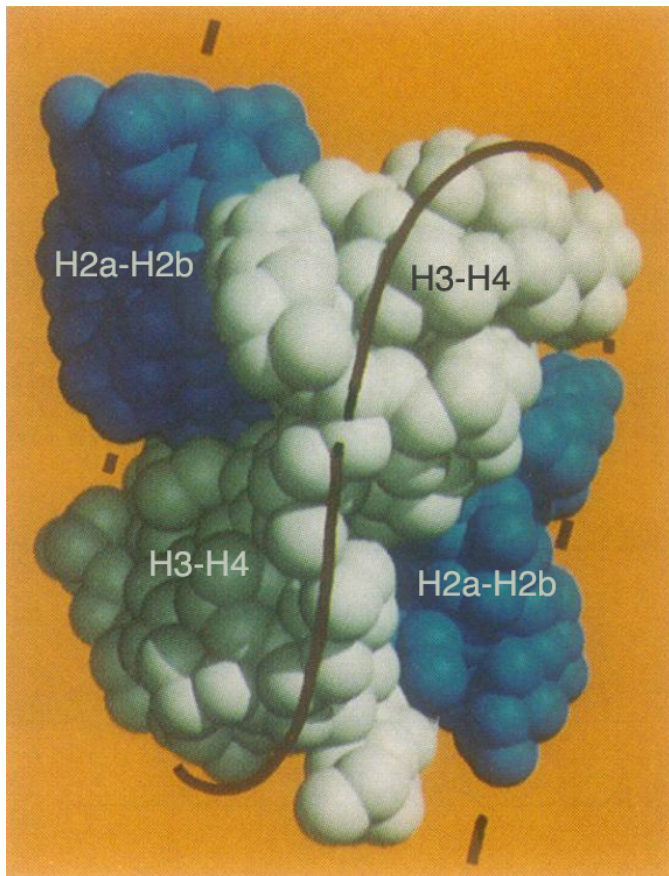


Figure 7. Left-handed protein superhelix structure of the histone octamer

The line indicates the path of the left-handed protein superhelix. The H2A-H2B dimers are indicated in dark blue at the beginning and end of the superhelix; the H3-H4 tetramer is lightly shaded in the middle. Figure adapted from ([Arents et al., 1991](#)).

Table 1: Classification of histone genes

Histone Super Family	Family	Subfamily	Gene Members	Importance for DNA synthesis (+, -)
Accessory (Linker)	H1	H1.F	H1F0, H1FNT, H1FOO, H1FX	-
		H1.H1	HIST1H1A, HIST1H1B, HIST1H1C, HIST1H1D, HIST1H1E, HIST1H1T	+
Core	H2A	H2A.F	H2AFB1, H2AFB2, H2AFB3, H2AFJ, H2AFV, H2AFX, H2AFY, H2AFY2, H2AFZ	+/-
		H2A.1	HIST1H2AA, HIST1H2AB, HIST1H2AC, HIST1H2AD, HIST1H2AE, HIST1H2AG, HIST1H2AI, HIST1H2AJ, HIST1H2AK, HIST1H2AL, HIST1H2AM	+
		H2A.2	HIST2H2AA3, HIST2H2AC	+
	H2B	H2B.F	H2BFM, H2BFS, H2BFWT	+/-
		H2B.1	HIST1H2BA, HIST1H2BB, HIST1H2BC, HIST1H2BD, HIST1H2BE, HIST1H2BF, HIST1H2BG, HIST1H2BH, HIST1H2BI, HIST1H2BJ, HIST1H2BK, HIST1H2BL, HIST1H2BM, HIST1H2BN, HIST1H2BO	+
		H2B.2	HIST2H2BE	+
	H3	H3.1	HIST1H3A, HIST1H3B, HIST1H3C, HIST1H3D, HIST1H3E, HIST1H3F, HIST1H3G, HIST1H3H, HIST1H3I, HIST1H3J	+
		H3.2	HIST2H3A, HIST2H3C, HIST2H3D	+
		H3.3	HIST3H3, H3F3A, H3F3B	-
	H4	H4.1	HIST1H4A, HIST1H4B, HIST1H4C, HIST1H4D, HIST1H4E, HIST1H4F, HIST1H4G, HIST1H4H, HIST1H4I, HIST1H4J, HIST1H4K, HIST1H4L	+
		H4.4	HIST4H4	+

1.4 Nucleosome assembly: an essential process for chromatin organization

In S phase, the step at which DNA synthesis occurs in preparation for cell division, following the expression of DNA replication-dependent variants of histone genes, newly synthesized histones can either be stored or trafficked to the nucleus for assembly into nucleosomes. Existing histones are separated between newly replicated DNA and the old DNA ([Sogo et al., 1986](#)). Nucleosome assembly begins by the deposition onto DNA of a (H3-H4)₂ tetramer, which can exist in an intermediate H3-H4 dimeric form (Fig. 5a). Two dimers of H2A-H2B are in turn associated to the (H3-H4)₂ tetramer bound to DNA. Histone chaperones play an essential role in acting as histone acceptors and donors in addition to disrupting and assembling nucleosomes ([Probst et al., 2009](#)). Chaperones are specific for particular histones or even a specific histone variant and control the local concentration of histones ([De Koning et al., 2007](#)).

To replenish nucleosomes, *de novo* complexes are formed with the help of histone chaperones. DNA synthesis-dependent nucleosome assembly is largely dependent on the activity of the chaperone, chromatin assembly factor 1 (CAF1). CAF1 associates to H3.1-H4 and is recruited to the replication fork ([Tagami et al., 2004](#)) through an interaction with the DNA polymerase cofactor, the DNA processivity factor proliferating cell nuclear antigen (PCNA) and other chromatin structural modifier proteins ([Probst et al., 2009](#)). Another H3-H4 chaperone, Asf1, binds to and functions synergistically with CAF1 ([Mello et al., 2002](#)) in DNA synthesis-dependent nucleosome assembly by acting as a donor of newly synthesized histones. Asf1 directly associates to replication fork machinery through interactions with components of the putative replicative helicase ([Groth et al., 2007](#)).

CAF1 and Asf1 chaperones are believed to play an added role in organizing newly synthesized histones with parental histones already deposited into nucleosomes (Fig. 8b) ([Probst et al., 2009](#)). During DNA replication, parental H3-H4 dimers can be split and removed from DNA by Asf1. Split H3-H4 dimers can be re-associated with old H3-H4 to DNA producing a nucleosome made up of parental histones. Split H3-H4 can also be assembled with newly synthesized H3-H4 by the association onto DNA of Asf1-deposited parental H3-H4 to CAF1-deposited new H3-H4 (Fig. 8b). Together, CAF1 and Asf1 provide the ability during replication to both replenish DNA with nucleosomes as well as reorganizing nucleosomes with a pool of parental and new histones ([Probst et al., 2009](#)).

Current studies aim to elucidate how nucleosome assembly during replication might affect transcriptional control.

Replication-independent nucleosome assembly encompasses a large number of biological processes for which nucleosome assembly may occur. Among those processes is maintenance of chromatin integrity during transcription, DNA damage repair, recombination, etc. The chaperone Hir-related protein A (HIRA) has the ability to reorganize nucleosomes during transcription. Nucleosome disassembly actively occurs at sites of active transcription. HIRA binds and recruits the H3.3-H4 dimer at sites of active transcription in order to maintain chromatin integrity ([Ahmad and Henikoff, 2002](#)). H3.3 nucleosomes are less stable than H3.1-containing nucleosomes ([Jin and Felsenfeld, 2007](#)). *In vivo*, H3.3 nucleosomes are observed to be more dynamic or amenable to displacement during transcription ([Probst et al., 2009](#)). Since DNA synthesis leads to a concomitant deposition of H3.1, the density of H3.3-containing nucleosomes is reduced. Other replication-independent processes are DNA damage repair and DNA recombination during which nucleosome assembly is essential for maintaining chromatin integrity. During DNA damage repair, CAF1-associated H3.1-H4 is recruited to sites of DNA damage ([Moggs et al., 2000](#); [Polo and Almouzni, 2006](#)). Characterizing the importance of nucleosome assembly on transcription is to identify the mechanisms governing nucleosome placement along the genome.

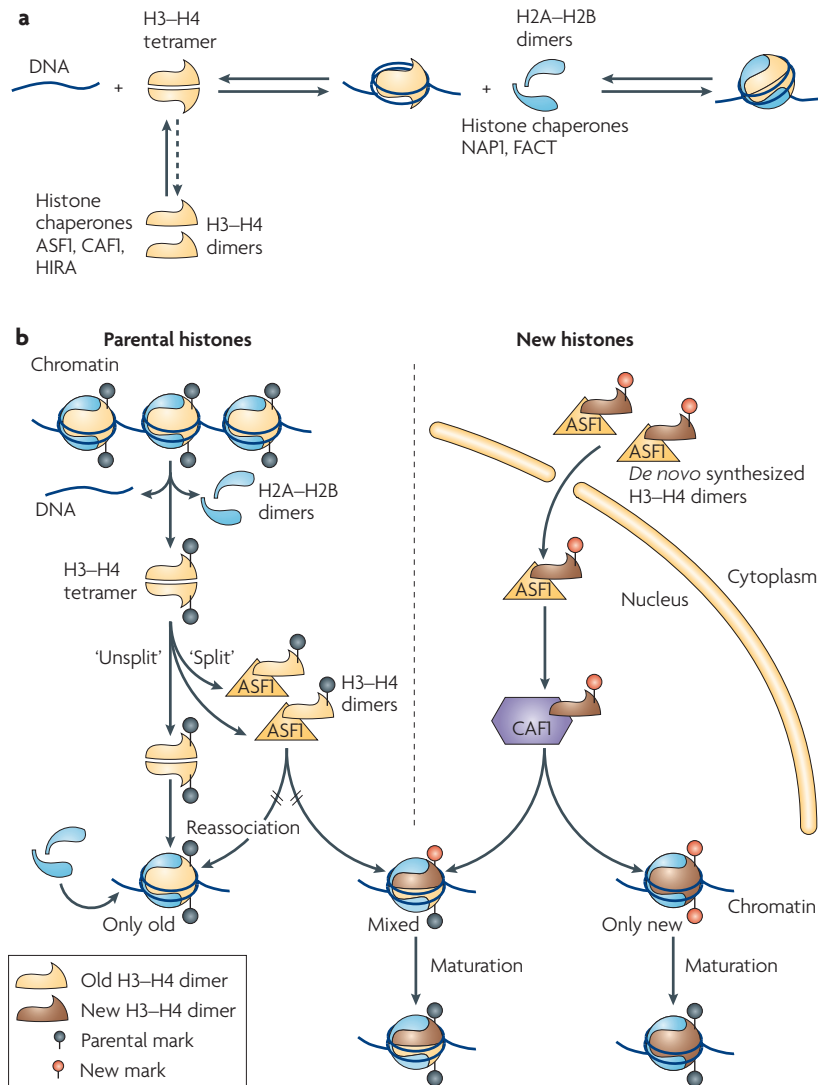


Figure 8. Nucleosome assembly. The incorporation of histone (H3-H4)₂ tetramers onto DNA, followed by the addition of two histone H2A-H2B dimers to form a nucleosome core particle (a). Prior to deposition, H3-H4 and H2A-H2B exist as dimers that are complexed to specific histone chaperones. On chromatin disruption at replication, parental H3-H4 tetramers with histone marks can either be preserved (unsplit) or broken up into dimers (split), potentially by interacting with the chaperone anti-silencing function 1 (ASF1) (b). Nucleosomes with only old H3-H4 are formed when unsplit parental tetramers are transferred directly onto daughter strands or when two parental H3-H4 dimers reassociate. Newly synthesized H3-H4 dimers with their typical marks are complexed with the chaperones ASF1 and chromatin assembly factor 1 (CAF1; also known as CHAF1). Nucleosomes might be formed on the daughter strands from one parental and one new H3-H4 dimer (indicated as mixed) or exclusively from two new H3-H4 dimers (indicated as only new). Nucleosomes that contain mixed and new histones undergo maturation after formation. FACT, facilitates chromatin transcription; HIRA, Hir-related protein A; NAP1, nucleosome assembly protein 1. (Probst et al., 2009)

1.5 Nucleosome positioning

Nucleosome positioning along the genome is a highly controlled process ([Loyola and Almouzni, 2007](#)), which plays an important role in regulating transcription. Nucleosome occupancy is correlated with transcriptional regulation. Transcriptional start sites (TSS), promoters, and enhancers all exhibit a high level of nucleosome occupancy, gradually diminishing at increasing distances from these sites ([Rando and Chang, 2009](#)). The differences in affinity for nucleosome occupancy of a DNA sequence dictates transcriptional outcome ([Segal et al., 2006](#); [Yuan and Liu, 2008](#)). DNA sequences not associated with nucleosomes and characterized by a repetitive double-stranded poly-(dA:dT) sequence have been described as “antinucleosomal” ([Rando and Chang, 2009](#)) and are sites where nucleosomes are excluded or not retained. There are two mechanisms by which transcriptional outcome is regulated based on nucleosome positioning. The first component dictating transcriptional outcome by controlling nucleosome positioning is the histone variants composing resident nucleosomes. Studies have associated histone variants with the ability to control the level of chromatin compaction, or recruit chromatin-modifying complexes. The second mechanism controlling transcriptional outcome is activity of chromatin-remodeling complexes in recruiting, stabilizing or repelling nucleosomes from a specific genomic locus. Together, these two mechanisms provide a considerable variety of possible nucleosome profiles associated to DNA, which can subsequently dictate the fate of transcription activity.

The histone variant residing at a specific genomic locus is critical for the first mechanism regulating transcription. One example is histone variant, H3.3, which is highly associated with regions of transcriptional activation and can be easily repositioned by transcriptional machinery (Table 2) ([Jin and Felsenfeld, 2007](#)). H3.3 can be pushed by transcriptional machinery leading to the dissociation of H3.3 from chromatin at DNA sequences unfavorable to nucleosome residency ([Tirosh and Barkai, 2008](#)). H3.3 nucleosomes are often enriched at promoters, gene regulatory elements, and genomic loci exhibiting a high level of transcriptional activity ([Elsaesser et al., 2010](#)). Furthermore, TSSs of genes associated with transcriptional activity are characterized by the loss of H2A.Z-containing nucleosomes (Table 2) ([Schones et al., 2008](#)). Together, these studies suggest that a loose association of H3.3 and H2A.Z with DNA allow for nucleosomes to be pushed away by transcriptional machinery. In contrast, H3.2 is assembled into genomic

regions that remain transcriptionally silent by contributing to chromatin compaction and opposing transcriptional machinery ([Akiyama et al., 2011](#)). Lastly, H3.1 is associated with both transcriptionally active and repressed DNA, which is dictated by the chromatin-modifying complexes associated with H3.1 catalyzing a change in H3.1-containing nucleosome positioning ([Hake et al., 2006](#)).

Chromatin remodeling complexes are a second factor regulating nucleosome positioning and governing transcriptional outcome. These complexes are recruited by sequence-specific DNA-binding factors and can regulate transcriptional activity ([Peterson and Logie, 2000](#); [Sudarsanam et al., 2000](#)). Catalyzed by ATPase domains, chromatin-remodeling factors such as Swi/Snf and NURF, are diverse in composition and biochemical activity ([Georgel et al., 1997](#); [Krebs et al., 2000](#); [Lee et al., 1999](#)). Sucrose nonfermentable 2 (SNF2) subfamily of remodelers can function to disrupt histone-DNA contacts in mono-nucleosomes ([Cairns et al., 1996](#); [Cote et al., 1994](#); [Fan et al., 2003](#); [Imbalzano et al., 1996](#)). Chromatin remodelers can modify nucleosome positioning by either facilitating mobilization along DNA, mediating the transfer of histone from one DNA template to a separate template, or by catalyzing nucleosome disassembly. In the first case, remodelers catalyze nucleosome mobilization (known as “sliding”), thus facilitating translocation of DNA along nucleosomes in an ATP-dependent manner or by laterally cross-transferring nucleosomes from one superhelical turn to an adjacent track (Fig. 9) ([Lusser and Kadonaga, 2003](#)). In this case, a DNA loop (or bulge) is generated to facilitate translocation of the remodeling factor. The chromatin-remodeling complex responsible for this translocation is the ISWI subfamily of the SNF2 superfamily, which has the general propensity for catalyzing nucleosome assembly rather than nucleosome disassembly ([Ito et al., 1997](#); [LeRoy et al., 2000](#)). The second proposed mechanism of nucleosome repositioning is by a lateral cross-transfer of DNA from one nucleosome to the next. In this model, the SWI/SNF complex (a SNF2 subfamily member) catalyzes the cross transfer of one superhelical turn of DNA (corresponding to about 80bp) to an adjacent track, while also dissociating another helical turn from the accepting nucleosome core particle ([Kassabov et al., 2003](#)). This model corresponds with the observations that SNF2 subfamily members disrupt nucleosomes ([Aalfs et al., 2001](#); [Imbalzano et al., 1996](#)). The third possible mechanism of remodeling is characterized by nucleosome disassembly, as assessed by the loss of DNA supercoiling of chromatin templates (Fig. 10) ([Aalfs et al.,](#)

[2001](#); [Gavin et al., 2001](#); [Guyon et al., 1999](#); [Jaskelioff et al., 2000](#); [Kwon et al., 1994](#); [Lorch et al., 2001](#); [Schnitzler et al., 1998](#)). Interestingly, these studies of how nucleosome positioning is modified by chromatin modifiers have largely focused on characterizing the mechanisms through which transcriptional control is programmed. Nucleosome positioning is one critical aspect to how transcriptional control is achieved. Chromatin-remodeling complexes target the histone C-terminal locus, which harbors many histone-histone and histone-DNA sites of association ([Lusser and Kadonaga, 2003](#)). Another critical aspect of how transcriptional control occurs, which is also dependent on chromatin modifying complexes is dependent on the targeting of the N-terminal tails of histones, which protrude out from the nucleosome core particle. The post-translational modification of the numerous target residues comprising histone N-terminal tails provides an added level of complexity and specificity to how transcriptional control can be programmed.

Table 2: Conservation and distribution of histone variants

Family	Variant/species	Conservation	Distribution
H3	H3 (canonical) / ubiquitous	<i>Sc, Sp</i> : H3 <i>Dm, Xl</i> : H3.2 <i>Mm, Hs</i> : H3.1 & H3.2	Global
	H3.3 / metazoan	<i>Dm, Xl, Mm, Hs</i> : H3.3	Promoters and active gene bodies, gene regulatory elements. <i>Mm</i> : telomeres, meiotic XY body. <i>Mm, Hs</i> : centromeres. <i>Dm, Mm</i> : paternal chromatin at fertilization.
	CenH3 / ubiquitous	<i>Sc</i> : Cse4 <i>Sp</i> : Cnp1 <i>Dm</i> : CID <i>Xl, Mm, Hs</i> : CENP-A	Centromeres. <i>Sc</i> : regions with high histone turnover, tRNA genes. <i>Hs</i> : DNA breaks
	H3t / mammals	<i>Mm, Hs</i> : H3t	ND (sperm) Nucleolus (somatic cells)
	H3.X/Y / primates	<i>Hs</i> : H3.X and H3.Y	Euchromatin
	H3.5 / hominids	<i>Hs</i> : H3.5	Testis-specific, euchromatin
H4	H4 (canonical) / ubiquitous	H4	Global
H2A	H2A (canonical) / ubiquitous	H2A	Global
	H2A.X / metazoan	<i>Dm</i> : H2Av <i>Xl, Mm, Hs</i> : H2A.X	Global
	H2AZ / ubiquitous	<i>Sc</i> : Htz1 <i>Sp</i> : Pht1 <i>Dm</i> : H2Av <i>Xl</i> : H2A.ZI <i>Mm, Hs</i> : H2AZ1 & H2AZ2	Promoters and the body of active and inducible genes, gene regulatory elements, nucleolus. <i>Sc, Sp</i> : subtelomeric regions. <i>Sp, Dm, Mm, Hs</i> : centromeres. <i>Mm</i> : meiotic XY body
	Macro H2A1,2 / amniotes	<i>Gg</i> : mH2A.1 and mH2A.2 <i>Mm, Hs</i> : mH2A.1-1, mH2A.1-2 & mH2A.2	Inactive X-chromosome, promoters of imprinted genes, promoters of inducible developmental genes, telomeres, centromeres, nucleolus, meiotic XY body
	H2AL1, L2 / rodent	<i>Mm</i> : H2AL1 & H2AL2	Centromeres (sperm)
	H2ABbd / mammals	<i>Mm, Hs</i> : H2ABbd	Euchromatin
H2B	H2B (canonical) / ubiquitous TSH2B / mammals	H2B <i>Mm, Hs</i> : TSH2B	Global
	H2BFWT / mammals	<i>Ms</i> : H2BL1 <i>Hs</i> : H2BWT	Telomeres (sperm)

ND, not determined; *Sc*, *S. cerevisiae*; *Sp*, *S. pombe*; *Dm*, *D. melanogaster*; *Xl*, *X. laevis*; *Gg*, *G. gallus*; *Mm*, *M. musculus*; *Hs*, *H. sapiens*. Table adapted from ([Boyarchuk et al., 2011](#)).

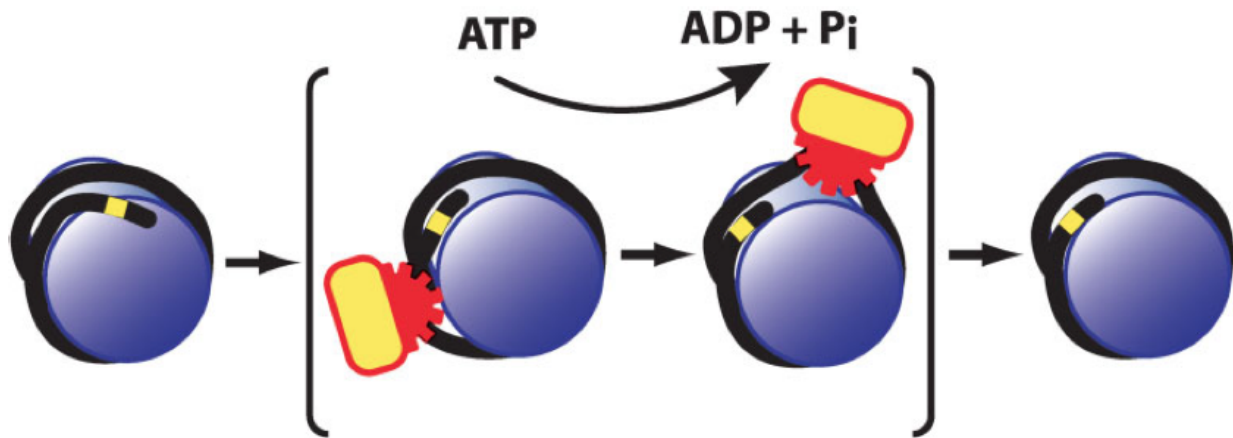


Figure 9. DNA translocation model for nucleosome remodeling.

A chromatin-remodeling complex possessing an ATP-dependent DNA-translocating enzyme disrupting the association of histones and DNA. Following the passage of the remodeling complex, histones and DNA re-associate into a canonical nucleosome located at a position shifted relative to the DNA template. ([Lusser and Kadonaga, 2003](#))

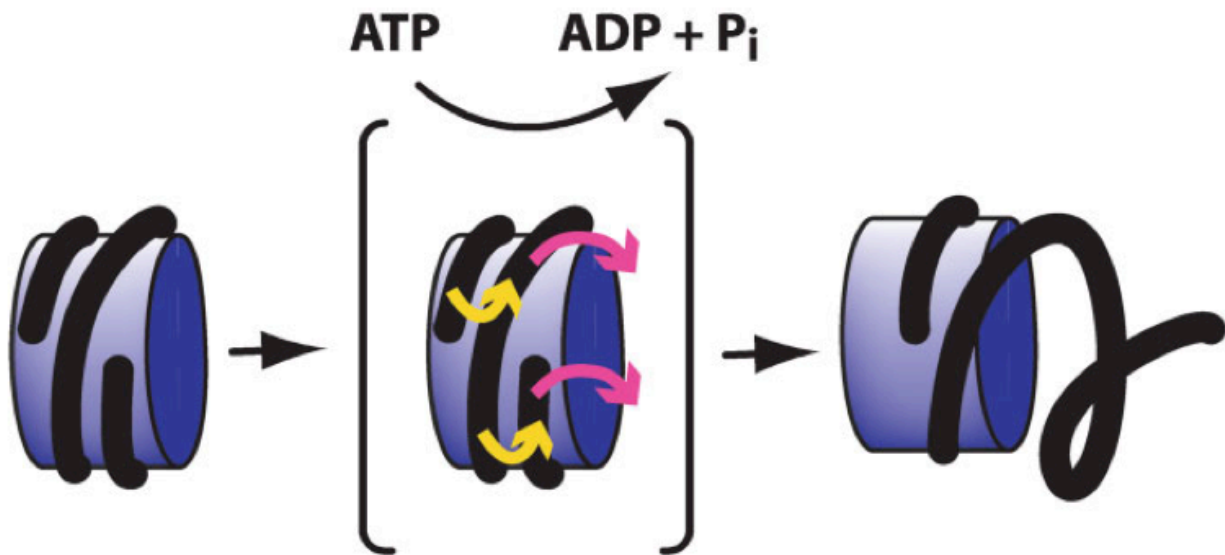


Figure 10. Lateral cross-transfer model for nucleosome remodeling.

The chromatin-remodeling complex catalyzes the rearrangement of one superhelical turn of nucleosomal DNA to the adjacent track on the histone octamer while the other superhelical turn of DNA is displaced from the nucleosome. ([Lusser and Kadonaga, 2003](#))

1.6 Histone Post-Translational Modifications

The N-terminal histone domain (tail) of core histones are less structured than C-terminal domains and are not essential for maintaining the integrity of nucleosome core particles ([Ausio et al., 1989](#); [Whitlock and Simpson, 1977](#)). Histone tails are thought to make secondary contacts with DNA and adjacent histones ([Luger et al., 1997](#)), thereby regulating or promoting the accessibility of the underlying genome. Covalent post-translational modifications (PTMs) to histone N-terminal tails underly the principal mechanism linking histone tail residues to transcriptional control. Numerous residues of the N-terminal tail of histones can undergo modification. Indeed a vast majority of PTMs occurring on histones takes place on N-terminal tail residues, whereas only a few globular core domain residues act as substrates for covalent modification ([Basu et al., 2009](#); [Latham and Dent, 2007](#)). The most common residues targeted for modification are lysine, serine, arginine, and threonine. Lysine residues undergo acetylation, methylation, ADP-ribosylation, ubiquitination, and even sumoylation. Serine and threonine residues undergo phosphorylation. Arginine residues are targeted for methylation (Fig. 11). Two models have been proposed to describe how histone modifications are associated to transcriptional control.

The first model suggests that a modification of histones influences chromatin states by modifying the charge of specific histone residues, leading to a change in steric interactions with DNA ([Shahbazian and Grunstein, 2007](#)). Steric interactions caused by histone modifications regulate the association of core histone particles with DNA. The addition of a modification, like an acetyl group to a lysine residue, effectively neutralizes the charge on lysine reducing its interaction with the negatively charged DNA. Phosphorylation confers a negative charge to serine residues, provoking a looser association with DNA. These histone modifications change the charge of the N-terminal tails, but whether they are sufficient alone to reverse transcriptional silencing through the modification of chromatin states remains unclear ([van Steensel, 2011](#)). Histone modifications do not prevent DNase I from accessing and cutting DNA ([Weintraub and Groudine, 1976](#)), nor do they prevent DNA methylation by the protein, DNA adenine methyltransferase ([Gottschling, 1992](#); [Kladde and Simpson, 1994](#); [Singh and Klar, 1992](#); [Wines et al., 1996](#)). Thus, it is difficult to conceive that histone modifications modifying chromatin states might control transcription if indeed factors and complexes promoting

transcription can indeed access DNA, even at regions of heterochromatin considered to be “closed” ([van Steensel, 2011](#)).

A second model proposes that histone modifications influence chromatin by providing binding platforms for transcription factor complex or repressor complex. The recruitment of multiprotein complexes to modified histone tail platforms is believed to be critical to control transcription. Repressor protein complexes cooperatively occupy and hinder transcriptional machinery from gaining access to DNA in a dense space. In the absence of any modification, histone tails exhibit a tight compaction with DNA. The specificity in the targeting of histone residues by histone modifiers is hypothesized to be dependent on both DNA sequence and pre-existing histone modifications. Specific DNA sequences are targeted by transcription factors, which complex with histone modifiers like histone acetyltransferases, and specify the nucleosomes that are to be modified. Accessory domains of histone-modifying enzymes called “readers” ([Gardner et al., 2011](#)) possess the unique function of recognizing and binding directly to modified histones, either free or bound to chromatin (Fig. 12). Histone-modifiers can also target their substrates by protein-protein interactions with other readers, in turn conferring specificity for substrates. This latter possibility has the added ability of integrating different histone modifications, in order to create specific patterns of histone modifications in a concerted and sequential order.

Eukaryotes have evolved a large array of tools for controlling the recruitment of histone modifiers to various histone substrates. The possibility for a histone modifier to target a specific site on histone tails as a result of the presence of a pre-existing modification on histones suggests that there is a complex interconnection between histone modifications. The patterns of how various histone modifications occur and how histone modifiers govern them is a major field of research in chromatin biology. The aim of such efforts is to decipher the “histone code” wherein histone modification patterns determine biological function ([Strahl and Allis, 2000](#)). Three major principles have emerged over the past ten years, building on the histone code hypothesis: 1) interactions between histone modifications are not limited to a single histone tail; 2) a single mark can recruit more than one chromatin-modifying protein; and 3) proteins acting alone or in the context of a macromolecular complex can contain multiple domains to facilitate binding to chromatin (Fig. 13).

Reader domains include: bromodomains, chromodomains, WD40 repeats, Tudor domains, and PHD fingers, which are all chromatin-binding domains that contribute to the recruitment of histone modifiers to chromatin (Table 3). Bromodomains confer the ability of proteins to be recruited based on its recognition and binding to an acetylated lysine residue. Chromodomains bind to methylated lysines and are present in a large number of enzymes acetylating neighboring lysine residues, suggesting that histone modifications can occur in various combinations.

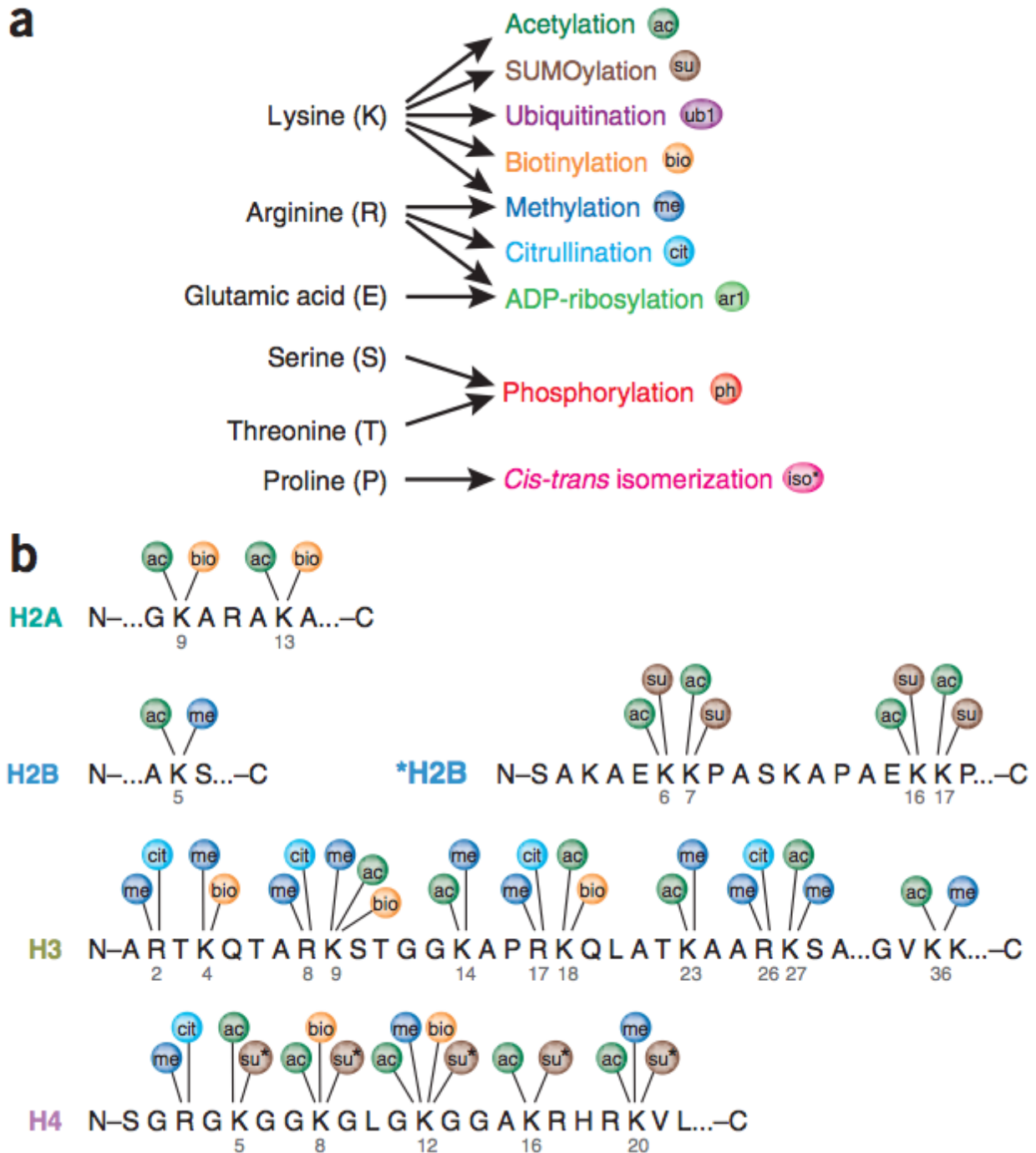


Figure 11. Histone modifications

(A) Known post-translational modifications and the amino acid residues they modify. (B) Residues that can undergo several different forms of post-translational modification or cross-talk *in situ*. Each modification inhibits subsequent modification. Histone amino acid sequence is from humans unless otherwise indicated; asterisk indicates that either the histone amino acid sequence or the modification is from *S. cerevisiae*. ac = acetylation; bio = biotinylation; cit = citrullination; me = methylation; su = SUMOylation. ([Latham and Dent, 2007](#))

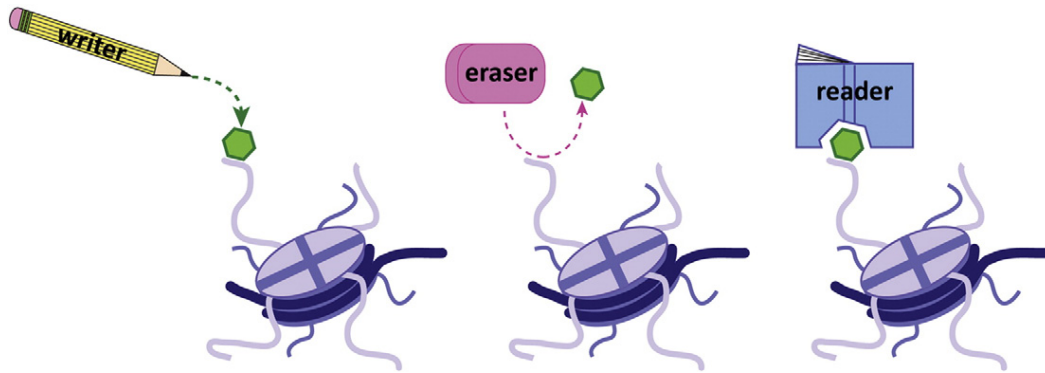


Figure 12. A toolkit for modifying the chromatin template

Schematic illustrating the concept that writers place PTMs on histone proteins (left), erasers remove such modifications from histone proteins (middle), and readers function to interpret these covalent modifications (right) to mediate diverse downstream processes. While these concepts are depicted on chromatin-bound histones ([Gardner et al., 2011](#))

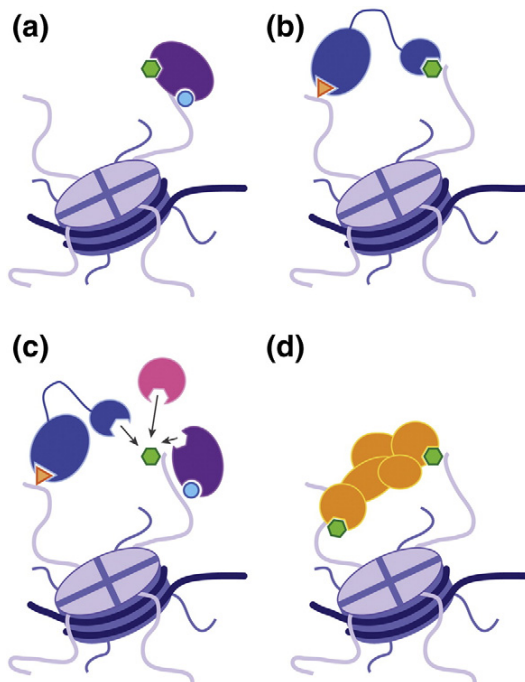









Figure 13. Mechanisms of histone-recognition modules

Binding of specialized domains to histone PTMs can occur in cis, where contact is made to a series of modifications on the same histone tail (a), or in trans, where contacts are made to distinct modifications across histone tails (b). Often, a single modification can serve as a docking site for more than one protein, in which secondary signals (e.g., other PTMs) may serve to dictate which protein is recruited to the specific mark (c). Proteins acting alone (a and b) or in the context of a macromolecular complex (d) can harbor multiple domains capable of facilitating chromatin recognition and binding. ([Gardner et al., 2011](#))

Table 3. Chromatin-binding domains

Domain	Structure	Proposed role	Complexes	Proteins
Bromo		Binds acetylated lysine	SAGA	Gcn5, Spt7
			NuA3	Yta7
Chromo		Binds methylated lysine	SAGA	Chd1
			NuA4	Esa1, Eaf3
Tudor		Binds methylated lysine and arginine	SAGA	Sgf29
SANT		Predicted to bind to histone tails	SAGA	Ada2
			NuA4	Eaf1, Eaf2
SWIRM		Predicted to regulate transcription through protein-protein interactions	SAGA	Ada2
WD40		Binds methylated lysine	SAGA	Spt8
			HatB	Hat2
			Elongator	Elp1, Elp2
PHD		Binds methylated lysine	NuA4	Yng2
			NuA3	Yng1, Nto1
YEATS	Unknown	Predicted to regulate transcription through protein-protein interactions	NuA4	Yaf9
			NuA3	Taf14
			SAS	Sas5
EPC-N	Unknown	Predicted to bind methylated lysine	NuA3	Nto1
			NuA4	Eaf6

1.7 Histone modifying enzymes

Histone modifications are catalyzed by histone modifying enzymes, which can either add or remove a mark (Fig. 10). Histone modifiers catalyze the addition of a specific modification to specific histone residues. The addition of a modification like a methyl group occurs by the activity of a methyltransferase. Adding a phospho-group is dependent on the activity of a kinase while acetyl groups are added by acetyltransferases. The removal of a methyl group occurs by a demethylase, removing a phospho-group by phosphatases, and acetyl-groups by deacetylases (HDACs). Histone modifications are dependent on the availability of coenzymes, which select for, 1) the types of modifications that can be made to histones and 2) for the class of histone modifiers to cause a modification. The source of acetyl marks is provided by Acetyl-Coenzyme A while S-Adenosyl methionine (SAM) serves as a methyl donor. Histone modifiers may also depend on metal ions as cofactors, as do the histone deacetylases or demethylases. For example, if zinc is available, then histone deacetylases of classes I, II, or IV may cause deacetylation. Otherwise, if NAD⁺ is made available, class III HDACs may catalyze a histone modification.

1.8 Biological impact of histone modifications

Histone modifications play an important role for nucleosome assembly as well as the organization of chromatin structure ([Han and Grunstein, 1988](#)). In yeast, following the production of histones, H4 lysine 5 and 12 ([Sobel et al., 1995](#)) and H3K56 undergo transient acetylation ([Rando and Chang, 2009](#)). These modifications to newly produced histones occur in the cytoplasm, before their relocalization to the nucleus and deposition on DNA. The chaperone, CAF1, is necessary for facilitating modifications to newly synthesized histones by interacting with histone modifiers and subsequently causing nucleosome assembly ([Das et al., 2009](#); [Probst et al., 2009](#)). H3K56 lies within a region of H3 that binds DNA at the entry and exit points of the nucleosome core particle. H3K56 in yeast undergoes deacetylation upon deposition of nucleosomes onto DNA, suggesting that the transient acetylation of H3K56 distinguishes resident histones from newly synthesized histones not yet deposited on chromatin ([Xu et al., 2005](#)). It is possible that acetylation of this residue perturbs electrostatic interactions between the histone and DNA such that H3K56 deacetylation promotes histone-DNA interactions. In higher eukaryotes, like mammals, there are more distinct histone modifications that can dictate

specific cell functions like nucleosome assembly, placement, removal, or reading of other histone modifications ([Rando and Chang, 2009](#)).

At a structural level, histone modifications are correlated with defining chromatin territories. Chromatin states are found in stretches known as territories. The process of maintaining or transforming a chromatin state is a highly controlled process. One example is the mechanism of heterochromatin spreading, which is the process of silencing transcriptional activity. Heterochromatin manifests by the concentration of nucleosomes along a chromatin territory, resulting in a genomic region where transcriptional machinery cannot associate. The mechanistic basis for understanding how certain genomic regions change chromatin states has been well characterized at the level of histone modifications in yeast and less in mammals.

In yeast, histone deacetylation correlates with heterochromatin spreading through the activity of HDACs causing a positive feedback loop of deacetylation and deacetylase recruitment to neighboring nucleosomes. The process of heterochromatin spreading in yeast is initiated by the binding to hypoacetylated H3 and H4 tails, of heterochromatin-spreading factors, called silent information regulators 3 and 4 (Sir3 and Sir4) ([Carmen et al., 2002](#); [Hecht et al., 1995](#)). The recruitment of Sir3 and Sir4 promotes the binding of Sir2, the founding member of the sirtuins class of deacetylases. Sir2 targets H3 K9 and 14 as well as H4 K16 and it seems that H4K16 deacetylation is crucial for Sir2 promoting silencing ([Cubizolles et al., 2006](#); [Imai et al., 2000a](#); [Johnson et al., 1992](#); [Thompson et al., 1994](#)). In parallel with H4K16 deacetylation, H3K9 methylation leads to H3K14 deacetylation ([Grewal and Moazed, 2003](#); [Suka et al., 2002](#)), suggesting that nucleosome compaction occurs by the cooperative deacetylation of H3 and H4. Deacetylated H4K16 is in turn bound by Sir3, which allows the recruitment of Sir proteins that will target neighboring nucleosomes ([Liou et al., 2005](#)).

A second example of a chromatin territory depending on histone modifications is euchromatin formation, which is characterized by H3K4 methylation and correlates with transcriptional activation in humans ([Noma et al., 2001](#)). H3S10 phosphorylation also marks transcriptional activation and the edge of euchromatic regions, known as heterochromatin boundaries ([Wang et al., 2011](#)). Together, these examples in both yeast and humans represent the various ways in which histone modifications play an important role in defining the state of chromatin and subsequently transcriptional control.

1.9 Impact of histone acetylation

Histone acetylation *in vivo* was first reported in 1964 ([Allfrey et al., 1964](#)). Since the first observations of histone acetylation, one major goal has been to understand its impact on transcriptional control, as initial studies demonstrated this modifications correlated with reduced transcription ([Allfrey and Mirsky, 1964](#)). Histone tails have a large number of lysine residues, which act as targets for histone acetyltransferases (HATs) and histone deacetylases (HDACs). Both hyper- and hypo-acetylation of individual lysines are associated with transcriptional regulation, enabling the establishment of unique patterns defining transcriptional state. Histone acetylation can affect transcription by causing a conformational change in the nucleosome core particle, allowing a greater accessibility to DNA. The acetylation of histone tails is proposed to loosen the association of the N-terminal tails around the nucleosome core particle, which results in a torsional strain opening the core particle and DNA (Fig. 14).

The acetylation by HATs of core histone N-terminal tails activates transcription. Examples of HATs are SAGA and SAGA-like HAT complexes, which acetylate both H2B and H3 at transcriptionally active genomic regions ([Kuo et al., 2000](#); [Suka et al., 2002](#)). Studies in yeast using chromatin immunoprecipitation of histone modifications mapped across the genome revealed that transcriptionally active gene regions correlate with one of two major groups of commonly occurring histone acetyl modifications. The first group of closely associated marks in yeast are: H2A K7, H3K9, K14, and K18, and H4K5 and K12, and the second group of closely associated marks are: H2B K16 and H4K8 and K16 ([Liu et al., 2005](#)). These groups of histone modifications can define distinct sets of activated and repressed genes. H3K18 and H4K16 can each correlate with transcriptional activation, however in a previous study they had also been identified to be the most anti-correlative marks ([Kurdistani et al., 2004](#)). These studies suggest that histone acetyl modifications, like H3K18 and H4K16, can both occur in an anti-correlative manner on the same nucleosomes and cooperatively affect the transcriptional outcome through their association with transcriptional modulators ([Kurdistani et al., 2004](#)), or they can occur independently of one another on distinct nucleosomes and separately affect transcriptional activity.

Gene activation can be controlled by HATs in a time-dependent ([Barbaric et al., 2001](#)). The absence of an acetyltransferase can merely delay gene activation or block its activity entirely ([Gregory et al., 1999](#); [Shahbazian and Grunstein, 2007](#)). The effect of acetylation on transcription is distinct depending on whether it occurs globally or locally along the genome. For example, global acetylation can facilitate transcription and increase the level of basal transcription ([Imoberdorf et al., 2006](#)). The local activation of gene expression through the targeted acetylation of histones in transcriptionally active regions is another way in which histone acetylation can facilitate gene activation. However, the mechanisms governing local and global acetylation are different. Readers and chromatin-modifying complexes recruit HATs causing global acetylation to chromatin. Specific transcription factors or repressors recruit HATs causing acetylation at specific genomic regions ([Shahbazian and Grunstein, 2007](#)). The acetyltransferase Gcn5, which is recruited to UAS elements, acetylates H3 tail lysines at promoters and the 5' end of coding regions ([Allard et al., 1999](#); [Kuo et al., 1998](#); [Liu et al., 2005](#); [Roh et al., 2004](#)).

Transcriptional regulation aside, histone acetylation is also implicated in an epigenetic program during replication wherein newly-synthesized chromatin can be distinguished from the old template strand by the histone modifications marking resident nucleosomes of each DNA copy ([Shahbazian and Grunstein, 2007](#)). The distinct histone modifications associated with newly synthesized DNA or template can be used to segregate chromosomes. In stem cells, this mechanism is hypothesized to dictate whether a newly divided daughter cell is to remain a stem cell or to differentiate ([Rocheteau et al.](#)). Yet other transcription-independent processes are dependent on histone acetylation, like X-chromosome inactivation, DNA damage repair, and DNA recombination ([Turner, 1993](#); [Yang and Seto, 2008](#)).

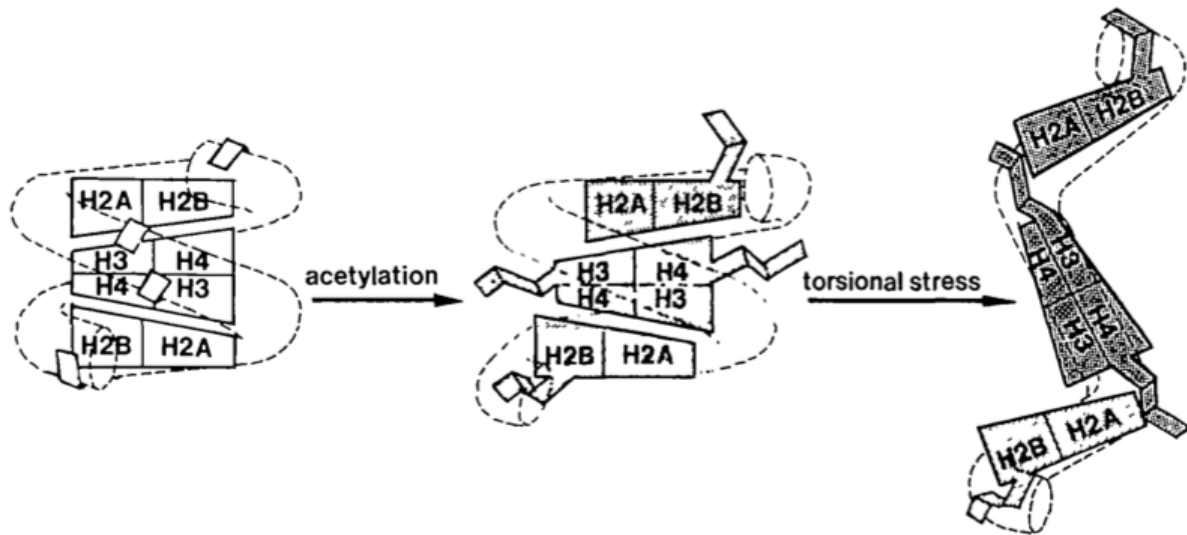


Figure 14. Unfolding of the nucleosome core particle by histone acetylation

Upon acetylation, the nucleosome core particle remains essentially in its folded native (unshaded particles) conformation. Yet, it adopts a slightly looser conformation (shaded particles) probably arising from the release of the N-terminal regions (tails) of the histone octamer. In the presence of torsional stress these particles may reversibly unfold into lexosome-like structures. It is possible that during this process some rearrangement of the core histones takes place. ([Ausio, 1992](#))

1.10 Classification and targeting of acetyltransferases

HATs are classified into two large groups distinguished by the sequence of their catalytic domains and accessory binding domains ([Sternier and Berger, 2000](#)). However, this two-group classification of HATs does not encompass all HATs, since some have distinct HAT catalytic domains and accessory binding domains.

Gcn5 is the founding member of the first group of HATs, the Gcn5 N-acetyltransferases (GNATs), which includes Gcn5, PCAF, Elp3, Hat1, Hpa2 and Nut1 (Table 4) ([Kimura et al., 2005](#)). GNATs are characterized by four highly conserved catalytic domain motifs (A-D) for which motif A contains an Arg/Gln-X-X-Gly-X-Gly/Ala sequence that is important for acetyl-CoA recognition and binding ([Roth et al., 2001](#)). The GNAT family of HATs target lysine residues of histone H2B, H3, and H4 ([Lee and Workman, 2007](#)). The second group includes PCAF, a p300/CBP(CREB-binding protein)-associated factor and Taf1 are two other major HAT families, which are nuclear residents. The nuclear HATs (GNATs and p300/CBP) possess bromodomains, which bind to acetyl-lysine residues ([Dhalluin et al., 1999a, b](#)) enhancing transcriptional activation by propagating the acetylation of nucleosomes across a specific region of the genome defined by the targeting with TFs. The Gcn5 bromodomain also is essential for the retention of the multi-subunit nuclear HAT complex, SAGA (Spt-Ada-Gcn5-acetyltransferase), on acetylated promoter nucleosomes ([Hassan et al., 2002](#)).

The second group of acetyltransferases is Morf, Ybf2, Sas2 and Tip60 comprise the founding members of the MYST family of HATs ([Sternier and Berger, 2000](#)). MYST family members are typically characterized by the presence of zinc fingers and chromodomains and they are found to acetylate lysine residues on histone H2A, H3, and H4. The chromodomain of Eaf3, a protein subunit of the HAT complex, NuA4, is essential for the binding to methylated H3K36 (Table 4) ([Joshi and Struhl, 2005](#)). These studies highlight the impact of *readers* in targeting the activity of HATs based on pre-existing acetyl or methyl marks of histones resulting in enhanced transcriptional activation.

Some HATs, like p300, have the added function of acetylating non-histone proteins and studies may reveal that non-histone proteins are more frequently targeted than histones. The HDAC, SIRT2, is one major target of p300 ([Black et al., 2008](#)). SIRT2 acetylation by p300 attenuates the deacetylase activity of this HDAC reducing its ability to

deacetylate histones and thereby raising the overall acetyl-level of histones ([Han et al., 2008](#)).

Table 4. Characteristics of HAT families

HAT group	HAT (and complexes associated with it)	Histones acetylated by recombinant HAT	Histones acetylated by HAT complex	Interactions with other HATs
GNAT	Gcn5 (SAGA, ADA, A2)	H3 \gg H4	H3, H2B	p300; CBP
	PCAF (PCAF)	H3 \gg H4	H3, H4	p300; CBP
	Hat1 (HatB)	H4 \gg H2A	H4, H2A ^a	
	Elp3 (elongator)	H2A, H2B, H3, H4		
	Hpa2	H3 > H4		
MYST	Esa1 (NuA4)	H4 \gg H3, H2A	H2A, H4	
	MOF (MSL)	H4 \gg H3, H2A	H4	
	Sas2	Unknown		
	Sas3 (NuA3)	Unknown	H3	
	MORF	H4 > H3		
	Tip60	H4 \gg H3, H2A		
	Hbo1 (ORC)		H3, H4	
p300/CBP	p300	H2A, H2B, H3, H4		PCAF; GCN5
	CBP	H2A, H2B, H3, H4		PCAF; GCN5
Basal transcription factors	TAFII250 (TFIID)	H3 \gg H2A		
	TFIIIC ^b		H3, H4 > H2A	
	Nut1 (mediator)		H3 \gg H4	
Nuclear receptor cofactors	ACTR ^c	H3 > H4		p300; CBP; PCAF
	SRC1	H3 > H4		p300; CBP; PCAF

^aH2A acetylation reported for human Hat1.

^bTFIIIC may contain up to three polypeptides with HAT activity ([Hsieh et al., 1999](#); [Kundu et al., 1999](#)).

^cAlso known as RAC3, AIB1, PCIP, and TRAM ([Rowan et al., 2000](#)).

1.11 Classification and targeting of histone deacetylases

The eighteen human deacetylases are divided into four major classes (Table 5) based on their similarity to homologs in *S. cerevisiae*. Class I HDACs are similar to the yeast transcriptional repressor Rpd3, class II HDACs to HDA1, class III to the silencing information regulator 2 (SIR2), and class IV is comprised of only one member, HDAC11, which is sometimes grouped into the Rpd3 class I HDACs. The features of each of these HDAC classes are distinct based on catalytic activity and structure.

Class I HDACs (HDAC1, 2, 3, & 8) share a compact structure and are predominantly nuclear proteins expressed in most tissues and cell lines ([Fischle et al., 2001](#)). Class IV, HDAC11, shares catalytic similarities to HDAC classes I and II. However, HDAC11 resembles the prokaryotic AcuC protein from *Bacillus subtilis* both structurally and in size, which although is believed to have evolved to give rise to class I HDACs ([Gao et al., 2002](#)). Class II HDACs are subdivided into two sub-classes based on sequence homology and domain organization, IIa (HDAC4, 5, 7, and 9 and its splice variant MITR) and IIb (HDAC6 and HDAC10). Sub-class IIa contains a highly conserved C-terminal catalytic domain homologous to HDA1. Sub-class IIb HDAC members are characterized by duplicated HDAC domains and some tissue specific gene expression ([Verdel and Khochbin, 1999](#); [Verdin et al., 2003](#)). HDAC classes I, II, and IV exhibit structural and domain organization that distinguish them, they all share some homology in their catalytic domain such that Zinc is used as a common catalytic cofactor.

In contrast, HDAC class III, the sirtuins, are catalytically distinct by their use of NAD⁺ as a cofactor, linking it to integral metabolic processes responsible for cell health and lifespan ([Houtkooper and Auwerx](#); [Houtkooper et al., 2012](#); [Imai et al., 2000a](#)). Seven mammalian sirtuins have to date been identified ([Frye, 1999](#)). The functions of sirtuins have been of exceptional interest since studies reported that they regulate mating in yeast by repressing MAT genes and also contribute to aging ([Imai et al., 2000b](#); [Michan and Sinclair, 2007](#)).

A sub-classification of mammalian sirtuins (classes I-IV) has been put forward based on phylogenetic analyses of core domains from different eukaryotic and prokaryotic genes. Class I sirtuins comprise mammalian SIRT1, 2, and 3, which share sequence similarity to Sir2 and Hst1 from *S. cerevisiae*. Class II represents SIRT4 and sirtuins from bacteria, *C. elegans*, nematodes, etc. Class III represents SIRT5, which is

widely spread across prokaryotes (bacteria and archaea). Class IV sirtuins are represented in mammals by SIRT6 and SIRT7 and are broadly distributed in metazoans, plants and vertebrates ([Michan and Sinclair, 2007](#)).

Among the mammalian sirtuins, SIRT1 and SIRT2 exhibit both cytoplasmic and nuclear localization, while SIRT6 and SIRT7 are exclusively reported in the nucleus. SIRT3, SIRT4, and SIRT5 are mitochondrial sirtuins and have an essential role in the metabolic cell processes. To date, Sirtuins 1, 2, 3, 5, and 7 have been observed to possess a deacetylase activity ([Michan and Sinclair, 2007](#)). Deacetylation by sirtuins occurs by transferring an acetyl group from Acetyl-Coenzyme A to a histone lysine residue, with the help of NAD⁺ as a key coenzyme (Fig. 15). Furthermore, Sirtuins 2, 4, and 6 have been observed to possess ADP-ribosyltransferase activity ([Frye, 1999](#); [Houtkooper et al., 2012](#)). SIRT5 has the added ability to demalonylate and desuccinylate mitochondrial targets ([Du et al.; Nakagawa et al., 2009](#); [Peng et al.](#)). Taken together, sirtuins possess important biochemical activities, which regulate biological functions through regulating cellular metabolism and transcriptional activity.

Table 5. Classification of mammalian HDACs

HDAC Classification				
Zinc*				NAD ⁺ *
I	IIa	IIb	IV	III
HDAC1	HDAC4	HDAC6	HDAC11	SIRT1
HDAC2	HDAC5	HDAC10		SIRT2
HDAC3	HDAC7			SIRT3
HDAC8	HDAC9			SIRT4
				SIRT5
				SIRT6
				SIRT7

* = Enzymatic cofactor

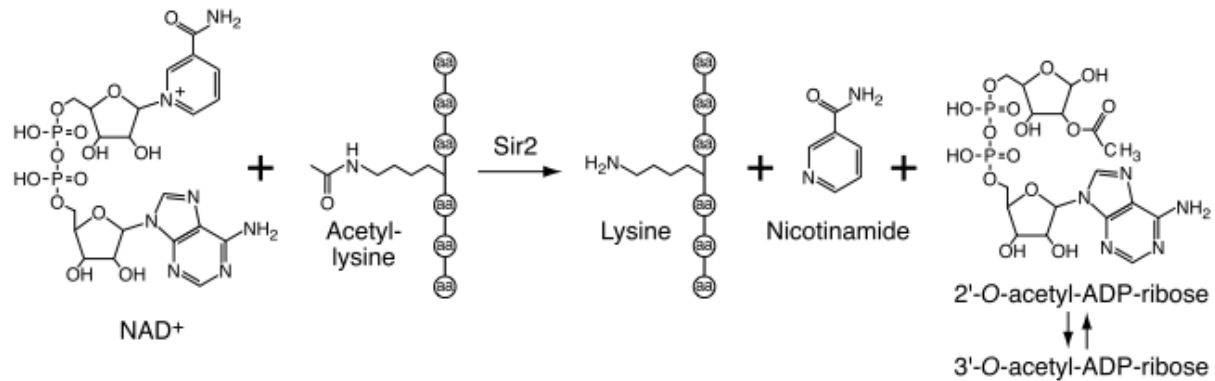


Figure 15. The NAD⁺ -dependent deacetylation reaction catalyzed by Sir2p ([Rusche et al., 2003](#)).

In conclusion, transcriptional control in eukaryotes is dependent on many principles that build on the basic concepts described by Jacob and Monod in the operon model in prokaryotes. The principles of eukaryotic transcriptional control are centered around the production of histones, assembly of nucleosomes, nucleosomal positioning, and retention at specific genomic regions. Underlying these functions of nucleosomes are histone modifications, which have been revealed to represent the state of transcription at specific genomic loci. One such important histone modification, acetylation, has been associated with transcriptional control for 60-years. Characterizing histone acetylation and deacetylation has the potential to shine light on the numerous programs encoded in cells controlling transcription.

Section 2:

2.1 Host-Microbe Interactions

Humans act as hosts to countless numbers of microbes. The host's ability to maintain homeostasis in health is dependent on a host's ability to recognize pathogenic microbes and react by mounting an immune response aimed at eliminating the microbe and/or damaged tissue. The host-microbe interaction begins with the association of factors of microbial origin like microbial-associated molecular patterns (MAMPs) to host sensors ([Ausubel, 2005](#)). These sensors of the host are referred to as pattern-recognition receptors (PRRs) ([Janeway, 1989](#)). The interaction of MAMPs and PRRs can elicit an innate immune response. The development of the host immune system depends on the presentation of MAMPs such that animals, which developed in a germ free context, mount a dysregulated immune response when presented with MAMPs in adulthood ([Vance et al., 2009](#)). Subsequently, the activation of an immune response by pathogen-associated molecular patterns (PAMPs) is believed to result in the host recognizing that a microbe is "non-self" ([Medzhitov and Janeway, 2002](#)). However, whether MAMPs or PAMPs activate an immune response, it is believed that the host is inevitably responding to a "danger" signal provoking tissue damage ([Matzinger, 2002](#)).

Host cells express PRRs both on the cell surface and in the cell cytoplasm. In mammals and insects, toll-like receptors (TLRs) function directly or indirectly as PRRs for microbe-associated molecules on the cell surface ([Beutler and Rehli, 2002](#); [Brennan and Anderson, 2004](#); [Hoffmann and Reichhart, 2002](#); [Janeway and Medzhitov, 2002](#); [Medzhitov and Janeway, 2000](#); [Royet, 2004](#)). The intracytosolic domain of TLRs was noted to have homology with the cytoplasmic domain of human interleukin 1 (IL-1) ([Gay and Keith, 1991](#)). The activation of TLR signaling induces the expression of NF- κ B-dependent genes encoding antimicrobial peptides ([Medzhitov et al., 1997](#)). TLRs target a range of microbial ligands, including lipopolysaccharide (TLR4), lipoproteins (TLR2), flagellin (TLR5), unmethylated CpG motifs in DNA (TLR9), double-stranded RNA (TLR3), and single-stranded RNA (TLR7 and TLR8) ([Akira et al., 2001](#); [Kawai and Akira, 2005](#)). TLR recognition of PAMPs leads to the production of reactive oxygen species (ROS), reactive nitrogen species (RNS), and expression of antimicrobial peptides (AMPs), all of which play a role in antimicrobial mechanisms. Nucleotide-binding oligomerization domain receptors (NOD-like receptors) act as intracellular PRRs.

Each infectious process occurring by a host-pathogen interaction can be interpreted as a “pattern of pathogenesis” ([Vance et al., 2009](#)), for which diverse species of bacteria use common host encoded mechanisms to drive infection. Microbial factors, which are recognized by PRRs are numerous and variable in composition and origin. Extracellular components of bacteria are a common pattern recognized by host sensors. For example, the host PRR, TLR5, recognizes bacterial flagellin as an extracellular-derived ligand, to induce a pro-inflammatory response. Intracytosolic bacterial flagellin is recognized by factors leading to Caspase 1-dependent and inflammasome activation ([Vance et al., 2009](#)). Perhaps the most common process of detection of secreted factors, which are produced by both extracellular and intracellular pathogens. Another circumstance for which pathogens can be recognized is upon adherence to the host cell surface. Extracellular pathogens like virulent strains of *E. coli* as well as several invasive pathogens are dependent on adherence to the host surface. Binding to host receptors both promotes adherence, but in certain instances can also induce signaling cascades within the host. Invasive pathogens have the added ability to induce bacterial entry, either by the injection of virulence effector molecules into the host, or by inducing internalization through the activation of host receptors. In both cases, injected effectors and the induction of host receptors can induce a signal transduction pathway to reprogram host cellular functions, while also providing the opportunity for the host to sense danger ([Matzinger, 2002](#)) or the presence of foreign factors ([Medzhitov and Janeway, 2002](#)). Some invasive pathogens remain inside a vacuole where they are capable of growing and dividing, by controlling the identity and composition of the vacuole. However, the release of bacterial DNA in the vacuole can be sensed by TLR3 or TLR9 and activate an inflammatory response ([Vance et al., 2009](#)). Other pathogens, facultative intracellular pathogens, catalyze their escape. Gaining access to the cytosol is both a benefit for these pathogens to grow and replicate, however the intimate proximity with host cellular sensors provides the greatest possibility to recognition of pathogenesis and destruction. Intracytosolic bacterial DNA can also activate a pro-inflammatory response ([Mariathasan et al., 2006](#)).

2.2 Pathogenesis governing host-pathogen interactions

Host sensors detect bacteria, both innocuous and pathogenic forms, in numerous different ways. During infection, pathogens come in contact with the host both at the surface of the cell and some invasive pathogens can be sensed inside the cell. Pathogenesis by diverse groups of pathogens follows common strategies of infection ([Finlay and Falkow, 1997](#)). Common bacterial molecules contributing to pathogenesis and host sensing are: bacterial surface-associated or secreted products interacting with host surface receptors inducing signal transduction cascades or toxic stress, factors facilitating adherence, mechanisms of host cell internalization, growth within a vacuole or in the cytosol, and hijacking cytoskeletal function ([Vance et al., 2009](#)). Pathogens exist in two main types: extracellular and intracellular. Both may come in contact with the host cell, by binding host cell surface receptors. The intracellular pathogens have the added ability to enter the host cell. Some of those pathogens remain inside the internalized vacuole while others catalyze their escape. Intracytosolic bacteria grow and divide in the cytosol and can polymerize actin enabling them to propel themselves throughout the cytoplasm and into neighboring cells. Many of these processes are now being described as correlating with or directly associated to a reprogramming of the host through various processes among which is transcriptional control. Indeed, most processes previously described on a subcellular level to contribute to pathogenesis are now being rediscovered to play a role in causing a modification in the host transcriptome. This suggests that host programs during infection are integrated at the chromatin and DNA level. Uncovering how host-pathogen interactions results in the modulation of specific host transcriptional programs may provide critical insight about infection.

Extracellular factors:

Pathogens produce many extracellular components and secreted substances that are directly or indirectly toxic to host cells. The detection of these factors occurs through the binding of host cell receptors on the cell surface or in the intracytosolic space. Toxins can be detected by the sensing of cellular stress. There are generally two types of toxins: endotoxins and exotoxins. Endotoxins are non-proteinaceous substances that can cause damage to host tissue. The pro-inflammatory LPS, an endotoxin, comprises a major component of the Gram-negative cell wall ([Finlay and Falkow, 1997](#)). Mice, which are

mutants for the *Lps* gene, exhibit resistance to LPS shock, but are susceptible to infection with Gram-negative bacteria ([Poltorak et al., 1998](#)). Contrary to endotoxins, exotoxins are microbial proteins that usually harm cells by an enzymatic activity. Exotoxins play a major role in the onset of clinical features described for the pathogens that produce them. This is apparent as the addition of purified exotoxin from *Vibrio cholerae*, *Clostridium tetani*, or *Corynebacterium diphtheriae*, to cells largely mimics pathogenesis of infection. Many exotoxins are comprised of two-component systems, resembling A-B toxins. The B subunit mediates binding to host cell receptors and facilitates delivery to the host of the A subunit, a toxic enzyme. Among the types of toxins are (1) proteolytic toxins, cleaving proteins by their endoprotease activities, like botulinum and tetanus toxins; (2) pore forming toxins, whose prototype member is the *Escherichia coli* hemolysin (*hlyA*) among Gram-negatives, but not exclusive to them as *Streptococcus pyogenes* is an example of a Gram-positive pathogen expressing the pore-forming pH-sensitive, streptolysin O. The Gram-positive bacterium, *Streptococcus pyogenes*, uses the pore-forming toxin streptolysin O to create portals for delivering bacterial products to the host cytosol ([Madden et al., 2001](#)). The action of toxins to induce pro-inflammatory signaling or cause a cell stress response represent an important mechanism through which the host is induced to counter the presence of bacterial toxins.

Host cell surface adherence:

Adherence is an essential step of pathogenesis, which occurs by the action of various adhesins. Adhesion allows for extracellular pathogens to remain bound to the cell surface and induce the reprogramming of the host cell. Extracellular pathogens such as enterohemorrhagic *E. coli* (EHEC) or Enteropathogenic *E. coli* (EPEC) employ unique mechanisms of adherence to host cells ([Finlay and Falkow, 1997](#)). EHEC express surface molecules known as fimbriae (*E. coli* common pilus, ECP), which are pili-like factors promoting cell surface attachment. EPEC lack fimbriae, but they use bundle-forming pili ([Giron et al., 1991](#)) and an adhesin known as Intimin ([Jerse and Kaper, 1991](#)), to bind host intestinal cells. The amino acid sequence of Intimin is highly similar to those of the invasins of *Yersinia pseudotuberculosis* and *Y. enterocolitica*. However, unlike invasins of *Yersinia* species, which associate to the $\beta 1$ family of integrin receptors and induce uptake of bacteria, intimin is necessary, though not sufficient to cause invasion ([Van Nhieu and](#)

[Isberg, 1991](#); [Yu and Kaper, 1992](#)). Invasive pathogens can adhere to host cell surfaces in order to provoke bacterial entry into non-phagocytic cells. Pathogens are reported to have dozens of different expressed adhesins, all contributing in varying degrees to bacterial adhesion. Adhesins are divided into pili (fimbriae) and non-pilus adhesins (afimbrial adhesins). Apart from the role of adhesins in binding to the host cell surface by interacting with receptors, adherence can also occur with the extracellular matrix. The necessity for adherence is as important for extracellular pathogens as for the following step of infection of intracellular pathogens, invasion.

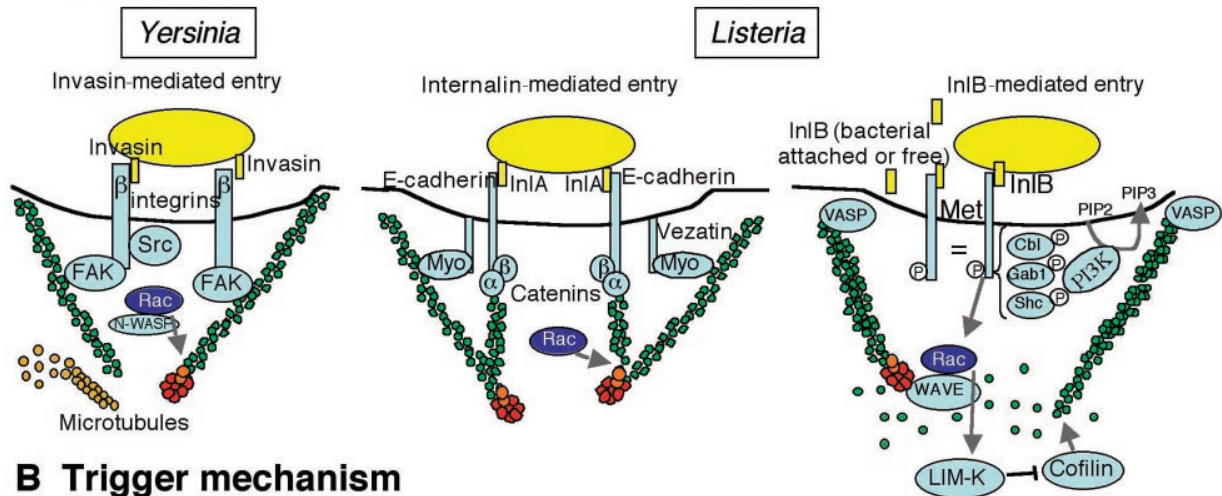
The binding to receptors at the host cell surface provides a major avenue through which to induce signal transduction cascades that will propagate a reprogramming of host cell functions through among other processes, transcriptional modulation. The activation of receptors like Tumor Necrosis Factor (TNF- α), Interferon (IFN- γ), or Toll-Like receptors (TLRs), all have been observed to result in host transcriptional modulation (Fig. 18). The result is a modulation of host immune response, innate and signaling to mount an adaptive immune response ([Cossart and Sansonetti, 2004](#)).

Bacterial internalization:

Among the pathogens that adhere to host cells, several are capable of inducing bacterial entry (Fig. 16). Two major mechanisms are employed by different sets of bacteria to facilitate entry into non-phagocytic cells. *Yersinia pseudotuberculosis* and *Listeria monocytogenes* induce entry through a process dubbed the zipper mechanism. The underlying mechanism for entry of these pathogens is the rearrangement of actin cytoskeletal components after (I) adhering to and activating transmembrane receptors, (II) forming an internalization cup, and (III) closing the vacuole ([Cossart and Sansonetti, 2004](#)). In contrast to the mechanism employed by *L. monocytogenes* and *Y. pseudotuberculosis*, *Shigella* and *Salmonella* employ a trigger mechanism of entry. Both *Shigella* and *Salmonella* express a secretion system apparatus, called the type III secretion system (TTSS), which plays an essential role in entry. Essential components of TTSS are the pore forming factors, SipB/C in *Salmonella* and IpaB/C in *Shigella* and allow for the creation of a continuum between bacterial and eukaryotic cytoplasm ([Finlay and Falkow, 1997](#); [Galan, 2001](#); [Sansonetti, 2001](#); [Young and Collier, 2007](#)). Effector molecules injected into the host facilitate actin cytoskeletal rearrangements, characterized by

membrane ruffling and culminating in the uptake of *Shigella* and *Salmonella* (Fig. 16). Some Gram-positive pathogens employ a secretion system in a functionally similar way as their Gram-negative cousins. Unlike pathogens entering non-phagocytic cells by the zipper or trigger mechanisms, *Mycobacterium tuberculosis* is taken up by macrophages, which are professional phagocytes. *M. tuberculosis* expresses the ESX-1 secretion system, an evolutionarily distinct secretion system, but delivers bacterial products to the host cytosol inducing entry ([Simeone et al., 2009](#)). In parallel with the various actin-cytoskeletal rearrangements that host cells undergo during internalization of invasive pathogens, signaling transduction cascades leading to the host nucleus allow for the host to sense pathogens by modulating transcription. It is not well known how host cells sense the secretion systems of pathogens, but two hypotheses consider the possibility that either cells recognize the PAMPs secreted through the injection apparatus, or by the physical damage associated with bacterial structures penetrating the cell membrane and the “sanctity of the cytosol” ([Lamkanfi and Dixit, 2009](#); [Shin and Cornelis, 2007](#); [Viboud and Bliska, 2005](#)).

A Zipper mechanism



B Trigger mechanism

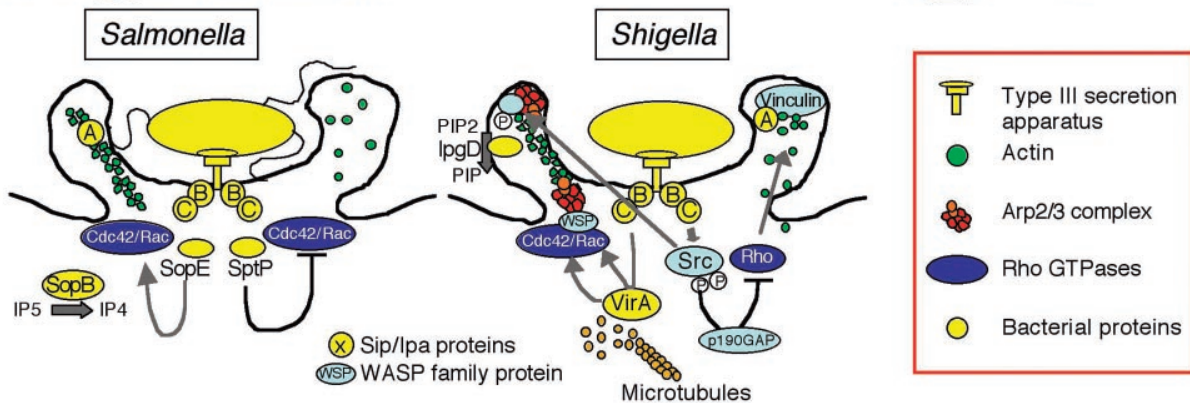


Figure 16. Mechanisms used by bacteria to enter cells. (A) The zipper mechanism used by *Yersinia* and *Listeria monocytogenes*. (B) The trigger mechanism used by *Salmonella* and *Shigella*. ([Cossart and Sansonetti, 2004](#))

Vacuolar life:

Newly internalized pathogens are entrapped within a vacuole. Some pathogens like *Salmonella*, *Yersinia*, or *Chlamydia*, reprogram this vacuole while others escape in order to gain access the cytoplasm. Cytosolic access is for some pathogens a critical component of their virulence strategy for growth and spread, such that mutants with abnormal auxiliary or pore-forming systems are typically avirulent. For the facultative intracytosolic pathogens sensitive to the lytic enzymes of the maturing vacuole, catalyzing their escape is obligatory. *Shigella* escapes from the vacuole by the activity of IpaB, highlighting the pleiotropic functions of this virulence factor. *Rickettsia rickettsii* is also known to escape from the vacuole in order to pursue host cytoplasmic parasitism ([Theriot, 1995](#)).

Bacterial growth:

Bacterial growth is perhaps the most common of patterns associated with pathogenesis, which can be sensed by the host cell. While pathogens like *Salmonella* or *Chlamydia* replicate within the confines of their reconditioned vacuoles, several species of intracellular pathogens including *Listeria*, *Shigella*, and *Mycobacterium marinum* replicate in the host cytosol ([Gouin et al., 2005](#)). Bacteria residing in the vacuole must adapt to and resist the hostile conditions of a maturing vacuole or else alter the biogenesis and dynamics of the vacuole such that the compartment is rendered permissive to survival and growth. Examples of vacuolar bacteria are *Salmonella*, *Chlamydia*, *Coxiella burnetti*, *Mycobacterium tuberculosis*, *Legionella pneumophila*, *Chlamydia trachomatis*, etc. *Coxiella burnetti* is capable of surviving the bactericidal agents that the host cell delivers to the phago-lysosome. *Salmonella typhimurium*, *Legionella*, and *Mycobacterium* render the vacuolar compartment permissive to bacterial growth by regulating the fusion of the vacuole with lysosomal compartments. After only a few hours following cell internalization by *Salmonella*, the vacuolar compartment resembles neither a late endosome fusing with lysosomal compartments, nor an early endosome ([Holden, 2002](#)). The reprogramming of vacuolar fate away from a lysosomal endpoint is dependent on the interaction of type three secretion system (TTSS) effectors and host factors, which contribute to the maintenance of a vacuole permissive to *Salmonella* growth and virulence. The *Salmonella* effector, SifA, causes the reduction in hydrolytic enzymes transported to the *Salmonella*-containing vacuole (SCV) by sequestering the host transporter, Rab9, which is necessary for the accumulation of mannose-6-phosphate receptor-associated hydrolases ([McGourty et al., 2012](#)).

Sensing of PAMPs is essential for host resistance to microbial pathogens. Toll-like receptors contribute as PRRs to recognizing pathogens and activating an innate immune response. Host sensing of *Salmonella typhimurium* is largely mediated by TLR2, TLR4, and TLR5 ([Feuillet et al., 2006](#); [Hapfelmeier et al., 2005](#); [O'Brien et al., 1980](#); [Royle et al., 2003](#); [Smith et al., 2003](#); [Uematsu et al., 2006](#); [Vazquez-Torres et al., 2004](#)). However, mice lacking additional TLRs (like TLR9) involved in *S. typhimurium* sensing are less susceptible to infection. These mice exhibiting less susceptibility to infection also exhibit *S. typhimurium* with a delayed up-regulation of the *Salmonella* pathogenicity island (SPI-2) genes. SPI-2 induction occurs upon acidification of the internalized vacuole, which is

dependent on TLR signaling ([Arpaia et al., 2011](#)). Therefore, the paradox of TLRs contributing to *S. typhimurium* infection is dependent on TLR9 activation of the innate immune system leading to vacuolar acidification, which acts as a cue induction of SPI-2 gene expression.

Intracellular pathogenesis:

Once free in the cytoplasm, *S. flexneri*, is observed surrounded by actin, which they then organize into a polar comet-like tail using the virulence factor, IcsA, respectively ([Kocks et al., 1995](#)). The polar organization of actin acts to propel the bacterium through the cytoplasm and into adjacent cells ([Cossart and Sansonetti, 2004](#)). *Listeria*, *Shigella*, *Mycobacterium marinum*, and Rickettsial species, as well as poxvirus all exploit host cell cytoskeletal components for catalyzing actin-based motility ([Gouin et al., 2005](#)). Bacterial spread into neighboring cells is the culmination of host colonization by pathogens, with dangerous and painful consequences for the host if not treated. Numerous other bacterial pathogens disrupt the host cytoskeleton for distinct purposes. *Salmonella* manipulates host actin during host cell invasion ([Galan and Wolf-Watz, 2006](#)), while other pathogens disrupt host actin in order to block phagocytosis ([Viboud and Bliska, 2005](#)).

Each process of pathogenesis, from the action of secreted factors and toxins, to adherence, entry, vacuolar escape, bacterial growth, and cytoskeletal hijacking are all patterns acting as signals for host cells to recognize pathogens. There is also a deeper, subtler pattern that has largely remained underdeveloped in the general understanding of patterns of pathogenesis. That pattern is of modulating the transcriptional state of the host through the global or directed reorganization of chromatin and it can occur during any of the processes of pathogenesis. Chromatin modifications occurring during infection is a burgeoning field of research wherein there are an increasing number of reports linking chromatin and histone modifications to both virulence and the host immune response to pathogens.

2.3 Histone modifications induced by bacterial infection

Bacterial infections influence transcriptional expression of the host in one of two ways: either the host senses PAMPs through the activity of PRRs, like TLRs, or bacteria impose changes on the host transcriptome in order to promote infection. In the first instance, mammalian TLRs bind PAMPs, leading to the activation of a signaling cascade whereby mitogen-activated protein kinases induce stress-related transcription factors like NF- κ B to cause large-scale transcriptional reprogramming ([Ausubel, 2005](#)). The impact of NF- κ B-dependent leads to an increase of transcriptional expression of cytokines or defensins, leading to a pro-inflammatory response to danger signals ([Matzinger, 2002](#)). Cells undergo a large scale transcriptional reprogramming that surpasses the activation of only innate immune factors. The transcriptional upregulation of genes coding co-stimulatory molecules on dendritic cells are essential for the activation of the adaptive immune response through T-cells ([Kawai and Akira, 2007](#)).

The second instance wherein host transcription is modified during infection is by microbial pathogens. Bacteria employ a variety of mechanisms to influence transcriptional control of the host. Infection often imposes global changes, which cannot be easily explained by the modulation of specific transcription factors. Rather, in recent years, studies have shown that bacterial pathogens induce host chromatin modifications to broadly affect transcription ([Arbibe et al., 2007](#); [Hamon et al., 2007](#); [Paschos and Allday, 2010](#)). Reprogramming transcription by pathogens can alter cell processes such as innate immunity, cell death, survival, adhesion, motility, cellular differentiation, or cell division ([Jenner and Young, 2005](#)). Histone modifications, through transcriptional regulation, are implicated in the control of the host response. Without such control, the host response is stimulated by the recognition of numerous patterns of pathogenesis resulting in the attenuation of bacterial infection ([Paschos and Allday, 2010](#)). Pathogens have evolved three general mechanisms by which to modify chromatin: 1) effectors directly cause histone modifications through their own enzymatic activity, 2) effectors complex with histone modifiers in order to promote histone-modifying activity, and 3) effectors induce signal transduction leading to histone modifications, indirectly ([Bierne and Cossart, 2012](#)).

2.4 Direct histone modification by virulence factors

The first mechanism by which pathogens can provoke histone modifications is by secreting or injecting virulence factors into the host, which will relocalize to the nucleus and directly target and catalyze modifications to histones. Such factors have been named, nucleomodulins ([Bierne and Cossart, 2012](#)). Perhaps the best evidence to date for a pathogenic virulence product contributing to pathogenesis through chromatin modification comes from studies characterizing the *Chlamydia trachomatis* effector, Nuclear Effector (NUE). NUE is reported to relocalize from the chlamydial inclusion body to the nucleus and has been shown *in vitro* to methylate mammalian histones (Fig. 17) ([Pennini et al., 2010](#)). Another mechanism of a nucleomodulin is the binding ankyrin-repeat (Ank) proteins, which mediate protein-protein interactions implicated in transcriptional regulation ([Mosavi et al., 2004](#)). *Anaplasma phagocytophilum* encodes the Ank-containing protein, AnkA, which was reported to bind chromatin structures resulting in the regulation of gene expression ([Park et al., 2004](#)). AnkA upregulates the expression of HDACs in infected cells contributing to silencing of host defense genes by deacetylation of histones (Fig. 17) ([Garcia-Garcia et al., 2009](#)). Other pathogens like *Coxiella*, *Legionella*, *Rickettsia*, and *Orientia* also encode Ank proteins ([Bierne and Cossart, 2012](#)), suggesting that these proteins might constitute a conserved family of chromatin modifiers contributing to infection.

Bacterial-encoded proteins targeting histones represent a new aspect of host-pathogen interactions and few examples have yet emerged reporting such histone modifying activities of bacterial factors. CobB is a protein produced by *Escherichia coli* and *Salmonella* species and is demonstrated to use NAD⁺ as a cofactor to catalyze mono-ADP-ribosyltransferase activity by transferring [³²P]NAD to bovine serum albumin (BSA) ([Frye, 1999](#)) and is predicted to possess deacetylase activity ([Richardson et al.](#)). Pathogenic bacteria utilize NAD⁺ as an enzymatic cofactor for catalyzing O-acetyltransferase activity outside the host cell, in order to evade host detection of patterns of pathogenesis ([Aubry et al.](#)). While this most direct mechanism of chromatin modification is conceivable, few bacterial factors with chromatin modifying activity have yet been identified in the nucleus of host cells. Indeed, direct chromatin modification by bacterial factors is certainly not the only way in which bacteria manipulate host chromatin.

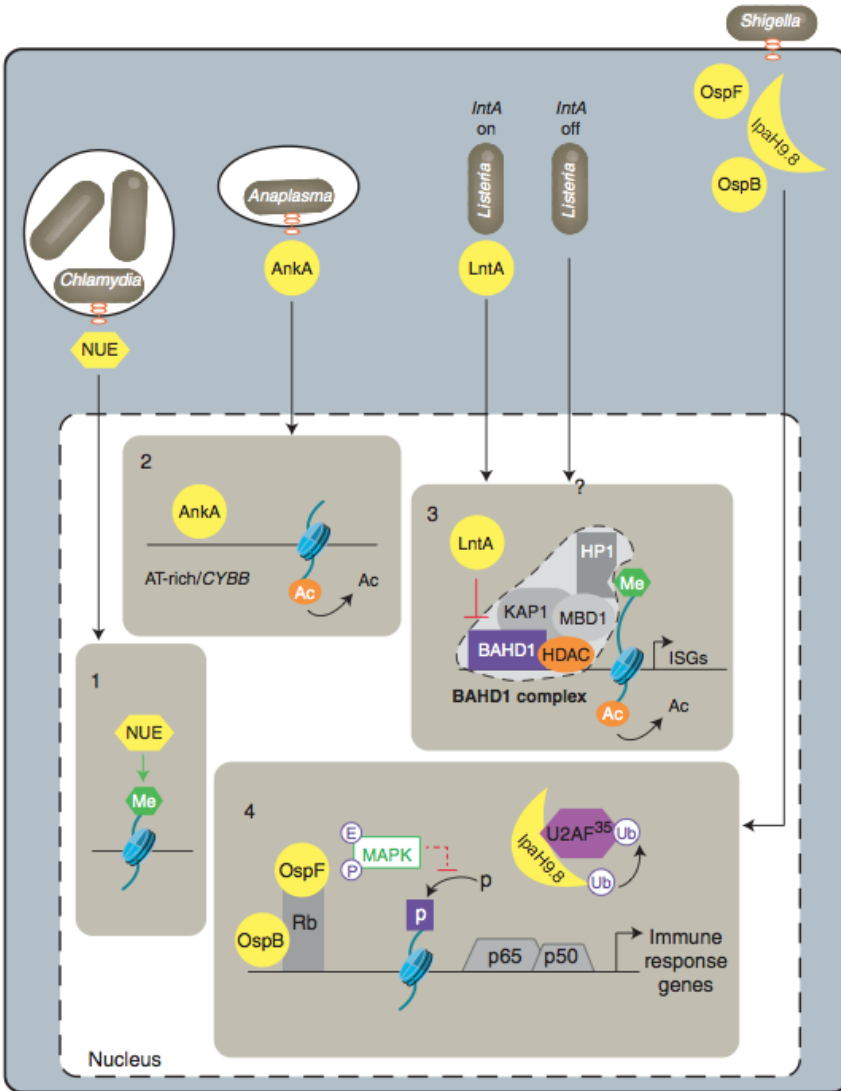


Figure 17. Bacterial nucleomodulins targeting chromatin.

Schematic representation of *Chlamydia*, *Anaplasma*, *Listeria*, and *Shigella* secreted factors involved in the control of gene expression in the nucleus of host cells. Bacterial nucleomodulins are in yellow. 1) *Chlamydia* histone-methyltransferase NUE methylates mammalian histones. However, target genes remain unknown. 2) Binding to AT-rich sequences and silencing of *CYBB* expression by *Anaplasma* Ank effector AnkA. 3) Inhibition of the BAHD1-associated heterochromatic complex and induction of interferon-stimulated genes by *Listeria* LntA. On *Listeria* infection, an unknown signaling pathway drives the BAHD1-associated chromatin complex to repress interferon-stimulated genes. When *Listeria* produces and secretes LntA, this factor enters the nucleus and interacts with BAHD1, destabilizes the silencing complex, restores histone acetylation (Ac), and enhances the expression of ISGs. 4) Control of a set of NF- κ B (p65-p50) regulated genes by *Shigella* post-translational modifiers OspE, which eliminates MAP kinases preventing phosphorylation of histone H3, and IpaH9.8, which ubiquitinylates and promotes degradation of the splicing factor U2AF. OspF and another effector, OspB, bind the retinoblastoma protein (Rb), which potentially recruits several chromatin-remodeling enzymes. Ac = Acetylation; Me = Methylation; P = Phosphorylation; E = elimination; Ub = ubiquitinylation. (Bierne and Cossart, 2012)

2.5 Histone modifiers regulated by virulence factors

Virulence factors that are either secreted or injected into the host cytosol can induce histone modifications in one of two ways: 1) bind and modulate the activity of histone modifiers, or 2) induce/regulate signaling cascades leading to chromatin modifications by host-encoded chromatin modifying machinery. The first mechanism by which virulence factors can cause histone modifications is by regulating chromatin-modifying enzymes. To date, several patterns have emerged to describe how virulence factor-host histone modifier interactions modulate host histone modifications. These mechanisms consist of mimicking the function of eukaryotic chaperones, regulating host heterochromatin forming complexes, or regulating ankyrin-dependent gene expression. One example is of a virulence factor interacting with host histones and functioning as a chaperone, directing histone deposition on DNA. The plant pathogen *Agrobacterium tumefaciens* injects a tumorigenic vector (Ti plasmid) into the host, which is integrated into the host genome. Ti encodes the 6b protein, which interacts with histone H3 and contributes to nucleosome formation, much like eukaryotic histone chaperones. Transcriptome analysis of transgenic 6b-expressing plants demonstrated that genes are differentially regulated as compared to control plants, suggesting that histone chaperone activity is one mechanism by which pathogens hijack the host. The *Ehrlichia chaffeensis* encoded ankyrin protein, p200, interacts with specific adenine-rich motifs of host promoters and intronic *Alu* elements ([Zhu et al., 2009](#)).

Pathogens can cause histone modifications through the induction of signaling cascades either at the cell surface, or by modifying signaling receptors or intermediates in the cytoplasm. *Bacillus anthracis*, *M. tuberculosis*, and the carcinogenic *Helicobacter pylori* activate innate immune receptors at the cell surface, causing activation of the MAPK signaling pathway and leading to a change in the expression of cytokines and chemokines through histone modifications ([Bierne and Cossart, 2012](#)). *B. anthracis* and *M. tuberculosis* induce the expression of innate immune ligands TNF α and IFN γ , which respectively engage their corresponding receptor on the surface of the host cell and cause histone modifications downstream (Fig. 18). The expression of lipoproteins by *H. pylori* and *M. tuberculosis* activate TLR2 signaling, which also leads to MAPK signaling and histone modifications (Fig. 18). *H. pylori* and *Porphyromonas gingivalis* are also capable to cause histone modifications independently of binding innate immune receptors. The type IV

secretion system (T4SS) of *H. pylori* is necessary for causing a transient H3 dephosphorylation and later rephosphorylation by engaging the IKK α -dependent pathway and H4 deacetylation ([Ding et al., 2010](#); [Fehri et al., 2009](#)). *P. gingivalis* produces a metabolite, butyric acid, which inhibits the activity of HDACs (Fig. 18). Butyric acid, produced by *P. gingivalis*, is correlated with the reactivation of latent viruses, like human immunodeficiency virus (HIV) and Epstein-Barr virus (EBV) ([Imai et al., 2012](#); [Imai et al., 2009](#)).

Pathogens that activate signaling from inside the cytoplasm do so by either targeting intracellular PRRs, like NOD-like receptors (NLRs), or by regulating signaling intermediates, like signaling kinases. Cytoplasmic *L. monocytogenes* is sensed by the NOD1 receptor, leading to MAPK signaling-dependent IL-8 up-regulation of gene expression, correlated with histone acetylation (Fig. 18) ([Opitz et al., 2006](#); [Schmeck et al., 2005](#)). Flagellin of *Legionella pneumophila* and LPS have similar effects on IL-8 gene expression in lung epithelial cells and dendritic cells, respectively ([Saccani et al., 2002](#); [Schmeck et al., 2008](#)). The *Shigella* encoded factors OspB, OspF and IpaH9.8 (Fig. 17) ([Bierne and Cossart, 2012](#); [Zurawski et al., 2009](#)) modify signaling through binding various host receptors and signaling intermediates. OspF is a pleiotropic chromatin-modifying factor influencing the onset of chromatin modifications by dephosphorylating mitogen-activated protein kinases (MAPKs) and abrogating H3 phosphorylation at a set of innate immune genes ([Arbibe et al., 2007](#)) and interacting, as does OspB, in the nucleus with the human retinoblastoma protein Rb, which is known itself to bind several chromatin remodeling factors ([Zurawski et al., 2009](#)). It is also possible that virulence factors inhibit the activity of intracellular signaling factors and have downstream effects on chromatin modifications. For example, the lethal toxin (LT) from *Bacillus anthracis* cleaves and inactivates mitogen-activated protein kinase kinase (MAPKK) (Fig. 18) ([Bardwell et al., 2004](#)), thereby blocking downstream signaling and leading to H3S10 dephosphorylation and H3K14 deacetylation at the promoters of a subset of genes ([Raymond et al., 2009](#)). Taken together, these studies highlight the increasing number of virulence factors originating from a diverse array of bacterial pathogens leading to a modulation of chromatin through indirect mechanisms.

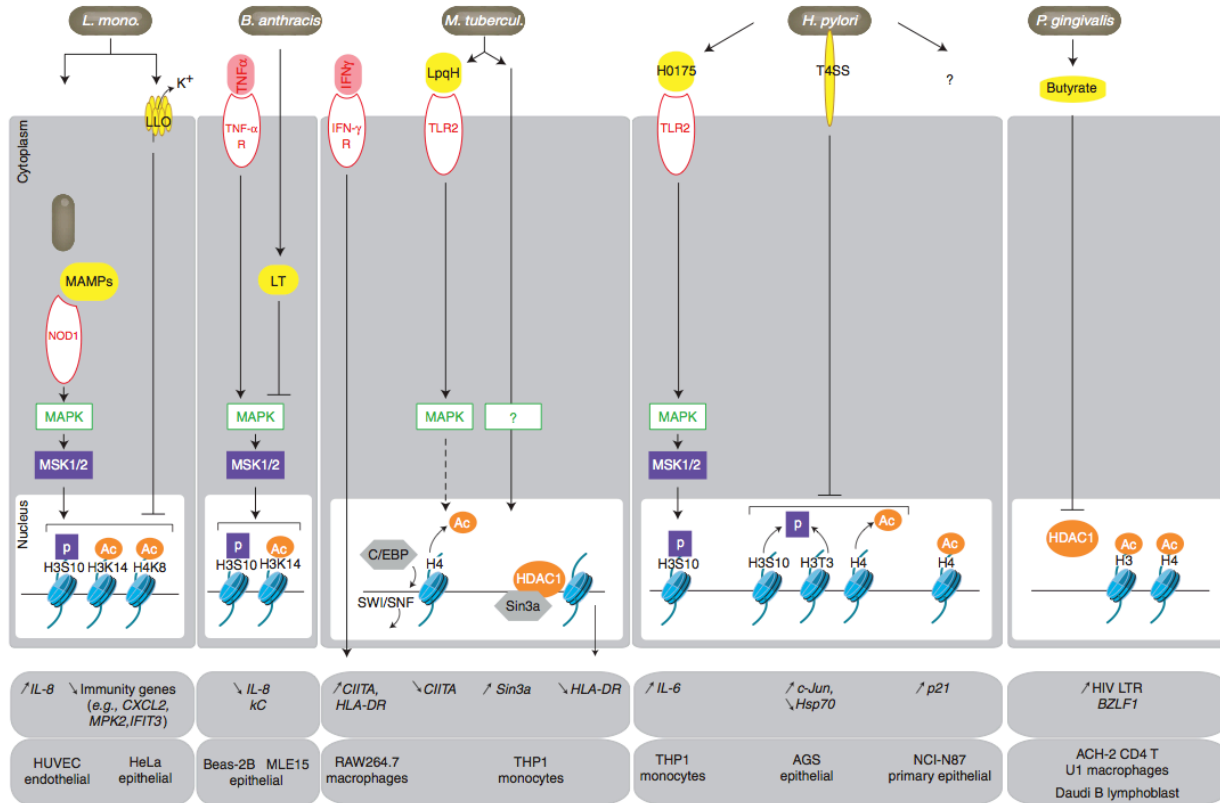


Figure 18. Bacterial signaling to histones and transcriptional response.

Schematic representation of *Listeria monocytogenes*, *Bacillus anthracis*, *Mycobacterium tuberculosis*, *Helicobacter pylori*, or *Porphyromonas gingivalis*-induced signaling pathways leading to histone modifications. Bacterial products inducing host cellular signaling are in yellow. Membrane (TNF- α , IFN- γ , TLR2, TLR4) or cytosolic (NDO1) receptors are indicated by a red oval. Effects on target genes are indicated by arrows (up for activation and down for repression). ([Bierne and Cossart, 2012](#))

2.6 Histone modifications resulting from infection-induced signaling

The third general group of virulence factors influencing chromatin modifications is factors secreted, shed, or liberated in the extracellular space. These virulence factors induce chromatin modifications through host-encoded pathways. To date, studies have revealed that bacterial virulence factors affect host innate immunity, however many other cellular processes may be modulated through histone modifications.

Examples of virulence factors inducing histone modifications are the cholesterol-dependent pore-forming toxins like the listerial LLO, perfringolysin O (PFO) of *Clostridium perfringens*, pneumolysin (PLY) of *Streptococcus pneumoniae* ([Hamon et al., 2007](#)). Interestingly, these and other toxins like aerolysin from *Aeromonas hydrophila* function by inducing intracellular signaling sensitive to potassium efflux ([Hamon and Cossart, 2011](#)). While many pathogens do express toxins leading to chromatin modifications by both intra- and extra- cellular spaces, many other virulence factors binding at the surface of the host cell also cause histone modifications. Those virulence factors may function as molecular mimics of pre-existent host agonists. The hijacking of these signaling cascades highlights the impressive evolutionary ability of pathogens to select for and reactivate native signaling pathways and reprogram host cells in order to prepare niches for pathogens to survive and grow.

Virulence factors causing histone modifications can also be classified based on the types of responses they encode, like immunological tolerance. The gram-negative LPS is recognized by the PRR, toll-like receptor 4 (TLR4), which induces downstream signaling of the nuclear factor- κ B (NF- κ B) and mitogen activated protein kinase (MAPK) signaling cascades, leading to increased gene expression of pro-inflammatory cytokines ([Akira and Takeda, 2004](#)). LPS-induced MAPK signaling induces H3S10 phosphorylation and H3K14 acetylation, crucial marks implicated in only one of several mechanisms sufficient for causing NF- κ B recruitment to pro-inflammatory cytokine genes ([Saccani et al., 2002](#)). Taken together, these studies demonstrate that pathogens can both activate and inhibit key immune signaling cascades to promote pathogenesis.

Section 3.

3.1 *Listeria monocytogenes* pathogenesis

Listeria monocytogenes is a Gram-positive facultative intracellular pathogen, which causes disease in humans called, listeriosis ([Vazquez-Boland et al., 2001](#)). The disease originates mainly from the ingestion of contaminated food. The target populations most at risk for developing listeriosis are immunocompromized individuals, pregnant women and newborns. The pathological conditions manifested by listeriosis are gastroenteritis, meningitis, encephalitis, and septicemia. These pathologies result in the death of nearly 30% of documented listeriosis cases. The crossing of three main host barriers by *L. monocytogenes* explains why patients diagnosed with listeriosis may suffer from a diverse array of pathologies. Once ingested, *L. monocytogenes* crosses the intestinal epithelium, thereby gaining access to the bloodstream and subsequently the liver and spleen where it continues to grow and divide. In severe cases, *L. monocytogenes* has the unique ability to cross the blood-brain barrier, a process that is not yet adequately understood. Access to the brain and meninges leads to patients regressing to a state of comatose at which point the prevalence of death is quite high. Pregnant women are particularly at risk as *L. monocytogenes* is able to cross the feto-placental barrier, leading to a high probability of mortality for the fetus.

L. monocytogenes has for several decades played a key role as a tool for understanding pathogenesis, as a consequence of characterizing host cell processes. The ability for *L. monocytogenes* to invade and replicate within cells underlines the intimate relationship between *Listeria* and a diverse array of host cells. The study of *L. monocytogenes* infection has played an important role in advancing the understanding of host-microbial interactions as represented by the various patterns of pathogenesis indicated previously.

Pathogenesis by *L. monocytogenes* is dependent on the expression and action of virulence factors. A RNA thermosensor encoded by the gene, *prfA* controls virulence in *L. monocytogenes* ([Johansson et al., 2002](#)). Once at 37°C, the untranslated mRNA (UTR) upstream of the *prfA* transcript becomes accessible for translation to occur. The protein product, PrfA, activates the expression of virulence genes essential to the progression through the stages of pathogenesis.

The virulence factors internalin A (InlA) and InlB are expressed on the surface of *Listeria* and are necessary for bacterial entry by binding to surface trans-membrane receptors of the host cell ([Drams et al., 1995](#); [Gaillard et al., 1991](#)). InlA binds the host receptor E-cadherin whereas InlB binds the receptor cMet. The interaction of InlA or InlB with their host receptor induces an actin cytoskeletal rearrangement that culminates in the internalization of *L. monocytogenes* into the host cell. *L. monocytogenes* then escapes the vacuole principally by the activity of the secreted virulence factor LLO, which disrupts the integrity of the vacuolar membrane by forming pores. Upon gaining access to the host cytoplasm, *L. monocytogenes* undergoes replication. By the expression of the virulence factor ActA, *L. monocytogenes* is capable of polarizing actin to confer the bacterium motility and the ability to spread into neighboring cells. Survival in the host cytoplasm is dependent on a close interaction of *L. monocytogenes* with the host, which implies important modifications to host cell processes.

3.2 Host chromatin modifications induced by *Listeria monocytogenes*

As highlighted above, chromatin modifications are provoked by a diverse array of mechanisms during pathogenesis. *L. monocytogenes* is known to cause various modifications on histones H3 and H4. To date, a few studies have aimed at describing what histone modifications occur during infection with *L. monocytogenes* and characterizing the bacterial and host mechanisms involved. These studies together demonstrate the variety of histone modifications that occur in a cell-type dependent manner highlighting the diversity of interactions that *Listeria* has with its host.

Histones in host cells infected with *Listeria* have been reported to undergo a time-dependent H4K8 acetylation and co-phosphorylation/acetylation to H3S10/K14 globally, at the IL8 promoter, of human umbilical vein endothelial cells, HUVEC ([Schmeck et al., 2005](#)). The zinc-dependent deacetylase, HDAC1, is evicted from the IL8 promoter, which results in an increase of H4 acetylation leading to gene activation, suggesting that the basal level of gene expression is low due to the presence of HDAC1 and once it is removed transcriptional activity increases. These modifications are dependent on NOD1-mediated sensing of cytosolic bacteria and MAPK signaling ([Opitz et al., 2006](#)), suggesting that histone modifications might represent a host response.

In another study, Hamon and colleagues reported that *L. monocytogenes* causes a variety of histone modifications including H3S10 dephosphorylation and global H3 and H4 deacetylation in the human cervical epithelial cell line, HeLa ([Hamon et al., 2007](#)). Significantly, this report identified that the listerial virulence factor, LLO, was both necessary and sufficient to cause H3S10 dephosphorylation and H4 deacetylation early on in infection. These histone modifications were correlated with a down-regulation of a key subset of innate immunity genes. Importantly, along with LLO, several other pore forming toxins produced by other pathogens were observed to cause H3S10 dephosphorylation and H4 deacetylation. A later study reported that potassium efflux, provoked by LLO-dependent pore formation, is required to cause H3S10 dephosphorylation (Fig. 19) ([Hamon and Cossart, 2011](#)). Taken together, these results demonstrated for the first time a listerial virulence factor as being important for inducing histone modifications.

A third independent study used a yeast-two-hybrid screen to identify interactors to the nuclearly targeted listerial protein, LntA, and the nuclear heterochromatin complexing factor bromo adjacent homology domain containing protein 1 (BAHD1) ([Bierne et al., 2009](#)). BAHD1 is a nuclear protein, which together localize to CpG-rich promoters and the inactive X chromosome (Xi), suggesting that this complex contributes to heterochromatin formation ([Bierne et al., 2009](#)). In conditions of overexpression, BAHD1 targets specific nuclear sites characterized by H3K27 tri-methylation and phase-dense nuclear material corresponding to heterochromatin. Among the proteins reported to complex with BAHD1 are chromatin-modifying enzymes like methyltransferases of histones KMT1E and DNMT3 and of DNA in MBD1, as well as the deacetylase HDAC5. During the course of *L. monocytogenes* infection, the BAHD1 repressor complex represses type III interferon (IFN)-stimulated genes (ISGs). However, if *L. monocytogenes* expresses and secretes the virulence factor, LntA, a type III IFN response is stimulated (Fig. 19) ([Lebreton et al., 2011](#)). The mechanism of IFN stimulation during listerial infection is dependent on the action of LntA preventing BAHD1 recruitment to ISGs. Furthermore, an increase in H3K9 acetylation occurs at ISGs in cells where LntA is bound to BAHD1. The mechanism of immune activation is therefore dependent on the expression of LntA through its interaction with the heterochromatin factor, BAHD1.

Studies conducted in listerial-infected endothelial and epithelial cells have characterized the various modifications occurring over time and their impact on these

host tissue. However, adaptive immune cells remained uncharacterized until a recent report demonstrated that the infection with *L. monocytogenes* of naïve CD8⁺ T cells, which is necessary for the differentiation of memory T cells, was correlated with histone H3K9 and K14 acetylation ([Dispirito and Shen, 2010](#)). These results suggest that H3 acetylation might play a role in the differentiation of naïve T cells into memory T cells, possibly through the activation of ISGs. Taken together, these reports have revealed a number of histone modifications occurring during infection with *L. monocytogenes*. Interestingly, *Listeria*-dependent histone modifications occur in a cell type-dependent manner. Where naïve CD8⁺ T-cells undergo histone H3 acetylation during infection and umbilical vein endothelial cells undergo H3S10 phosphorylation and H3K14 acetylation, epithelial cells undergo H3 and H4 deacetylation.

In epithelial cells, the outcome of infection may possibly be more complex. The specific histone modifications observed to occur early during infection by the action of the secreted LLO, are correlated with the repression of a subset of key innate immunity genes ([Hamon et al., 2007](#)). At a later stage of infection however, ISGs can be stimulated by the activity of intracellular PRRs during infection with *L. monocytogenes*, through IFN- γ -dependent signaling. However, if the listerial factor, LntA, is expressed and localized in epithelial cells, it can block the BAHD1 complex from regulating ISG activation, thereby driving a positive genetic feedback loop reminiscent of a classical epigenetic switch ([Lebreton et al., 2011](#)). These results suggest that histones are dynamic substrates that are manipulated by both the pathogen and the host, with the goal of promoting infection early on and mounting a host defense later on during infection. Here, we explore the mechanism underlying a new histone modification, H3 deacetylation, and how it contributes to *L. monocytogenes* infection.

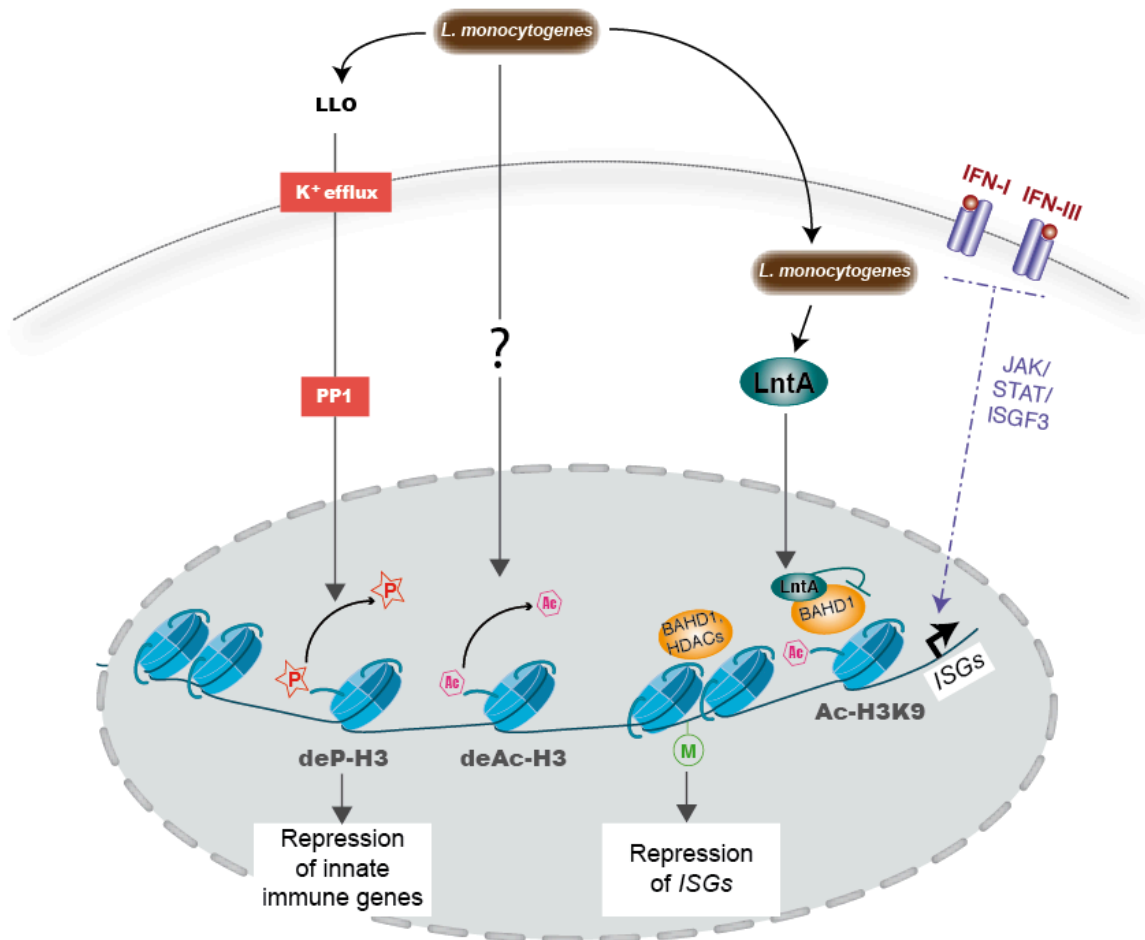


Figure 19. *L. monocytogenes*-induced host chromatin modifications

Schematic representation of chromatin modifications induced in host cells infected with *L. monocytogenes*. Pores formed in the cell membrane by *L. monocytogenes* virulence factor, LLO, causes potassium efflux, which induces a relocalization of the phosphatase, PP1, to the nucleus, resulting in H3 dephosphorylation. The infection with *L. monocytogenes* causes H3 deacetylation in a LLO-independent manner. The heterochromatin factor, BAHD1, associates with class I HDACs to cause repression of interferon-stimulated genes (ISGs). However, the expression of the listerial virulence factor LntA inhibits BAHD1 function, causing an increase in H3K9 acetylation and the expression of ISGs. White boxes indicate gene expression. P = phosphorylation; Ac = acetylation; M = methylation; K^+ = potassium ions. ([Bierne et al., 2009](#); [Hamon et al., 2007](#); [Hamon and Cossart, 2011](#); [Lebreton et al., 2011](#)).

Section 4:

Thesis Objectives

- 1) Characterization of histone H3 deacetylation
- 2) Search for the listerial factor(s) causing H3 deacetylation
- 3) Identification of the genomic loci where H3 deacetylation occurs
- 4) Study H3 acetylation patterns *in vivo*
- 5) Generalizing the findings to other bacterial pathogens

Summary of my thesis work

In this thesis report, I highlight the experiments conducted, which led to the identification of H3 K18 as a host histone H3 target residue for deacetylation during infection with *L. monocytogenes*, a mark that has remained largely uncharacterized in biology until recently when studies have highlighted the reduction in H3 K18 acetylation predicting poor prognosis for patients with various cancer types ([Barber et al., 2012](#); [Seligson et al., 2009](#)). SIRT2, a member of the class III HDACs (γ Sir2 homolog) is necessary to target H3 K18 during infection. SIRT2 has largely been characterized as a tubulin deacetylase in the cytoplasm ([North et al., 2003](#)), however our results demonstrate an unsuspected nuclear recruitment of SIRT2 causing a targeted H3 K18 deacetylation at the transcriptional start sites of a subset of tested repressed genes during infection. The mechanistic basis for the association of SIRT2 to chromatin remains to be thoroughly characterized. However, preliminary results suggest that SIRT2 undergoes dephosphorylation at its N-terminus. The biological function of SIRT2 was assessed at the transcriptional level and at the infection level. Strikingly, SIRT2 was observed to be necessary for the repression of nearly all genes detected to be repressed during infection. The infection in SIRT2^{-/-} mice is significantly diminished, strongly suggesting that SIRT2 is critical for a listerial infection.

Results

Section 1:

Manuscript in revision at the journal, *Science*.

Title: A role for SIRT2-dependent histone H3K18 deacetylation in bacterial infection

Authors: Haig A Eskandarian^{1,2,3}, Francis Impens^{1, 2, 3, 4, 5}, Marie-Anne Nahori^{1,2,3}, Guillaume Soubigou⁶, Jean-Yves Coppée⁶, Pascale Cossart^{1,2,3,*}, Mélanie Hamon^{1,2,3,*}

Affiliations:

¹Unité des Interactions Bactéries-Cellules, Institut Pasteur, Paris F-75015, France.

²Inserm, Unité 604, Paris F-75015, France.

³Institut National de la Recherche Agronomique, Unité Sous Contrat 2020, Paris F-75015, France.

⁴Department of Medical Protein Research, VIB, Ghent, Belgium

⁵Department of Biochemistry, Ghent University, Ghent, Belgium

⁶Plate-forme 2, Transcriptome et Epigénome, Génopole, Institut Pasteur, Paris F-75015, France

*Correspondence: hamon@pasteur.fr (M.H.), pcossart@pasteur.fr (P.C.).

Section 2:

Title: Generalizing Histone H3K18 deacetylation to other bacterial pathogens

Section 3:

Title: *Listeria monocytogenes* infection does not inhibit CBP/p300 Histone Acetyltransferase to cause H3K18 deacetylation

Section 4:

Title: SIRT2 N-terminal dephosphorylation regulates nuclear localization

Overview of Results:

Section 1:

A role for SIRT2-dependent histone H3K18 deacetylation in bacterial infection

The manuscript entitled, “A role for SIRT2-dependent histone H3K18 deacetylation in bacterial infection,” has been accepted for publication at the peer-review journal *Science*. It comprises the majority of my thesis work in which we aimed to characterize the mechanistic basis for infection-induced host histone H3 deacetylation and its impact on infection. This manuscript addresses the first four of my thesis objectives. Below, I will briefly highlight how we addressed each of these thesis objectives in this manuscript.

1) Characterization of histone H3 deacetylation

In the initial study by Mélanie Hamon, published in 2007, she identified that infection with *Listeria monocytogenes* caused H3 deacetylation, in a LLO-independent manner ([Hamon et al., 2007](#)). She used a H3 pan-acetyl antibody raised against di-acetylated H3 K9 and K14 in order to quantify H3 acetyl levels, as these residues had to date been the most commonly studied H3 N-terminal acetyl marks. However, her experiments further demonstrated that H3 K9 and K14 did not undergo deacetylation during infection ([Hamon et al., 2007](#)). Therefore, I will aim to determine whether other lysine residues, like H3 K18 undergo deacetylation during infection.

While Mélanie Hamon’s studies were conducted in non-phagocytic epithelial cells, in tissue culture, it is not yet known whether other cell types also undergo similar histone modifications during infection. I will aim to determine which cell types undergo H3 deacetylation during infection. For this purpose, organs will be harvested from mice infected with *L. monocytogenes*, namely the liver and spleen. The liver is composed of mainly hepatocytes and endothelial cells, while the spleen is composed of tissue of mesenchymal origin and is a major point of interaction of host immune cells like dendritic cells and macrophages.

2) Search for the listerial factor(s) causing H3 deacetylation

In order to identify the listerial factor causing deacetylation during infection a methodical approach was undertaken that conceptually interrogates whether each

specific process of infection are involved. The process of infection with *Listeria monocytogenes* is characterized by 1) attachment to the host cell and inducing bacterial entry, 2) escaping the internalized vacuole, 3) growing and replicating in the cytoplasm, 4) and polymerizing actin to propel *Listeria* throughout the cytoplasm and into neighboring cells in order to promote spread of the infection. Each of these processes are dependent on the expression of specific listerial virulence factors. The secreted listerial factor, InlB, promotes attachment by binding the host cell receptor, cMet, and subsequently inducing bacterial entry. LLO induces escape of *Listeria* from the internalized vacuole and ActA provokes the polymerization of actin to promote spreading. Cells infected with an InlB mutant *Listeria* do not exhibit H3 K18 deacetylation.

3) Identification of the genomic loci where H3 deacetylation occurs

We next aimed to determine whether H3 deacetylation is correlated with a change in gene transcription. A two-step process was undertaken in order to identify genomic regions where H3 K18 deacetylation occurs during infection and subsequently whether SIRT2 localizes to these same genomic loci. The first step was to define the transcriptional profile of by microarray analysis of cells uninfected or infected and under conditions where SIRT2 is active or inactive. This transcriptome would identify genes that are controlled by SIRT2 during infection with *L. monocytogenes*. These genes provided a more acute view into where deacetylation might be occurring. Previous ChIP-sequencing studies mapped H3 K18 acetyl levels across the whole genome ([Rando and Chang, 2009](#); [Wang et al., 2008](#)) and determined that H3K18 acetylation is enriched at TSSs, promoters, and enhancer regions. Unlike enhancers and promoters, which are identified using predictive computational algorithms, TSSs are well annotated and transcriptionally verified by qPCR. Therefore, I aimed to determine whether the TSSs of the SIRT2-dependent genes modified during infection undergo H3 K18 deacetylation and SIRT2 recruitment, by ChIP-PCR. Interestingly, those genes that are repressed during infection in a SIRT2-dependent manner undergo SIRT2 recruitment and H3 K18 deacetylation at their TSSs, but not at exon 2. In contrast, SIRT2-activated genes undergo an increase in H3 K18 acetylation.

4) Study H3 acetylation patterns *in vivo*

The infection of mice with *L. monocytogenes* crosses the intestinal epithelium and enters the bloodstream. A secondary infection ensues wherein the liver and spleen exhibit high counts of growing and replicating bacteria. Further infection can lead to a crossing of the blood-brain barrier and the feto-placental barrier. Traditionally, the liver and spleen have been used to quantify infection load as they represent major niches for bacterial growth and replication. Furthermore, the spleen is an important interface where bacteria are in close contact with cells of the immune system both innate and adaptive.

We aimed to determine whether H3 K18 deacetylation occurred in both the liver and spleen and whether the block of deacetylation would negatively affect listerial infection as I had observed that it does in cell culture. With the help of Marie-Anne Nahori and Mélanie Hamon, I was able to observe that H3 K18 deacetylation occurs in the spleen and that in SIRT2^{-/-} mice deacetylation is abolished. Our attempts to quantify H3 K18 acetyl levels in the liver were less conclusive. However, in both the spleen and liver, infection levels were significantly reduced in SIRT2^{-/-} mice in comparison to wildtype. Importantly, if mice are infected with a mutant of *Listeria* knocked out for InlB expression, no differences in infection levels or H3 K18 deacetylation was observed. These studies suggest that SIRT2 promotes bacterial infection.

Interestingly, SIRT2 is shown to be most highly expressed in the CNS and brain, which is also a site of infection by *Listeria monocytogenes* and resulting in a high level of mortality. Unfortunately, due to technical issues, I was not able to obtain infected mouse brains for quantifying H3 K18 acetyl levels and the impact of SIRT2 on infection in this organ.

Taken together, this manuscript provides evidence for the listerial InlB causing SIRT2 to relocalize to the nucleus where it causes H3 K18 deacetylation at the TSS of genes that are subsequently transcriptionally repressed. Furthermore, I identify that SIRT2 is a host factor promoting bacterial infection. Soluble catalytic inhibitors of SIRT2 could possibly act as novel therapeutics for controlling bacterial infections.

Section 2:

Listeria monocytogenes infection does not inhibit CBP/p300 Histone Acetyltransferase to cause H3 K18 deacetylation

My thesis aims one, two, and three each focussed on the identification and characterization of H3 K18 deacetylation and its consequence at the genomic level. The manuscript in results section one provided ample evidence that the histone deacetylase, SIRT2, is essential for H3 K18 deacetylation during infection. Conceptually, however, the initial observation of a reduction in H3 K18 acetyl levels upon infection does not necessarily have to depend on the activity of a deacetylase. Another possibility is that infection represses the activity of a histone acetyltransferase, thereby reducing the basal level of H3 K18 acetylation. Indeed, studies have demonstrated that adenovirus causes H3 K18 hypoacetylation through the block of CBP/p300 acetyltransferase ([Ferrari et al., 2008](#); [Horwitz et al., 2008](#)). This section highlights the experiments aimed at determining whether the reduction in H3 K18 acetylation is dependent on the block of p300 activity. Results demonstrate that blocking p300 activity by chemical inhibition causes a decrease in H3 K18 acetyl levels, however infection still causes a similar level of H3 K18 deacetylation as compared to uninfected cells. Furthermore, treatment of cells with a p300 activator caused an increase in basal H3 K18 acetyl levels, however infection still caused similar levels of H3 K18 deacetylation in comparison to uninfected. In conclusion, p300 activity does not affect H3 K18 acetyl levels during infection.

Section 3:

SIRT2 N-terminal dephosphorylation regulates nuclear localization

In order to go a step further from my thesis objectives, I have aimed to characterize the mechanistic basis of SIRT2-dependent H3 K18 deacetylation and role in promoting listerial infection. SIRT2 is observed to relocalize to the nucleus and associate to chromatin upon infection, however the underlying mechanistic basis for this change in sub-cellular has remained uncharacterized. Therefore, I aimed to characterize the mechanism governing SIRT2 sub-cellular localization. For this, I initially observed that infection-induced, chromatin-bound SIRT2 migrates faster on a denaturing polyacrylamide gel than SIRT2 isolated in nuclear soluble and cytosolic fractions. It was

believed that this shift in SIRT2 band migration was dependent on a post-translational modification, as it has previously been reported that SIRT2 a target for phosphorylation at its serine residues located at the C-terminus ([North and Verdin, 2007b](#)). Experiments aim to determine whether the C-terminal phospho-domain of SIRT2 dictates sub-cellular localization or whether another site of phosphorylation is involved.

Sections 4:

4) Generalizing Histone H3K18 deacetylation to other bacterial pathogens

The manuscript presented in results section 1 highlights the large body of work addressing the first four of the five aims of my thesis. Results section 4 addresses the fifth thesis aim, which is to generalize our findings to other bacterial pathogens. To this end, we describe in two experiments that *E. coli* engineered to express invasin from *Yersinia pseudotuberculosis* causes a relocalization of SIRT2 to the nucleus and H3 K18 deacetylation. In contrast, *Salmonella typhimurium* and *Shigella flexneri* both cause SIRT2 nuclear exclusion and no change to H3 K18 acetyl levels. In conclusion, the integrin-associating invasin-expressing *E. coli* and cMet-engaging InlB of *L. monocytogenes* cause SIRT2 nuclear localization and H3 K18 deacetylation.

Section 1:

Manuscript in revision for the journal, *Science*.

Title: A role for SIRT2-dependent histone H3K18 deacetylation in bacterial infection

Authors: Haig A Eskandarian^{1,2,3}, Francis Impens^{1,2,3}, Marie-Anne Nahori^{1,2,3}, Guillaume Soubigou⁴, Jean-Yves Coppée⁴, Pascale Cossart^{1,2,3,*}, Mélanie Hamon^{1,2,3,*}

Affiliations:

¹Unité des Interactions Bactéries-Cellules, Institut Pasteur, Paris F-75015, France.

²Inserm, Unité 604, Paris F-75015, France.

³Institut National de la Recherche Agronomique, Unité Sous Contrat 2020, Paris F-75015, France.

⁴Plate-forme 2, Transcriptome et Epigénome, Génopole, Institut Pasteur, Paris F-75015, France

*Correspondence: hamon@pasteur.fr (M.H.), pcossart@pasteur.fr (P.C.).

Abstract

Pathogens dramatically affect host cells transcription programs for their own profit during infection, but in most cases the underlying mechanisms remain elusive. We discovered that during infection with the bacterium *Listeria monocytogenes*, the host deacetylase SIRT2 translocates to the nucleus, in a manner dependent on the bacterial factor InlB, and associates to the transcription start sites of a subset of genes repressed during infection, and deacetylates histone H3 on lysine 18. We further show that infecting cells in which SIRT2 activity was blocked, or SIRT2^{-/-} mice resulted in a significant impairment of bacterial infection. Together these data uncover a crucial role for SIRT2-mediated H3K18 deacetylation in infection and a new epigenetic mechanism imposed by a pathogenic bacterium to reprogram its host.

Main Text:

Chromatin is a dynamic and highly regulated structure composed of DNA wrapped around an octamer of histone proteins, H2A, H2B, H3 and H4, ([Kornberg and Lorch, 1999](#)). Post-translational modification of histones is a well-documented mechanism by which the chromatin structure is modulated to regulate gene expression. Acetylation of histones, mediated by histone acetyl transferases, allows chromatin to adopt a more relaxed structure and the transcription machinery to be recruited. Deacetylation,

mediated by histone deacetylases (HDACs), counteracts the effects of acetylation and is associated with transcriptional repression. Sirtuins are a class of HDACs, which have received special attention for their role in the regulation of aging and cancer, and to which a growing number of biological processes are being connected ([Denu and Gottesfeld, 2012](#)). However, the role of these enzymes in bacterial infection has never been investigated.

Listeria monocytogenes is a food-borne pathogen, which mainly causes disease in immunocompromized patients and pregnant women. This facultative intracellular pathogen invades host cells, evades killing, and exploits cellular functions through the activity of its numerous virulence factors ([Cossart, 2011](#)). Increasing evidence is uncovering the strong impact of bacterial pathogens on host chromatin ([Arbibe, 2008](#); [Bierne and Cossart, 2012](#); [Hamon and Cossart, 2008](#)). However, our knowledge of the impact of histone modifications and of chromatin modifiers on infection is in its infancy.

An infection-induced modification, H3 deacetylation, was previously observed upon infection with *L. monocytogenes*, but not characterized ([Hamon et al., 2007](#)). We first determined which lysine residue(s) was deacetylated upon infection. We observed H3 lysine 18 (H3K18) deacetylation by 3 hours of infection of HeLa or Caco2 cells which continued through 24 hours of infection (fig 1A, B, S1A, B, S2). In contrast, no deacetylation was observed at other known acetylated targets or histones such as tubulin, H3K9, H3K14, H4K16, suggesting that under the conditions tested, we only observe modifications of H3K18 during infection (fig 1A). H3K18 deacetylation was then assessed *in vivo*. The spleens of Balb/c mice were collected after intravenous infection with *L. monocytogenes*, and compared to uninfected mice. Strikingly, similar to *in vitro* infection, deacetylation of H3K18, but not H3K9 or H3K14, was observed in the spleens harvested after 72 and 96 hours of infection (figure 1C, S1C). This is the first report of H3K18 being targeted during a bacterial infection.

To identify the host factor involved in infection-induced H3K18 deacetylation, we blocked the activity of HDAC classes with specific chemical inhibitors and tested their effect on H3K18 acetyl levels in infected cells. The activity of HDAC classes I and II was

blocked with Trichostatin A (TSA) and that of class III, the sirtuins, was blocked with Nicotinamide (NIC). TSA treatment did not inhibit infection-induced deacetylation, while, NIC treatment completely blocked H3K18 deacetylation, suggesting a role for sirtuins in deacetylation (fig S3A). We further used specific inhibitors of the sirtuin family. Our results show that, whereas a SIRT1 inhibitor, CTCC, had no effect, a SIRT2 inhibitor, AGK2, blocked infection-induced deacetylation of H3K18. We also knocked down by siRNA, SIRT1, SIRT2, SIRT6 or SIRT7, which have reported deacetylase activity and are localized either in the cytoplasm or nucleus. In agreement with results obtained with chemical inhibitors, only the SIRT2 siRNA blocked H3K18 deacetylation upon infection, suggesting that SIRT2 is the HDAC responsible for this modification (fig 2A). Complementation of SIRT2 siRNA treated cells with a plasmid encoding wild type siRNA-insensitive SIRT2, restored infection-induced deacetylation to SIRT2 knocked down cells (fig S3B). However, deacetylation was not restored when cells were transfected with a plasmid encoding a catalytically inactive siRNA-insensitive SIRT2 plasmid, even though SIRT2 still relocalized to the nucleus (fig S3C). Taken together, these results demonstrate for the first time, that in cells SIRT2 is responsible for deacetylating H3K18, in agreement with previous *in vitro* data ([Black et al., 2008](#)). Interestingly, H3K18 was recently found to be deacetylated by SIRT7 in cancer cells ([Barber et al., 2012](#)), suggesting that different deacetylases act on this residue under different conditions.

SIRT2 has mainly been characterized in the cytoplasm of interphasic cells ([North and Verdin, 2007a](#)). We therefore examined the localization of SIRT2 during infection. Interestingly, as shown by immunofluorescence, cells infected with *L. monocytogenes* showed a clear nuclear labeling whereas in uninfected cells the distribution of SIRT2 was ubiquitous (fig 2B). We next fractionated cells into cytosolic, nuclear, and chromatin soluble fractions. The two main SIRT2 splice variants previously described ([North and Verdin, 2007b](#)) were detected in the cytosol, and the large isoform was seen in the nuclear fraction of uninfected and infected cells. Strikingly, only in infected cells, SIRT2 localized to the chromatin fraction, where H3 deacetylation was observed (fig 2C, S4). We further assessed whether retaining SIRT2 in the nucleus with leptomycin B (without infection) was sufficient to deacetylate H3K18. Interestingly, leptomycin B caused SIRT2 accumulation in the nucleus, but did not lead to H3K18 deacetylation (fig S5A, B).

Therefore, infection induces targeting of SIRT2 to the chromatin fraction where deacetylation of H3K18 occurs.

To identify the bacterial factor(s) necessary for inducing H3K18 deacetylation, we screened *L. monocytogenes* mutants defective for infection. One mutant, *ΔinlB*, which is defective for invasion of HeLa cells, did not exhibit H3K18 deacetylation, suggesting that either the InlB protein itself, or entry of bacteria, is important for inducing H3K18 deacetylation (fig 1D). InlB is a surface protein of *Listeria*, which upon interaction with the cell surface receptor c-Met mediates entry of bacteria or beads into non-phagocytic cells. We then tested whether a non-invasive species *Listeria innocua*, which when engineered to express InlB is able to enter into HeLa cells, can induce H3K18 deacetylation. Figure 1D shows that while *L. innocua* has no effect, *L. innocua* expressing InlB led to H3K18 deacetylation levels similar to those induced by *L. monocytogenes*, strongly suggesting that no other virulence factor besides InlB is necessary for H3K18 deacetylation. Similar results were obtained with polystyrene beads coated with InlB, which induced H3 deacetylation, whereas uncoupled beads had no effect. Furthermore, purified InlB was sufficient to induce H3K18 deacetylation. Interestingly, when treating cells with the natural c-Met ligand, the hepatocyte growth factor (HGF), deacetylation was also observed to similar levels and with the same kinetics as with purified InlB (figure 1D, S6A-C). In contrast, cells treated with epidermal growth factor (EGF), which binds the EGF-receptor (EGF-R), had no effect (fig 1D, S6A, C). The correlation between deacetylation of H3K18 and SIRT2 relocalization was also assessed with purified InlB, HGF and EGF. Strikingly, immunofluorescence analysis of cells treated with either InlB or HGF shows that the nuclear accumulation of SIRT2 was observed in all conditions where deacetylation occurred, and did not occur upon EGF treatment (fig 2D). Together these data show that InlB or HGF, through the c-Met receptor, are sufficient to induce SIRT2 nuclear translocation and H3K18 deacetylation.

We then addressed the effect of the signaling cascade downstream of c-Met on H3K18 deacetylation. We treated cells with inhibitors of tyrosine phosphorylation, PI3K and Akt, all known to be activated upon binding of InlB to c-Met, and assessed acetyl H3K18 levels and SIRT2 relocalization. When cells were treated with genistein to block

tyrosine phosphorylation, neither InlB nor HGF induced H3K18 deacetylation or SIRT2 nuclear targeting within the time assayed (fig 2D, S6A). Next, we showed using either chemical inhibition of PI3K, with wortmannin or LY294002, or expression of a dominant negative p85 regulatory subunit, that PI3K activity is necessary for SIRT2 nuclear accumulation and H3K18 deacetylation (fig 2D, S6B, D, E). We further assessed the role of Akt by using the chemical inhibitor HIMO. This compound blocked InlB- and HGF-dependent H3K18 deacetylation and nuclear relocalization of SIRT2 (fig S6C, 2D). Together, these results establish that the signaling cascade mediated by the cell receptor c-Met and the downstream signaling factors PI3K and Akt is one essential pathway linking *L. monocytogenes* to SIRT2 and H3K18 deacetylation.

To further characterize the role of SIRT2 during infection, we searched for genes modulated during infection, in a SIRT2-dependent manner. Transcriptome analyses were carried out comparing 4 different conditions: uninfected HeLa cells, cells infected for 5 hours with *L. monocytogenes*, and AGK2 pretreated cells with or without infection. Strikingly, when comparing uninfected cells, treated or not with AGK2, we did not identify any genes that were differentially regulated in a significant manner, suggesting that SIRT2 has no effect on resting cells (fig 3A). This observation is consistent with our cell fractionation data, which show that in resting cells only a small fraction of SIRT2 is chromatin bound. In contrast, AGK2 had a significant effect on gene transcription induced by infection. Indeed, in the absence of AGK2, infection with *L. monocytogenes* led to activation of 158 genes, and repression of 272 genes. Remarkably, pretreatment with AGK2 significantly decreased the number of infection-induced activated and repressed genes to 30 and 1 respectively. Using these data, we categorized genes as SIRT2-independent if AGK2 pretreatment had no effect on their expression, and SIRT2-dependent if AGK2 affected their expression, and validated these results by quantitative PCR on a subset of genes (fig S7). Our data strongly suggested that gene repression during infection with *L. monocytogenes* is almost entirely dependent on SIRT2 activity, and mediated by InlB (fig 3A, S8). The 271 genes identified as SIRT2-dependent repressed genes are diverse and participate in many essential cellular functions (table S1). Of note, are genes involved in immune response regulation such as regulators of B and T cell receptor signaling (RASGRP1, MAPK14, PIK3R3, PTPNG, SOS1, VAV3, ABL1, CAMK26,

MAP2K6, LEF1), the chemokine CXCL12 which is strongly chemotactic for lymphocytes, and the interferon transcription factor IRF2. In addition a significant number of repressed genes are DNA binding proteins and/or are implicated in transcriptional regulation, strongly suggesting that *L. monocytogenes* is hijacking SIRT2 in order to impose a transcriptional control on the host.

Previous studies have shown in T-cells, that H3K18 acetylation levels are enriched at transcriptional start sites (TSSs) and enhancers of active mammalian genes ([Rando and Chang, 2009](#); [Wang et al., 2008](#)). We thus probed the TSSs of SIRT2-regulated genes for SIRT2 recruitment and H3K18 deacetylation by chromatin immunoprecipitation (ChIP). Remarkably, all tested SIRT2-dependent repressed genes (MYLIP, EHHADH, SYDE2, ERCC5, and LEF1) exhibited a more than 10 fold recruitment of SIRT2 and a significant decrease in the level of acetylated H3K18 upon infection (fig 3C). All other genes assayed showed the opposite, i.e. an increase in acetylated H3K18, and a loss of SIRT2 at their TSSs (fig 3B). Interestingly, SIRT2 recruitment and H3K18 deacetylation were only observed at the TSSs, and not at exon 2, strongly supporting a role for SIRT2 in transcriptional regulation (fig S9). Since H3 deacetylation is observed globally by western blot, we predict it must also occur in other regions besides the TSS of specific genes, perhaps in intergenic regions as reported for Adenovirus infections ([Ferrari et al., 2012](#)). We further verified that other histone residues were not modified upon SIRT2 recruitment. ChIP experiments using anti-AcH3K9, AcH3K14, and AcH4K16 antibodies showed that none of the corresponding residues were deacetylated at the genes where SIRT2 was recruited (fig S10). Interestingly, acetylation of H3K18 and H4K16 are anti-correlated, which is in agreement with what had previously been described ([Kurdistani et al., 2004](#)). Therefore, our data support a model in which infection targets SIRT2 to a subset of genes, where it specifically imposes H3K18 deacetylation and gene repression.

We next assessed the impact of SIRT2 on infection. We first performed experiments in tissue culture cells using either a siRNA approach or a pharmacological approach. Infection was quantified either by western blot, measuring the levels of a secreted bacterial factor, InlC, which accumulates during infection ([Gouin et al., 2010](#)), or by FACS analysis of host cells infected with GFP-expressing *L. monocytogenes*. Treating

cells with siRNA against SIRT1, 6 or 7, or a SIRT1 chemical inhibitor, CTCC had no effect on infection (fig 4A, S11). In contrast, cells treated with a SIRT2 siRNA or inhibitor, AGK2, were significantly less infected than untreated cells (fig 4A, S12). It should be noted that SIRT2 is not toxic to bacteria, nor does it affect the host's cell cycle (data not shown and fig S10). Interestingly, although the initial stages of infection progress similarly in the presence or absence of AGK2, at later times of infection, the levels of InlC or the GFP fluorescence detected in untreated cells was significantly greater than in cells treated with AGK2 (fig S12). We also showed that there was no motility or cell-to-cell spread defect in response to AGK2 treatment (fig S12). Therefore SIRT2 is required for the late stages of a listerial infection, most probably for bacterial replication, in tissue cultured cells.

The impact of SIRT2 on infection was also determined *in vivo* in *Sirt2^{tm1a(EUCOMM)Wtsi}* mice (*Sirt2*^{-/-}) generated at the Sanger Institute. Wild type or *Sirt2*^{-/-} mice were infected intravenously with *L. monocytogenes* and the spleens and livers were collected for bacterial enumeration. In agreement with our *in vitro* data, the spleens of *Sirt2*^{-/-} mice were significantly less infected than those of wild type mice, confirming the crucial role of SIRT2 on infection *in vivo* (fig 4B). We further tested the role of InlB by comparing infection of a *ΔinlB* mutant in both wild type and *Sirt2*^{-/-} mice. Our results show that in contrast to wild type *L. monocytogenes*, a *ΔinlB* mutant infects both wild type and *Sirt2*^{-/-} mice strains similarly (fig 4B), confirming the importance of InlB in hijacking SIRT2 *in vivo*. We further assessed the levels of H3K18 acetylation in the spleens of infected mice. Interestingly, whereas deacetylation occurred in wild type mice, it did not in *Sirt2*^{-/-} mice, or in wild type mice infected with a *ΔinlB* mutant (fig 4C). Together our data definitively establish that *in vivo* the activity of SIRT2 on H3K18 is important for infection, and that InlB is the bacterial factor triggering this activity.

In summary, our study reveals that *L. monocytogenes* hijacks the host HDAC, SIRT2 to impose a transcriptional program on the host. We have uncovered a nuclear function for SIRT2 in deacetylating H3 specifically on lysine 18 in response to infection, and to activation of the PI3K/AKT signaling cascade. To our knowledge this is the first report demonstrating that a histone modifier is essential for infection.

Figure 1

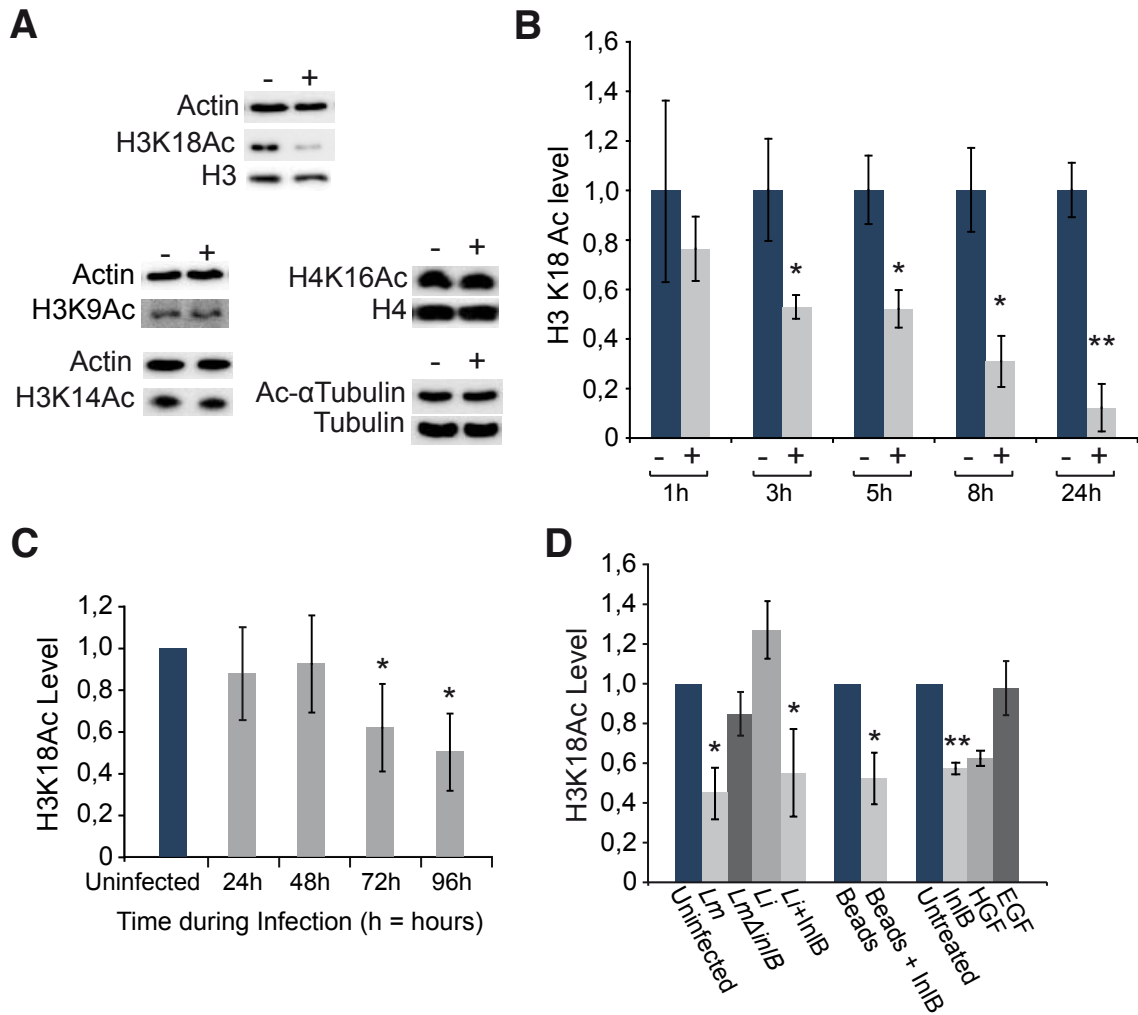


Figure 1. Infection induces deacetylation of H3K18

(A) Acetylation levels in uninfected HeLa (-) and *L. monocytogenes* infected cells (+) as detected by immunoblotting. (B-D) Quantification of acetylated H3K18 immunoblots in HeLa cells (B & D) ($n \geq 3$) and spleen of Balb/c mice ($n \geq 4$ mice per time point) (C). (D) Quantification of acetylated H3K18 immunoblots in HeLa cells infected with *Listeria innocua* or *Listeria monocytogenes* mutant stains or treated with purified proteins. Error bars represent the standard error of the mean (s.e.m.). Statistical significance was calculated using a student t-test. * $p < 0.05$; ** $p < 0.001$.

Figure 2

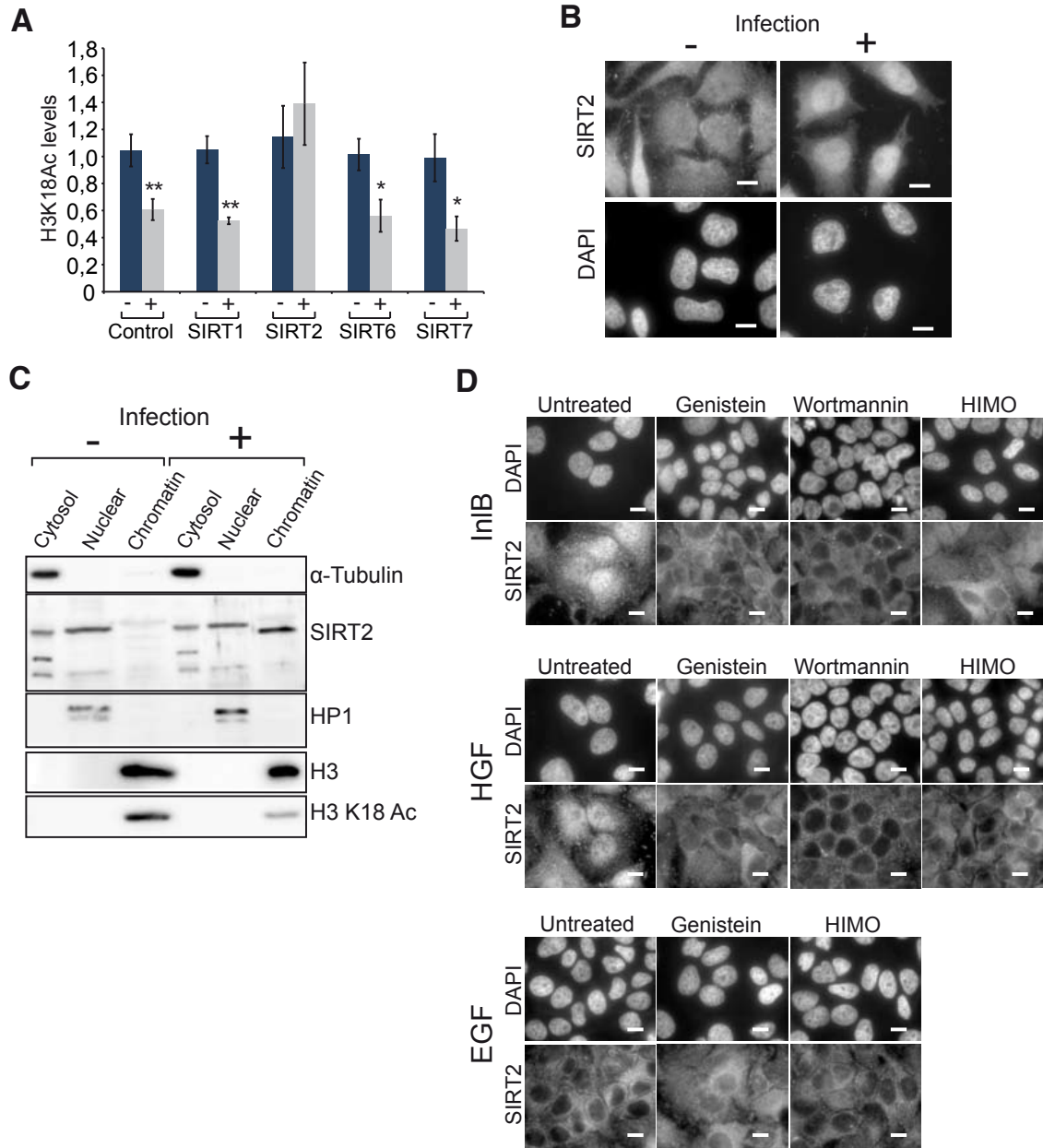


Figure 2. SIRT2 deacetylates H3K18 and is relocalized to the nucleus upon infection.

(A) Quantification of acetylated H3K18 immunoblots in uninfected (-) or infected (+) cells knocked down for the expression of sirtuins by siRNA. (B & D) Endogenous SIRT2 was detected by immunofluorescence of HeLa cells uninfected (-) or infected (+) or treated with purified signaling factors and treated with chemical inhibitors. Scale bar = 10 μ m. (C) Immunoblots of cell fractionation. Experiments represent $n \geq 3$. Error bars are SEM. Statistical significance was calculated using a student t-test. * $p < 0.05$; ** $p < 0.001$.

Figure 3

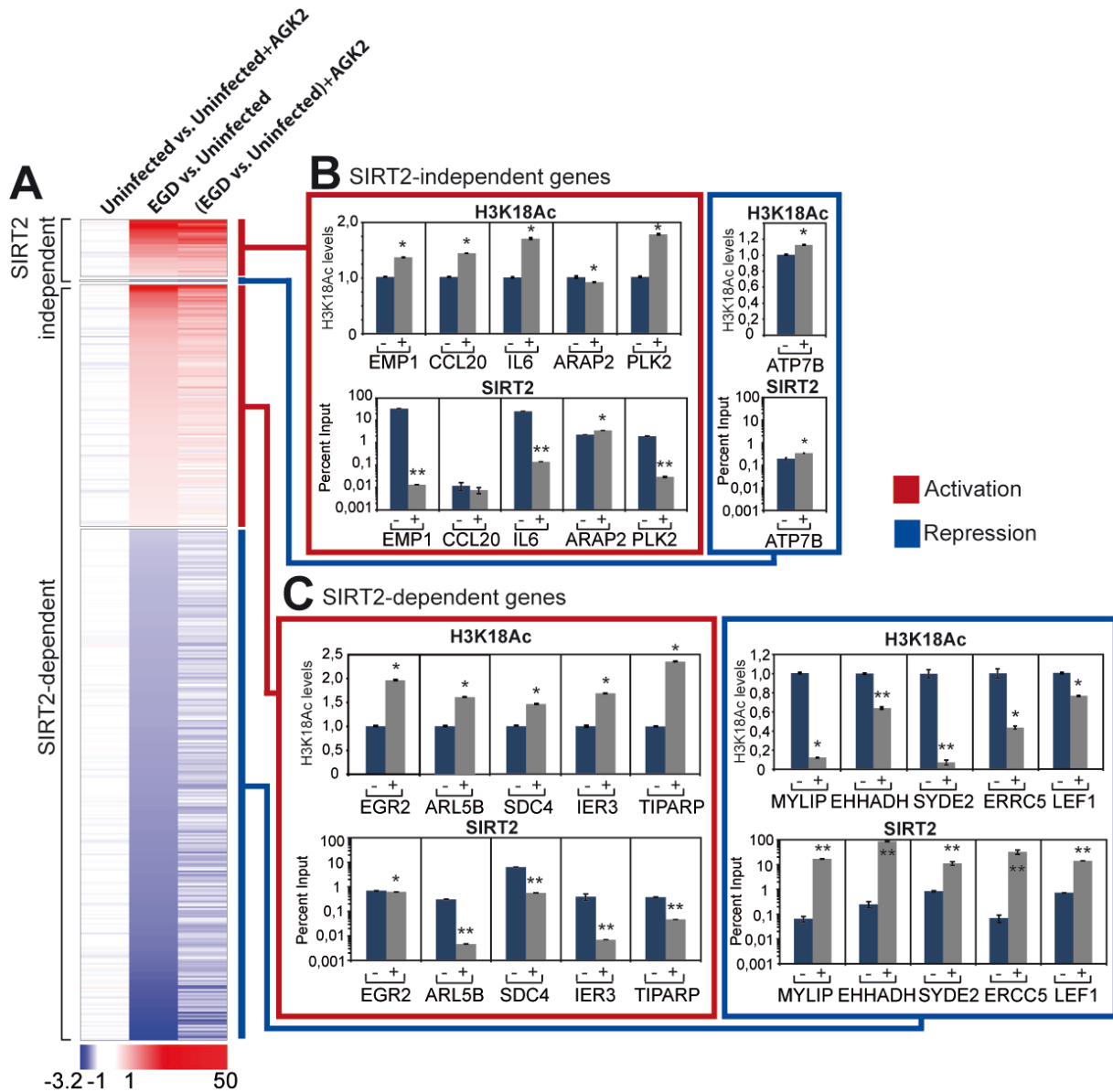


Figure 3. SIRT2 regulates genes during infection. (A) Heatmap representation of the mean fold-change in gene expression as determined by transcriptome analysis of Caco2 cells infected for 5h ($n \geq 2$). Red represents gene activation while blue gene repression. (B & C) Chromatin immunoprecipitation using antibodies targeting SIRT2, H3K18Ac, and H3 was quantified by qPCR ($n \geq 3$). H3K18Ac qPCRs are normalized to H3 qPCRs, and SIRT2 qPCR results are represented as % of the input. Error bars are SEM. Statistical significance was calculated using a student t-test. $p^* p < 0.05$; $** p < 0.001$.

Figure 4

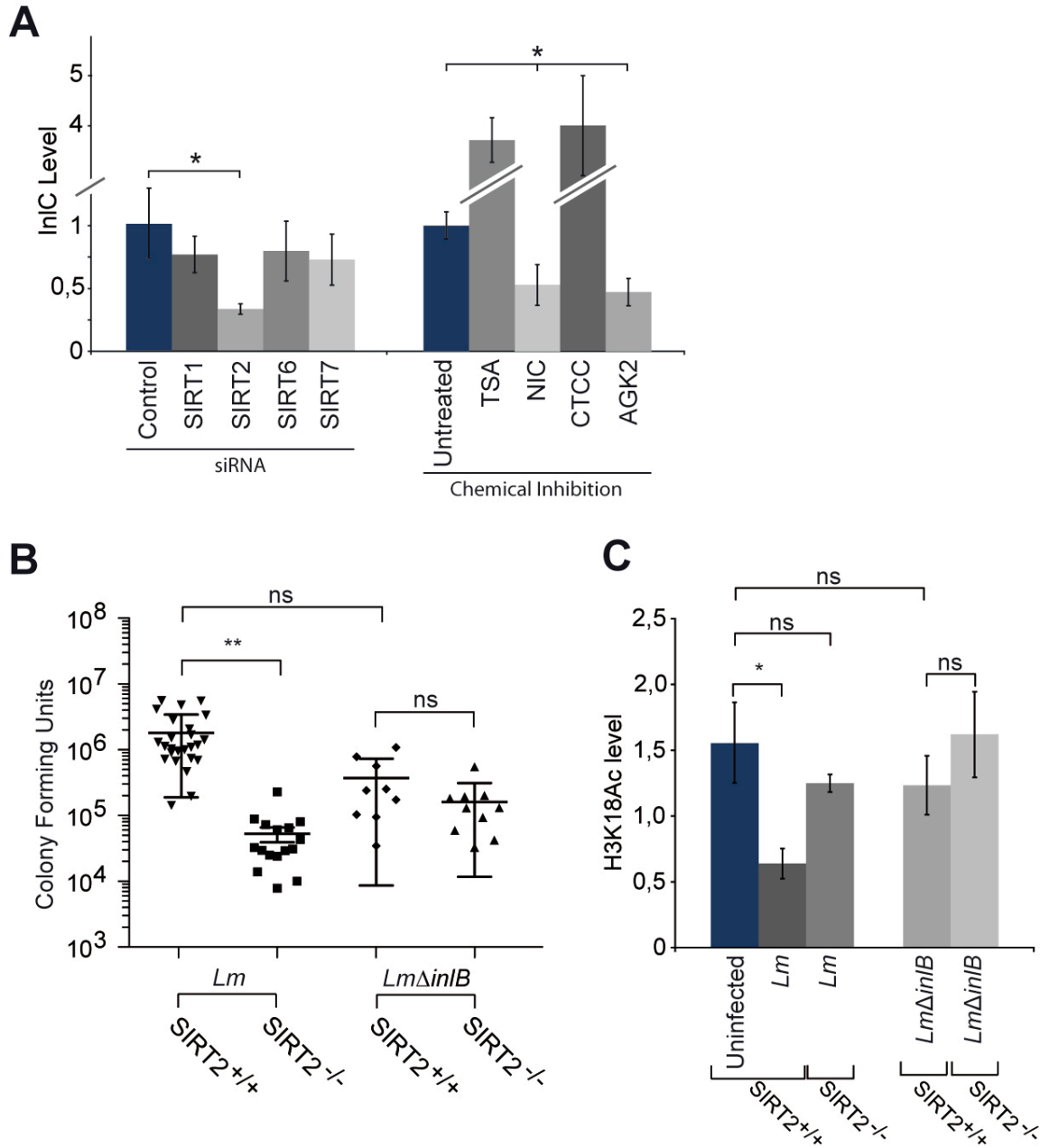


Figure 4. SIRT2 is necessary for infection. (A) Quantification of immunoblots detecting the bacterial protein InIC in 5h-infected HeLa cells knocked down for SIRTs 1, 2, 6, and 7 by siRNA or in cells treated with chemical deacetylase inhibitors. (B) Colony forming units in spleens of SIRT2^{+/+} or SIRT2^{-/-} mice infected for 72h with *L. monocytogenes* (*Lm*) or Δ *inIB* (Δ *inIB*). Each symbol represents one mouse. (C) Immunoblot analysis of H3K18 acetylation levels in mice spleens. Error bars are SEM. Statistical significance was calculated using a student t-test. * p< 0.05; ** p< 0.001; ns = non significant.

SUPPORTING MATERIAL FOR:

A role for SIRT2-dependent histone H3K18 deacetylation in bacterial infection

Authors: Haig A Eskandarian^{1,2,3}, Francis Impens^{1,2,3}, Marie-Anne Nahori^{1,2,3}, Guillaume Soubigou⁴, Jean-Yves Coppée⁴, Pascale Cossart^{1,2,3,*}, Mélanie Hamon^{1,2,3,*}

Affiliations:

¹Unité des Interactions Bactéries-Cellules, Institut Pasteur, Paris F-75015, France.

²Inserm, Unité 604, Paris F-75015, France.

³Institut National de la Recherche Agronomique, Unité Sous Contrat 2020, Paris F-75015, France.

⁴Plate-forme 2, Transcriptome et Epigénome, Génopole, Institut Pasteur, Paris F-75015, France

*Correspondence: hamon@pasteur.fr (M.H.), pcossart@pasteur.fr (P.C.).

Supplementary text

- Infection-induced deacetylation occurs specifically at H3K18
- *Listeria* induces H3K18 deacetylation through a different mechanism than adenovirus

Supplementary figures

Figure S1. *L. monocytogenes* induces H3K18 deacetylation

Figure S2. Quantification of H3K18 deacetylation

Figure S3. The catalytic activity of SIRT2 is necessary for H3K18 deacetylation

Figure S4. SIRT2 is relocalized to the nuclear and chromatin fractions upon infection

Figure S5. Nuclear localization of SIRT2 is not sufficient for inducing H3K18 deacetylation

Figure S6. H3K18 deacetylation is induced through activation of the PI3K/AKT pathway

Figure S7. Validation of microarray analysis

Figure S8. InlB and HGF are sufficient to modulate SIRT2-dependent genes

Figure S9. H3K18 deacetylation does not occur at exon 2

Figure S10. Deacetylation at TSS is specific to H3K18

Figure S11. AGK2 does not affect the cell cycle

Figure S12. SIRT2 is essential for a listerial infection *in vivo*

Supplementary text

Infection-induced deacetylation occurs specifically at H3K18

We have demonstrated that SIRT2 plays an essential role in deacetylating H3K18. Its effect on H3K18 during infection appears to be specific, as deacetylation of other H3 lysines or known targets, such as tubulin and H4K16, does not occur (fig 1A). Furthermore, this specificity holds true *in vivo* since deacetylation of H3K9 or H3K14 does not occur (fig S1C). In addition, we verified at the gene level whether other lysines were deacetylated at the same position as where SIRT2 was recruited. Figure S9 shows that other lysines are not deacetylated at the TSS of genes repressed by SIRT2. Therefore, even though we cannot exclude that SIRT2 is targeting other proteins during infection, we were unable to identify any other residue besides H3K18 that was deacetylated by SIRT2.

Listeria induces H3K18 deacetylation through a different mechanism than adenovirus

Adenovirus infection causes a threefold reduction in total cellular histone H3K18 acetylation, through binding and sequestering the HATs CBP and p300 to a specific subset of host genes ([Horwitz et al., 2008](#)). We have found that *L. monocytogenes* induces H3K18 deacetylation through SIRT2 recruitment to specific host genes. We thus verified that CBP was not being recruited to the same genes where SIRT2 was binding (figure S8). We have thus ruled out that listeria induced H3K18 deacetylation through sequestering of CBP. However, for adenovirus-induced H3K18 deacetylation, it is possible that SIRT2 could be involved as well as CBP.

Supplementary figures

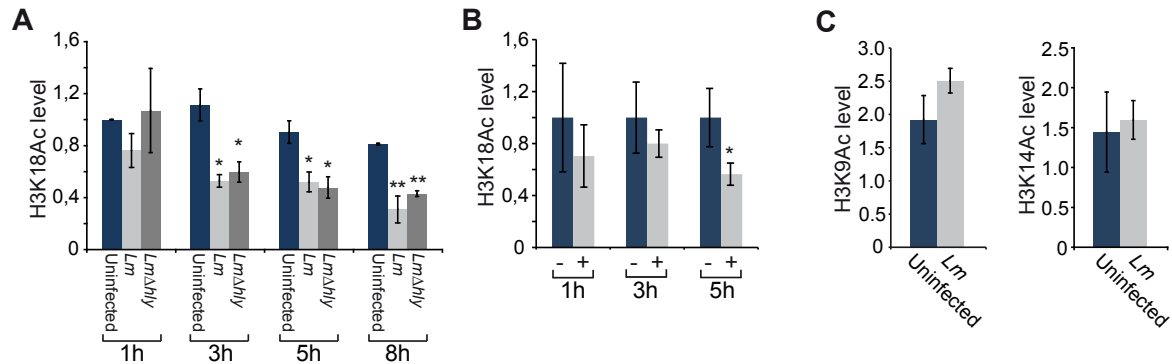


Figure S1. *L. monocytogenes* induces H3K18 deacetylation. (A) H3K18 acetylation levels were measured by western blot of HeLa cells infected with either wild type *L. monocytogenes* (*Lm*) or a mutant lacking LLO (*Lm* Δ *hly*). H3K18 deacetylation is induced by *L. monocytogenes* independently of listeriolysin O (LLO), as *Lm* Δ *hly* mutant induces the same amount of H3K18 deacetylation as a wild type strain. (B) Quantification of by western blot analysis CaCO₂ cells uninfected (-) or infected (+) with *L. monocytogenes*. H3K18 deacetylation occurs in CaCO₂ cells similarly to HeLa cells upon infection. (C) Quantification of H3K9 and H3K14 acetylation levels in spleens of C57BL/6 mice uninfected or infected with *L. monocytogenes* (*Lm*). No H3K9 or H3K14 deacetylation is observed *in vivo*, which is consistent with *in vitro* data showing that lysine 18 is the residue detected as being deacetylated. Quantitation of western blots was performed on n \geq 3. Error bars are standard error of the mean (SEM). Statistical significance was calculated using a student t-test. * p < 0.05; ** p < 0.001.

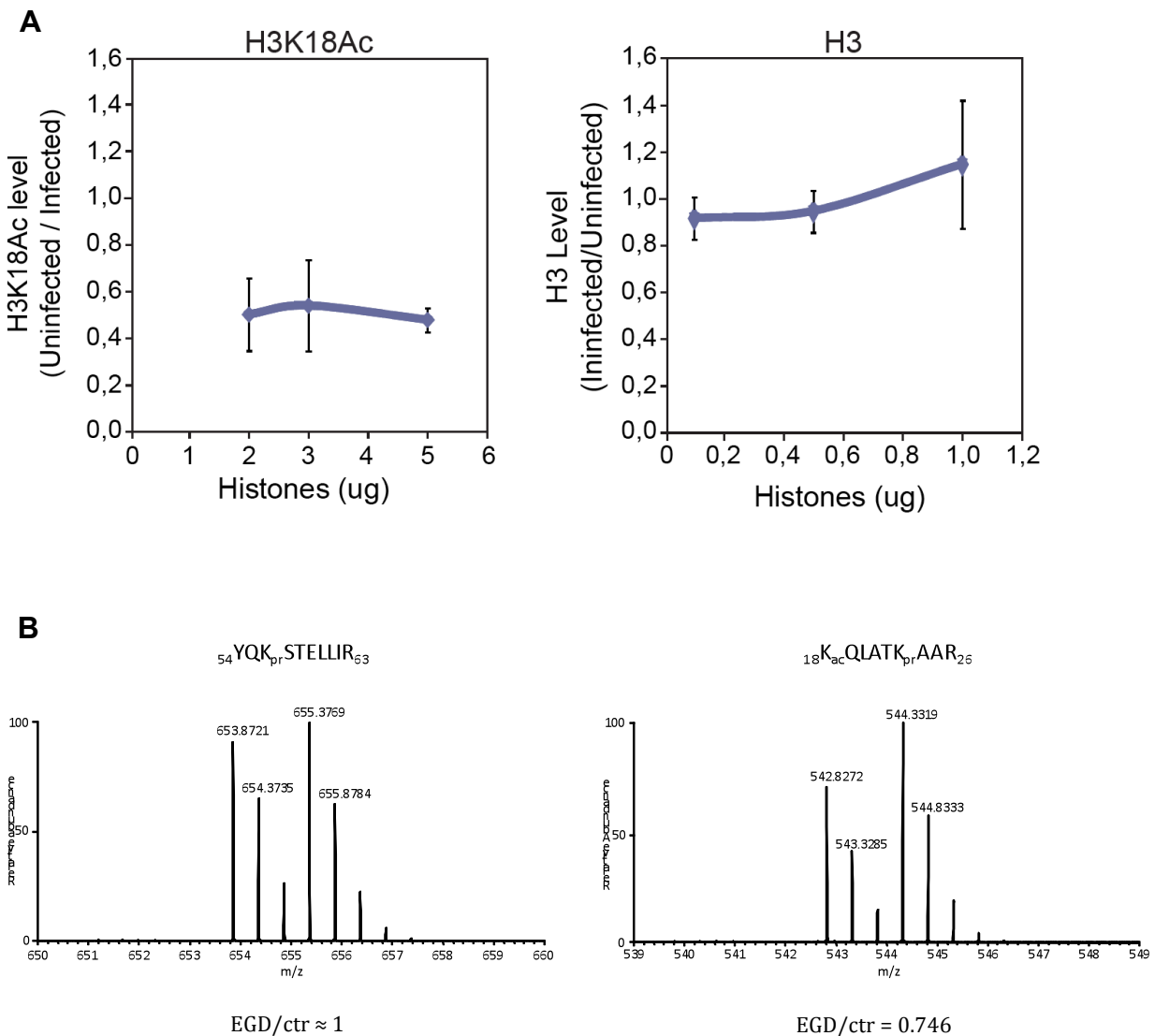


Figure S2. Quantification of H3K18 deacetylation levels by mass spectrometry.

(A) Different concentrations of Purified histones were immunoblotted for H3K18 acetylation and H3. Plots of the quantified values are shown as a ratio of uninfected samples/infected for 3 experiments. Error bars are SEM. These results show that over a range of histone concentrations deacetylation of H3K18 is linear, and therefore infection induces deacetylation of H3K18 of approximately 50% at 5h of infection. (B) Deacetylation of H3K18 was confirmed by differential mass spectrometry (MS) using an adapted version of the protocol of Garcia et. al. ([Garcia et al., 2007](#)). Briefly, histones purified from HeLa cells infected or not with *Listeria EGD* were separated by SDS-PAGE and stained by coomassie blue. Protein bands corresponding to histone H3 were cut and modified by in-gel differential propionylation ([Damme et al., 2013](#); [Staes et al., 2011](#)). Modification of free lysine residues with propionyl resulted in longer histone H3 peptides upon trypsin digestion (mimicking Arg-C digestion), which are better detectable by MS, and the use of isotopically light ($^{12}\text{C}_3$, *EGD*) and heavy ($^{13}\text{C}_3$, uninfected) labeled reagents allowed relative

quantification of peptides after mixing equal amounts of both samples. The MS spectrum of YQK_{pr}STELLIR, a peptide near the C-terminus of histone H3 (pr=propionyl group). The lysine residue at position 56 was exclusively identified in its light (m/z=653.8721, *EGD*) or heavy (m/z=655.3769, uninfected) propionylated form, indicating that this residue was not modified *in vivo*. The observed ion ratio is roughly 1:1, demonstrating equal mixing of both samples. The MS spectrum of K_{ac}QLATK_{pr}AAR, the peptide carrying acetylated K18 at its N-terminus (pr=propionyl group, ac=acetyl group). Doublet peaks at 542.8272 and 544.3319 m/z correspond to forms of the peptide with light or heavy propionylated K23, derived from the *EGD* infected and uninfected sample, respectively. The lower presence of this peptide in the *EGD* infected sample indicated deacetylation of K18 with 25.4%.

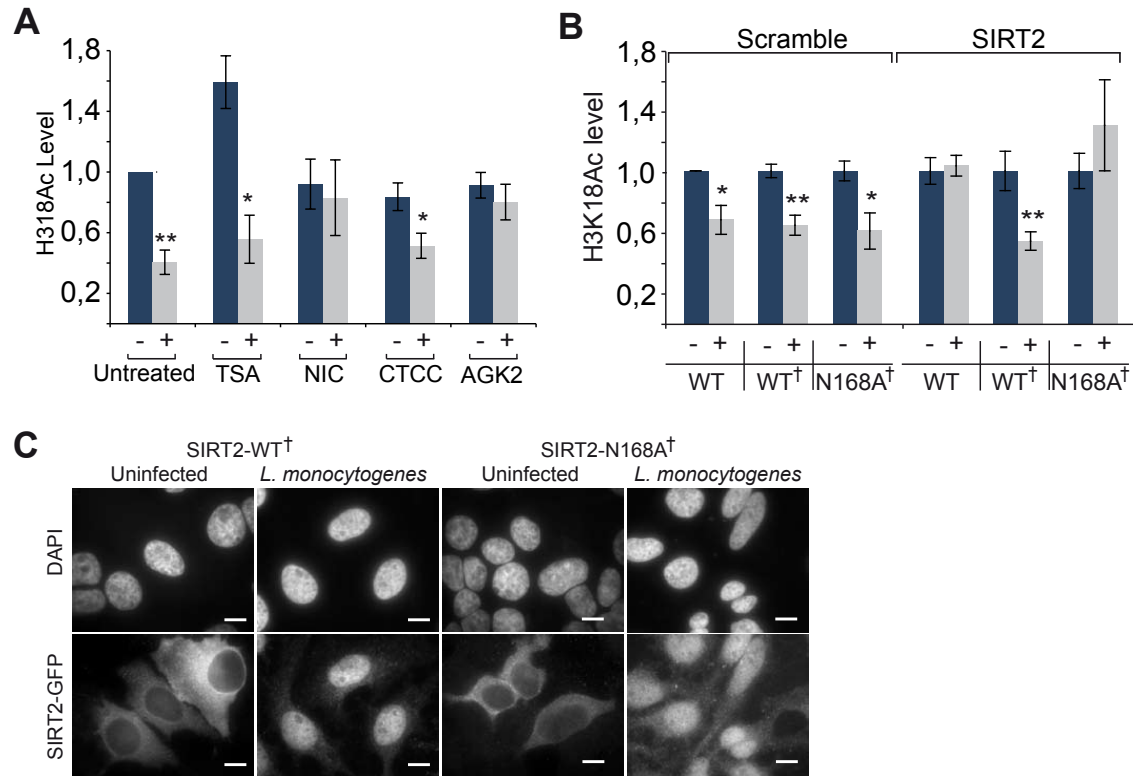


Figure S3. The catalytic activity of SIRT2 is necessary for H3K18 deacetylation

(A) HeLa cells are pretreated with HDAC inhibitors and the signal intensity of H3K18 acetylation levels are quantified from immunoblots. Cells are either uninfected (-) or infected (+) with *L. monocytogenes*. Abbreviation are as follows: TSA-trichostatin A (class I & II inhibitors), NIC- Nicotinamide (class III inhibitor), CTCC (SIRT1 inhibitor) or AGK2 (SIRT2 inhibitor). NIC and AGK2 are the only inhibitors that block infection-induced deacetylation, suggesting that SIRT2 is important for H3K18 deacetylation. (B) Cells are transfected either with scramble or SIRT2 siRNA, and with a plasmid expressing wild type SIRT2 (WT), a siRNA insensitive SIRT2 (WT⁺) or a catalytically inactive siRNA insensitive SIRT2 (N168A⁺). Levels of H3K18 acetylation are measured by immuoblot in uninfected (-) or *L. monocytogenes*-infected (+) cells. Deacetylation is blocked upon SIRT2 siRNA treatment, and is restored upon transfecting siRNA-insensitive SIRT2. Complementation of SIRT2 siRNA treatment with a catalytically inactive SIRT2 does not restore deacetylation, showing that the catalytic activity of SIRT2 is necessary for H3K18 deacetylation upon infection. $n \geq 3$. Error bars are SEM. Statistical significance was calculated using a student t-test. * < 0.05; ** < 0.001. (C) SIRT2 is visualized by immunofluorescence microscopy in HeLa cells knocked down for the endogenous expression of SIRT2 by siRNA and complemented with siRNA insensitive SIRT2-GFP constructs, catalytically active (WT⁺) or inactive (N168A⁺). The catalytically inactive SIRT2 relocalizes to the nucleus upon infection similarly to the wild type SIRT2. Scale bar = 10 μ m

	# MS/MS spectra (unique peptides) uninfected	# MS/MS spectra (unique peptides) <i>L. monocytogenes</i>
cytoplasm	959 (65)	455 (46)
nucleus	50 (14)	1090 (58)
chromatin	26 (7)	279 (39)

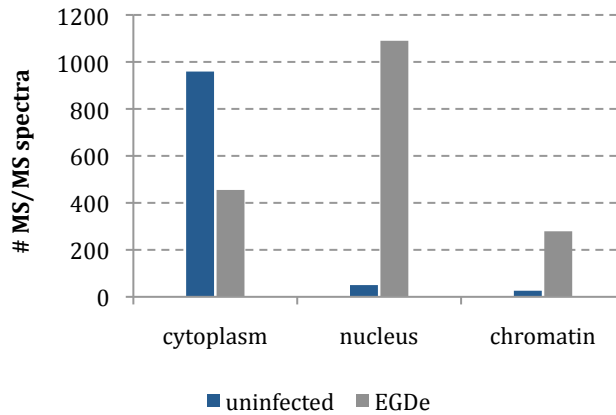


Figure S4: SIRT2 is relocalized to the nuclear and chromatin fractions upon infection

Immunoprecipitation of SIRT2-FLAG from the cytosolic, nuclear and chromatin fraction of *L. monocytogenes* infected and uninfected cells were analyzed by mass spectrometry. The number of spectra detected by mass spectrometry are indicated in the table and in parenthesis is the number of unique and different spectra detected. A graphical representation of the numbers found in the table is also shown. These numbers confirm nuclear translocation and chromatin association of SIRT2 upon infection with *Listeria* EGDe, and show that a baseline level of nuclear and chromatin-associated SIRT2 is detected in uninfected cells.

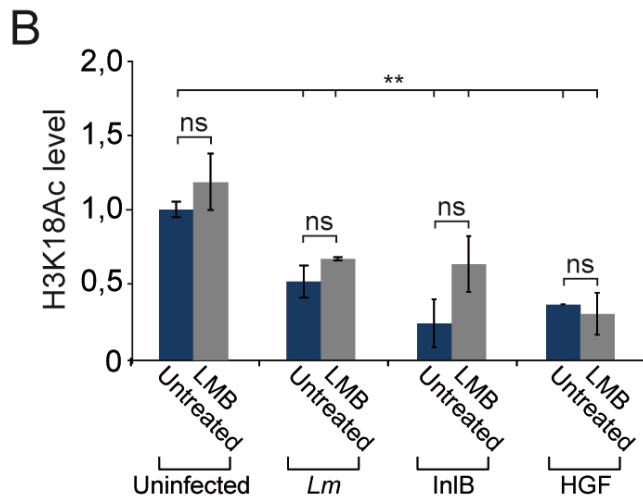
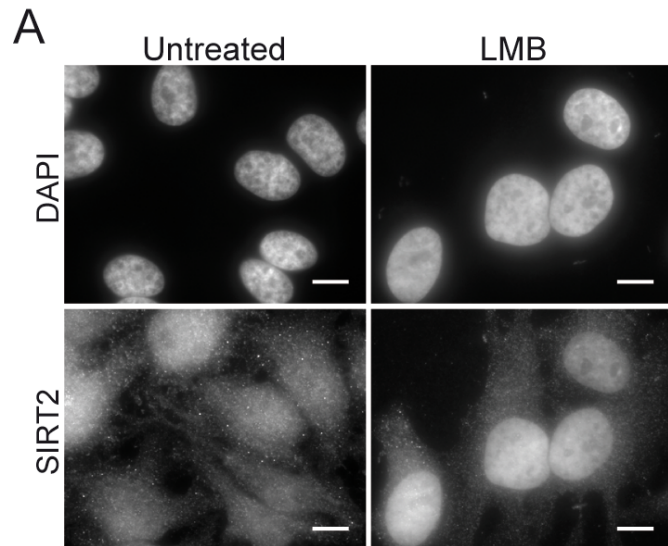


Figure S5. Nuclear localization of SIRT2 is not sufficient for inducing H3K18 deacetylation

(A) SIRT2-GFP is visualized by immunofluorescence microscopy assessed in HeLa cells. SIRT2 is retained in the nucleus upon treatment with leptomycin B (LMB). Scale bar = 10 μ m

(B) Quantification of H3K18 acetylation levels in HeLa cells untreated or treated with Leptomycin B (LMB). Cells are either infected for 5h with *L. monocytogenes* (Lm) or treated with 10ng/ml InlB or HGF for 3h. Leptomycin B treatment does not lead to H3K18 deacetylation, therefore nuclear translocation of SIRT2 is not sufficient to induce H3K18 deacetylation. $n \geq 3$. SEM. ** < 0.001; ns: non significant as measured with a student t-test.

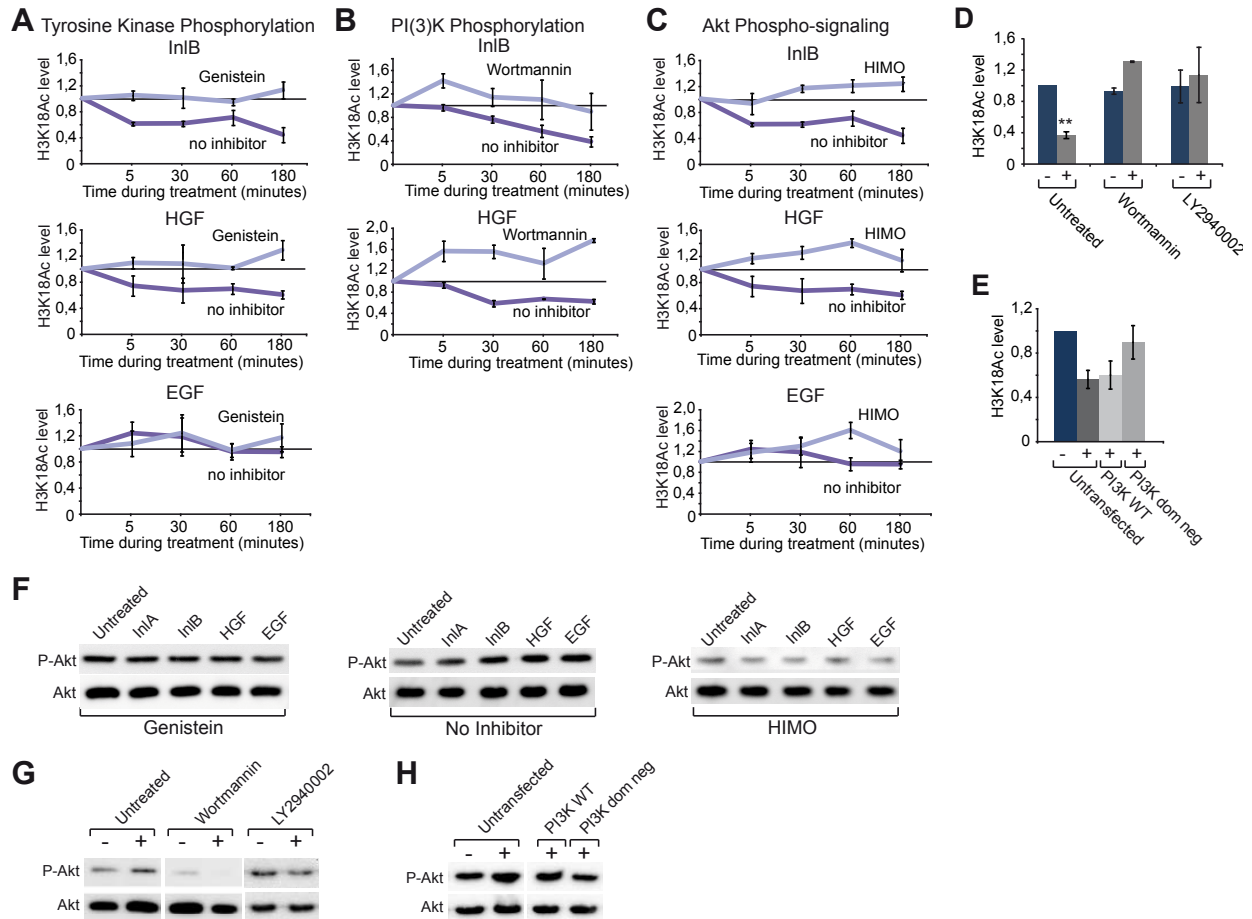
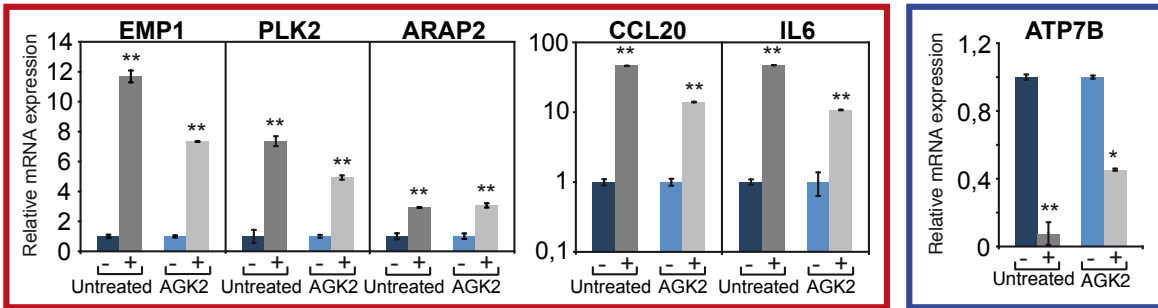


Figure S6. H3K18 deacetylation is induced through activation of the PI3K/AKT pathway

(A-C) HeLa cells are pretreated with inhibitor (Genistein, Wortmannin, or HIMO) and stimulated with InIB, HGF or EGF for different times. H3K18 acetylation levels as detected by immunoblotting, are quantified over time. Results are shown as a ratio of treated cells (InIB, HGF or EGF) to untreated cells. The baseline of 1 is shown as a black line. All inhibitors, Genistein, Wortmannin and HIMO block InIB or HGF induced deacetylation. (D) HeLa cells are pretreated with Wortmannin or LY2940002 prior to infection (+). Both Wortmannin and LY2940002 block infection induced deacetylation. (E) Plasmids expressing either wild type PI3K or a dominant negative PI3K were transfected into HeLa cells which were infected with *L. monocytogenes* (+). Transfection of the dominant negative form of PI3K blocks infection induced H3K18 deacetylation. H3K18 levels are measured by western blot. $n \geq 3$, error bars are SEM, * < 0.05 ; ** < 0.001 as measured with a student t-test. (F-H) Phospho-Akt levels were measured by Immunoblotting of cells treated with inhibitors. Genistein, HIMO, wortmannin, LY2940002, and the PI3K dominant negative mutant inhibit Akt phosphorylation at the concentrations used in our assays. The inhibitors used were therefore active in the above experiments. $n \geq 3$.

SIRT2-independent genes



SIRT2-dependent genes

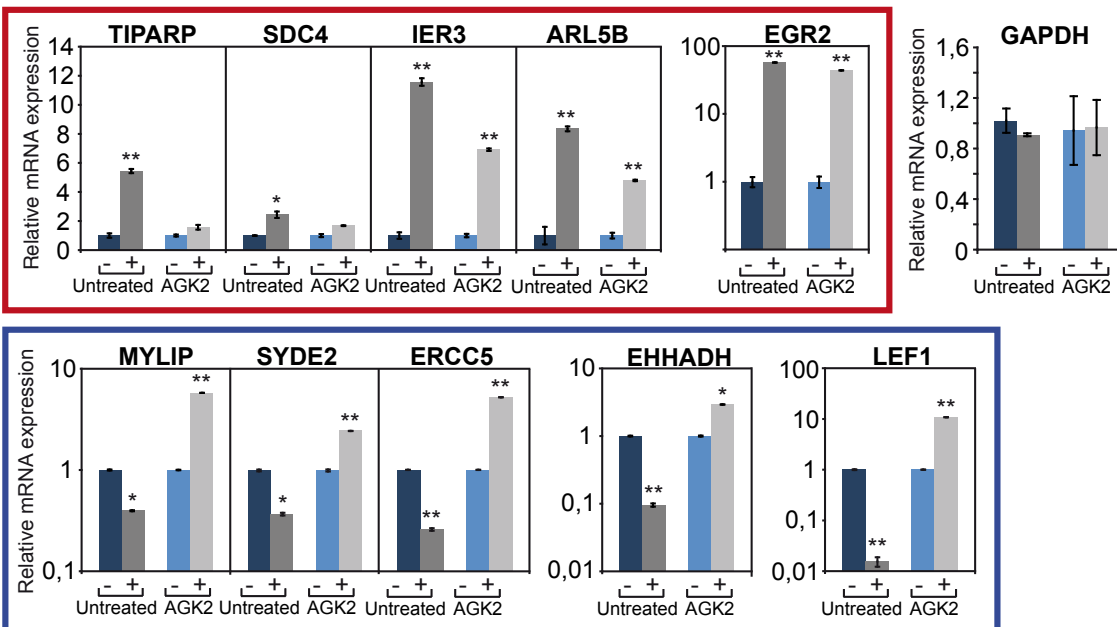
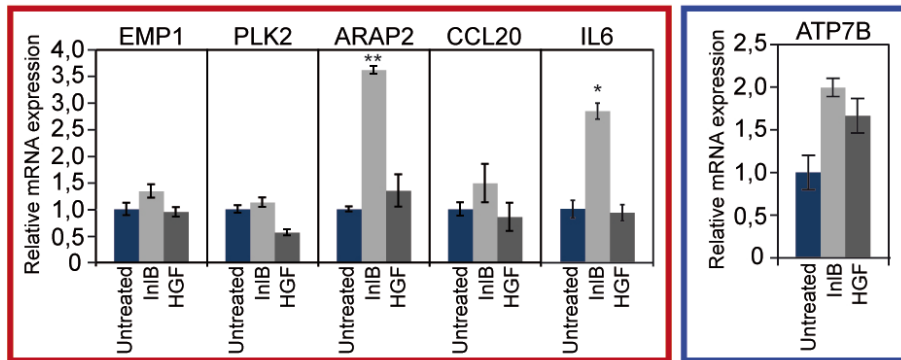


Figure S7. Validation of microarray analysis

Caco2 cells are either uninfected (-) or infected (+) for 5h with *L. monocytogenes*. The relative mRNA expression as detected by quantitative PCR is shown normalized to uninfected untreated samples and to GAPDH, a control unmodified by infection or AGK2 treatment. Infection-dependent activated genes are highlighted in a red box while repressed genes are highlighted by a blue box. Histograms are representative of $n \geq 3$ individual replicates. Error bars on histograms are SEM. * < 0.05; ** < 0.001 as measured with a student t-test.

SIRT2-independent genes



SIRT2-dependent genes

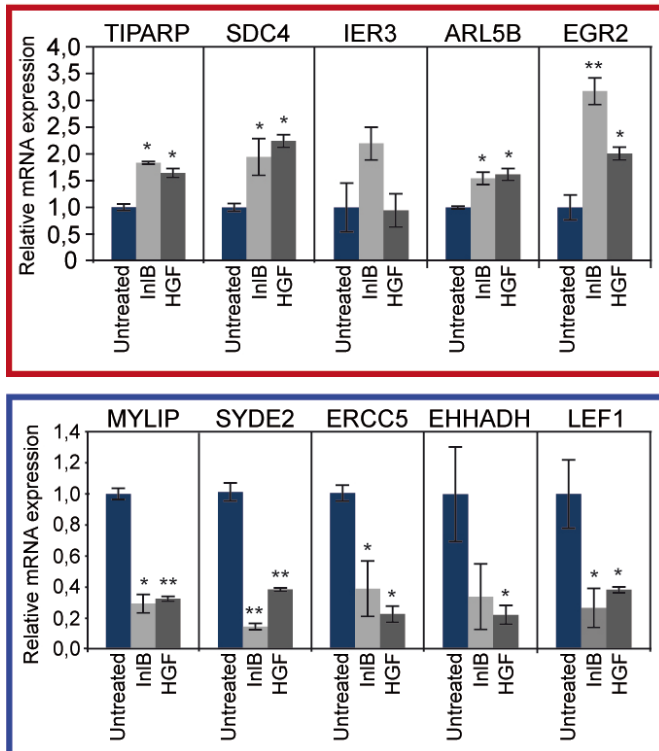
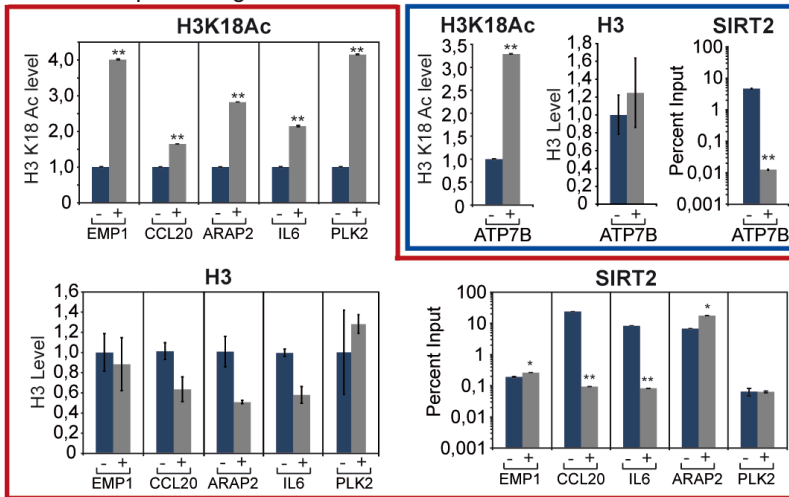


Figure S8. InIB and HGF are sufficient to modulate SIRT2-dependent genes

Caco2 cells untreated or treated with InIB or HGF (10ng/ml) for 3h. The relative mRNA expression as detected by quantitative PCR is shown normalized to untreated samples and to GAPDH (Figure S6). Activated genes are highlighted in a red box and repressed genes are highlighted by a blue box. SIRT2-repressed genes are similarly controlled by InIB and HGF as with infection. $n \geq 3$. SEM. * < 0.05 ; ** < 0.001 as measured with a student t-test.

SIRT2-independent genes



SIRT2-dependent genes

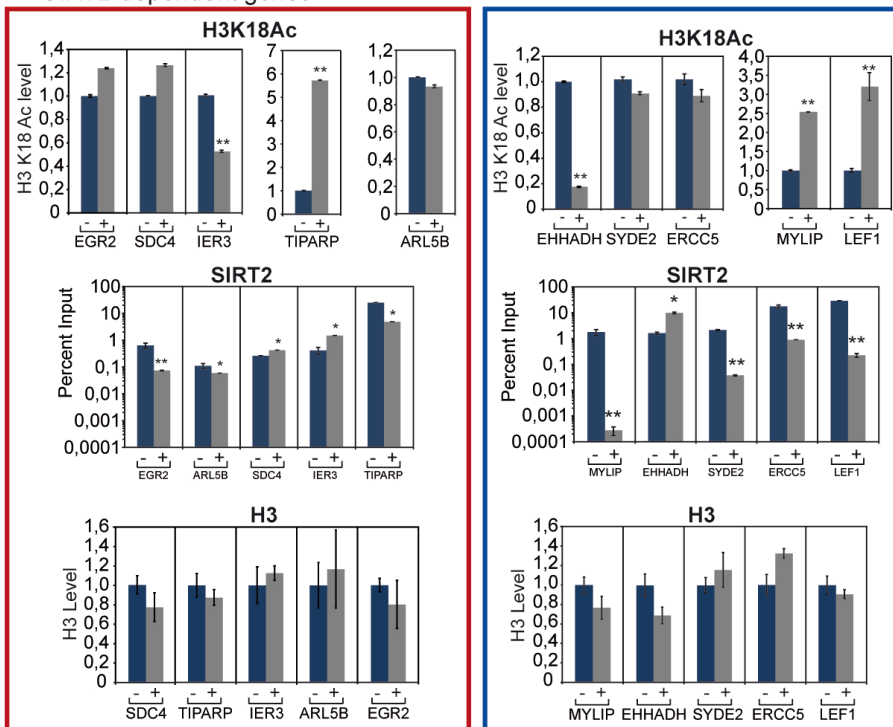


Figure S9. H3K18 deacetylation does not occur at exon 2

Chromatin immunoprecipitations using antibodies targeting SIRT2, H3K18Ac, and H3 were quantified by qPCR ($n \geq 3$) for the region representing the second exon of each selected gene. Activated genes are highlighted in red boxes and repressed genes in blue boxes. H3K18 is not deacetylated and SIRT2 is not recruited to the second exon of genes. Error bars represent the SEM. * < 0.05; ** < 0.001.

SIRT2-activated genes

SIRT2-repressed genes

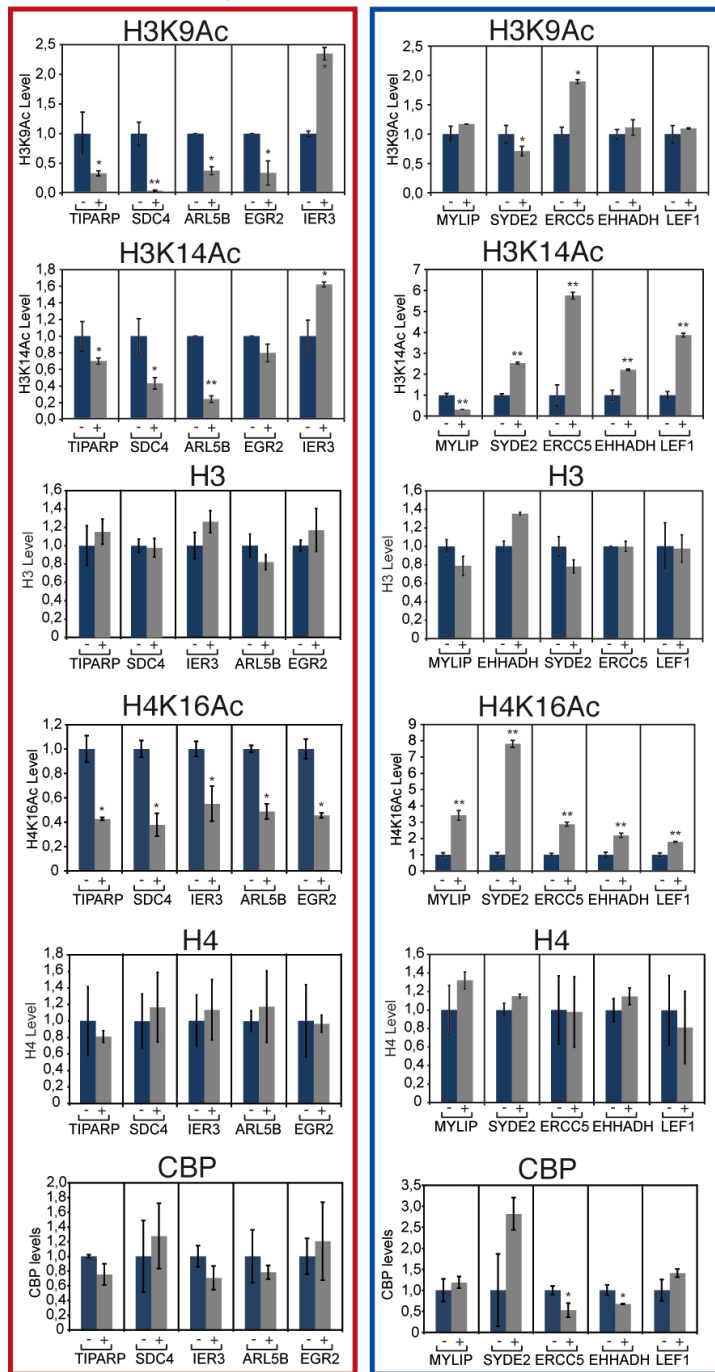


Figure S10. Deacetylation at TSS is specific to K18

ChIP conducted using antibodies targeting H3K9Ac, H3K14Ac, H3, H4K16Ac, H4, and CBP was quantified by qPCR ($n \geq 3$) for the TSS of selected genes modulated during infection in a SIRT2-dependent manner. Deacetylation of H3K9, H3K18 or H4K16, or CBP recruitment was not observed at genes where SIRT2 is recruited. Activated genes are highlighted in red boxes and repressed genes in blue boxes. Error bars represent the SEM. * < 0.05; ** < 0.001.

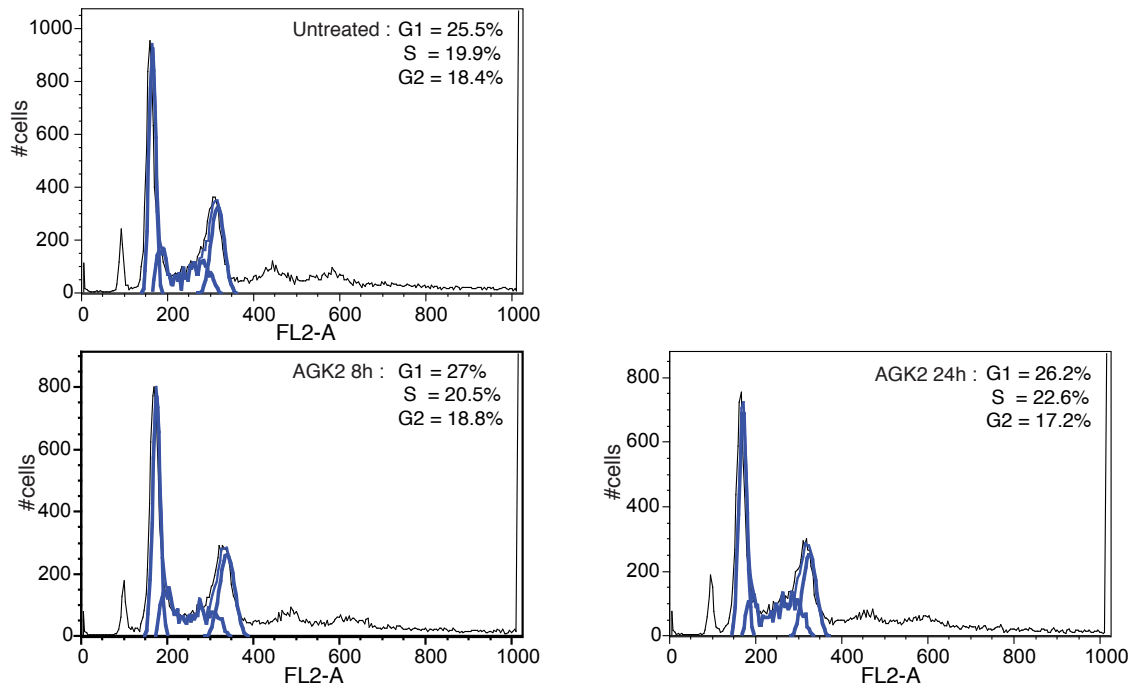


Figure S11. AGK2 does not affect the cell cycle. FACS analysis of 10,000 propidium iodide stained cells Caco2 cells. Cells are untreated or treated for the indicated times with AGK2. Percentage of cells in each stage of the cell cycle is calculated with Flowjo software. $n \geq 3$

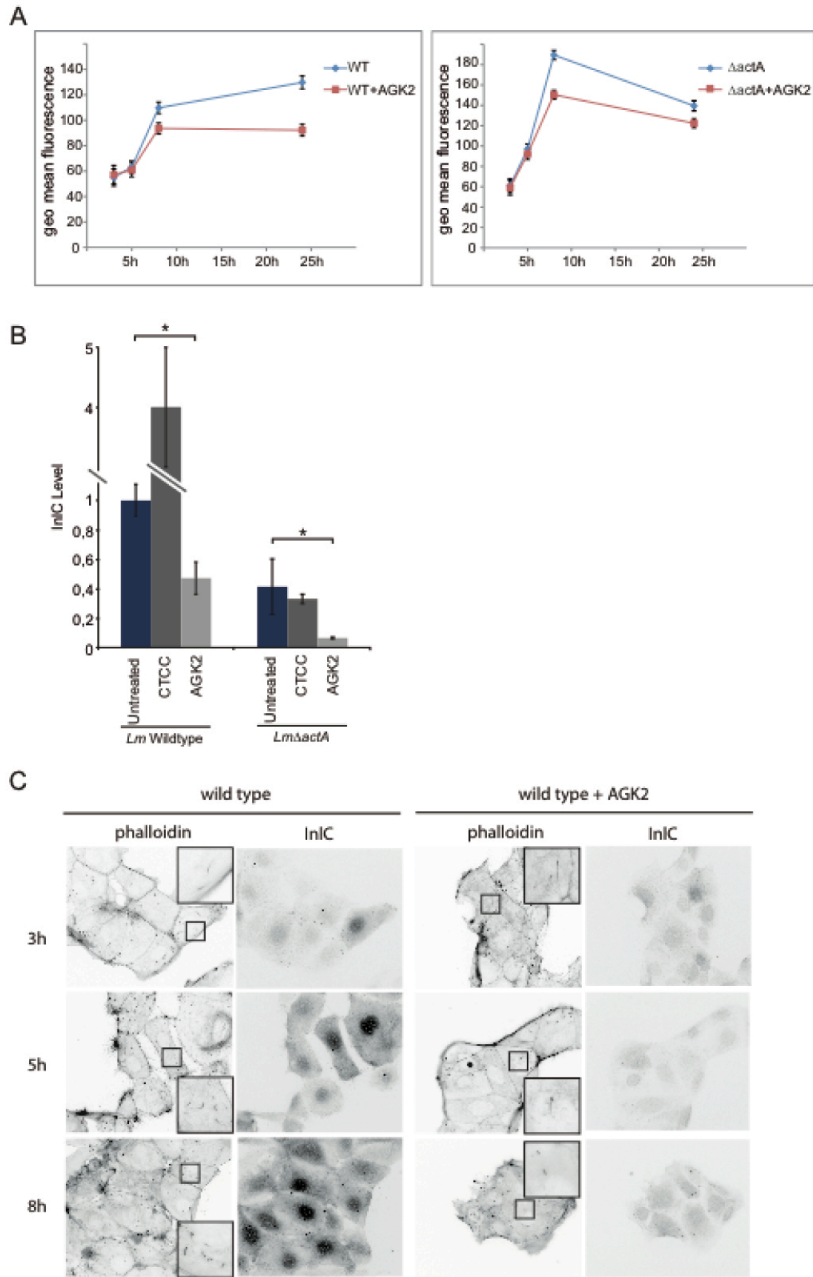


Figure S12. SIRT2 is essential for a listerial infection

(A) The level of *L. monocytogenes* infection is measured by FACS analysis of Caco2 cells, where the geometric mean (y-axis) represents the number of intracellular bacteria (10,000 cells measured; $n \geq 3$). Error bars are SEM. * < 0.05 as measured with a student t-test. Cells infected with a *L. monocytogenes*Δ*actA* mutant have on average more bacteria per cell and therefore are dying at 24h of infection. These results show that both wild type and a Δ*actA* mutant are defective in intracellular growth in cells pretreated with the SIRT2 inhibitor, AGK2. (B) The level of intracellular *L. monocytogenes* at 5h of infection is measured by western blot against InlC, a listerial protein secreted when bacteria are intracellular. HeLa cells are pretreated with a SIRT1 inhibitor, CTCC or a SIRT2 inhibitor AGK2 for 2 hours prior to infection. As for the FACS analysis, these results show that both wild type and a

$\Delta actA$ mutant are defective in intracellular growth in cells pretreated with the SIRT2 inhibitor, Error bars are SEM. * < 0.05 as measured with a student t-test (C)
Immunofluorescence of Caco2 cells infected with wild type *L. monocytogenes*. Phalloidin is marking actin and therefore shows intracellular listeria that are polymerizing actin. InlC is a listerial protein secreted when bacteria are intracellular. Immunofluorescence images are shown as negatives for better visualization. Scale bar = 50 μ m.

Section 2:

CBP/p300 does not antagonize H3K18 deacetylation during infection with *Listeria monocytogenes*

The mechanism of histone H3K18 deacetylation during infection is shown to depend on SIRT2 expression and activity, as well as to be correlated with chromatin association. SIRT2 has been shown to deacetylate H3K18 in biochemical assays, *in vitro* ([Dryden et al., 2003](#)). SIRT2 has also been shown to deacetylate the HAT, p300, *in vitro*, thereby regulating its ability to acetylate lysine residues ([Black et al., 2008](#)), which has previously been shown to target H3K18 for acetylation ([Ferrari et al., 2008](#)). Taken together, we investigated the possibility that p300 activity would regulate H3K18 acetylation levels during infection.

Results:

The activity of p300 was modulated by chemical treatments in HeLa cells. If p300 plays a role in antagonizing SIRT2-dependent H3K18 deacetylation during infection, then the inhibition of p300 would cause a decrease in the basal level of H3K18 acetyl and infection would cause a greater level of H3K18 deacetylation as compared to uninfected cells. HeLa cells treated with the p300 chemical inhibitor, anacardic acid, were infected for 3 and 5 hours before quantifying H3K18 acetyl levels by immunoblotting. Preliminary results from figure 1 show that H3K18 acetyl levels decrease in uninfected anacardic acid-treated cells as compared to untreated cells in a concentration-dependent manner. The infection with *L. monocytogenes* caused a decrease in H3K18 acetyl levels, as compared to uninfected samples. However, the levels of H3K18 deacetylation during infection in the treated samples are not drastically lower than in the untreated sample, suggesting that p300 does not play a role in antagonizing H3K18 deacetylation during infection.

In order to determine whether p300 activity can cause H3K18 acetylation, HeLa cells were treated with a potent chemical activator p300, CTPB (N-(4-Chloro-3-trifluoromethyl-phenyl)-2-ethoxy-6-pentadecyl-benzamide). H3K18 acetyl levels were assessed in cells uninfected and infected with *L. monocytogenes* in order to observe whether deacetylation occurs in spite of raising basal H3K18 acetyl levels. Figure 2 shows preliminary results for which p300 activation increases the basal level of H3K18 acetylation. However, infected

cells treated with CTPB exhibited H3K18 deacetylation at levels comparable to that exhibited by infected, untreated cells. Taken together, these results suggest that p300 activation does not antagonize H3K18 deacetylation during infection and therefore, infection does not lead to H3K18 deacetylation by inhibiting HAT activity.

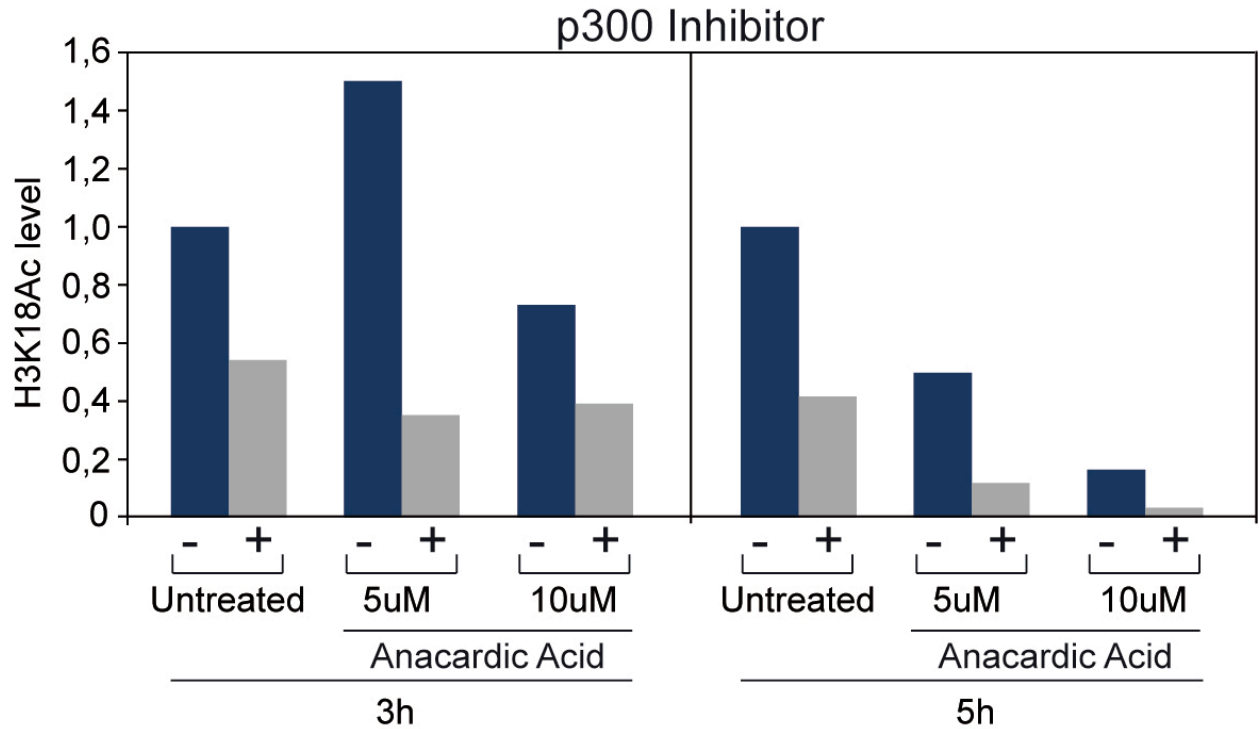


Figure 1. p300 activity regulates basal H3K18 acetyl levels, but does not antagonize H3K18 deacetylation during infection

Quantification of H3K18 acetyl levels in immunoblots conducted on HeLa cells treated with anacardic acid (a potent chemical inhibitor of p300) and infected for 3 and 5 hours with *L. monocytogenes*. Basal levels of H3K18 acetylation decrease by 5 hours of infection. H3K18 deacetylation is observed during infection as compared to uninfected cells.

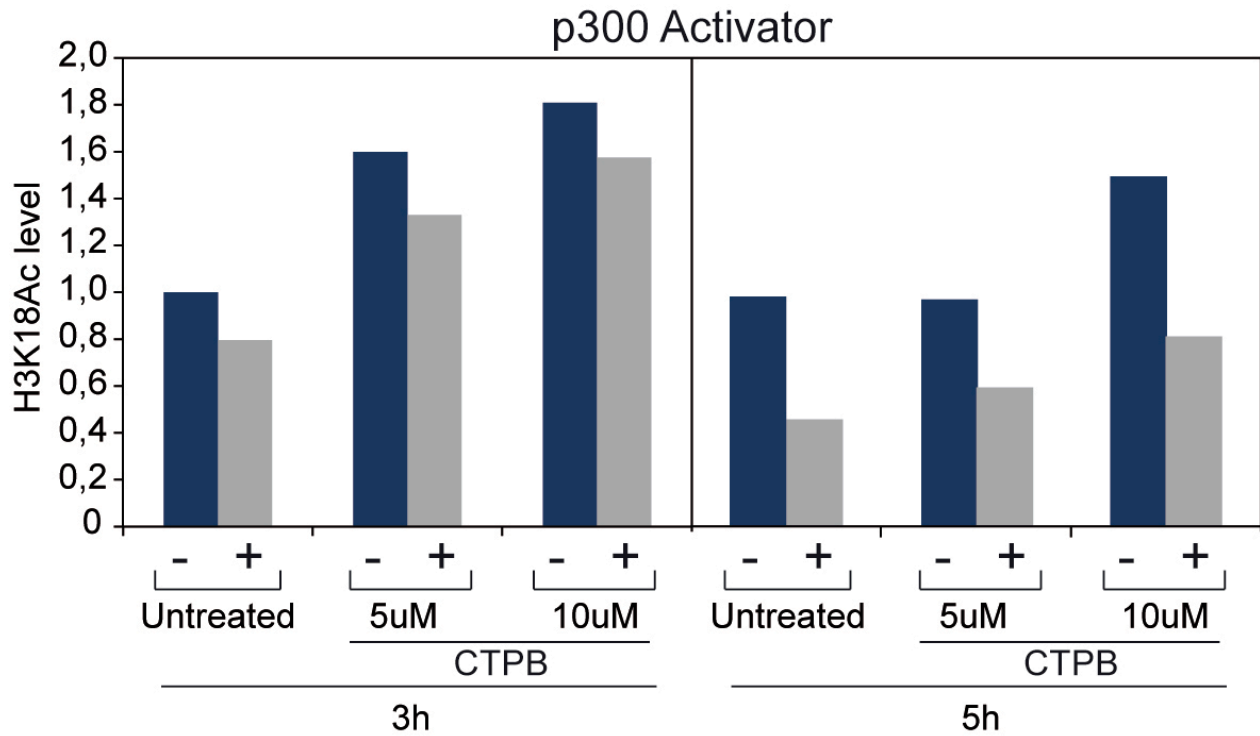


Figure 2. p300 activation increases basal H3K18 acetyl levels at 3 hours, but does not inhibit H3K18 deacetylation during infection.

Quantification of H3K18 acetyl levels in immunoblots conducted on HeLa cells treated with CTPB (a potent chemical activator of p300) and infected for 3 and 5 hours with *L. monocytogenes*. Basal levels of H3K18 acetylation increased by 3 hours and were sustained at 10 μ M of CTPB, at 5 hours. H3K18 deacetylation is observed during infection as compared to uninfected cells.

Section 3:

SIRT2 N-terminal dephosphorylation causes nuclear recruitment

Initial studies on the deacetylase activity of human SIRT2 reported predominantly in the cytoplasm ([North et al., 2003](#); [Vaquero et al., 2006](#)). The localization of SIRT2, however is reported to be nuclear during mitosis ([Black et al., 2008](#); [Dryden et al., 2003](#); [Inoue et al., 2007](#)) while constitutively shuttling through the nucleus in interphase cells ([North and Verdin, 2007a](#)). Vaquero and colleagues observed a co-localization of SIRT2 with histones by immunofluorescence, and an importance of SIRT2 activity for H4K16 deacetylation ([Vaquero et al., 2006](#)). However, they did not identify a mechanistic cue regulating SIRT2 nuclear localization or association with histones. Black and colleagues next proposed that SIRT2 targets and regulates the activity of the histone acetyltransferase, p300, in the nucleus ([Black et al., 2008](#)). However, a signal for SIRT2 nuclear localization or chromatin association had never before been identified.

SIRT2 is reported to be a substrate for phosphorylation at the C-terminal residue, serine 368, by cyclin dependent kinase 1 (Cdk1) and dephosphorylated by the phosphatases, CDC14A and CDC14B ([Dryden et al., 2003](#); [North and Verdin, 2007b](#)). While one study suggested that the modification of this site, S331 (corresponding to S368 of SIRT2.1) on the short isoform of SIRT2 (SIRT2.2; 352aa) regulated catalytic activity ([Pandithage et al., 2008](#)), other studies reported that the modification of SIRT2.1 S368 only slightly effects catalytic activity ([Nahhas et al., 2007](#)).

My data have shown that upon infection, SIRT2 relocated to the nucleus as observed by immunofluorescence (section 2, figure 1b). SIRT2 levels were also detected in chromatin soluble fractions of infected samples isolated by cell fractionation. Only the long form of SIRT2 (389aa) was detected in the chromatin fraction of infected cells, representing variant SIRT2.1 (section 1, figure 2c). Surprisingly, the chromatin band SIRT2.1 migrated further than SIRT2.1 bands in both cytosolic and nuclear soluble fractions, suggesting that SIRT2 is a target for post-translational modification (PTM).

The aim of this section is to characterize the mechanistic basis for the SIRT2 PTM, with the hopes of determining its impact in SIRT2 nuclear localization and/or chromatin association. Revealing the molecular factors important for such a PTM would potentially clarify how the PI3K/Akt signaling cascade dictates SIRT2 nuclear relocalization and chromatin association.

Results:

SIRT2 C-terminal phospho-site does not regulate sub-cellular localization

SIRT2 had previously been observed to undergo phosphorylation at residues S368 and S372 ([Nahhas et al., 2007](#)). To determine whether the SIRT2 residue S368 is important for the nuclear localization of SIRT2 during infection, HeLa cells were transfected with SIRT2-GFP S368 mutants mimicking either a dephosphorylated (S368A) or phosphorylated (S368E) state. Figure 1 shows by immunofluorescence microscopy that SIRT2-GFP wildtype and mutants in cells uninfected and infected with *L. monocytogenes* all exhibited a nuclear localization of SIRT2, independent of whether S368 was modified. These results suggest that SIRT2 nuclear recruitment occurs during infection, independent of the phosphorylation status of S368.

Chromatin association of SIRT2-GFP S368 mutants was next assessed by immunoblotting of cell fractions. SIRT2-GFP was not detected in nuclear and chromatin fractions of uninfected cells, whereas SIRT2-GFP was detectable in the chromatin fraction of 5h-infected samples (figure 2). Furthermore, both SIRT2-GFP S368 mutants were observed in the chromatin fractions of infected, but not uninfected cells. Curiously, while immunofluorescence microscopy determined that SIRT2-GFP mutants were present in the nucleus of uninfected and infected cells, SIRT2-GFP levels were only detected in the chromatin fraction of infected cells. What accounts for this discrepancy is not known. Nevertheless, these results suggest that the phospho-status of SIRT2 at residue S368 does not affect association to chromatin as both the phospho-mimetic (SIRT2-GFP S368E) and dephospho-mimic (SIRT2-GFP S368A) both associated to chromatin during infection similarly to wildtype SIRT2.

SIRT2 undergoes dephosphorylation at a novel N-terminal phospho-site

Previous studies predicted potential sites of phosphorylation at both C-terminal and N-terminal regions of SIRT2 ([Nahhas et al., 2007](#)). However, no phosphorylation sites besides the targeting of the C-terminal S368 has been studied in cells. In order to exhaustively identify all SIRT2 peptides harboring phospho-sites, mass spectrometry was conducted by Francis Impens on FLAG-immunoprecipitated cell fractions of SIRT2-FLAG-transfected HeLa cells uninfected or infected for 5 hours with *L. monocytogenes*.

Mass spectrometry revealed the status of SIRT2 phosphorylation by detecting the unique mass of phosphorylated/dephosphorylated SIRT2 peptides. Figure 3 shows the status of SIRT2 phosphorylation at the N-terminal Serine 25 and the C-terminal Serine 368. SIRT2 exhibits phosphorylation in all cellular fractions of uninfected and infected cells at the C-terminal S368, suggesting the infection has no effect of S368 phosphorylation. Phosphorylation was equally present at the N-terminal S25 in cytosolic and nuclear fractions of both uninfected and infected samples. Strikingly, chromatin fractions of both uninfected and infected cells exhibited a dephosphorylation, suggesting that SIRT2 undergoes post-translational modification at the N-terminus, during infection and this is correlated with an association to chromatin.

Mass spectrometry provides a semi-quantitative measure of SIRT2 serine phosphorylation. Since serines 23, 25, and 27 are present on the same peptide of digested SIRT2 protein, phosphorylation of serines 23, 25, or 27 yield peptides of the same mass making the phosphorylated peptides indistinguishable. Therefore, the exact residue undergoing dephosphorylation during infection at the N-terminus remains unclear.

SIRT2 dephosphorylation is necessary for nuclear relocalization

In order to address the importance SIRT2 N-terminal phospho-site identified by mass spectrometry on nuclear localization, SIRT2 mutants were engineered to either mimic a phosphorylated (SIRT2-GFP S23/S25/S27E) or dephosphorylated (SIRT2-GFP S23/S25/S27A) state. The SIRT2-GFP S23/S25/S27 mutants were transfected into HeLa cells and assessed for their sub-cellular localization during infection. Figure 4 shows uninfected cells transfected with the dephosphorylated mimics, SIRT2-GFP S23/S25/S27A,

exhibited a nuclear localization, in contrast to wildtype SIRT2-GFP in uninfected cells. This result is in sharp contrast to cells transfected with either SIRT2-GFP WT or phospho-mimetic S23/S25/S27E, suggesting that SIRT2 N-terminal dephosphorylation is correlated with nuclear localization. The infection of cells transfected with both WT and S23/S25/S27A exhibited a nuclear relocalization of SIRT2, while the S23/S25/S27E phospho-mimetic mutant failed to relocalize to the nucleus. Taken together, these results suggest that SIRT2 nuclear localization depends at least partially on the dephosphorylation of the N-terminal phospho site of SIRT2.

Protein phosphatase 1B is necessary for H3K18 deacetylation during infection

In order to identify what proteins might associate with SIRT2 during infection, cell fractions of uninfected and infected cells transfected with SIRT2-FLAG were immunoprecipitated with a FLAG peptide in order to purify SIRT2 and its interactors. Mass spectrometry analysis conducted by Francis Impens on SIRT2-FLAG interactors revealed an association between SIRT2 and protein phosphatase 1B (PPM1B), in the cytoplasmic fraction of infected cells and the chromatin fraction of both uninfected and infected cells (Table 1). The abundance of PPM1B was 4 times greater in the chromatin fraction of the infected sample, as compared to the uninfected chromatin fraction. The cytoplasmic interaction between SIRT2 and PPM1B was only observed during infection. Taken together, these data suggest that infection causes an interaction between SIRT2 and PPM1B in the cytoplasm and chromatin fractions.

In order to address whether PPM1B is necessary for H3K18 deacetylation during infection, the expression of PPM1B was knocked down by siRNA in HeLa cells that were either uninfected or infected with *L. monocytogenes* for 5 hours. H3K18 acetylation levels were quantified by immunoblotting. Preliminary results are represented in figure 5, which shows that *L. monocytogenes* infection caused H3K18 deacetylation in cells expressing PPM1B, whereas cells knocked down for PPM1B exhibited no change in H3K18 acetylation as compared to levels in uninfected cells. These results suggest that PPM1B is necessary for H3K18 deacetylation during infection.

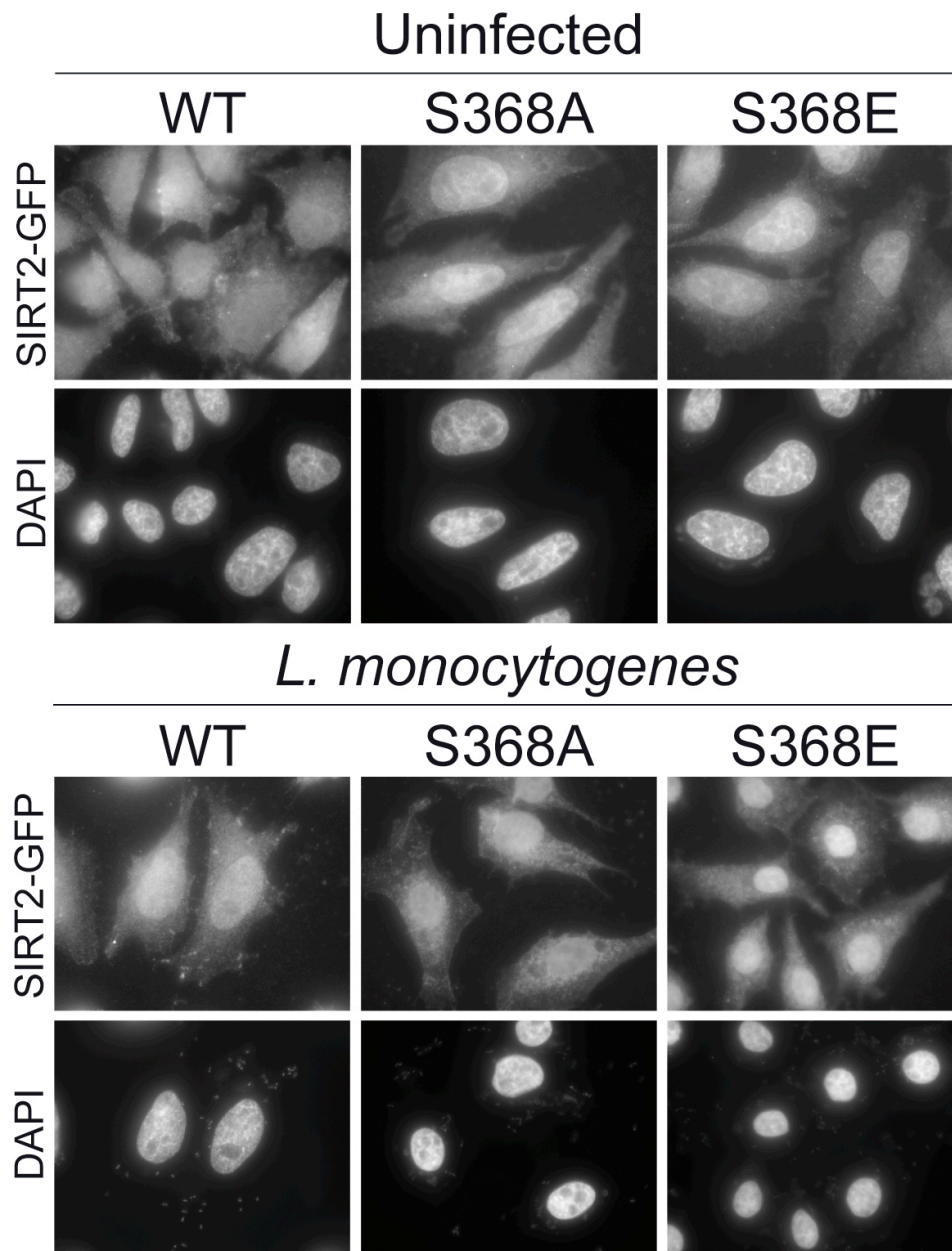


Figure 1. SIRT2 S368 phospho status does not dictate sub-cellular localization.

Immunofluorescence microscopy of SIRT2-GFP conducted on HeLa cells transfected with SIRT2-GFP S368 WT, or S368A/E mutants and infected for 5 hours with *L. monocytogenes*. n = 3. Immunofluorescence magnification: 100x.

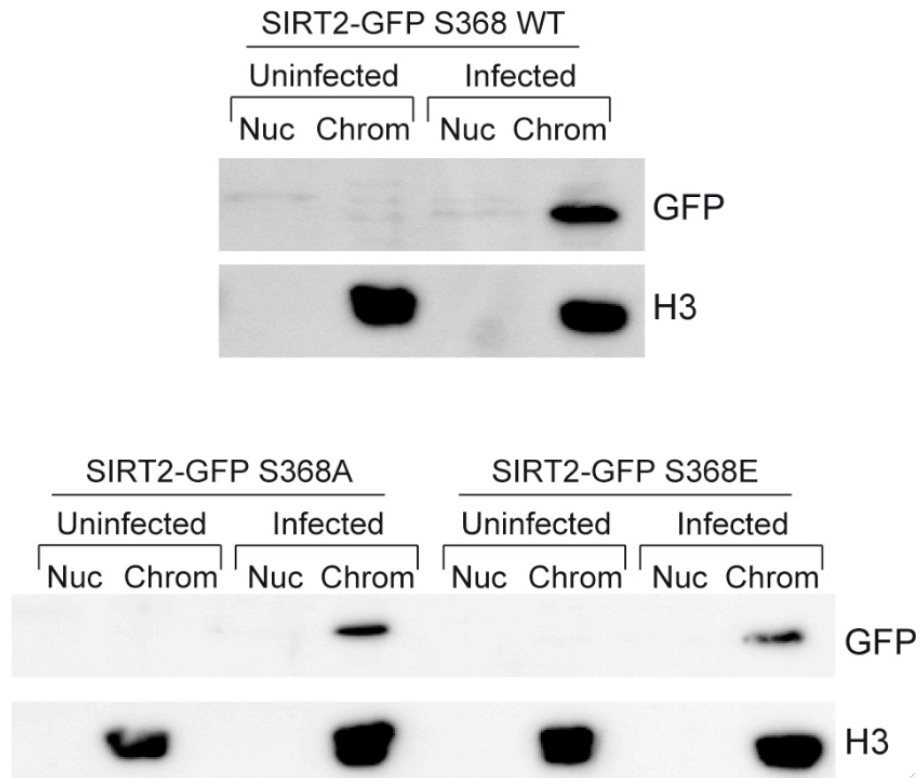


Figure 2. Sub-nuclear localization of SIRT2-GFP S368 mutants

Immunoblot of SIRT2-GFP and H3 isolated from nuclear and chromatin fractions prepared from HeLa cells transfected with SIRT2-GFP S368 WT, or S368A/E mutants and infected for 5 hours with *L. monocytogenes*. n = 3.

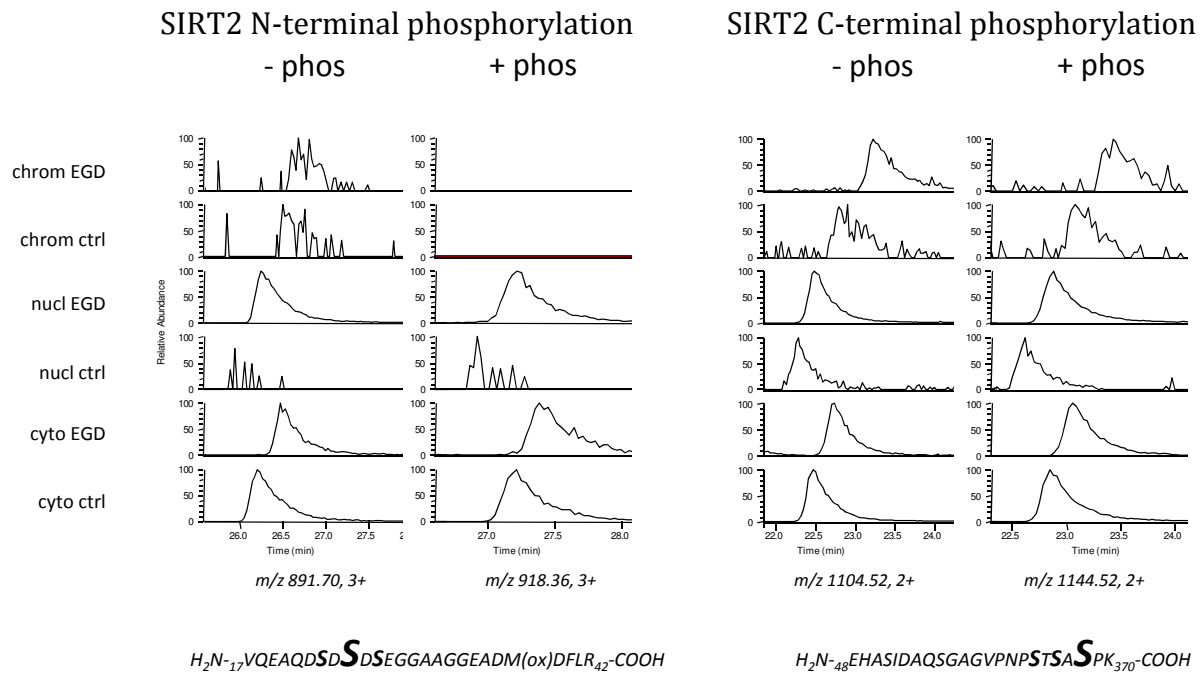


Figure 3. SIRT2 phosphorylation status of N- and C-terminal phospho sites.

MS/MS spectra plots for SIRT2 S25 or S368 are represented on the y-axis as the relative abundance of spectra and the x-axis represents the time of flight (seconds). *L. monocytogenes*-infected samples are represented as “EGD” and uninfected samples are represented as “ctrl”. Fractions “cyt” = cytosolic, “nucl” = nuclear, and “chrom” = chromatin. Spectral plots for “- phos” represent SIRT2 dephosphorylated peptides and “+ phos” represents phosphorylated SIRT2.

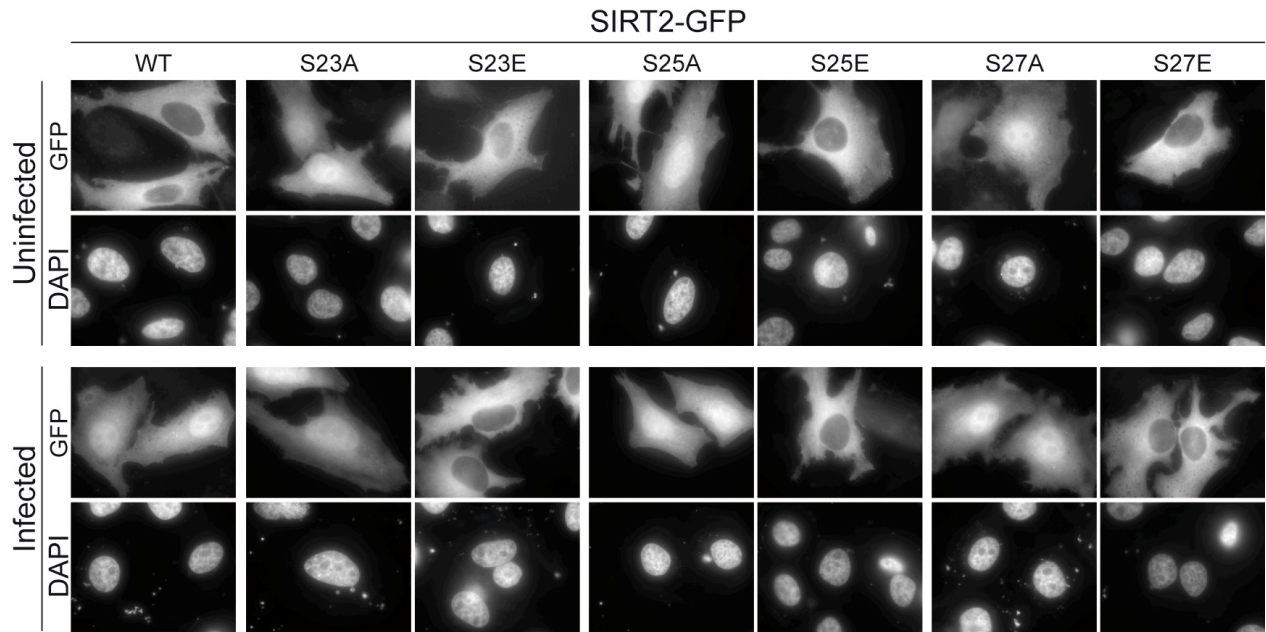


Figure 4. SIRT2 S23/S25/S27 phosphorylation regulates SIRT2 nuclear recruitment. Immunofluorescence microscopy of SIRT2-GFP S23/S25/S27 A/E mutants transfected into HeLa cells, uninfected or 5h infected with *L. monocytogenes* (MOI 50:1). Microscopy magnification: 100x.

Table 1: Mass spectrometric quantification of PPM1B peptides

	# MS/MS spectra (unique peptides) Uninfected	# MS/MS spectra (unique peptides) Infected
cytoplasm	0 (0)	40 (40)
nucleus	0 (0)	0 (0)
chromatin	12 (6)	42 (26)

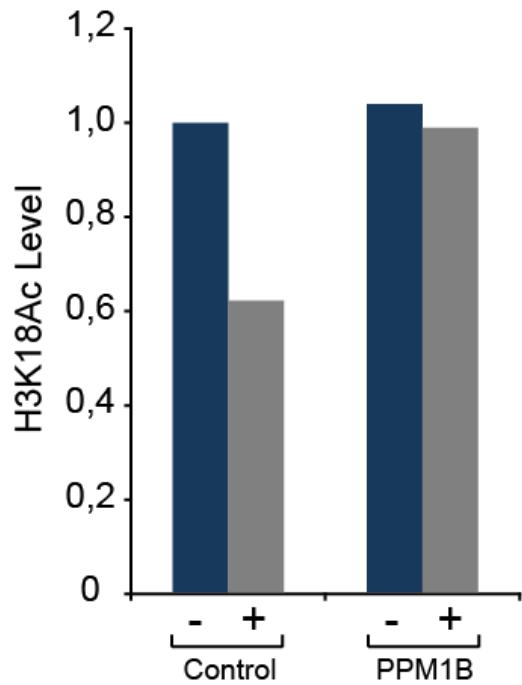


Figure 5. PPM1B is necessary for H3K18 deacetylation during infection

Quantification of H3K18 acetylation levels by immunoblotting using antibodies raised against H3K18 acetylation and Actin. Whole cell lysates collected from HeLa cells transfected with control or PPM1B siRNA and either uninfected or infected for 8h with *L. monocytogenes*. n = 1.

Section 4:

Generalizing Histone H3K18 deacetylation to other bacterial pathogens

Infection of host epithelial cells with *L. monocytogenes* causes both an enrichment of SIRT2 in the nucleus and H3K18 deacetylation. Both SIRT2 nuclear relocalization and H3K18 deacetylation are dependent on Met-induced signaling. We aimed to determine whether any other bacteria besides *L. monocytogenes* induce SIRT2 nuclear recruitment and H3K18 deacetylation. We selected *Salmonella typhimurium*, *Shigella flexneri*, and *Escherichia coli* engineered to express Invasin from *Yersinia pseudotuberculosis* to test for H3K18 acetyl levels and SIRT2 sub-cellular localization, during infection.

Results:

Cells were infected with *Shigella flexneri* (strain M90T), *Salmonella typhimurium*, and a strain of *E. coli* engineered to express invasin (*inv*), from *Yersinia pseudotuberculosis* ([Isberg and Falkow, 1985](#)), in order to mimic entry of *Yersinia*. Infections with both *S. flexneri* and *S. typhimurium* led to no detectable change in H3K18 acetyl levels (figure 1A). In contrast, infection with invasin-expressing *E. coli* caused H3K18 deacetylation upon infection (figure 1A). These results suggest H3K18 deacetylation is a feature of specific bacterial infections.

We also looked at SIRT2 cellular localization by immunofluorescence microscopy. HeLa cells infected for 5 hours with *L. monocytogenes* or *E. coli* expressing invasin induced a relocalization of SIRT2 to the nucleus (figure 1A). In contrast, HeLa cells infected with *S. typhimurium* or *S. flexneri* caused SIRT2 exclusion from the nucleus. Together, these results suggest that SIRT2 sub-cellular localization is a highly controlled process. While *L. monocytogenes* and *E. coli* expressing invasin facilitate SIRT2 nuclear retention, *S. flexneri* and *S. typhimurium* block the shuttling of SIRT2 from the cytoplasm to the nucleus. These results highlight the first identified cues, which modify the sub-cellular localization and the dynamics of SIRT2 shuttling.

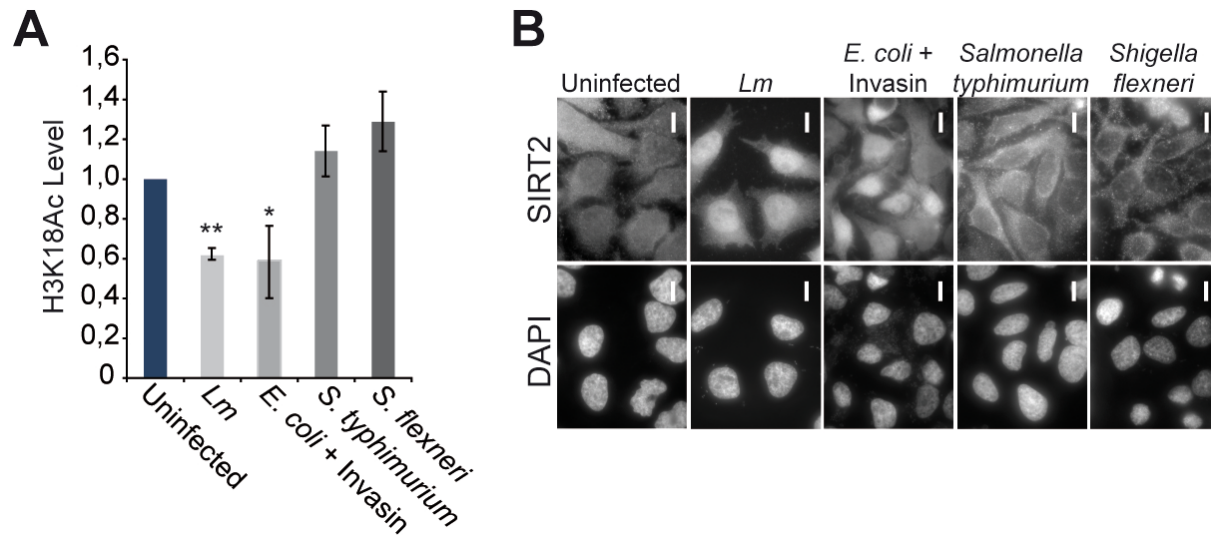


Figure 1. Invasin expressing *E. coli* causes H3K18 deacetylation and SIRT2 nuclear relocalization, like *L. monocytogenes*. HeLa cells were infected for 5h with *L. monocytogenes* (MOI 50:1), *E. coli* expressing Invasin from *Yersinia pseudotuberculosis*, *Salmonella typhimurium*, or *Shigella flexneri* (MOI 100:1 for *E.c* + Inv, *S.t.*, and *S.f.*). (A) Acetylated H3K18 levels were quantified by western blot analysis after infection with the indicated bacteria. (B) SIRT2 sub-cellular localization was visualized by immunofluorescence microscopy after infection with the indicated bacteria. Scale bar is 10 μ m. $n \geq 3$. Error bars are SEM (* < 0.05 ; ** < 0.001).

Discussion

The work presented here reports a novel role for the deacetylase, SIRT2, in transcriptionally reprogramming a cell during infection with a bacterial pathogen. The interaction of the listerial factor, InlB, with the host surface receptor, c-Met, causes an activation of the PI3K/Akt signaling cascade, which is critical for a relocalization of SIRT2 to the nucleus and association to chromatin. The N-terminal dephosphorylation of SIRT2 is a novel site, which plays an important role in the sub-cellular relocalization upon stimulation of the host cell by infection. Furthermore, the catalytic activity of SIRT2 is essential for causing H3K18 deacetylation at a global level. SIRT2 is targeted specifically to the TSSs of genes, which undergo transcriptional repression during infection. Strikingly, SIRT2 expression and activity are critical for *L. monocytogenes* infection.

Manipulating host histone acetylation

The study of pathogen-induced histone modifications is an emerging field of research. To date, few bacterial pathogens have been reported to provoke a modification to histone acetyl levels during infection. During infection with *Mycobacterium tuberculosis*, histone deacetylation occurs at the promoters of specific genes, HLA-DR α , HLA-DR β and CIITA, correlating with the transcriptional repression ([Kincaid and Ernst, 2003](#); [Wang et al., 2005](#)). Infection of gastric epithelial cells by *Helicobacter pylori* was shown to induce deacetylation of H3K23 ([Pathak et al., 2006](#)). *Anaplasma phagocytophilum* infection activates the expression of genes encoding HDAC1 and 2, which correlated with transcriptional repression of key immunity genes and a decrease in histone acetylation at the promoter of these same genes ([Garcia-Garcia et al., 2009](#)). It has also been observed that listeriolysin O of *L. monocytogenes* induces a global deacetylation of H4, correlating with a transcriptional repression of a subset of host genes ([Hamon et al., 2007](#)). While these studies reported modifications to histone acetyl levels during infection, they remain largely correlative and the underlying mechanisms uncharacterized. Nevertheless, histone deacetylation appears to be a frequent target of bacterial pathogens during infection, suggesting a high importance for regulating host chromatin. Our results suggest that host histone deacetylation caused by an infection with *Listeria monocytogenes* promotes

infection by rendering the host environment permissive to bacterial growth, demonstrating that deacetylation is important for the infectious process.

While the discovery of *L. monocytogenes* or *Y. pseudotuberculosis* targeting H3K18 is novel, bacterial pathogens are not alone as viral infection by adenovirus also regulates host transcription by targeting H3K18, highlighting further the importance of deacetylation during infection ([Ferrari et al., 2008](#); [Horwitz et al., 2008](#)). Upon expression of the adenovirus protein, e1a, cell cycle and growth genes are activated, caused by an enrichment of p300/CBP and H3K18 acetylation at the promoters of these genes ([Ferrari et al., 2008](#)). Interestingly, e1a causes a repression of antiviral genes by causing H4K16 acetylation ([Horwitz et al., 2008](#)), a modification associated with transcriptional repression ([Kurdistani et al., 2004](#)). As a result, cell cycling increases and the virus is disseminated into a greater numbers of cells, leading to a spread of the viral infection. Taken together, deacetylation appears to be a crucial mechanism during infection, as it is a target of microbial pathogens.

***L. monocytogenes* imposes a histone code**

With the proposal of the “histone code” hypothesis ([Strahl and Allis, 2000](#)) emerged the aim to characterize how and why along the genome certain patterns of histone modifications occur and whether specific patterns could predict cellular outcomes. The histone code hypothesizes that histone modifications can occur cooperatively or sequentially to assert transcriptional control ([Carmen et al., 2002](#); [Kurdistani et al., 2004](#); [Liu et al., 2005](#)). Studies of *L. monocytogenes* infection of host cells have provided key insight into what modifications occur and what the transcriptional consequence of these modifications is ([Bierne and Cossart, 2012](#)).

Infection with *L. monocytogenes* has been shown to cause transcriptional repression by the action of different virulence factors. Host transcription is modulated through the action of LLO, which causes H3 dephosphorylation and H4 deacetylation ([Hamon et al., 2007](#)) and InlB, which causes H3K18 deacetylation. How these distinct histone modifications, induced by listerial virulence factors, direct changes to host transcriptional programs still remains to be further characterized. Interestingly, it is observed that LLO is responsible for the significant reduction in the size of host nuclei (Fig. 1). Cells infected with a strain of *L. monocytogenes* knocked out for the expression of LLO does not provoke a

change in the size of nuclei. Whether there is a link between these histone modifications and nuclear size is not known. However, in yeast, it has been described that H4K16 deacetylation is responsible for chromatin compaction during cell cycling ([Kurdistani and Grunstein, 2003](#); [Vaquero et al., 2006](#)). Taken together, these studies suggest that the link between LLO-dependent H4 deacetylation and the reduction in nuclear size might be chromatin compaction and in this way transcriptional control.

Genes undergoing transcriptional silencing in a LLO-dependent manner also exhibit H4 deacetylation ([Hamon et al., 2007](#)). However, these suppressed genes are distinct from those genes repressed during infection with *L. monocytogenes* in an InlB-induced SIRT2-dependent manner. These results suggest that InlB and LLO suppress transcription at different gene sets. Curiously though, H4 deacetylation is observed at a subset of genes that are repressed in a LLO-dependent manner and at genes that are activated in a SIRT2-dependent manner. Conceptually, in order to understand how possibly these histone modifications may account for transcriptional status during infection I propose a model described in figure 2, below. The state of acetylation for H3K18 and H4K16 might function as an embedded binary switch to encode the transcriptional status of the cell. InlB and LLO simply modulate these switches in order to fine-tune the transcriptional response and possibly, additively promote infection. In this model, H4 deacetylation, caused by LLO treatment could provoke transcriptional silencing ([Hamon et al., 2007](#)). Acetylating H4K16 loosens chromatin and is necessary but not sufficient to cause transcriptional activation (Fig. 2). Transcriptional activation ensues from the targeted acetylation of H3K18 at genomic regions exhibiting H4K16 acetylation. The regulation of transcriptionally active genomic regions is dependent on InlB-induced H3K18 deacetylation. The LLO-induced transcriptional silencing occurs at regions that exhibit deacetylated H3K18, because the deacetylation of H4K16 at regions where H3K18 is acetylated corresponds to transcriptionally active DNA. Taken together, the listerial virulence factors, InlB and LLO, could cooperatively function to regulate gene expression in a way that each individual factor does not. Nevertheless, the impact of each of these factors individually is paramount to infection.

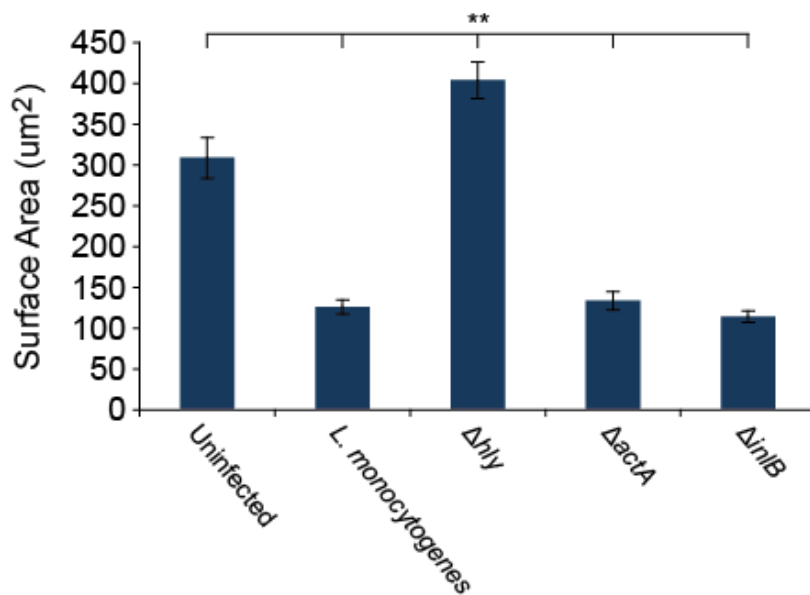
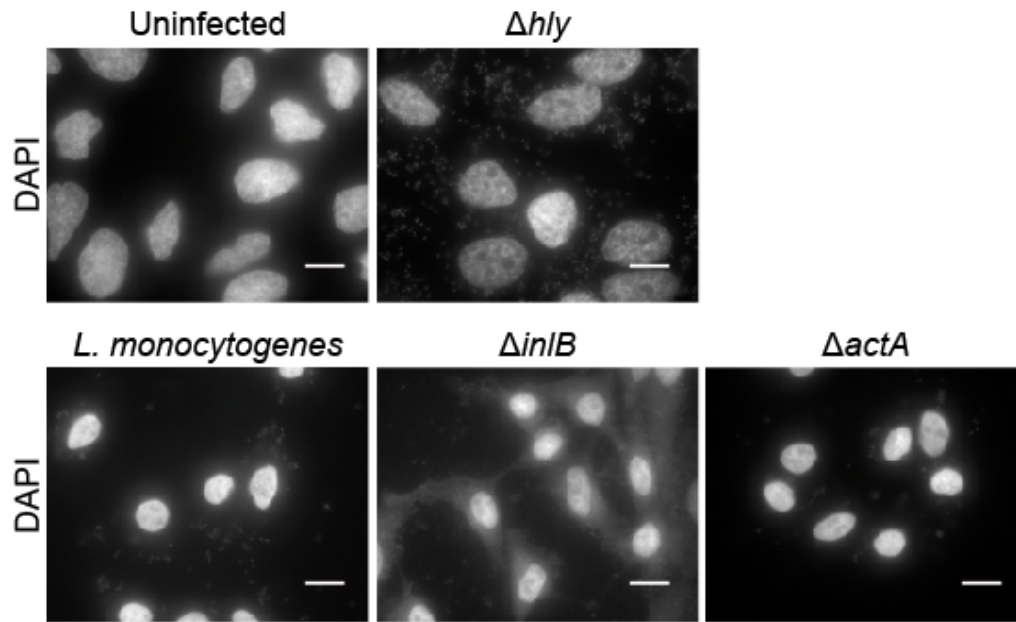


Figure 1. LLO causes a reduction in host nuclear size

Immunofluorescence microscopy of HeLa cell nuclei stained with DAPI. Cells 5h-infected (MOI 50:1) exhibit a reduction in nuclear surface area in a *hly*-dependent manner. Nuclear surface area was measured using Image J measurement tools. Scale bar = 10μm.

Immunofluorescence experiment is representative of $n \geq 3$. SEM. ** < 0.001.

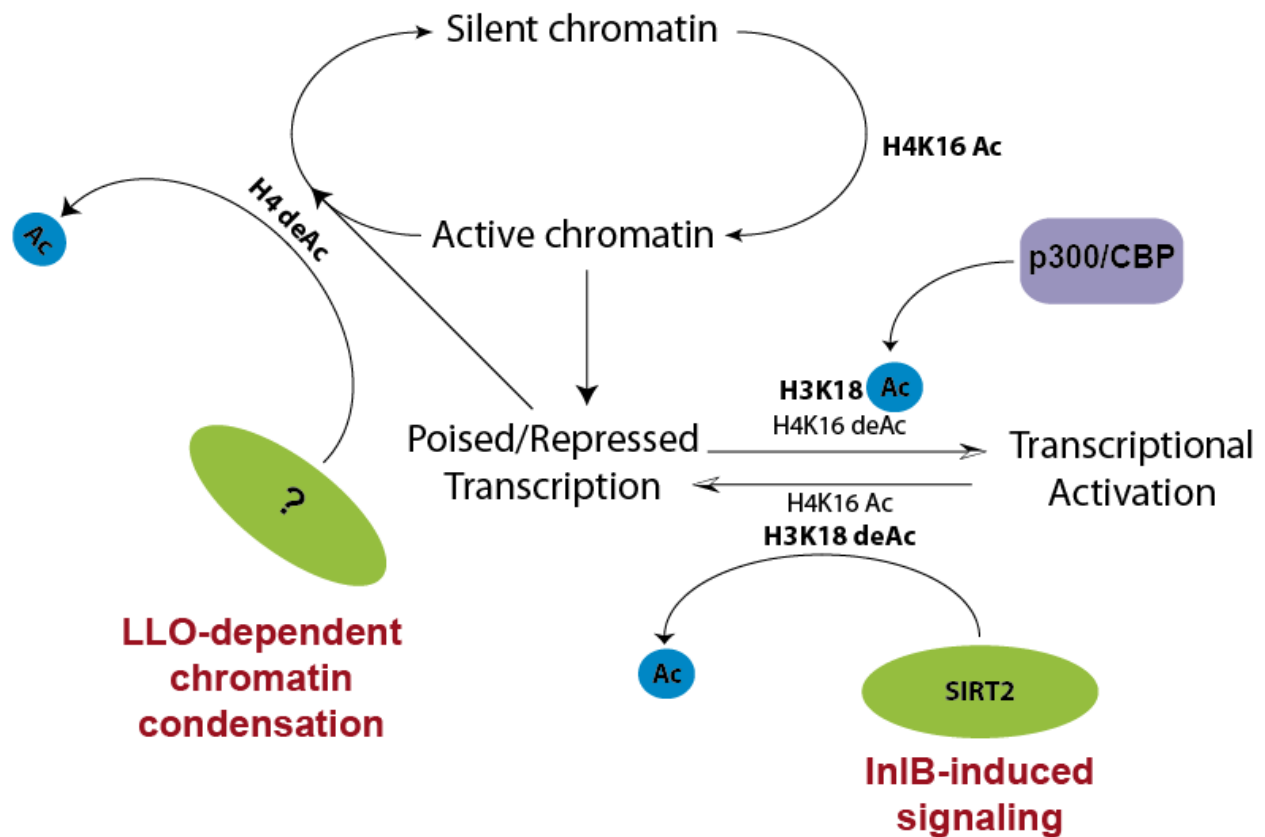


Figure 2. H3K18/H4K16 acetylation dictates state of chromatin and transcription.

In euchromatin, the state of H3K18 acetylation is epistatic over H4K16 acetylation for transcriptional regulation, whereas in heterochromatin the state of H4K16 acetylation is epistatic over H3K18 acetylation. Transcriptional repression can occur by either deacetylating H3K18, or by promoting heterochromatin formation through H4K16 deacetylation (Vaquero et al., 2006). LLO causes H4 deacetylation, which is correlated with transcriptional repression (Hamon et al., 2007). InI β induces H3K18 deacetylation and subsequently, gene repression.

***L. monocytogenes* induces SIRT2-dependent transcriptional control**

Initial characterization of SIRT2 function focused attention on the cytoplasm where it regulates microtubule dynamics through the deacetylation of α -tubulin ([Dryden et al., 2003](#); [North et al., 2003](#)). Cytoplasmic SIRT2 was characterized to control adipocyte differentiation ([Jing et al., 2007](#)) and autophagy ([Zhao et al., 2010](#)) through deacetylation of the transcription factor, FOXO1. Another FOXO transcription factor, FOXO3, undergoes SIRT2-dependent deacetylation in response to oxidative stress and caloric restriction ([Houtkooper et al., 2012](#)). Indeed, FOXO transcription factors are common targets for SIRT2, suggesting that SIRT2-dependent transcriptional regulation can occur through the targeting of transcription factors. However, further studies identifying the targets of SIRT2 revealed several nuclear factors, such as the transcription factor p53, the histone acetyltransferase p300, and histones H3 & H4 ([Houtkooper et al., 2012](#)).

With the identification of nuclear targets of SIRT2 emerged the hypothesis that SIRT2 is a regulator of transcription. Transcriptional control can occur by either directly targeting histones or by regulating the activity of chromatin modifiers. *In vitro* biochemical studies identified that SIRT1, 2, & 3 can deacetylate H3K18 and H4K16 and that p300 is specifically targeted by SIRT2 ([Black et al., 2008](#)). Deacetylation of p300 might be a mechanism by which to regulate transcriptional activation, whereas the direct deacetylation of H3K18 results in transcriptional repression. While conceptually gene expression can depend on both p300-dependent H3K18 acetylation and SIRT2-dependent repression, my results suggest that SIRT2 directly represses gene expression through H3K18 deacetylation as opposed to regulating transcriptional activation by targeting p300. Furthermore, p300/CBP does not seem to play a role in maintaining the activation of SIRT2-repressed genes during infection, since CBP levels remain unchanged across all ChIP PCR-tested SIRT2-repressed genes.

Impact of SIRT2-dependent gene regulation

In identifying the genes regulated by SIRT2 during infection, several key gene ontologies were identified, which could impact *L. monocytogenes* infection. Genes regulating transcription, cell survival, and immune activation were all identified targets of SIRT2-dependent modulation during infection. While H3K18 deacetylation has previously been

correlated with cell cycling and oncogenic transformation, genes promoting such changes were not observed to be modulated during infection.

Although many histone deacetylases have a role in transcriptional regulation, no such role has been directly attributed to SIRT2, as it has not previously been shown to target chromatin *in vivo*. A gene ontology annotation of the 271 SIRT2-dependent repressed genes strikingly reveals that nearly one quarter of them are DNA-binding proteins (51 genes) and/or implicated in transcriptional regulation (55 genes). A few prominent examples are SMAD1, FOXM1, transcription factors participating in proliferation, differentiation, apoptosis, regulator of interferon response activated during infection, etc., IRF2, SMARCA2, which is a member of the SWI/SNF family of chromatin remodelers that alter the chromatin structure in an ATP-dependent manner, SAP130, which is part of the Sin3A repressor complex important in transcriptional repression. These data suggest that *L. monocytogenes* hijacks SIRT2 in order to impose a transcriptional control on the host.

Further gene annotation analysis identified a group of 36 genes regulated by SIRT2, all required for cell survival. Self-renewal of tissues is essential for preserving tissue homeostasis, and is crucial for limiting bacterial colonization. Self-renewal is characterized by apoptosis of damaged cells and induction of cell cycling in undamaged cells. Our results demonstrate that SIRT2 promotes the growth of *L. monocytogenes* within invaded cells and irrespective of ActA-dependent bacterial spread, suggesting that host cells are programmed to tolerate greater numbers of *L. monocytogenes* before dying off. In addition, bacterial pathogens, including *Shigella flexneri* and *Helicobacter pylori* have been shown to dampen rapid turnover of epithelial cells, thereby prolonging colonization within intestinal epithelial cells ([Iwai et al., 2007](#); [Mimuro et al., 2007](#)). With the SIRT2-dependent repression of 22 genes involved in cell cycle progression, *L. monocytogenes* seems to also dampen cell turnover through InlB. Taken together, these results suggest that InlB-induced SIRT2 transcriptional control could promote intestinal epithelial cell colonization through the up-regulation of survival and down-regulation of cell cycling.

Another interesting finding from the transcriptome analysis is that a significant number of SIRT2-repressed genes are involved in immune response regulation. Many genes are regulators of B and T cell receptor signaling (RASGRP1, MAPK14, PIK3R3, PTPNG, SOS1, VAV3, ABL1, CAMK26, MAPK26, and LEF1). The chemokine, CXCL12, which is strongly

chemotactic for lymphocytes, and the interferon transcription factor IRF2, are also repressed. In conclusion, SIRT2 manipulates many essential cellular functions in order to promote a listerial infection.

Previously, H3K18 hypoacetylation was highly correlated with a poor prognosis for prostate carcinoma patients ([Seligson et al., 2009](#)), suggesting that H3K18 acetyl levels may be linked to oncogenic transformation ([Manuyakorn et al., 2010](#)). Infection of quiescent human cells with adenovirus resulted in the stimulation of cell cycling and the inhibition of antiviral responses and cell differentiation ([Ferrari et al., 2008](#)). The mechanism governing adenovirus-dependent cell cycling results from the eviction of CBP/p300 from a specific set of host genes repressing cell cycle progression ([Horwitz et al., 2008](#)). A more recent study found that H3K18 deacetylation is implicated in the stabilization of the transformed state of cancer cells ([Barber et al., 2012](#)). The NAD⁺-dependent deacetylase, SIRT7, is a nuclear resident ([Mostoslavsky et al., 2010](#)) and is specifically targeted to the promoters of a set of genes where it deacetylates H3K18 and promotes transcriptional repression ([Barber et al., 2012](#)). SIRT7-dependent H3K18 deacetylation is necessary for maintaining essential features of human cancer cells, including anchorage-independent growth and escape from contact inhibition. In contrast to these studies, SIRT2-dependent gene regulation did not significantly upregulate the expression of genes involved in cell cycling or the stabilization of oncogenic transformation, despite SIRT2 being activated downstream of the signaling receptor, c-Met. The oncogenic receptor, c-Met, activates PI3K/Akt signaling culminating in H3K27 tri-methylation (H3K27me3) at a set of genes associated with oncogenic transformation in breast cancer cell lines ([Zuo et al., 2011](#)). To date, my results show no evidence that SIRT2-dependent H3K18 deacetylation is correlated with oncogenesis.

Perspectives

A nuclear function for SIRT2 during *L. monocytogenes* infection

SIRT2 sub-cellular localization:

SIRT2 was initially reported localized mainly in the cytoplasm of interphase cells, although further scrutiny revealed that it constitutively shuttles through the nucleus ([Dryden et al., 2003](#); [North and Verdin, 2007a](#)). During the G2-M transition of the cell cycle, SIRT2 relocates to the nucleus and causes H4K16 deacetylation, which promotes heterochromatin formation ([Vaquero et al., 2006](#)). However, the mechanism governing the equilibrium in SIRT2 nucleo-cytoplasmic localization remains uncharacterized. My results demonstrate that *L. monocytogenes* infection causes SIRT2 nuclear relocation and chromatin association. Nevertheless, it is not fully clear how SIRT2 is induced to relocate to the nucleus. One hypothesis is that the SIRT2 nucleo-cytoplasmic equilibrium promotes SIRT2 to flow into the nucleus because nuclear SIRT2 is associating to chromatin, during infection. Another possibility is that the SIRT2 nucleo-cytoplasmic equilibrium shifts from being mainly cytoplasmic to nuclear. While the first hypothesis might provide for the recruitment of some SIRT2 into the nucleus, the latter hypothesis is supported by mass spectrometry data, which revealed that SIRT2 shifts from a 93% cytoplasmic localization in uninfected cells to a 75% nuclear localization in infected cells. Therefore, further study will aim at characterizing the underlying mechanism governing the nucleo-cytoplasmic equilibrium of SIRT2 sub-cellular localization.

State of SIRT2 N-terminal phosphorylation governing sub-cellular localization:

One aspect of SIRT2 sub-cellular localization might be governed by the post-translational modification of SIRT2 during infection. Together with Francis Impens, we discovered an N-terminal phospho-site of SIRT2 (S23/S25/S27), which is dephosphorylated only in the chromatin fraction of cells. This N-terminal region of SIRT2 represents the long SIRT2.1 isoform, which lies outside of the catalytic domain of SIRT2 ([Finnin et al., 2001](#)). The correlation between chromatin association and SIRT2 dephosphorylation, suggests an importance in the mechanism of dephosphorylation for

allowing access to chromatin. Further evidence provided by immunofluorescence microscopy suggests that nuclear localization altogether is dependent on SIRT2 N-terminal dephosphorylation. Whether N-terminal dephosphorylation governs chromatin association or nuclear access, this post-translational modification can regulate SIRT2 sub-cellular localization and impact the cell during infection. Further studies will aim to characterize how SIRT2 is dephosphorylated and relocalized to the nucleus.

Interestingly, SIRT2 is not the only protein or deacetylase whose sub-cellular localization is governed by its state of phosphorylation. FOXO and class IIa HDACs also exhibit a phospho-switch governing their sub-cellular localization. Under conditions of low insulin signaling in *C. elegans*, the transcription factor, FOXO, is mainly localized in the nucleus, where it engages transcriptional machinery at many genomic loci, most of them cooperatively with the SWI/SNF chromatin-remodeling complex ([Calnan and Brunet, 2008](#); [Riedel et al., 2013](#)). Upon activation of insulin signaling through PI3K/Akt, FOXO becomes phosphorylated and is bound by 14-3-3 proteins, which is necessary for cytosolic sequestration, possibly through the exposure of a nuclear export sequence (NES). Cytosolic FOXO associated with protein 14-3-3 causes ubiquitylation of and degradation. The HDAC class IIa members, HDAC4/5/7/9 possess two or three N-terminal serine residues, whose phosphorylation provokes cytoplasmic sequestration ([Verdin et al., 2003](#)). The sequence of the phosphorylation sites of class IIa HDACs closely relates to the phosphorylation sites for Ca²⁺/CaM-dependent protein kinases (CamKs) ([McKinsey et al., 2000a](#)). CaMK-mediated phosphorylation of class IIa HDACs promotes their association with 14-3-3 proteins and stimulates nuclear export ([Kao et al., 2001](#); [McKinsey et al., 2000b, 2001](#); [Wang et al., 2000](#)). How the phosphorylation of the N-terminus of class IIa HDACs could cause cytoplasmic sequestration is not fully understood. However, it is thought that phosphorylation-dependent binding of 14-3-3 proteins masks the nuclear localization sequence (NLS), thus preventing import of class IIa HDACs. Taken together, it is not yet fully understood how 14-3-3 proteins are involved in causing cytosolic sequestration of transcriptional operators, nevertheless, phosphorylation plays a major role in dictating the sub-cellular localization of many factors affecting transcription.

While no NLS has yet been identified for SIRT2, a comparable mechanism for SIRT2 sub-cellular localization is possible. The sequence of the SIRT2 phosphorylation sites is

distinct from that exhibited by class IIa HDACs, but BLAST analysis of the sequence QDSDSDSE indicates that this sequence is present in proteins like: NF- κ B, rab-like protein 6, cadherin EGF LAG seven pass G-type receptor. Interestingly, this phosphorylation site has not previously been attributed a biological function for the proteins expressing it. Therefore, further study of this SIRT2 N-terminal phospho-site may lead to a novel discovery of how the sub-cellular localization may be controlled for proteins expressing this sequence.

Identification of a phosphatase targeting SIRT2:

Preliminary evidence suggests that SIRT2 may be dephosphorylated by PPM1B. PPM1B is a member of the PP2C family of serine/threonine phosphatases and is reported to terminate TNF α -dependent signaling by dephosphorylating the signaling intermediate, IKK β ([Sun et al., 2009](#)). Together with Francis Impens, we observed by mass spectrometry that PPM1B interacts with SIRT2 in cytoplasmic and chromatin fractions of infected cells. In cells transfected with SIRT2-GFP mutants for N-terminal serine residues only dephosphorylated SIRT2 mimics undergo nuclear translocation, suggesting that PPM1B targets SIRT2 in the cytoplasm. My results infer a link between PPM1B-dependent SIRT2 dephosphorylation PI3K/Akt signaling, although future experiments are necessary to determine the intermediate mechanism.

The downstream impact of PPM1B has been assessed in a preliminary experiment demonstrating that PPM1B is necessary for H3K18 deacetylation during infection. Future experiments will aim to determine whether PPM1B is necessary for dephosphorylating the N-terminal phospho-site of SIRT2. Furthermore, the link between PPM1B and upstream signal transduction mediators, PI3K/Akt, during infection will be investigated.

Conclusion

This thesis provides evidence that *L. monocytogenes* hijacks the host HDAC, SIRT2 to impose host transcriptional control. Our results report an important mechanism of host transcriptional regulation by pathogenic bacteria. Transcriptional repression occurs by the targeting of the chromatin modifier, SIRT2, to the nucleus. SIRT2 relocalization and histone H3 K18 deacetylation significantly promote bacterial infection.

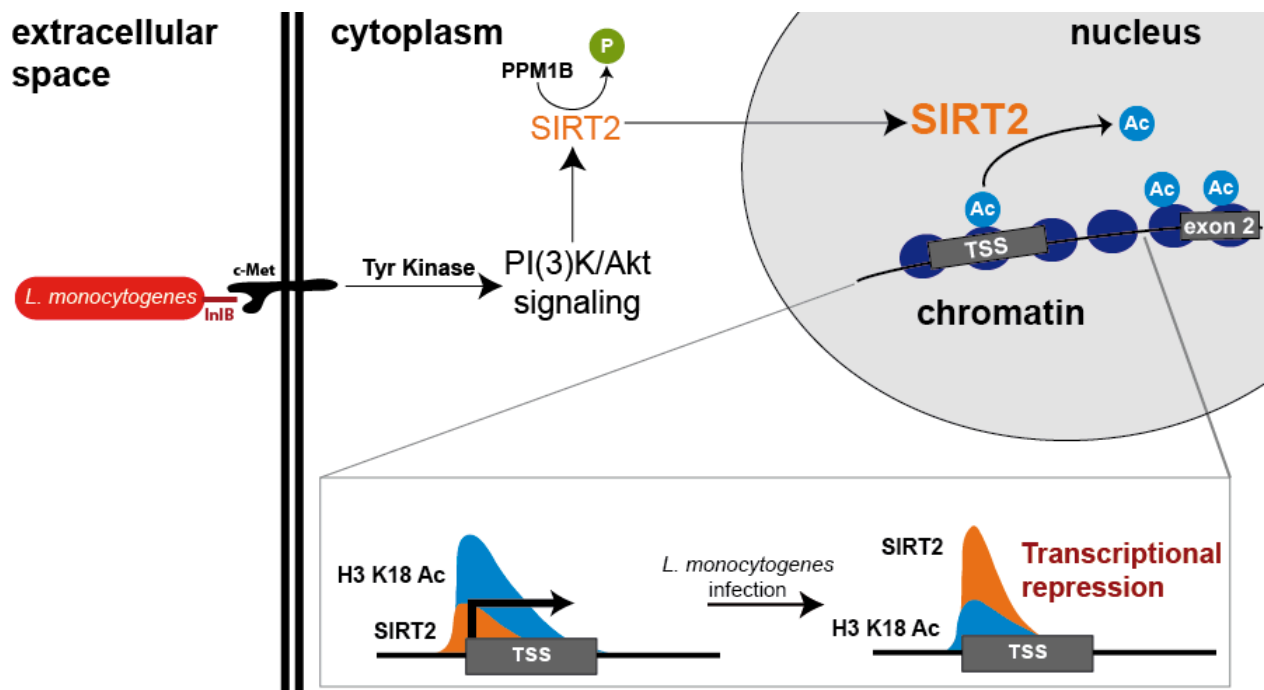


Figure 3. Model of *L. monocytogenes*-induced SIRT2-dependent H3K18 deacetylation

Annex:

Materials and methods

- Antibodies
- Cell culture, infections, and inhibitors
- Cloning
- Transfections
- Immunoblotting and cell fractionation
- Immunofluorescence and FACS analysis
- Microarray analysis
- qRT-PCR
- Chromatin Immunoprecipitation
- *Sirt2* mice
- Bacterial strains
- Plasmids
- Cloning primers
- qPCR primers

Data:

- Microarray analysis results

References:

Materials and Methods:

Antibodies

Rabbit polyclonal antibodies used were anti-Acetyl-Histone H3 K9 (Cell Signaling, 9671), anti-Acetyl-Histone H3 K14 (Cell Signaling, 4318), anti-Acetyl-Histone H3K18 (Cell Signaling, 9675), anti-Histone H3 (Cell Signaling, 9715), anti-Histone H4 (AbCam, ab10158), anti-Acetyl-Histone H4 K16 (Millipore, 06-762), anti-trimethyl-Histone H3 K9 (Upstate, 07-442), anti-SIRT2 (Thermo Scientific, PA3-200). Mouse monoclonal antibodies used were anti-HP1-1 α (Euromedex, 2HP-1H5-AS), anti- α -Tubulin (Sigma, T6074), anti-Actin (Sigma, A5441).

Cell culture, infections, and inhibitors

HeLa (ATCC CCL-2) and CaCO₂ (ATCC HTB-37) cells were cultured in MEM plus GlutaMAX (GIBCO) supplemented with 1mM sodium pyruvate (GIBCO), 0,1mM non-essential amino acid solution (GIBCO) and 10% (HeLa) or 20% (CaCO₂) fetal calf serum (FCS). RAW 264.7 cells (ATCC TIB-71) were cultured in DMEM plus GlutaMAX (GIBCO) supplemented with 2mM glutamine (GIBCO), 1mM sodium pyruvate and 10% FCS.

HeLa, and CaCO₂ were grown to semi-confluence at which point they were serum starved (serum low medium: MEM plus GlutaMAX, 1mM Na²⁺ Pyruvate, 0,1mM non-essential amino acid solution, 0,25% FCS) for 24 hours before use in experiments. Exponential phase bacteria were washed twice in the above-mentioned serum-low medium and added to cells at a multiplicity of infection (MOI) of 50:1 (HeLa & CaCO₂). After 1h of infection, cells were washed with serum-low medium and 10 μ g/ml gentamycin was added. Infections were carried out for 5h unless otherwise indicated.

InlB was isolated as per Ireton *et al.* ([Ireton et al., 1999](#)). Cells were treated with purified PBS, InlB (100nM), Hepatocyte Growth Factor (100nM HGF, Sigma, Cat#H5791), or Epidermal Growth Factor (100nM EGF, Sigma, Cat#E9644). Beads Polystyrene carboxyl P(S/V-COOH/1) 1.1 μ m (Bang Laboratories, Inc., via biovalley.fr, Cat#PC04N-7740-1I) were coated with InlB as per protocol Bang Laboratories, Beads Above the Rest, TechNote 205, Covalent Coupling.

For experiments involving pharmacological inhibitors, cells were pre-treated for 2 h prior to infection with Trichostatin A (5 μ M TSA, Sigma, Cat#T8552), Nicotinamide (5 μ M NIC, Sigma, N0636), 6-Chloro-2,3,4,9-tetrahydro-1H-carbasole-1-carboxamide (5 μ M CTCC, Enzo Life Sciences, ALX-270-437), 2-Cyano-3-[5-(2,5-dichlorophenyl)-2-furanyl]-N-5-quinolinyl-2-propenamamide (5 μ M AGK2, Enzo Life Sciences, ALX-270-484), or for 30 m with PBS, DMSO, Wortmannin (100nM, Sigma, W1628), Genistein (10 μ M, Sigma, G6776), and 1-L-6-hydroxymethyl-chiro-inositol 2-(R)-2-methyl-3-O-octadecylcarbonate (10 μ M HIMO, Alexis Biochemicals, ALX-270-292).

Cloning

For overexpression of wild type SIRT2, we used a SIRT2-GFP construct (pEGFP-c1 backbone), which was a kind gift from Brian North ([North and Verdin, 2007a](#)). siRNA insensitive SIRT2 and siRNA insensitive SIRT2 N168A were constructed by PCR amplification of the SIRT2-GFP construct with primer pairs: 1) SIRT2 fwd + SIRT2 05 rev; 2) SIRT2 05 fwd + SIRT2 rev; 3) SIRT2 fwd + SIRT2 rev (see supplemental experimental procedures for primer sequences), followed by insertion at the EcoRI site of the pEGFP-c1 vector.

SIRT2-GFP S27A/E mutants were constructed using site specific primers harboring modifications to the codon sequence of S27. Primers pairs were used to amplify two strands of SIRT2 overlapping at the site of mutation. Primary PCR products were produced (called front and back, below) for the two overlapping sections of SIRT2, harboring the S27 mutation in the middle. Front and back fragments of each SIRT2 S27 mutant are used as template DNA in order to amplify a full SIRT2 PCR product harboring the S27A/E mutation.

Construction of SIRT2-GFP S27A: dephosphorylated mimic

Primers SIRT2-fwd-full (TCCGAATTCTATGGCAGAGCCAGACCCCTCT) and SIRT2-S27A-rev (TCCTCCCTCAGCGTCTGAATC) amplify the SIRT2 S27A front fragment while primers SIRT2-S27A-fwd (GATTCAGACGCTGAGGGAGGA) and SIRT2-end-rev (CTCCGAATTCCTGGGGTTTCTCC) amplify the back fragment.

Construction of SIRT2-GFP S27E: phospho-mimetic

Primers SIRT2-fwd-full (TCCGAATTCTATGGCAGAGCCAGACCCCTCT) and SIRT2-S27E-rev (TCCTCCCTCTTCGTCTGAATC) amplify the SIRT2 S27E front fragment while primers SIRT2-S27E-fwd (GATTCAGACGAAGAGGGAGGA) and SIRT2-end-rev (CTCCGAATTCCTGGGGTTTCTCC) amplify the back fragment.

Transfections

DharmaFECT (Dharmacon) transfection was used to introduce RNAi knockdown SIRT1 (Thermo Scientific, siGENOME SMARTpool M-003540_01_0005), SIRT2 (Thermo Scientific, siGENOME SMARTpool M-004826-02-0005, or siRNA fragment D-004826-05), or control scramble siRNA (On-TARGETplus SMARTpool). Cells were assayed 72h after siRNA transfection.

SIRT2-FLAG, or SIRT2N168A-FLAG were rendered siRNA sensitive by the addition of three point mutations by PCR amplification using primers SIRT2 fwd with SIRT2 rev 05 and SIRT2 fwd 05 with SIRT2 rev (see supplemental table 2 for primer list)

Immunoblotting and cell fractionation

Total cell lysates were harvested by removing growth medium and adding lysis buffer [1M Tris HCl (pH 6,8 at 25°C), 10% SDS, 50% glycerol, 0,05% bromophenol blue, 10% β -mercaptoethanol]. Spleen and liver samples were collected as described in ([Ribet et al., 2010](#)). Samples were boiled for 5-10 min, sonicated for 5 s, and loaded of a 15% acrylamide gel. A semi-dry transfer was conducted for 1 h, at 32 mA per transfer, followed by blocking of the Hybond P-PVDF membranes (GE Healthcare) in TBS-Tween [Tris 50mM (pH8), NaCl 15mM, 0,1% Tween] supplemented with 10% milk. Transferred membranes were incubated with previously mentioned primary antibodies for 2 h at 25°C or ON at 4°C. Membranes were washed and incubated with horseradish peroxidase-conjugated goat α -rabbit or α -mouse antibodies (Biosys Laboratories). Quantification of Western blots was performed using the G:box-ichemi machine (SynGene).

Cell fractionation was conducted as follows. Cells were resuspended in Buffer A (consisting of 20mM HEPES (pH 7,0), 0,15mM EDTA, 0,15mM EGTA, and 10mM KCl). 1% NP40 was added followed by SR Buffer [50mM HEPES (pH 7,0), 0,25 EDTA, 10mM KCl, 70% (m/v) saccharose]. Samples were centrifuged for 5 min at 2,000 g. The supernatant was

isolated as the cytosolic fraction and re-centrifuged for 20 min at 20,000 g to eliminate cell nuclear debris. The pellet was washed in Buffer B [10mM HEPES (pH 8,0), 0,1mM EDTA, 100mM NaCl, 25% (v/v) glycerol] and centrifuged for 5 min at 2,000 g. Buffers A, B, and SR were supplemented with 0,15mM spermidine, 0,15 spermine, 1mM DTT, and 1x Complete®. The washed pellet was resuspended in sucrose buffer [20mM Tris (pH 7,65), 60mM NaCl, 15mM KCl, 0,34M sucrose, 0,15mM spermine, 0,15mM spermidine] followed by the addition of a high salt buffer [20mM Tris (pH 7,65), 0,2mM EDTA, 25% glycerol, 900mM NaCl, 1,5mM MgCl₂] in order to obtain a final salt concentration of 250mM. Samples were incubated for 25 min and centrifuged for 10 min at 10,000 rpm. The supernatant was isolated as the nuclear soluble fraction from the pellet, which represents chromatin and nuclear insoluble material. The pellet was resuspended in sucrose buffer + MNase (0,0025U/uL) and 1mM CaCl₂, and incubated at 37°C for 10 min. EDTA 4mM was added and samples were sonicated using the Bioruptor (Diagenode) for 7,5 min (15 sec ON and 1 min OFF) and centrifuged for 15 m at 13,000 rpm. The supernatants represent a soluble chromatin fraction.

Immunofluorescence and FACS analysis

Cells were grown on glass cover slides. After infection, cells were fixed in 4% paraformaldehyde and permeabilized in 0.3% triton for 15 min. Immunostaining was performed with an anti-SIRT2 antibody (Thermo Scientific, PA3-200) in 1% BSA+ 0.1% tween 100. Infections for immunofluorescence and for FACS were carried out with GFP expressing *L. monocytogenes*. Infected cells were monitored with a FACScalibur (BD bioscience), and analysis was done with Flowjo software.

Microarray analysis

Total mRNA from uninfected and infected cells, pre-treated or untreated with AGK2 (5µM for 2h), was extracted and purified as per RNeasy kit (Qiagen, Valencia, CA). Quality assessment and normalization of the arrays was performed with the tools available in Expression Console v1.1 (Affymetrix, Inc., Santa Clara, CA) and Bioconductor packages. 200ng of total RNA was reverse transcribed and amplified per the manufacturer's protocols using the Applause WTA Amp-Plus System (Nugen Technologies, Inc. 5510-24), fragmented

and biotin labeled using the Encore Biotin Module, (Nugen Technologies, Inc. 4200-12). Gene expression was determined by hybridization of the labeled template to *HuGene 1.0 ST* microarrays (Affymetrix, Inc., Santa Clara, CA). Hybridization cocktail and post-hybridization processing was performed according to the “Target Preparation for Affymetrix GeneChip® Eukaryotic Array Analysis” protocol found in the appendix of the Nugen protocol of the fragmentation kit. Arrays were hybridized for 18 hours and washed using fluidics protocol FS450_0007 on a GeneChip Fluidic Station 450 (Affymetrix, Inc.) and scanned with an Affymetrix Genechip Scanner 3000, generating CEL files for each array. Three Biological replicates were run for each condition.

Gene-level expression values were derived from the CEL file probe-level hybridization intensities using the model-based Robust Multichip Average algorithm (RMA) ([Bolstad et al., 2003](#)). RMA performs normalization, background correction and data summarization. An analysis is performed using the Limma t-test ([Wettenhall and Smyth, 2004](#)), and a p-value threshold of $p < 0.05$ is used as the criterion for expression. The estimated false discovery rate (FDR) of this analyse was calculated using the BH approach ([Benjamini and Hochberg, 1995](#)) in order to correct for multiple comparisons.

qRT-PCR

Total mRNA was extracted using the RNeasy kit (Qiagen). Reverse transcription was performed with the iScript cDNA Synthesis kit (BioRad). qPCR was done using the SsoFast EvaGreen Supermix (BioRad) and run on a MyIQ device (BioRad). Data were analyzed by the $\Delta\Delta C_t$ method.

Chromatin Immunoprecipitation

Preparation of ChIP samples was adapted from Lebreton *et al.* ([Lebreton et al., 2011](#)). Chromatin inputs corresponding to 1.8×10^5 cells for each individual ChIP assay. All buffers were supplemented with Complete EDTA-free protease inhibitor cocktail tablets (Roche). Formaldehyde-fixed cells were washed in PBS and lysed in 10 mM Tris (pH 8) 10 mM EDTA, 0.5 mM EGTA, 0.25% Triton X-100 for 5 min on ice. The nuclear pellets were recovered by brief centrifugation at $3,000 \times g$, and the soluble nuclear fraction was extracted with 250 mM NaCl, 50 mM Tris (pH 8), 1 mM EDTA, 0.5 mM EGTA for 30 min on

ice. After brief centrifugation at 16,000 x g, chromatin pellets were resuspended in 10 mM Tris (pH 8), 1 mM EDTA, 0.5 mM EGTA, 0.5% SDS, and then sonicated with a Bioruptor (Diagenode) to shear chromatin to a final size of 150-600 bp. Extracts were quantified by $A_{260\text{nm}}$, and material quantities were adjusted accordingly. Samples were then diluted to obtain the following IP buffer composition: 150 mM NaCl, 10 mM Tris (pH 8), 0.1% SDS, 1% Triton X-100, 0.1% sodium deoxycholate, 1 mM EDTA, 0.5 mM EGTA. Immunoprecipitation (IP) was carried out ON at 4 °C with anti - SIRT2, H3, H3K18 Ac, H4, and H4 K16 Ac. Immunocomplexes were recovered with Dynabeads Protein G (Invitrogen) added for 90 min at 4°C and then washed 5 times in a succession of isotonic and saline buffers as described (Boukarabila *et al.*, 2009). After a final wash in 10 mM Tris pH8, 1mM EDTA, 0.01% Igepal, bound material was eluted by the addition of water containing 10% Chelex (Bio-Rad), followed by boiling for 10 min to reverse the crosslink. Samples were then incubated with proteinase K (100 µg/mL) for 30 min at 55 °C with some shaking, and then boiled for another 10 min. Finally, the ChIP DNA fraction was separated from beads and Chelex matrix by centrifugation. Recovered supernatants were quantified by qRT-PCR using the $\Delta\Delta\text{Ct}$ method. Results for samples immunoprecipitated with AcH3K18 were normalized to samples immunoprecipitated with H3. The sequences for the primers used are given in Table S1.

***Sirt2* mice**

Sirt2^{tm1a(EUCOMM)Wtsi} mice were obtained from the Sanger center. For details see <http://www.informatics.jax.org/javawi2/servlet/WIFetch?page=alleleDetail&key=606707>. Infections were performed by intra venous injection of 10⁵ bacteria per animal. Experiments were performed according to the Institut Pasteur guidelines for animal experimentation.

Immunoprecipitation

Immunoprecipitation of SIRT2-FLAG was performed with M2-FLAG affinity gel (Sigma A2220), according to manufacturer's protocol. Elution was performed in 0.1 M glycine HCl, pH 3.5.

SDS-PAGE and LC-MS/MS analysis

Proteins were separated by SDS-PAGE on a 4-15% polyacrylamide gel (Bio-Rad) and stained by colloid coomassie blue (Invitrogen). For every sample the gel lane was cut in five consecutive gel slices which were washed with H₂O, incubated for 15' with water/acetonitrile (1:1, v/v) and incubated for 15' with 100% acetonitrile before they were dried completely in a vacuum concentrator. 0.25 µg sequencing-grade trypsin (Promega) in 50 mM ammonium bicarbonate in water/acetonitrile (9:1, v/v) was added to the dried gel slices and proteins were digested overnight at 37 °C. Peptides eluted from every gel slice were dried completely in a vacuum concentrator and redissolved in 15 µl solvent A (0.1% formic acid in water/acetonitrile (98:2, v/v)) of which 5 µl was used for LC-MS/MS analysis on an Ultimate 3000 HPLC system (Dionex) in line connected to an LTQ Orbitrap Velos mass spectrometer (Thermo Electron). Trapping was performed at 10 µl/min for 4 min in solvent A on a PepMap™ C₁₈ column (0.3 mm inner diameter × 5 mm (Dionex)), and following back-flushing from the trapping column, the sample was loaded on a reverse-phase column (made in-house, 75 µm I.D. × 150 mm, 3 µm beads C18 Reprosil-HD, Dr. Maisch). Peptides were eluted by a linear increase from 2 to 55% solvent B (0.08% formic acid in water/acetonitrile (2:8, v/v)) over 30 minutes at a constant flow rate of 300 nl/min.

The mass spectrometer was operated in data-dependent mode, automatically switching between MS and MS/MS acquisition for the ten most abundant ion peaks per MS spectrum. Full-scan MS spectra (300-2000 m/z) were acquired at a resolution of 60,000 in the orbitrap analyzer after accumulation to a target value of 1000,000. The ten most intense ions above a threshold value of 5000 were isolated for fragmentation by CID at a normalized collision energy of 35% in the linear ion trap (LTQ) after filling the trap at a target value of 5000 for maximum 50 ms. From the MS/MS data in each LC-run, Mascot generic files (mgf) were created using the Mascot Distiller software (version 2.4.3.3, Matrix Science Ltd.). When generating peak lists, grouping of spectra was performed with 0.005 m/z tolerance on the precursor ion, a maximum intermediate retention time of 30 s and a maximum intermediate scan count of 5. A peak list was only generated when the MS/MS

spectrum contained more than 10 peaks, no deisotoping was performed and the relative signal to noise limit was set at 2.

Generated peak lists were then searched with Mascot using the Mascot Daemon interface (version 2.3.0, Matrix Science Ltd.) against the human proteins in the Swiss-Prot database (database release version of July 7, 2012 containing 20235 human protein sequences). Variable modifications were set to oxidation of methionine residues, pyroglutamate formation of N-terminal glutamine residues, acetylation of peptide N-termini and lysine residues, di-glycine modification of lysine residues and phosphorylation of serine, threonine and tyrosine residues. Mass tolerance of the precursor ions was set to 10 ppm and mass tolerance of the fragment ions was set to 0.5 Da. The peptide charge was set to 1+, 2+, or 3+, and one missed tryptic cleavage site was allowed. Also, the C13 setting of Mascot was to 1. Only peptides that were ranked first and scored above the threshold score set at 99% confidence were withheld. For processing of all MS data, the ms_lims software platform was used (PMID 20058248).

Histone Purification

Histones were purified according to protocol published in ([Shechter et al., 2007](#)) using TCA precipitation.

Bacterial strains

The bacterial strains used in these experiments and their growth conditions are heretofore indicated.

L. monocytogenes strain EGD (BUG600) was grown in brain-heart infusion (BHI) medium (Difco, Detroit, MI) at 37°C until OD_{600nm}=1. *S. flexneri* strain M90T (BUG2505) was cultured in trypticase soy (TCS) until OD_{600nm}=0,6. Wildtype *S. typhimurium* (BUG2939) and *E. coli* expressing invasin from *Yersinia pseudotuberculosis* (BUG2940) was cultured in Luria Broth (LB) until OD_{600nm}=0,8.

Bacterial species	Genotype	Strain Number
<i>L. monocytogenes</i>	Wildtype EGD	BUG600
<i>L. monocytogenes</i>	EGD Δ inlB	BUG1047
<i>L. monocytogenes</i>	EGD-GFP	BUG2539

<i>L. innocua</i>	Wildtype	BUG499
<i>L. innocua</i>	<i>inlB</i> (pAT18pprot + LRR-IR <i>inlB</i> -SPA)	BUG1638

Plasmids

	Strain Number
SIRT2-GFP	BUG3340
SIRT2 ⁺ -GFP (siRNA insensitive)	BUG3341
SIRT2N168A ⁺ -GFP (siRNA insensitive)	BUG3342
pSR α -wp85 – IK85 from K. Ireton collection	BUG3371
pSR α - Δ p85 – IK86 from K. Ireton collection	BUG3372

Cloning primers

SIRT2 fwd	GCTTCGAATTCAGTCGCAATCACTCTCGGCATGGACGAG
SIRT2 rev	GAAGCCTTAAGGACTGCCTAGTAAAACCTCTACAAATGTGGTATGG
SIRT2 rev 05	CTTAGCGGATACTCATGCCGGC
SIRT2 fwd 05	GCCGGCATGAGTATCCGCTAAG

qPCR Primers

For all genes, primers _1 and _2 amplify TSS, _3 and _4 exon 2, and _5 and 6 are used for expression validation of transcriptome analysis

oligoname	sequence
ARL5B_1	TGTGGTAGGTAGGTGGGTACAGA
ARL5B_2	ACCGGACAGCCCTTTGTTTCGAG
ARL5B_3	TAATTAGGCTGCACCTGGGCGTAT
ARL5B_4	TGAGGCAGGAGAATGGCTTGAAC
ARL5B_5	ACTGAACAGTGGCCAAAGGAAAGC
ARL5B_6	CATCCCACACACACCACAAACCAT
IER_1	AATGCCCACTTCGGCGATACTCA
IER_2	TGAGATCTTCACCTTCGACCCTCT
IER_3	GCTCCGAAGTCAGATTAAGGGCT
IER_4	TCTTTCTGCTGCTCACCATCGTCT
IER_5	TGGAAC TGCGGCAAAGTAGGAGAA
IER_6	AGTTGAGATGCTGGAGGATGCAGT
TIPARP_1	TTCTCGGAACAAAGTGACCCCTCCA
TIPARP_2	AGTTCTGTGCGGTGGACTTATGCT
TIPARP_3	AAGCTCCAGAACGAGTGGTTCCAA
TIPARP_4	TGGAAGTGAGCTGGTGTGGAATCT
TIPARP_5	TCTCAGGAGCACTTGGAAAGA
TIPARP_6	ACACGTTTATGGCATTCAAA
EGR2_1	CAGTTCGGCATTTGGAAAAGATGGT
EGR2_2	AGGTTGTGCGAGGAGCAAATGATG
EGR2_3	TCTGGGATCATTGGGAAGAGACCT
EGR2_4	TTATTTGGCTGTGCAGGAGACCT
EGR2_5	TTGACCAGATGAACGGAGTG
EGR2_6	AGCAAAGTCTGCTGGGATATG
SDC4_1	AACCTCCAAGCACCCACCGACTC
SDC4_2	TTCTCCAGTCCGCGGTGCCAT
SDC4_3	ATCCAAGTCTCAAGGCATGGTCAC
SDC4_4	TTTGAGCTGTCTGGCTCTGGAGAT
SDC4_5	CTGTTCTCTGAGCGGAGT
SDC4_6	CTCATCGTCTGGTAGGGCTC
MYLIP_1	CAGCCATGCTGTGTTATGTGACGA
MYLIP_2	TCACCTGGTTGAGGCAGTCCT
MYLIP_3	TGGACTGCAGTTTACGGGTAGCAA
MYLIP_4	TGAGGCTCCACGAAGAACTTGACT
MYLIP_5	AAGTCTTCTGTTGGAGCCTCA
MYLIP_6	CTCTGGGGAACACAAGAGGT
EHHADH_1	CGTTACCTGATCGGTTGACCG
EHHADH_2	TGCCCTCGGTGATAGAGGAAACAT
EHHADH_3	TTGGTCTCAGTCTGTGGCTGGATT
EHHADH_4	GTGATTTGTGGAGCAGAGGGCAA
EHHADH_5	CTCAGACCCGGTTGAAGAAG
EHHADH_6	CTGAATTGGCTTGTTCAGCA
SYDE2_1	GGGAAGCTGTGATCCGCCAA
SYDE2_2	ACCCAGTTGCGAGAGGCTATTAT
SYDE2_3	TTGACAGCAGGGAGCTTCAACA
SYDE2_4	CCCATTCTGAGGATGATGACCTT
SYDE2_5	AAGCAGAGCGGCATACTGAAGACT
SYDE2_6	AACATGGGACTGTCTCCACCATT
ERCC5_1	TTTAATGCGCTCCATTAGTGCCG
ERCC5_2	AATTCTTCTACGACGGACTGCACC
ERCC5_3	CAAGCACTTAAAGGAGTCCGGGAT

oligoname	sequence
ERCC5_4	GCAGAGCCGATGAAACAAAGTGAG
ERCC5_5	GGAAGCTGCTGGAGTGCT
ERCC5_6	CCGGACTCCTTTAAGTGCTTG
LEF1_1	CCGGGATGATTCAGACTCGTTCA
LEF1_2	CGAGATCAGTCATCCGAAGAGGAA
LEF1_3	TGCTTGTCTGGCCACCTAACATCA
LEF1_4	CCAGCGCACACACATTTGTACCAT
LEF1_5	TGGATCTCTTTCTCCACCCA
LEF1_6	CACGTGAAGTGATGAGGGGG
EMP1_1	TAGCAGGGCGTAGCTTACCAACAA
EMP1_2	GGGTGTGTAATGGGCGGTTCTTT
EMP1_3	TTGCTGGCTGGTATCTTTGTGGTC
EMP1_4	GCAAGGGCTGTGGCTTAAACTTCT
EMP1_5	TGCGGTACATACTTCCAGA
EMP1_6	GAGTTCTGAAGGGTCCCAGC
CCL20_1	ACAGCACTCCCAAGAAGTGGGTA
CCL20_2	ACATCAAAGCAGCCAGGAGCAAAC
CCL20_3	GCAAGCAACTTTGACTGCTGTCTGG
CCL20_4	GCATTGATGTCACAGCCTTATTGGC
CCL20_5	GTGCTGCTACTCCACCTCTG
CCL20_6	CGTGTGAAGCCCAATAAAA
IL6_1	ACCGGAAACGAAAGAGAAGCTCTA
IL6_2	TGGCAGTTCAGGGCTAAGGATTT
IL6_3	AAATTCGGTACATCCTCGACGGCA
IL6_4	TGCTCTAGAACCAGCAAAGACCT
IL6_5	AGTGAGGAACAAGCCAGAGC
IL6_6	GTGAGGGGTGGTTATTGCAT
ARAP2_1	TCCAGACAGGGTCTCCCA
ARAP2_2	TTTCGAACTCCGCGACCCGA
ARAP2_3	TCGCGTTTAGGAGGAGACAGCTTA
ARAP2_4	CACCGCAGTTGGAGACTGTTAGAA
ARAP2_5	GGAGCATCTGCAAAGAAGGT
ARAP2_6	GCCATCAAATTTACCCATC
PLK2_1	TTGTCACCTTTCCAGCACTTTGC
PLK2_2	ACCATCACCACCATTCCGACT
PLK2_3	GGGCCATCCTTGACACAAAGAAA
PLK2_4	TGTTTCTTTCCAGGGTGGCTTTGC
PLK2_5	AGATCTCGGGATTATCGTC
PLK2_6	TCGTAACATTTTGCAAAGCC
ATP7B_1	AACTCACTTTCCGACTGGCCC
ATP7B_2	TCAGAGAAGAATTCGGTGTCCGTG
ATP7B_3	TCAATTTGGTCCCAGGCTTAAAGGA
ATP7B_4	AGGCCGTACACTTATCAGCCTT
ATP7B_5	AGATCACAGCCAGAGAAGGG
ATP7B_6	GCCAACATTGTCAAAGCAA
GAPDH for.	AATGAAGGGTTCATTGATGG
GAPDH rev.	AAGGTGAAGTTCGGAGTCAA

Microarray Analysis Results:

Transcriptome of *L. monocytogenes* infection

Rows in bold font represent genes from the microarray analysis whose change in expression were verified by qRT-PCR. Rows labeled in purple represent genes that were modulated during infection, independent of SIRT2 activity.

Fold Change	P.Value	Gene Symbol	Gene Accession	Affymetrix Probe ID	Gene Name
5.68667	0.00006	TFPI2	NM_006528	8141016	tissue factor pathway inhibitor 2
4.15833	0.00247	IL6	NM_000600	8131803	interleukin 6 (interferon, beta 2)
3.37333	0.01566	ITGA2	NM_002203	8105267	integrin, alpha 2 (CD49B, alpha 2 subunit of VLA-2 receptor)
3.08333	0.00641	ETS1	NM_001143820	7952601	v-ets erythroblastosis virus E26 oncogene homolog 1 (avian)
3.06167	0.03877	NPPB	NM_002521	7912520	natriuretic peptide B
3.01667	0.04005	ANKRD1	NM_014391	7934979	ankyrin repeat domain 1 (cardiac muscle)
2.95500	0.00791	SNAI2	NM_003068	8150698	snail homolog 2 (Drosophila)
2.85000	0.00641	CCL20	NM_004591	8048864	chemokine (C-C motif) ligand 20
2.78000	0.00826	TRIM55	NM_033058	8146669	tripartite motif-containing 55
2.62500	0.00641	PLK2	NM_006622	8112202	polo-like kinase 2
2.61833	0.03277	TGFB2	NM_001135599	7909789	transforming growth factor, beta 2
2.60833	0.01501	CYR61	NM_001554	7902687	cysteine-rich, angiogenic inducer, 61
2.57500	0.00006	ARL14	NM_025047	8083743	ADP-ribosylation factor-like 14
2.51333	0.00641	MIR21	NR_029493	8008885	microRNA 21
2.49333	0.00130	EMP1	NM_001423	7954090	epithelial membrane protein 1
2.42500	0.00791	BIRC3	NM_001165	7943413	baculoviral IAP repeat-containing 3
2.38333	0.01501	NNMT	NM_006169	7943998	nicotinamide N-methyltransferase
2.33333	0.01566	---	---	8012906	---
2.29833	0.02164	F2RL1	NM_005242	8106403	coagulation factor II (thrombin) receptor-like 1
2.28500	0.02072	C15orf48	NM_032413	7983478	chromosome 15 open reading frame 48 carcinoembryonic antigen-related cell adhesion molecule 1 (biliary glycoprotein)
2.26333	0.03166	CEACAM1	NM_001712	8037205	(biliary glycoprotein)
2.24333	0.00130	MMP1	NM_002421	7951271	matrix metalloproteinase 1 (interstitial collagenase)
2.24000	0.02059	ART4	NM_021071	7961507	ADP-ribosyltransferase 4 (Dombrock blood group)
2.23167	0.01219	SGMS2	NM_001136258	8096733	sphingomyelin synthase 2
2.16000	0.04844	EDN1	NM_001955	8116921	endothelin 1
2.13167	0.01234	C8orf4	NM_020130	8146115	chromosome 8 open reading frame 4

2.13000	0.03062	PTGS2	NM_000963	7922976	prostaglandin-endoperoxide synthase 2 (prostaglandin G/H synthase and cyclooxygenase)
2.12333	0.00891	EGR1	NM_001964	8108370	early growth response 1
2.12167	0.02718	LMCD1	NM_014583	8077490	LIM and cysteine-rich domains 1
1.96500	0.01095	ITGB6	NM_000888	8056184	integrin, beta 6
1.95667	0.01641	DUSP1	NM_004417	8115831	dual specificity phosphatase 1
1.94167	0.00641	BTG2	NM_006763	7908917	BTG family, member 2
1.94167	0.02492	CCL2	NM_002982	8006433	chemokine (C-C motif) ligand 2
1.91000	0.01501	SERPINB2	NM_001143818	8021635	serpin peptidase inhibitor, clade B (ovalbumin), member 2
1.90000	0.01241	ANXA1	NM_000700	8155849	annexin A1
1.89167	0.01095	RGS2	NM_002923	7908409	regulator of G-protein signaling 2, 24kDa
1.86333	0.03179	HEG1	NM_020733	8090193	HEG homolog 1 (zebrafish)
1.85000	0.04005	UPP1	NM_003364	8132725	uridine phosphorylase 1
1.80167	0.02325	FOS	NM_005252	7975779	FBJ murine osteosarcoma viral oncogene homolog
1.79167	0.00641	TRIB1	NM_025195	8148304	tribbles homolog 1 (Drosophila)
1.77500	0.02325	MUC13	NM_033049	8090180	mucin 13, cell surface associated
1.77000	0.00791	GPR87	NM_023915	8091515	G protein-coupled receptor 87
1.72500	0.02380	KLF6	NM_001300	7931810	Kruppel-like factor 6
1.62500	0.02325	BHLHE40	NM_003670	8077441	basic helix-loop-helix family, member e40
1.61500	0.01834	CYP24A1	NM_000782	8067140	cytochrome P450, family 24, subfamily A, polypeptide 1
1.56667	0.03836	TNS4	NM_032865	8015016	tensin 4
1.55833	0.04490	GLIPR1	NM_006851	7957260	GLI pathogenesis-related 1
1.55667	0.01832	ACSL5	NM_016234	7930498	acyl-CoA synthetase long-chain family member 5
1.55167	0.03143	GCNT3	NM_004751	7984001	glucosaminyl (N-acetyl) transferase 3, mucin type
1.54667	0.04168	EREG	NM_001432	8095728	epiregulin
1.52833	0.04168	CD44	NM_000610	7939341	CD44 molecule (Indian blood group)
1.50667	0.03020	FGFBP1	NM_005130	8099467	fibroblast growth factor binding protein 1
1.47500	0.04389	VGLL3	NM_016206	8088979	vestigial like 3 (Drosophila)
1.45833	0.01505	HSPB8	NM_014365	7959102	heat shock 22kDa protein 8
1.44667	0.03918	PPP1R15A	NM_014330	8030128	protein phosphatase 1, regulatory (inhibitor) subunit 15A
1.41667	0.02325	IER3	NM_003897	8178435	immediate early response 3
1.40000	0.01095	KRTAP3-1	NM_031958	8015173	keratin associated protein 3-1
1.40000	0.01095	KRTAP3-1	NM_031958	8019593	keratin associated protein 3-1
1.38833	0.00791	ERRFI1	NM_018948	7912157	ERBB receptor feedback inhibitor 1
1.36667	0.03693	NEDD9	NM_001142393	8123936	neural precursor cell expressed, developmentally down-regulated 9

1.36333	0.03058	ATF3	NM_001040619	7909610	activating transcription factor 3
1.34500	0.04284	NOSTRIN	NM_001039724	8046099	nitric oxide synthase trafficker
1.33333	0.02985	LIMA1	NM_001113546	7963187	LIM domain and actin binding 1
1.32833	0.02070	UGCG	NM_003358	8157216	UDP-glucose ceramide glucosyltransferase
1.32667	0.03475	SERPINE2	NM_006216	8059376	serpin peptidase inhibitor, clade E (nexin, plasminogen activator inhibitor type 1), member 2
1.32667	0.02316	STOM	NM_004099	8163896	stomatin
1.31833	0.04760	ARHGDI3	NM_001175	7961532	Rho GDP dissociation inhibitor (GDI) beta
1.31333	0.04005	NUAK2	NM_030952	7923753	NUAK family, SNF1-like kinase, 2
1.31000	0.01172	TXNRD1	NM_003330	7958174	thioredoxin reductase 1
1.30833	0.01834	NFKBIZ	NM_031419	8081386	nuclear factor of kappa light polypeptide gene enhancer in B-cells inhibitor, zeta
1.30833	0.00641	KLF4	NM_004235	8163002	Kruppel-like factor 4 (gut)
1.30000	0.01234	DDIT4	NM_019058	7928308	DNA-damage-inducible transcript 4
1.28167	0.01258	DUSP5	NM_004419	7930413	dual specificity phosphatase 5
1.27333	0.04490	INPP1	NM_001128928	8047069	inositol polyphosphate-1-phosphatase
1.27333	0.01845	IDS	NM_000202	8175593	iduronate 2-sulfatase
1.26667	0.01626	SSFA2	NM_001130445	8046726	sperm specific antigen 2
1.25667	0.01095	ARL5B	NM_178815	7926531	ADP-ribosylation factor-like 5B
1.25500	0.00641	KRTAP2-4	NM_033184	8015210	keratin associated protein 2-4
1.25500	0.00641	KRTAP2-4	NM_033184	8019576	keratin associated protein 2-4
1.24833	0.04629	SLC20A1	NM_005415	8044499	solute carrier family 20 (phosphate transporter), member 1
1.24333	0.02230	PLIN2	NM_001122	8160297	perilipin 2
1.24000	0.01641	EGR2	NM_000399	7933872	early growth response 2
1.23833	0.02985	TNFAIP3	NM_006290	8122265	tumor necrosis factor, alpha-induced protein 3
1.23833	0.03475	GEM	NM_005261	8151816	GTP binding protein overexpressed in skeletal muscle
1.22500	0.03526	DUSP6	NM_001946	7965335	dual specificity phosphatase 6
1.21333	0.02718	IER3	NM_003897	8124848	immediate early response 3
1.21333	0.02718	IER3	NM_003897	8179704	immediate early response 3
1.20833	0.04080	TIPARP	NM_015508	8083569	TCDD-inducible poly(ADP-ribose) polymerase
1.20000	0.02164	ZFP36	NM_003407	8028652	zinc finger protein 36, C3H type, homolog (mouse)
1.19833	0.01832	SMAD3	NM_005902	7984364	SMAD family member 3
1.19167	0.00641	MCL1	NM_021960	7919751	myeloid cell leukemia sequence 1 (BCL2-related)
1.18667	0.04529	MOSPD1	NM_019556	8175288	motile sperm domain containing 1
1.17833	0.01237	ZBED2	NM_024508	8089467	zinc finger, BED-type containing 2
1.16167	0.01834	ARAP2	NM_015230	8099760	ArfGAP with RhoGAP domain, ankyrin repeat and PH

domain 2				
1.15667	0.01641	KLF10	NM_005655	8152215 Kruppel-like factor 10
1.15333	0.04857	PLAU	NM_002658	7928429 plasminogen activator, urokinase
1.14000	0.02325	HEY1	NM_012258	8151457 hairy/enhancer-of-split related with YRPW motif 1
1.13667	0.02718	---	---	8116952 ---
1.12667	0.02164	UCA1	NR_015379	8026490 urothelial cancer associated 1 (non-protein coding)
1.11833	0.01641	S100P	NM_005980	8093950 S100 calcium binding protein P
1.10667	0.03657	ELL2	NM_012081	7921344 elongation factor, RNA polymerase II, 2
1.09833	0.03179	SERPINB8	NM_002640	8021653 serpin peptidase inhibitor, clade B (ovalbumin), member 8
1.09667	0.02059	FERMT2	NM_006832	7979204 fermitin family member 2
1.07333	0.02449	SCHIP1	NM_014575	8083677 schwannomin interacting protein 1
1.06833	0.01469	TIMP3	NM_000362	8075635 TIMP metalloproteinase inhibitor 3
1.06000	0.04313	MALL	NM_005434	8054479 mal, T-cell differentiation protein-like
1.04500	0.04490	CTPS	NM_001905	7900510 CTP synthase
1.03833	0.03149	EGLN3	NM_022073	7978544 egl nine homolog 3 (C. elegans)
1.02833	0.02349	ELL2	NM_012081	8113220 elongation factor, RNA polymerase II, 2
1.02500	0.02059	GCLC	NM_001498	8127158 glutamate-cysteine ligase, catalytic subunit
1.01500	0.03166	CGNL1	NM_032866	7983867 cingulin-like 1
1.01000	0.02807	ITGA6	NM_000210	8046380 integrin, alpha 6
1.00333	0.01775	PCDH7	NM_032456	8094520 protocadherin 7
0.99167	0.01095	KRT6A	NM_005554	7963421 keratin 6A
0.99000	0.02316	NCRNA00152	NR_024204	8043363 non-protein coding RNA 152
0.97833	0.02164	PHLDA1	NM_007350	7965040 pleckstrin homology-like domain, family A, member 1
0.97333	0.03877	RASA2	NM_006506	8083094 RAS p21 protein activator 2
0.96833	0.02200	GDF15	NM_004864	8027002 growth differentiation factor 15
0.96500	0.02449	NCRNA00152	NR_024204	8054611 non-protein coding RNA 152
0.95500	0.04844	SDC4	NM_002999	8066513 syndecan 4
0.95500	0.03836	USP53	NM_019050	8097098 ubiquitin specific peptidase 53
0.95333	0.02673	GREM1	NM_013372	7982377 gremlin 1
0.94000	0.04365	SNORD51	NR_002589	8047778 small nucleolar RNA, C/D box 51
0.93000	0.02164	---	---	7899560 ---
0.92500	0.04309	SH3RF1	NM_020870	8103630 SH3 domain containing ring finger 1
0.92167	0.01426	PRKAG2	NM_016203	8143961 protein kinase, AMP-activated, gamma 2 non-catalytic subunit
0.90833	0.04389	OXTR	NM_000916	8085138 oxytocin receptor
0.90500	0.02316	ARHGAP12	NM_018287	7932885 Rho GTPase activating protein 12
0.90500	0.03684	ZFAND5	NM_001102420	8161747 zinc finger, AN1-type domain 5

0.90333	0.03114	KCTD9	NM_017634	8149857	potassium channel tetramerisation domain containing 9
0.89000	0.02413	NR1D2	NM_005126	8078272	nuclear receptor subfamily 1, group D, member 2
0.89000	0.04614	NIPAL1	NM_207330	8094938	NIPA-like domain containing 1
0.88167	0.02985	ANKRD37	NM_181726	8098604	ankyrin repeat domain 37
0.86833	0.02200	TNFRSF12A	NM_016639	7992789	tumor necrosis factor receptor superfamily, member 12A
0.86333	0.03277	---	---	8108376	---
0.85833	0.01834	RABGEF1	NM_014504	8133176	RAB guanine nucleotide exchange factor (GEF) 1
0.85000	0.03156	LOC151760	ENST00000383686	8089464	hypothetical LOC151760
0.84833	0.03684	CPEB4	NM_030627	8110055	cytoplasmic polyadenylation element binding protein 4
0.84000	0.04556	ARHGAP42	NM_152432	7943349	Rho GTPase activating protein 42
0.83000	0.04482	PPFIBP1	NM_003622	7954559	PTPRF interacting protein, binding protein 1 (liprin beta 1)
0.82333	0.02325	C3orf52	NM_024616	8081645	chromosome 3 open reading frame 52
0.82333	0.04844	HMGCS1	NM_001098272	8111941	3-hydroxy-3-methylglutaryl-CoA synthase 1 (soluble)
0.81833	0.02718	---	---	8157798	---
0.81667	0.03684	PHLDA2	NM_003311	7945781	pleckstrin homology-like domain, family A, member 2
0.81167	0.03588	BCL10	NM_003921	7917338	B-cell CLL/lymphoma 10
0.81167	0.02807	KRTAP5-4	NM_001012709	7945657	keratin associated protein 5-4
0.80500	0.04168	AXL	NM_021913	8029006	AXL receptor tyrosine kinase BTB and CNC homology 1, basic leucine zipper transcription
0.80167	0.04490	BACH1	NR_027655	8068105	factor 1
0.80000	0.03448	SMURF2	NM_022739	8017651	SMAD specific E3 ubiquitin protein ligase 2
0.79500	0.04650	ZNF668	NM_001172668	7995030	zinc finger protein 668
0.79500	0.04504	HBEGF	NM_001945	8114572	heparin-binding EGF-like growth factor
0.79167	0.04168	SGK1	NM_001143676	8129677	serum/glucocorticoid regulated kinase 1
0.78500	0.02988	RIOK3	NM_003831	8020508	RIO kinase 3 (yeast)
0.77333	0.02644	FAM92B	BC093665	8003193	family with sequence similarity 92, member B
0.77167	0.04168	NR4A1	NM_002135	7955589	nuclear receptor subfamily 4, group A, member 1
0.77167	0.04883	CPM	NM_001874	7964834	carboxypeptidase M
0.75167	0.02957	JUNB	NM_002229	8026047	jun B proto-oncogene
0.74667	0.04883	KRTAP2-1	NM_001123387	8015208	keratin associated protein 2-1
0.74333	0.04482	FOSL1	NM_005438	7949532	FOS-like antigen 1
0.74167	0.04650	---	---	7930376	---
0.74167	0.04490	SPHK1	NM_182965	8010061	sphingosine kinase 1
0.73167	0.03166	CCL3	NM_002983	8014369	chemokine (C-C motif) ligand 3 UDP-Gal:betaGlcNAc beta 1,4- galactosyltransferase,
0.72500	0.03937	B4GALT5	NM_004776	8066939	polypeptide 5

0.72333	0.04168	RNF19A	NM_183419	8152041	ring finger protein 19A
0.71500	0.04465	ESPNP	NR_026567	7912854	espin pseudogene
0.71500	0.04844	ABCB8	ENST00000356058	8137330	ATP-binding cassette, sub-family B (MDR/TAP), member 8
0.71333	0.04745	LOC442132	NR_033906	8110916	golgin A6 family-like 1 pseudogene
0.71000	0.03020	C10orf54	NM_022153	7934185	chromosome 10 open reading frame 54
0.69500	0.04003	FAM84B	NM_174911	8152812	family with sequence similarity 84, member B
0.69167	0.02374	WEE1	NM_003390	7938348	WEE1 homolog (S. pombe)
0.68667	0.03094	ITCH	NM_031483	8061986	itchy E3 ubiquitin protein ligase homolog (mouse)
0.68000	0.04005	RAPGEF5	NM_012294	8138504	Rap guanine nucleotide exchange factor (GEF) 5
0.66833	0.03516	MMD	NM_012329	8016832	monocyte to macrophage differentiation-associated
0.65333	0.04857	---	---	8149146	---
0.65167	0.03166	---	---	7907351	---
0.65167	0.02959	SDCBP	NM_005625	8146550	syndecan binding protein (syntenin)
0.64500	0.03100	EGR4	NM_001965	8053022	early growth response 4
0.63500	0.04005	TES	NM_015641	8135576	testis derived transcript (3 LIM domains)
0.61833	0.04168	GADD45B	NM_015675	8024485	growth arrest and DNA-damage-inducible, beta
0.61667	0.04830	ESYT2	NM_020728	8144184	extended synaptotagmin-like protein 2
0.59833	0.04844	KRTAP2-4	NM_033184	8015214	keratin associated protein 2-4
0.59833	0.04844	KRTAP2-4	NM_033184	8019574	keratin associated protein 2-4
0.58833	0.04745	TNFAIP8	NM_014350	8107520	tumor necrosis factor, alpha-induced protein 8
-0.53167	0.04704	ARHGAP19	NM_032900	7935403	Rho GTPase activating protein 19
-0.56000	0.04733	MBNL3	NM_018388	8175177	muscleblind-like 3 (Drosophila)
-0.56167	0.04650	MCM3	NM_002388	8127031	minichromosome maintenance complex component 3
-0.56667	0.04883	EML1	NM_001008707	7976698	echinoderm microtubule associated protein like 1
-0.56833	0.04595	HMG20A	NM_018200	7985119	high-mobility group 20A
-0.56833	0.04883	ZNF234	NM_006630	8029392	zinc finger protein 234
-0.57667	0.04977	TGFBRAP1	NM_004257	8054364	transforming growth factor, beta receptor associated protein 1
-0.58500	0.04683	PJA1	NM_145119	8173340	praja ring finger 1
-0.58667	0.04143	MRFAP1L1	NM_203462	8099235	Morf4 family associated protein 1-like 1
-0.59167	0.04309	TNFRSF19	NM_148957	7968015	tumor necrosis factor receptor superfamily, member 19
-0.60167	0.03156	RPA1	NM_002945	8003679	replication protein A1, 70kDa
-0.61000	0.04504	METTL13	NM_015935	7907353	methyltransferase like 13
-0.61000	0.03836	ZNF607	NM_032689	8036436	zinc finger protein 607
-0.61333	0.04143	POLR3B	NM_018082	7958275	polymerase (RNA) III (DNA directed) polypeptide B
-0.61500	0.04465	ZNF226	NM_001032372	8029399	zinc finger protein 226
-0.62500	0.04730	BCL9	NM_004326	7904907	B-cell CLL/lymphoma 9

-0.62667	0.04857	MFSD5	NM_001170790	7955729	major facilitator superfamily domain containing 5
-0.63167	0.04733	ZNF616	NM_178523	8038954	zinc finger protein 616
-0.63167	0.03475	MCCC1	NM_020166	8092328	methylcrotonoyl-CoA carboxylase 1 (alpha)
-0.63333	0.03693	WDR53	NM_182627	8093141	WD repeat domain 53
-0.64333	0.03544	CYB5D1	NM_144607	8004694	cytochrome b5 domain containing 1
-0.64667	0.04490	COQ5	NM_032314	7967072	coenzyme Q5 homolog, methyltransferase (S. cerevisiae)
-0.64667	0.02959	PKP4	NM_003628	8045860	plakophilin 4
-0.64667	0.03877	GALNT11	NM_022087	8137448	UDP-N-acetyl-alpha-D-galactosamine:polypeptide N-acetylgalactosaminyltransferase 11 (GalNAc-T11)
-0.64833	0.04452	CCDC77	NM_032358	7952914	coiled-coil domain containing 77
-0.65000	0.03094	ATP7B	NM_000053	7971731	ATPase, Cu⁺⁺ transporting, beta polypeptide
-0.65000	0.03116	MTSS1	NM_014751	8152764	metastasis suppressor 1
-0.65500	0.04212	DDB2	NM_000107	7939738	damage-specific DNA binding protein 2, 48kDa
-0.65833	0.03020	PPIL3	NM_130906	8058147	peptidylprolyl isomerase (cyclophilin)-like 3
-0.66333	0.04309	sept-08	NM_015146	8114050	septin 8
-0.67000	0.03684	NIF3L1	NM_021824	8047356	NIF3 NGG1 interacting factor 3-like 1 (S. pombe)
-0.67167	0.04005	ANAPC5	NM_016237	7967149	anaphase promoting complex subunit 5
-0.67167	0.04313	NARF	NM_001038618	8010804	nuclear prelamin A recognition factor
-0.67333	0.04168	PARP1	NM_001618	7924733	poly (ADP-ribose) polymerase 1
-0.67333	0.04168	UROS	NM_000375	7936937	uroporphyrinogen III synthase
-0.67833	0.04458	MCM9	AK299076	8129214	minichromosome maintenance complex component 9
-0.68000	0.04711	USP21	NM_001014443	7906671	ubiquitin specific peptidase 21
-0.68167	0.03149	NDUFB10	NM_004548	7992402	NADH dehydrogenase (ubiquinone) 1 beta subcomplex, 10, 22kDa
-0.68333	0.04168	C10orf26	NM_017787	7930162	chromosome 10 open reading frame 26
-0.68500	0.03526	MKS1	NM_017777	8016909	Meckel syndrome, type 1
-0.68500	0.03116	RPL39L	NM_052969	8092654	ribosomal protein L39-like
-0.68833	0.04168	CALB2	NM_001740	7997139	calbindin 2
-0.69000	0.02959	SMAP2	NM_022733	7900426	small ArfGAP2
-0.69000	0.03836	FAN1	NM_014967	7982309	FANCD2/FANCI-associated nuclease 1
-0.69333	0.03684	MARVELD2	NM_001038603	8105899	MARVEL domain containing 2
-0.69333	0.03684	MARVELD2	NM_001038603	8177498	MARVEL domain containing 2
-0.69667	0.04704	MTIF2	NM_001005369	8052250	mitochondrial translational initiation factor 2
-0.69833	0.04168	PHF17	NM_199320	8097417	PHD finger protein 17
-0.70000	0.02775	SAT2	NM_133491	8012247	spermidine/spermine N1-acetyltransferase family member 2
-0.70333	0.03116	WDR5B	NM_019069	8089993	WD repeat domain 5B

-0.70667	0.03475	SMAGP	NM_001033873	7963280	small cell adhesion glycoprotein
-0.70833	0.03179	TIMELESS	NM_003920	7964145	timeless homolog (Drosophila)
-0.71000	0.03918	RBFOX2	NM_001082578	8075673	RNA binding protein, fox-1 homolog (C. elegans) 2
-0.71167	0.04303	KCTD1	NM_001136205	8022646	potassium channel tetramerisation domain containing 1
-0.71167	0.03475	PTCH1	NM_001083603	8162533	patched 1
-0.71167	0.03683	MAP7D2	NM_001168465	8171725	MAP7 domain containing 2
-0.71333	0.03836	NQO2	NM_000904	8116610	NAD(P)H dehydrogenase, quinone 2
-0.71500	0.02325	KIAA0319L	NM_024874	7914809	KIAA0319-like
-0.71667	0.03877	KIAA1217	NM_019590	7926679	KIAA1217
-0.71667	0.04635	PAAF1	NM_025155	7942476	proteasomal ATPase-associated factor 1 bone morphogenetic protein receptor, type II (serine/threonine kinase)
-0.71667	0.04482	BMPR2	NM_001204	8047538	kinase)
-0.72000	0.04080	ZNF510	NM_014930	8162631	zinc finger protein 510
-0.72000	0.03877	GOLGA1	NM_002077	8164105	golgin A1
-0.72167	0.02059	FAM83D	NM_030919	8062571	family with sequence similarity 83, member D membrane associated guanylate kinase, WW and PDZ domain containing 3
-0.72500	0.02540	MAGI3	NM_152900	7904106	containing 3
-0.72500	0.02325	STIM2	NM_001169118	8094501	stromal interaction molecule 2
-0.72833	0.03116	CCDC56	NM_001040431	8015712	coiled-coil domain containing 56
-0.73000	0.02713	RGS4	NM_001102445	7906919	regulator of G-protein signaling 4
-0.73000	0.03116	PRPSAP1	NM_002766	8018694	phosphoribosyl pyrophosphate synthetase-associated protein 1
-0.73833	0.03877	IPP	NM_005897	7915775	intracisternal A particle-promoted polypeptide
-0.73833	0.04005	PGAP1	NM_024989	8057959	post-GPI attachment to proteins 1
-0.74000	0.01677	TRAFD1	NM_001143906	7958828	TRAF-type zinc finger domain containing 1
-0.74333	0.03552	UBE4B	NM_001105562	7897527	ubiquitination factor E4B (UFD2 homolog, yeast)
-0.74333	0.03021	---	---	7957549	---
-0.74333	0.02463	VPS39	NM_015289	7987840	vacuolar protein sorting 39 homolog (S. cerevisiae)
-0.74333	0.03062	FTSJD2	NM_015050	8119198	FtsJ methyltransferase domain containing 2
-0.75167	0.03664	HRASLS	NM_020386	8084838	HRAS-like suppressor
-0.75167	0.02325	MDC1	NM_014641	8124813	mediator of DNA-damage checkpoint 1
-0.75167	0.02325	MDC1	NM_014641	8178404	mediator of DNA-damage checkpoint 1
-0.75333	0.01834	NR1H3	NM_005693	7939751	nuclear receptor subfamily 1, group H, member 3
-0.75333	0.01955	BBS2	NM_031885	8001507	Bardet-Biedl syndrome 2
-0.75833	0.02070	TMTC4	NM_032813	7972579	transmembrane and tetratricopeptide repeat containing 4
-0.75833	0.02316	TEX2	NM_018469	8017582	testis expressed 2
-0.76167	0.03526	C8orf31	BC073830	8148580	chromosome 8 open reading frame 31

-0.76667	0.04733	MKI67	NM_002417	7937020	antigen identified by monoclonal antibody Ki-67
-0.76667	0.03877	ATF7IP	NM_018179	7954104	activating transcription factor 7 interacting protein
-0.76667	0.03683	NCOA1	NM_147223	8040552	nuclear receptor coactivator 1
-0.76833	0.02540	DTX4	NM_015177	7940160	deltex homolog 4 (Drosophila)
-0.76833	0.03978	ACPP	NM_001099	8082673	acid phosphatase, prostate
-0.76833	0.03683	SH2D4A	NM_022071	8144880	SH2 domain containing 4A
-0.77000	0.04309	AARS	NM_001605	8002347	alanyl-tRNA synthetase
-0.77333	0.02595	NHLRC3	NM_001012754	7968703	NHL repeat containing 3
-0.77333	0.02536	WDR92	NM_138458	8052703	WD repeat domain 92
-0.77333	0.04465	C8orf40	NM_001135674	8146225	chromosome 8 open reading frame 40
-0.77333	0.01830	DOCK8	NM_203447	8153959	dedicator of cytokinesis 8 v-myc myelocytomatosis viral related oncogene, neuroblastoma derived (avian)
-0.77500	0.03516	MYCN	NM_005378	8040419	derived (avian)
-0.77500	0.03257	SAP130	NM_001145928	8055104	Sin3A-associated protein, 130kDa
-0.77500	0.03293	CC2D2A	NM_001080522	8094190	coiled-coil and C2 domain containing 2A
-0.77667	0.02449	NEO1	NM_002499	7984704	neogenin 1
-0.77667	0.03156	FTSJ3	NM_017647	8017437	FtsJ homolog 3 (E. coli)
-0.77833	0.04882	ZNF678	NM_178549	7910198	zinc finger protein 678
-0.78000	0.04890	MYST4	NM_012330	7928491	MYST histone acetyltransferase (monocytic leukemia) 4
-0.78000	0.04320	AIF1L	NM_031426	8158771	allograft inflammatory factor 1-like
-0.78000	0.02718	C9orf116	NM_001048265	8165024	chromosome 9 open reading frame 116
-0.78333	0.02200	SLC39A11	NM_001159770	8018082	solute carrier family 39 (metal ion transporter), member 11 protein-L-isoaspartate (D-aspartate) O-methyltransferase domain containing 1
-0.78333	0.03877	PCMTD1	NM_052937	8146427	domain containing 1
-0.78500	0.04857	VPS11	NM_021729	7944382	vacuolar protein sorting 11 homolog (S. cerevisiae) Sep (O-phosphoserine) tRNA:Sec (selenocysteine) tRNA synthase
-0.78500	0.03020	SEPSECS	NM_016955	8099696	synthase
-0.78833	0.02718	USP40	NM_018218	8059801	ubiquitin specific peptidase 40
-0.78833	0.01501	TMPRSS2	NM_001135099	8070467	transmembrane protease, serine 2 excision repair cross-complementing rodent repair deficiency, complementation group 4
-0.79167	0.03156	ERCC4	NM_005236	7993298	complementation group 4
-0.79167	0.03978	TRIM24	NM_015905	8136473	tripartite motif-containing 24
-0.79333	0.02316	SMAD1	NM_005900	8097657	SMAD family member 1
-0.79667	0.01842	VPS33A	NM_022916	7967240	vacuolar protein sorting 33 homolog A (S. cerevisiae)
-0.79667	0.04005	NARG2	NM_024611	7989347	NMDA receptor regulated 2
-0.79667	0.04320	MND1	NM_032117	8097857	meiotic nuclear divisions 1 homolog (S. cerevisiae)
-0.79833	0.03179	CACHD1	NM_020925	7901993	cache domain containing 1

-0.80167	0.04313	ZFP161	NM_001143823	8022110	zinc finger protein 161 homolog (mouse)
-0.80667	0.04005	ITPR2	NM_002223	7961900	inositol 1,4,5-triphosphate receptor, type 2
-0.80833	0.04109	INTS3	NM_023015	7905631	integrator complex subunit 3
-0.80833	0.02518	RNF214	NM_207343	7944096	ring finger protein 214
-0.80833	0.04490	C18orf54	NM_173529	8021286	chromosome 18 open reading frame 54
-0.81000	0.02908	VPS33B	NM_018668	7991427	vacuolar protein sorting 33 homolog B (yeast)
-0.81167	0.02962	KBTBD7	NM_032138	7971218	kelch repeat and BTB (POZ) domain containing 7
-0.81500	0.04401	EXOC7	NM_001145297	8018620	exocyst complex component 7
-0.81500	0.01501	TTC30A	NM_152275	8056999	tetratricopeptide repeat domain 30A
-0.81500	0.04504	ST3GAL6	NM_006100	8081219	ST3 beta-galactoside alpha-2,3-sialyltransferase 6
-0.81667	0.01834	MAPK14	NM_001315	8119000	mitogen-activated protein kinase 14
-0.81667	0.03578	WDR67	NM_145647	8148158	WD repeat domain 67
-0.81833	0.02325	PBX1	NM_002585	7906954	pre-B-cell leukemia homeobox 1
-0.81833	0.03138	TRAF3IP1	NM_015650	8049635	TNF receptor-associated factor 3 interacting protein 1
-0.82000	0.04905	SLC33A1	NM_004733	8091637	solute carrier family 33 (acetyl-CoA transporter), member 1
-0.82000	0.04452	CDK5RAP2	NM_018249	8163733	CDK5 regulatory subunit associated protein 2
-0.82167	0.04005	SSBP3	NM_145716	7916403	single stranded DNA binding protein 3
-0.82833	0.02496	RASGRP1	NM_005739	7987405	RAS guanyl releasing protein 1 (calcium and DAG-regulated)
-0.82833	0.02463	ANKRD6	NM_014942	8121095	ankyrin repeat domain 6
-0.83500	0.03308	OBFC1	NM_024928	7936134	oligonucleotide/oligosaccharide-binding fold containing 1
-0.83833	0.03166	PEX11B	NM_003846	7904755	peroxisomal biogenesis factor 11 beta
-0.84000	0.04704	TIGD1	NM_145702	8059770	tigger transposable element derived 1
-0.84000	0.02957	TACC3	NM_006342	8093500	transforming, acidic coiled-coil containing protein 3
-0.84167	0.03877	DCAF5	NM_003861	7979849	DDB1 and CUL4 associated factor 5
-0.84333	0.04005	TMEM136	NM_001198670	7944554	transmembrane protein 136
-0.84333	0.04650	NUDT7	NM_001105663	7997332	nudix (nucleoside diphosphate linked moiety X)-type motif 7
-0.84333	0.04836	C7orf49	NR_024185	8143065	chromosome 7 open reading frame 49
-0.84500	0.01641	VPS26B	NM_052875	7945275	vacuolar protein sorting 26 homolog B (S. pombe)
-0.84500	0.04490	TLE4	NM_007005	8156060	transducin-like enhancer of split 4 (E(sp1) homolog, Drosophila)
-0.84667	0.03116	KIF22	NM_007317	7994620	kinesin family member 22
-0.84667	0.03877	CRISPLD1	NM_031461	8146967	cysteine-rich secretory protein LCCL domain containing 1
-0.85000	0.04704	ABL1	NM_005157	8158725	c-abl oncogene 1, non-receptor tyrosine kinase
-0.85167	0.02962	SDCCAG8	NM_006642	7911017	serologically defined colon cancer antigen 8
-0.85167	0.01834	FGFR2	NM_000141	7936734	fibroblast growth factor receptor 2
-0.85167	0.02528	C7orf25	NM_001099858	8139228	chromosome 7 open reading frame 25
-0.85333	0.04168	ACSF2	NM_025149	8008321	acyl-CoA synthetase family member 2

-0.85500	0.03886	C20orf177	NM_022106	8063755	chromosome 20 open reading frame 177
-0.85833	0.04365	SOS1	NM_005633	8051670	son of sevenless homolog 1 (Drosophila)
-0.85833	0.02380	NEK1	NM_012224	8103646	NIMA (never in mitosis gene a)-related kinase 1
-0.86333	0.03836	PANK1	NM_148977	7934945	pantothenate kinase 1
-0.86500	0.01834	EPB41L3	NM_012307	8022118	erythrocyte membrane protein band 4.1-like 3
-0.86667	0.02070	C11orf52	NM_080659	7943795	chromosome 11 open reading frame 52
-0.86667	0.02090	NCOA2	NM_006540	8151254	nuclear receptor coactivator 2
-0.87000	0.02325	ROBLD3	NM_014017	7906072	roadblock domain containing 3
-0.87000	0.03166	AMOT	NM_133265	8174576	angiominin
-0.87500	0.01842	HSDL1	NM_031463	8003116	hydroxysteroid dehydrogenase like 1
-0.87500	0.02959	KIF22	NM_007317	8003583	kinesin family member 22
-0.87667	0.02957	PIK3R3	NM_003629	7915787	phosphoinositide-3-kinase, regulatory subunit 3 (gamma)
-0.88000	0.02200	PEX12	NM_000286	8014264	peroxisomal biogenesis factor 12
-0.88167	0.02518	BCL7A	NM_020993	7959354	B-cell CLL/lymphoma 7A
-0.88333	0.03475	TMEM218	NM_001080546	7952484	transmembrane protein 218
-0.88333	0.03937	ZNF415	NR_028343	8039044	zinc finger protein 415
-0.88333	0.03087	BRD8	NM_139199	8114365	bromodomain containing 8
-0.88500	0.02413	ZNF528	NM_032423	8030931	zinc finger protein 528
-0.88833	0.03190	R3HDM2	NM_014925	7964413	R3H domain containing 2
-0.88833	0.04844	KAT2B	NM_003884	8078227	K(lysine) acetyltransferase 2B
-0.89000	0.03323	ZNF652	NM_014897	8016546	zinc finger protein 652
-0.89000	0.04309	BCS1L	NM_004328	8048370	BCS1-like (S. cerevisiae)
-0.89167	0.04401	MSX2	NM_002449	8110084	msh homeobox 2
-0.89500	0.03448	MEGF8	NM_001410	8029273	multiple EGF-like-domains 8
-0.89667	0.04530	TLE1	NM_005077	8161919	transducin-like enhancer of split 1 (E(sp1) homolog, Drosophila)
-0.89833	0.01566	USP30	NM_032663	7958439	ubiquitin specific peptidase 30
-0.89833	0.04830	FOXN3	NM_001085471	7980680	forkhead box N3
-0.89833	0.02718	ISY1	NM_020701	8090533	ISY1 splicing factor homolog (S. cerevisiae)
-0.90000	0.02059	KIAA1377	NM_020802	7943376	KIAA1377
-0.90000	0.01501	CEP110	NM_007018	8157534	centrosomal protein 110kDa
-0.90667	0.02059	FAM184A	NM_024581	8129231	family with sequence similarity 184, member A
-0.90833	0.02496	VPS45	NM_007259	7905099	vacuolar protein sorting 45 homolog (S. cerevisiae)
-0.90833	0.02150	ZBTB8OS	NM_178547	7914550	zinc finger and BTB domain containing 8 opposite strand
-0.91000	0.02059	TDRKH	NM_001083965	7920057	tudor and KH domain containing
-0.91000	0.02059	C3orf1	NM_016589	8081867	chromosome 3 open reading frame 1
-0.91000	0.04962	RNF144B	NM_182757	8117106	ring finger protein 144B

-0.91167	0.01834	GIT2	NM_057169	7966268	G protein-coupled receptor kinase interacting ArfGAP 2
-0.92000	0.03516	SLC6A4	NM_001045	8013989	solute carrier family 6 (neurotransmitter transporter, serotonin), member 4
-0.92500	0.01852	UBAC1	NM_016172	8165064	UBA domain containing 1
-0.92833	0.03544	DCAF7	NM_005828	8009164	DDB1 and CUL4 associated factor 7
-0.93000	0.04490	CCDC111	NM_152683	8098556	coiled-coil domain containing 111
-0.93167	0.03020	ALG6	NM_013339	7901915	asparagine-linked glycosylation 6, alpha-1,3-glucosyltransferase homolog (<i>S. cerevisiae</i>)
-0.93167	0.02718	ANKRD44	NM_001195144	8057990	ankyrin repeat domain 44
-0.93333	0.03359	C12orf26	NM_032230	7957404	chromosome 12 open reading frame 26
-0.93500	0.01566	FAM54B	NM_019557	7899057	family with sequence similarity 54, member B
-0.93500	0.01834	FAM72D	AB096683	7909146	family with sequence similarity 72, member D
-0.93500	0.01834	C4orf42	NR_033339	8093456	chromosome 4 open reading frame 42
-0.93833	0.04836	DCLRE1A	NM_014881	7936408	DNA cross-link repair 1A
-0.93833	0.01611	FAM158A	BC002491	7978114	family with sequence similarity 158, member A
-0.94167	0.03877	FYB	NM_001465	8111739	FYN binding protein
-0.94333	0.01810	FAM72D	AB096683	7904452	family with sequence similarity 72, member D
-0.94833	0.03836	MTUS2	NM_001033602	7968307	microtubule associated tumor suppressor candidate 2
-0.95000	0.04320	DCPS	NM_014026	7945101	decapping enzyme, scavenger
-0.95667	0.03380	PTPN6	NM_080549	7953569	protein tyrosine phosphatase, non-receptor type 6
-0.95667	0.01566	STS	NM_000351	8165866	steroid sulfatase (microsomal), isozyme S
-0.96000	0.01834	DET1	NM_017996	7991216	de-etiolated homolog 1 (<i>Arabidopsis</i>)
-0.96333	0.01605	FAM72D	AB096683	8039928	family with sequence similarity 72, member D
-0.96500	0.03847	C13orf27	NM_138779	7972674	chromosome 13 open reading frame 27
-0.96500	0.01834	FAM117B	NM_173511	8047565	family with sequence similarity 117, member B
-0.96667	0.01810	TMEM163	NM_030923	8055350	transmembrane protein 163
-0.96667	0.01605	SNCA	NM_000345	8101762	synuclein, alpha (non A4 component of amyloid precursor)
-0.96833	0.04143	CENPF	NM_016343	7909708	centromere protein F, 350/400kDa (mitosin)
-0.96833	0.02799	C22orf46	NM_001142964	8073470	chromosome 22 open reading frame 46
-0.96833	0.02449	ARHGAP24	NM_001025616	8096160	Rho GTPase activating protein 24
-0.97000	0.02200	IRF2	NM_002199	8103911	interferon regulatory factor 2
-0.97333	0.02059	CAMK2G	NM_172171	7934477	calcium/calmodulin-dependent protein kinase II gamma
-0.97833	0.01474	USP27X	NM_001145073	8167601	ubiquitin specific peptidase 27, X-linked
-0.98333	0.02316	COQ9	NM_020312	7996041	coenzyme Q9 homolog (<i>S. cerevisiae</i>)
-0.98833	0.01566	GRHL2	NM_024915	8147697	grainyhead-like 2 (<i>Drosophila</i>)
-0.98833	0.02316	ZMYM3	NM_201599	8173457	zinc finger, MYM-type 3

-0.99000	0.03746	C12orf48	NM_017915	7958031	chromosome 12 open reading frame 48
-1.00167	0.01237	POP5	NM_015918	7967084	processing of precursor 5, ribonuclease P/MRP subunit (S. cerevisiae)
-1.00167	0.02492	SERPINF1	NM_002615	8003667	serpin peptidase inhibitor, clade F (alpha-2 antiplasmin, pigment epithelium derived factor), member 1
-1.00167	0.03116	C6orf70	NM_018341	8123467	chromosome 6 open reading frame 70
-1.00167	0.02297	VPS52	NM_022553	8125649	vacuolar protein sorting 52 homolog (S. cerevisiae)
-1.00167	0.04309	TBL1X	NM_005647	8165911	transducin (beta)-like 1X-linked
-1.00167	0.02297	VPS52	NM_022553	8178917	vacuolar protein sorting 52 homolog (S. cerevisiae)
-1.00333	0.03020	FPGT	NM_003838	7902308	fucose-1-phosphate guanylyltransferase sepiapterin reductase (7,8-dihydrobiopterin:NADP+ oxidoreductase)
-1.00500	0.04854	SPR	NM_003124	8042696	
-1.01000	0.02985	NR2F2	NM_021005	7986329	nuclear receptor subfamily 2, group F, member 2
-1.01167	0.03836	ZNF302	NM_018443	8027674	zinc finger protein 302
-1.01333	0.04005	AAAS	NM_015665	7963646	achalasia, adrenocortical insufficiency, alacrimia
-1.01333	0.03578	MRPL2	NM_015950	8126512	mitochondrial ribosomal protein L2
-1.01833	0.04005	BBS10	NM_024685	7965060	Bardet-Biedl syndrome 10
-1.02167	0.02985	PIGM	NM_145167	7921526	phosphatidylinositol glycan anchor biosynthesis, class M
-1.02167	0.02325	POLG2	NM_007215	8017621	polymerase (DNA directed), gamma 2, accessory subunit
-1.02333	0.02164	VPS52	NM_022553	8180123	vacuolar protein sorting 52 homolog (S. cerevisiae)
-1.02500	0.04143	TMTC2	NM_152588	7957417	transmembrane and tetratricopeptide repeat containing 2 solute carrier family 25 (mitochondrial carrier, Aralar), member 12
-1.02500	0.03521	SLC25A12	NM_003705	8056766	
-1.02667	0.04857	FAH	NM_000137	7985268	fumarylacetoacetate hydrolase (fumarylacetoacetase)
-1.02667	0.02959	CA8	NM_004056	8150978	carbonic anhydrase VIII
-1.03000	0.02959	NSD1	NM_022455	8110289	nuclear receptor binding SET domain protein 1
-1.03000	0.04465	SCIN	NM_001112706	8131550	scinderin
-1.03333	0.02325	ZNF223	NM_013361	8029360	zinc finger protein 223
-1.03500	0.02451	MAP2K6	NM_002758	8009476	mitogen-activated protein kinase kinase 6
-1.04000	0.03359	C18orf55	NM_014177	8021716	chromosome 18 open reading frame 55
-1.04000	0.01666	SESN1	NM_014454	8128698	sestrin 1 HECT, C2 and WW domain containing E3 ubiquitin protein ligase 2
-1.04833	0.04857	HECW2	NM_020760	8057898	
-1.05333	0.02230	CYP2R1	NM_024514	7946742	cytochrome P450, family 2, subfamily R, polypeptide 1
-1.06000	0.03151	---	---	7928907	---
-1.06333	0.00891	SIRT4	NM_012240	7959148	sirtuin 4
-1.06500	0.01641	FAM72D	AB096683	7919591	family with sequence similarity 72, member D

-1.06833	0.04807	GPAM	NM_020918	7936322	glycerol-3-phosphate acyltransferase, mitochondrial
-1.06833	0.00791	SPAG5	NM_006461	8013671	sperm associated antigen 5
-1.06833	0.01566	MTMR4	NM_004687	8017019	myotubularin related protein 4
-1.06833	0.04650	KIF20A	NM_005733	8108301	kinesin family member 20A
-1.07167	0.01234	MLYCD	NM_012213	7997525	malonyl-CoA decarboxylase
-1.07167	0.03116	NMI	NM_004688	8055702	N-myc (and STAT) interactor
-1.07167	0.02059	PHF6	NM_032458	8169969	PHD finger protein 6
-1.07667	0.01469	SESN3	NM_144665	7951077	sestrin 3
-1.08000	0.03475	COLEC12	NM_130386	8021946	collectin sub-family member 12
-1.08500	0.04284	ATP6V0A4	NM_020632	8143221	ATPase, H+ transporting, lysosomal V0 subunit a4
-1.08833	0.02200	PHF21A	NM_001101802	7947624	PHD finger protein 21A
-1.09000	0.01396	RPRD2	NM_015203	7905185	regulation of nuclear pre-mRNA domain containing 2
-1.09000	0.01474	FOXM1	NM_202002	7960340	forkhead box M1
-1.09167	0.04836	ABCF3	NM_018358	8084360	ATP-binding cassette, sub-family F (GCN20), member 3
-1.09333	0.03877	DHRS11	NM_024308	8006655	dehydrogenase/reductase (SDR family) member 11
-1.09500	0.02755	ZNF682	NM_033196	8035782	zinc finger protein 682
-1.10500	0.00947	ZSCAN16	NM_025231	8117640	zinc finger and SCAN domain containing 16
-1.11500	0.00641	RNF20	NM_019592	8156945	ring finger protein 20
-1.11667	0.01469	NAA40	NM_024771	7940824	N(alpha)-acetyltransferase 40, NatD catalytic subunit, homolog (S. cerevisiae)
-1.11667	0.03978	MTERFD3	NM_001033050	7966046	MTERF domain containing 3
-1.12167	0.01501	OLFML1	NM_198474	7938225	olfactomedin-like 1
-1.12333	0.03823	SLC35D1	NM_015139	7916808	solute carrier family 35 (UDP-glucuronic acid/UDP-N-acetylgalactosamine dual transporter), member D1
-1.12500	0.04389	CENPE	NM_001813	8102076	centromere protein E, 312kDa
-1.13000	0.03475	NAPEPLD	NM_001122838	8141872	N-acyl phosphatidylethanolamine phospholipase D
-1.15000	0.01847	---	---	7942520	---
-1.15000	0.01834	ASB8	NM_024095	7962783	ankyrin repeat and SOCS box-containing 8
-1.15167	0.01845	CXCL12	NM_000609	7933194	chemokine (C-X-C motif) ligand 12
-1.15500	0.01501	ATF7IP2	NM_024997	7993167	activating transcription factor 7 interacting protein 2
-1.16500	0.00641	ACAD8	NM_014384	7945283	acyl-CoA dehydrogenase family, member 8
-1.17000	0.01095	BBX	NM_001142568	8081465	bobby sox homolog (Drosophila)
-1.17167	0.03116	PLA2G10	NM_003561	7999588	phospholipase A2, group X
-1.17333	0.02059	PHF12	NM_001033561	8013812	PHD finger protein 12
-1.18333	0.00791	SLC25A37	AF495725	8145291	solute carrier family 25, member 37
-1.18667	0.02316	GABRA3	NM_000808	8175696	gamma-aminobutyric acid (GABA) A receptor, alpha 3

-1.18833	0.02463	PLEKHM3	NM_001080475	8058509	pleckstrin homology domain containing, family M, member 3
-1.19167	0.04695	STARD5	NM_181900	7990839	StAR-related lipid transfer (START) domain containing 5
-1.19167	0.04808	SCRN3	NM_024583	8046502	secernin 3
-1.19667	0.00857	EME1	NM_001166131	8008310	essential meiotic endonuclease 1 homolog 1 (S. pombe)
-1.21000	0.01641	SYDE2	NM_032184	7917322	synapse defective 1, Rho GTPase, homolog 2 (C. elegans)
-1.22000	0.01501	GOLPH3L	NM_018178	7919780	golgi phosphoprotein 3-like
-1.22333	0.01258	DAPK1	NM_004938	8156199	death-associated protein kinase 1
-1.22500	0.04068	FAM185A	NR_026879	8135211	family with sequence similarity 185, member A
-1.25000	0.02230	RAB5C	NM_201434	8015545	RAB5C, member RAS oncogene family
-1.25333	0.02200	LRRN1	NM_020873	8077366	leucine rich repeat neuronal 1
-1.27167	0.01647	ERCC5	NM_000123	7969935	excision repair cross-complementing rodent repair deficiency, complementation group 5
-1.27500	0.04595	PBX2	NM_002586	8083221	pre-B-cell leukemia homeobox 2
-1.29333	0.03836	CCDC88C	NM_001080414	7980828	coiled-coil domain containing 88C
-1.30333	0.01219	SETDB2	NM_031915	7969114	SET domain, bifurcated 2
-1.30833	0.04005	TET2	NM_001127208	8096675	tet oncogene family member 2
-1.31333	0.01599	LEF1	NM_016269	8102232	lymphoid enhancer-binding factor 1
-1.32667	0.01842	GRAMD1C	NM_017577	8081758	GRAM domain containing 1C
-1.33167	0.01095	DLG2	NM_001364	7950764	discs, large homolog 2 (Drosophila)
-1.36167	0.02595	TDRD5	NM_173533	7907749	tudor domain containing 5
-1.37000	0.04143	TSHZ1	NM_005786	8021768	teashirt zinc finger homeobox 1
-1.37667	0.00857	PRUNE	NM_021222	7905299	prune homolog (Drosophila)
-1.38333	0.01955	C6orf203	NM_016487	8121312	chromosome 6 open reading frame 203
-1.39167	0.01258	MYLIP	NM_013262	8117020	myosin regulatory light chain interacting protein
-1.43833	0.00641	HYLS1	NM_145014	7945040	hydrolethalus syndrome 1
-1.44000	0.01666	EHHADH	NM_001966	8092523	enoyl-CoA, hydratase/3-hydroxyacyl CoA dehydrogenase
-1.44167	0.04760	BMP7	NM_001719	8067185	bone morphogenetic protein 7
-1.45000	0.01234	SUOX	NM_000456	7956097	sulfite oxidase
-1.45833	0.02325	MEIS1	NM_002398	8042356	Meis homeobox 1
-1.46500	0.01501	SLAIN1	NM_001040153	7969533	SLAIN motif family, member 1
-1.48167	0.04733	DLX5	NM_005221	8141140	distal-less homeobox 5
-1.52000	0.04490	---	---	7926297	---
-1.54000	0.01834	MPP1	NM_002436	8176174	membrane protein, palmitoylated 1, 55kDa
-1.55167	0.03877	GPR155	NM_001033045	8056837	G protein-coupled receptor 155
-1.56000	0.01501	CAB39L	NM_030925	7971590	calcium binding protein 39-like
-1.58000	0.03648	CNPY4	NM_152755	8134730	canopy 4 homolog (zebrafish)

-1.63500	0.03021	HIST1H2AJ	NM_021066	8124518	histone cluster 1, H2aj
-1.63500	0.03553	ORM1	NM_000607	8157446	orosomuroid 1
-1.64000	0.01834	MEIS2	NM_172316	7987385	Meis homeobox 2
-1.64333	0.02799	DEPDC1	NM_001114120	7916898	DEP domain containing 1
-1.64667	0.01566	C3orf70	BC137178	8092520	chromosome 3 open reading frame 70 SWI/SNF related, matrix associated, actin dependent regulator
-1.66667	0.03020	SMARCA2	NM_003070	8154059	of chromatin, subfamily a, member 2
-1.69000	0.01234	VAV3	NM_006113	7918157	vav 3 guanine nucleotide exchange factor

References

- Aalfs, J.D., Narlikar, G.J., and Kingston, R.E. (2001). Functional differences between the human ATP-dependent nucleosome remodeling proteins BRG1 and SNF2H. *J Biol Chem* 276, 34270-34278.
- Ahmad, K., and Henikoff, S. (2002). The histone variant H3.3 marks active chromatin by replication-independent nucleosome assembly. *Mol Cell* 9, 1191-1200.
- Akira, S., and Takeda, K. (2004). Functions of toll-like receptors: lessons from KO mice. *C R Biol* 327, 581-589.
- Akira, S., Takeda, K., and Kaisho, T. (2001). Toll-like receptors: critical proteins linking innate and acquired immunity. *Nature immunology* 2, 675-680.
- Akiyama, T., Suzuki, O., Matsuda, J., and Aoki, F. (2011). Dynamic replacement of histone H3 variants reprograms epigenetic marks in early mouse embryos. *PLoS Genet* 7, e1002279.
- Albig, W., and Doenecke, D. (1997). The human histone gene cluster at the D6S105 locus. *Hum Genet* 101, 284-294.
- Albig, W., Kioschis, P., Poustka, A., Meergans, K., and Doenecke, D. (1997). Human histone gene organization: nonregular arrangement within a large cluster. *Genomics* 40, 314-322.
- Allard, S., Utley, R.T., Savard, J., Clarke, A., Grant, P., Brandl, C.J., Pillus, L., Workman, J.L., and Cote, J. (1999). NuA4, an essential transcription adaptor/histone H4 acetyltransferase complex containing Esa1p and the ATM-related cofactor Tra1p. *EMBO J* 18, 5108-5119.
- Allfrey, V.G., Faulkner, R., and Mirsky, A.E. (1964). Acetylation and Methylation of Histones and Their Possible Role in the Regulation of Rna Synthesis. *Proc Natl Acad Sci U S A* 51, 786-794.
- Allfrey, V.G., and Mirsky, A.E. (1964). Structural Modifications of Histones and their Possible Role in the Regulation of RNA Synthesis. *Science* 144, 559.
- Arbibe, L. (2008). Immune subversion by chromatin manipulation: a 'new face' of host-bacterial pathogen interaction. *Cell Microbiol* 10, 1582-1590. Epub 2008 May 1514.
- Arbibe, L., Kim, D.W., Batsche, E., Pedron, T., Mateescu, B., Muchardt, C., Parsot, C., and Sansonetti, P.J. (2007). An injected bacterial effector targets chromatin access for transcription factor NF-kappaB to alter transcription of host genes involved in immune responses. *Nat Immunol* 8, 47-56.
- Arents, G., Burlingame, R.W., Wang, B.C., Love, W.E., and Moudrianakis, E.N. (1991). The nucleosomal core histone octamer at 3.1 A resolution: a tripartite protein assembly

and a left-handed superhelix. Proceedings of the National Academy of Sciences of the United States of America *88*, 10148-10152.

Arpaia, N., Godec, J., Lau, L., Sivick, K.E., McLaughlin, L.M., Jones, M.B., Dracheva, T., Peterson, S.N., Monack, D.M., and Barton, G.M. (2011). TLR signaling is required for *Salmonella typhimurium* virulence. *Cell* *144*, 675-688.

Aubry, C., Goulard, C., Nahori, M.A., Cayet, N., Decalf, J., Sachse, M., Boneca, I.G., Cossart, P., and Dussurget, O. OatA, a peptidoglycan O-acetyltransferase involved in *Listeria monocytogenes* immune escape, is critical for virulence. *J Infect Dis* *204*, 731-740.

Ausio, J. (1992). Structure and dynamics of transcriptionally active chromatin. *Journal of cell science* *102 (Pt 1)*, 1-5.

Ausio, J., Dong, F., and van Holde, K.E. (1989). Use of selectively trypsinized nucleosome core particles to analyze the role of the histone "tails" in the stabilization of the nucleosome. *J Mol Biol* *206*, 451-463.

Ausubel, F.M. (2005). Are innate immune signaling pathways in plants and animals conserved? *Nat Immunol* *6*, 973-979.

Barbaric, S., Walker, J., Schmid, A., Svejstrup, J.Q., and Horz, W. (2001). Increasing the rate of chromatin remodeling and gene activation--a novel role for the histone acetyltransferase Gcn5. *EMBO J* *20*, 4944-4951.

Barber, M.F., Michishita-Kioi, E., Xi, Y., Tasselli, L., Kioi, M., Moqtaderi, Z., Tennen, R.I., Paredes, S., Young, N.L., Chen, K., *et al.* (2012). SIRT7 links H3K18 deacetylation to maintenance of oncogenic transformation. *Nature* *000*.

Bardwell, A.J., Abdollahi, M., and Bardwell, L. (2004). Anthrax lethal factor-cleavage products of MAPK (mitogen-activated protein kinase) kinases exhibit reduced binding to their cognate MAPKs. *The Biochemical journal* *378*, 569-577.

Basu, A., Rose, K.L., Zhang, J., Beavis, R.C., Ueberheide, B., Garcia, B.A., Chait, B., Zhao, Y., Hunt, D.F., Segal, E., *et al.* (2009). Proteome-wide prediction of acetylation substrates. *Proc Natl Acad Sci U S A* *106*, 13785-13790.

Benjamini, Y., and Hochberg, Y. (1995). Controlling the false discovery rate: A practical and powerful approach to multiple testing, Vol 57 (Blackwell Publishing).

Beutler, B., and Rehli, M. (2002). Evolution of the TIR, tolls and TLRs: functional inferences from computational biology. *Current topics in microbiology and immunology* *270*, 1-21.

Bierne, H., and Cossart, P. (2012). When bacteria target the nucleus: the emerging family of nucleomodulins. *Cell Microbiol* *14*, 622-633.

Bierne, H., Tham, T.N., Batsche, E., Dumay, A., Leguillou, M., Kerneis-Golsteyn, S., Regnault, B., Seeler, J.S., Muchardt, C., Feunteun, J., *et al.* (2009). Human BAHD1 promotes heterochromatic gene silencing. *Proc Natl Acad Sci U S A* *106*, 13826-13831. Epub 12009 Aug 13823.

Black, J.C., Mosley, A., Kitada, T., Washburn, M., and Carey, M. (2008). The SIRT2 deacetylase regulates autoacetylation of p300. *Mol Cell* *32*, 449-455.

Bolstad, B.M., Irizarry, R.A., Astrand, M., and Speed, T.P. (2003). A comparison of normalization methods for high density oligonucleotide array data based on variance and bias. *Bioinformatics* *19*, 185-193.

Boyarchuk, E., Montes de Oca, R., and Almouzni, G. (2011). Cell cycle dynamics of histone variants at the centromere, a model for chromosomal landmarks. *Current opinion in cell biology* *23*, 266-276.

Brennan, C.A., and Anderson, K.V. (2004). *Drosophila*: the genetics of innate immune recognition and response. *Annual review of immunology* *22*, 457-483.

Cairns, B.R., Lorch, Y., Li, Y., Zhang, M., Lacomis, L., Erdjument-Bromage, H., Tempst, P., Du, J., Laurent, B., and Kornberg, R.D. (1996). RSC, an essential, abundant chromatin-remodeling complex. *Cell* *87*, 1249-1260.

Calnan, D.R., and Brunet, A. (2008). The FoxO code. *Oncogene* *27*, 2276-2288.

Carey, M. (1998). The enhanceosome and transcriptional synergy. *Cell* *92*, 5-8.

Carmen, A.A., Milne, L., and Grunstein, M. (2002). Acetylation of the yeast histone H4 N terminus regulates its binding to heterochromatin protein SIR3. *J Biol Chem* *277*, 4778-4781.

Chen, L., and Widom, J. (2005). Mechanism of transcriptional silencing in yeast. *Cell* *120*, 37-48.

Cossart, P. (2011). Illuminating the landscape of host-pathogen interactions with the bacterium *Listeria monocytogenes*. *Proceedings of the National Academy of Sciences of the United States of America* *108*, 19484-19491.

Cossart, P., and Sansonetti, P.J. (2004). Bacterial invasion: the paradigms of enteroinvasive pathogens. *Science* *304*, 242-248.

Cote, J., Quinn, J., Workman, J.L., and Peterson, C.L. (1994). Stimulation of GAL4 derivative binding to nucleosomal DNA by the yeast SWI/SNF complex. *Science* *265*, 53-60.

Cubizolles, F., Martino, F., Perrod, S., and Gasser, S.M. (2006). A homotrimer-heterotrimer switch in Sir2 structure differentiates rDNA and telomeric silencing. *Mol Cell* *21*, 825-836.

- Damme, P., Arnesen, T., Ruttens, B., and Gevaert, K. (2013). In-Gel N-Acetylation for the Quantification of the Degree of Protein In Vivo N-Terminal Acetylation. In *Protein Acetylation*, S.B. Hake, and C.J. Janzen, eds. (Humana Press), pp. 115-126.
- Das, C., Lucia, M.S., Hansen, K.C., and Tyler, J.K. (2009). CBP/p300-mediated acetylation of histone H3 on lysine 56. *Nature* *459*, 113-117.
- De Koning, L., Corpet, A., Haber, J.E., and Almouzni, G. (2007). Histone chaperones: an escort network regulating histone traffic. *Nature structural & molecular biology* *14*, 997-1007.
- Denu, J.M., and Gottesfeld, J.M. (2012). Minireview series on sirtuins: from biochemistry to health and disease. *The Journal of biological chemistry* *287*, 42417-42418.
- Dhalluin, C., Carlson, J.E., Zeng, L., He, C., Aggarwal, A.K., and Zhou, M.M. (1999a). ¹H, ¹⁵N and ¹³C resonance assignments for the bromodomain of the histone acetyltransferase P/CAF. *J Biomol NMR* *14*, 291-292.
- Dhalluin, C., Carlson, J.E., Zeng, L., He, C., Aggarwal, A.K., and Zhou, M.M. (1999b). Structure and ligand of a histone acetyltransferase bromodomain. *Nature* *399*, 491-496.
- Ding, S.Z., Fischer, W., Kaparakis-Liaskos, M., Liechti, G., Merrell, D.S., Grant, P.A., Ferrero, R.L., Crowe, S.E., Haas, R., Hatakeyama, M., *et al.* (2010). Helicobacter pylori-induced histone modification, associated gene expression in gastric epithelial cells, and its implication in pathogenesis. *PloS one* *5*, e9875.
- Dispirito, J.R., and Shen, H. (2010). Histone acetylation at the single-cell level: a marker of memory CD8+ T cell differentiation and functionality. *J Immunol* *184*, 4631-4636.
- Dramsi, S., Biswas, I., Maguin, E., Braun, L., Mastroeni, P., and Cossart, P. (1995). Entry of Listeria monocytogenes into hepatocytes requires expression of inlB, a surface protein of the internalin multigene family. *Mol Microbiol* *16*, 251-261.
- Dryden, S.C., Nahhas, F.A., Nowak, J.E., Goustin, A.S., and Tainsky, M.A. (2003). Role for human SIRT2 NAD-dependent deacetylase activity in control of mitotic exit in the cell cycle. *Molecular and cellular biology* *23*, 3173-3185.
- Du, J., Zhou, Y., Su, X., Yu, J.J., Khan, S., Jiang, H., Kim, J., Woo, J., Kim, J.H., Choi, B.H., *et al.* Sirt5 is a NAD-dependent protein lysine demalonylase and desuccinylase. *Science* *334*, 806-809.
- Elsaesser, S.J., Goldberg, A.D., and Allis, C.D. (2010). New functions for an old variant: no substitute for histone H3.3. *Curr Opin Genet Dev* *20*, 110-117.
- Fan, Y., Nikitina, T., Morin-Kensicki, E.M., Zhao, J., Magnuson, T.R., Woodcock, C.L., and Skoultchi, A.I. (2003). H1 linker histones are essential for mouse development and affect nucleosome spacing in vivo. *Mol Cell Biol* *23*, 4559-4572.

- Fehri, L.F., Rechner, C., Janssen, S., Mak, T.N., Holland, C., Bartfeld, S., Bruggemann, H., and Meyer, T.F. (2009). Helicobacter pylori-induced modification of the histone H3 phosphorylation status in gastric epithelial cells reflects its impact on cell cycle regulation. *Epigenetics* 4, 577-586.
- Ferrari, R., Pellegrini, M., Horwitz, G.A., Xie, W., Berk, A.J., and Kurdistani, S.K. (2008). Epigenetic reprogramming by adenovirus e1a. *Science* 321, 1086-1088.
- Ferrari, R., Su, T., Li, B., Bonora, G., Oberai, A., Chan, Y., Sasidharan, R., Berk, A.J., Pellegrini, M., and Kurdistani, S.K. (2012). Reorganization of the host epigenome by a viral oncogene. *Genome research* 22, 1212-1221.
- Feuillet, V., Medjane, S., Mondor, I., Demaria, O., Pagni, P.P., Galan, J.E., Flavell, R.A., and Alexopoulou, L. (2006). Involvement of Toll-like receptor 5 in the recognition of flagellated bacteria. *Proceedings of the National Academy of Sciences of the United States of America* 103, 12487-12492.
- Filion, G.J., van Bommel, J.G., Braunschweig, U., Talhout, W., Kind, J., Ward, L.D., Brugman, W., de Castro, I.J., Kerkhoven, R.M., Bussemaker, H.J., *et al.* Systematic protein location mapping reveals five principal chromatin types in Drosophila cells. *Cell* 143, 212-224.
- Finlay, B.B., and Falkow, S. (1997). Common themes in microbial pathogenicity revisited. *Microbiol Mol Biol Rev* 61, 136-169.
- Finnin, M.S., Donigian, J.R., Cohen, A., Richon, V.M., Rifkind, R.A., Marks, P.A., Breslow, R., and Pavletich, N.P. (2001). Structures of a histone deacetylase homologue bound to the TSA and SAHA inhibitors. *Nature* 401, 188-193.
- Fischle, W., Kiermer, V., Dequiedt, F., and Verdin, E. (2001). The emerging role of class II histone deacetylases. *Biochem Cell Biol* 79, 337-348.
- Frye, R.A. (1999). Characterization of five human cDNAs with homology to the yeast SIR2 gene: Sir2-like proteins (sirtuins) metabolize NAD and may have protein ADP-ribosyltransferase activity. *Biochemical and biophysical research communications* 260, 273-279.
- Gaillard, J.L., Berche, P., Frehel, C., Gouin, E., and Cossart, P. (1991). Entry of L. monocytogenes into cells is mediated by internalin, a repeat protein reminiscent of surface antigens from gram-positive cocci. *Cell* 65, 1127-1141.
- Galan, J.E. (2001). Salmonella interactions with host cells: type III secretion at work. *Annu Rev Cell Dev Biol* 17, 53-86.
- Galan, J.E., and Wolf-Watz, H. (2006). Protein delivery into eukaryotic cells by type III secretion machines. *Nature* 444, 567-573.

Gao, L., Cueto, M.A., Asselbergs, F., and Atadja, P. (2002). Cloning and functional characterization of HDAC11, a novel member of the human histone deacetylase family. *J Biol Chem* 277, 25748-25755.

Garcia, B.A., Mollah, S., Ueberheide, B.M., Busby, S.A., Muratore, T.L., Shabanowitz, J., and Hunt, D.F. (2007). Chemical derivatization of histones for facilitated analysis by mass spectrometry. *Nat Protoc* 2, 933-938.

Garcia-Garcia, J.C., Barat, N.C., Trembley, S.J., and Dumler, J.S. (2009). Epigenetic silencing of host cell defense genes enhances intracellular survival of the rickettsial pathogen *Anaplasma phagocytophilum*. *PLoS Pathog* 5, e1000488. Epub 1002009 Jun 1000419.

Gardner, K.E., Allis, C.D., and Strahl, B.D. (2011). OPERating ON Chromatin, a Colorful Language where Context Matters. *Journal of Molecular Biology* 409, 36-46.

Gavin, I., Horn, P.J., and Peterson, C.L. (2001). SWI/SNF chromatin remodeling requires changes in DNA topology. *Mol Cell* 7, 97-104.

Gay, N.J., and Keith, F.J. (1991). *Drosophila* Toll and IL-1 receptor. *Nature* 351, 355-356.

Geanacopoulos, M., Vasmatazis, G., Lewis, D.E., Roy, S., Lee, B., and Adhya, S. (1999). GalR mutants defective in repressosome formation. *Genes & development* 13, 1251-1262.

Georgel, P.T., Tsukiyama, T., and Wu, C. (1997). Role of histone tails in nucleosome remodeling by *Drosophila* NURF. *EMBO J* 16, 4717-4726.

Giron, J.A., Ho, A.S., and Schoolnik, G.K. (1991). An inducible bundle-forming pilus of enteropathogenic *Escherichia coli*. *Science* 254, 710-713.

Gottschling, D.E. (1992). Telomere-proximal DNA in *Saccharomyces cerevisiae* is refractory to methyltransferase activity in vivo. *Proceedings of the National Academy of Sciences of the United States of America* 89, 4062-4065.

Gouin, E., Adib-Conquy, M., Balestrino, D., Nahori, M.A., Villiers, V., Colland, F., Dramsi, S., Dussurget, O., and Cossart, P. (2010). The *Listeria monocytogenes* InIC protein interferes with innate immune responses by targeting the I{kappa}B kinase subunit IKK{alpha}. *Proceedings of the National Academy of Sciences of the United States of America* 107, 17333-17338.

Gouin, E., Welch, M.D., and Cossart, P. (2005). Actin-based motility of intracellular pathogens. *Current opinion in microbiology* 8, 35-45.

Gregory, P.D., Schmid, A., Zavari, M., Munsterkotter, M., and Horz, W. (1999). Chromatin remodelling at the PHO8 promoter requires SWI-SNF and SAGA at a step subsequent to activator binding. *EMBO J* 18, 6407-6414.

- Grewal, S.I., and Moazed, D. (2003). Heterochromatin and epigenetic control of gene expression. *Science* 301, 798-802.
- Groth, A., Corpet, A., Cook, A.J., Roche, D., Bartek, J., Lukas, J., and Almouzni, G. (2007). Regulation of replication fork progression through histone supply and demand. *Science* 318, 1928-1931.
- Grunstein, M. (1990). Histone function in transcription. *Annu Rev Cell Biol* 6, 643-678.
- Guyon, J.R., Narlikar, G.J., Sif, S., and Kingston, R.E. (1999). Stable remodeling of tailless nucleosomes by the human SWI-SNF complex. *Mol Cell Biol* 19, 2088-2097.
- Hake, S.B., Garcia, B.A., Duncan, E.M., Kauer, M., Dellaire, G., Shabanowitz, J., Bazett-Jones, D.P., Allis, C.D., and Hunt, D.F. (2006). Expression patterns and post-translational modifications associated with mammalian histone H3 variants. *J Biol Chem* 281, 559-568.
- Hamon, M.A., Batsche, E., Regnault, B., Tham, T.N., Seveau, S., Muchardt, C., and Cossart, P. (2007). Histone modifications induced by a family of bacterial toxins. *Proc Natl Acad Sci U S A* 104, 13467-13472.
- Hamon, M.A., and Cossart, P. (2008). Histone modifications and chromatin remodeling during bacterial infections. *Cell Host Microbe* 4, 100-109.
- Hamon, M.A., and Cossart, P. (2011). K⁺ efflux is required for histone H3 dephosphorylation by *Listeria monocytogenes* listeriolysin O and other pore-forming toxins. *Infect Immun* 79, 2839-2846.
- Han, M., and Grunstein, M. (1988). Nucleosome loss activates yeast downstream promoters in vivo. *Cell* 55, 1137-1145.
- Han, Y., Jin, Y.H., Kim, Y.J., Kang, B.Y., Choi, H.J., Kim, D.W., Yeo, C.Y., and Lee, K.Y. (2008). Acetylation of Sirt2 by p300 attenuates its deacetylase activity. *Biochemical and biophysical research communications* 375, 576-580.
- Hapfelmeier, S., Stecher, B., Barthel, M., Kremer, M., Muller, A.J., Heikenwalder, M., Stallmach, T., Hensel, M., Pfeffer, K., Akira, S., *et al.* (2005). The Salmonella pathogenicity island (SPI)-2 and SPI-1 type III secretion systems allow Salmonella serovar typhimurium to trigger colitis via MyD88-dependent and MyD88-independent mechanisms. *Journal of immunology* 174, 1675-1685.
- Hassan, A.H., Prochasson, P., Neely, K.E., Galasinski, S.C., Chandy, M., Carrozza, M.J., and Workman, J.L. (2002). Function and selectivity of bromodomains in anchoring chromatin-modifying complexes to promoter nucleosomes. *Cell* 111, 369-379.
- Hecht, A., Laroche, T., Strahl-Bolsinger, S., Gasser, S.M., and Grunstein, M. (1995). Histone H3 and H4 N-termini interact with SIR3 and SIR4 proteins: a molecular model for the formation of heterochromatin in yeast. *Cell* 80, 583-592.

- Hereford, L.M., and Rosbash, M. (1977). Number and distribution of polyadenylated RNA sequences in yeast. *Cell* 10, 453-462.
- Hochschild, A., and Dove, S.L. (1998). Protein-protein contacts that activate and repress prokaryotic transcription. *Cell* 92, 597-600.
- Hoffmann, J.A., and Reichhart, J.M. (2002). *Drosophila* innate immunity: an evolutionary perspective. *Nature immunology* 3, 121-126.
- Holden, D.W. (2002). Trafficking of the *Salmonella* vacuole in macrophages. *Traffic* 3, 161-169.
- Horwitz, G.A., Zhang, K., McBrian, M.A., Grunstein, M., Kurdistani, S.K., and Berk, A.J. (2008). Adenovirus small e1a alters global patterns of histone modification. *Science* 321, 1084-1085.
- Houtkooper, R.H., and Auwerx, J. Exploring the therapeutic space around NAD⁺. *The Journal of cell biology* 199, 205-209.
- Houtkooper, R.H., Pirinen, E., and Auwerx, J. (2012). Sirtuins as regulators of metabolism and healthspan. *Nature reviews Molecular cell biology* 13, 225-238.
- Hsieh, Y.J., Kundu, T.K., Wang, Z., Kovelman, R., and Roeder, R.G. (1999). The TFIIIC90 subunit of TFIIIC interacts with multiple components of the RNA polymerase III machinery and contains a histone-specific acetyltransferase activity. *Molecular and cellular biology* 19, 7697-7704.
- Imai, K., Inoue, H., Tamura, M., Cueno, M.E., Takeichi, O., Kusama, K., Saito, I., and Ochiai, K. (2012). The periodontal pathogen *Porphyromonas gingivalis* induces the Epstein-Barr virus lytic switch transactivator ZEBRA by histone modification. *Biochimie* 94, 839-846.
- Imai, K., Ochiai, K., and Okamoto, T. (2009). Reactivation of latent HIV-1 infection by the periodontopathic bacterium *Porphyromonas gingivalis* involves histone modification. *Journal of immunology* 182, 3688-3695.
- Imai, S., Armstrong, C.M., Kaeberlein, M., and Guarente, L. (2000a). Transcriptional silencing and longevity protein Sir2 is an NAD-dependent histone deacetylase. *Nature* 403, 795-800.
- Imai, S., Johnson, F.B., Marciniak, R.A., McVey, M., Park, P.U., and Guarente, L. (2000b). Sir2: an NAD-dependent histone deacetylase that connects chromatin silencing, metabolism, and aging. *Cold Spring Harbor symposia on quantitative biology* 65, 297-302.
- Imbalzano, A.N., Schnitzler, G.R., and Kingston, R.E. (1996). Nucleosome disruption by human SWI/SNF is maintained in the absence of continued ATP hydrolysis. *J Biol Chem* 271, 20726-20733.

Imoberdorf, R.M., Topalidou, I., and Strubin, M. (2006). A role for gcn5-mediated global histone acetylation in transcriptional regulation. *Mol Cell Biol* 26, 1610-1616.

Inoue, T., Hiratsuka, M., Osaki, M., Yamada, H., Kishimoto, I., Yamaguchi, S., Nakano, S., Kato, M., Ito, H., and Oshimura, M. (2007). SIRT2, a tubulin deacetylase, acts to block the entry to chromosome condensation in response to mitotic stress. *Oncogene* 26, 945-957.

Ireton, K., Payrastre, B., and Cossart, P. (1999). The *Listeria monocytogenes* protein InlB is an agonist of mammalian phosphoinositide 3-kinase. *J Biol Chem* 274, 17025-17032.

Isberg, R.R., and Falkow, S. (1985). A single genetic locus encoded by *Yersinia pseudotuberculosis* permits invasion of cultured animal cells by *Escherichia coli* K-12. *Nature* 317, 262-264.

Ito, T., Bulger, M., Pazin, M.J., Kobayashi, R., and Kadonaga, J.T. (1997). ACF, an ISWI-containing and ATP-utilizing chromatin assembly and remodeling factor. *Cell* 90, 145-155.

Iwai, H., Kim, M., Yoshikawa, Y., Ashida, H., Ogawa, M., Fujita, Y., Muller, D., Kirikae, T., Jackson, P.K., Kotani, S., *et al.* (2007). A bacterial effector targets Mad2L2, an APC inhibitor, to modulate host cell cycling. *Cell* 130, 611-623.

Jacob, F., and Monod, J. (1961). Genetic regulatory mechanisms in the synthesis of proteins. *J Mol Biol* 3, 318-356.

Janeway, C.A., Jr. (1989). Approaching the asymptote? Evolution and revolution in immunology. *Cold Spring Harbor symposia on quantitative biology* 54 Pt 1, 1-13.

Janeway, C.A., Jr., and Medzhitov, R. (2002). Innate immune recognition. *Annual review of immunology* 20, 197-216.

Jaskelioff, M., Gavin, I.M., Peterson, C.L., and Logie, C. (2000). SWI-SNF-mediated nucleosome remodeling: role of histone octamer mobility in the persistence of the remodeled state. *Mol Cell Biol* 20, 3058-3068.

Jenner, R.G., and Young, R.A. (2005). Insights into host responses against pathogens from transcriptional profiling. *Nat Rev Microbiol* 3, 281-294.

Jerse, A.E., and Kaper, J.B. (1991). The *eae* gene of enteropathogenic *Escherichia coli* encodes a 94-kilodalton membrane protein, the expression of which is influenced by the EAF plasmid. *Infection and immunity* 59, 4302-4309.

Jin, C., and Felsenfeld, G. (2007). Nucleosome stability mediated by histone variants H3.3 and H2A.Z. *Genes & development* 21, 1519-1529.

Jing, E., Gesta, S., and Kahn, C.R. (2007). SIRT2 regulates adipocyte differentiation through FoxO1 acetylation/deacetylation. *Cell metabolism* 6, 105-114.

Johansson, J., Mandin, P., Renzoni, A., Chiaruttini, C., Springer, M., and Cossart, P. (2002). An RNA thermosensor controls expression of virulence genes in *Listeria monocytogenes*. *Cell* 110, 551-561.

Johnson, L.M., Fisher-Adams, G., and Grunstein, M. (1992). Identification of a non-basic domain in the histone H4 N-terminus required for repression of the yeast silent mating loci. *EMBO J* 11, 2201-2209.

Joshi, A.A., and Struhl, K. (2005). Eaf3 chromodomain interaction with methylated H3-K36 links histone deacetylation to Pol II elongation. *Mol Cell* 20, 971-978.

Kao, H.Y., Verdel, A., Tsai, C.C., Simon, C., Juguilon, H., and Khochbin, S. (2001). Mechanism for nucleocytoplasmic shuttling of histone deacetylase 7. *The Journal of biological chemistry* 276, 47496-47507.

Kassabov, S.R., Zhang, B., Persinger, J., and Bartholomew, B. (2003). SWI/SNF unwraps, slides, and rewraps the nucleosome. *Molecular cell* 11, 391-403.

Kawai, T., and Akira, S. (2005). Pathogen recognition with Toll-like receptors. *Curr Opin Immunol* 17, 338-344.

Kawai, T., and Akira, S. (2007). Signaling to NF-kappaB by Toll-like receptors. *Trends Mol Med* 13, 460-469.

Kimura, A., Matsubara, K., and Horikoshi, M. (2005). A decade of histone acetylation: marking eukaryotic chromosomes with specific codes. *J Biochem* 138, 647-662.

Kincaid, E.Z., and Ernst, J.D. (2003). *Mycobacterium tuberculosis* exerts gene-selective inhibition of transcriptional responses to IFN-gamma without inhibiting STAT1 function. *J Immunol* 171, 2042-2049.

Kladde, M.P., and Simpson, R.T. (1994). Positioned nucleosomes inhibit Dam methylation in vivo. *Proceedings of the National Academy of Sciences of the United States of America* 91, 1361-1365.

Kocks, C., Marchand, J.B., Gouin, E., d'Hauteville, H., Sansonetti, P.J., Carlier, M.F., and Cossart, P. (1995). The unrelated surface proteins ActA of *Listeria monocytogenes* and IcsA of *Shigella flexneri* are sufficient to confer actin-based motility on *Listeria innocua* and *Escherichia coli* respectively. *Mol Microbiol* 18, 413-423.

Kornberg, R.D., and Lorch, Y. (1999). Twenty-five years of the nucleosome, fundamental particle of the eukaryote chromosome. *Cell* 98, 285-294.

Krebs, J.E., Fry, C.J., Samuels, M.L., and Peterson, C.L. (2000). Global role for chromatin remodeling enzymes in mitotic gene expression. *Cell* 102, 587-598.

- Kundu, T.K., Wang, Z., and Roeder, R.G. (1999). Human TFIIIC relieves chromatin-mediated repression of RNA polymerase III transcription and contains an intrinsic histone acetyltransferase activity. *Molecular and cellular biology* *19*, 1605-1615.
- Kuo, M.H., vom Baur, E., Struhl, K., and Allis, C.D. (2000). Gcn4 activator targets Gcn5 histone acetyltransferase to specific promoters independently of transcription. *Mol Cell* *6*, 1309-1320.
- Kuo, M.H., Zhou, J., Jambeck, P., Churchill, M.E., and Allis, C.D. (1998). Histone acetyltransferase activity of yeast Gcn5p is required for the activation of target genes in vivo. *Genes & development* *12*, 627-639.
- Kurdistani, S.K., and Grunstein, M. (2003). Histone acetylation and deacetylation in yeast. *Nature reviews Molecular cell biology* *4*, 276-284.
- Kurdistani, S.K., Tavazoie, S., and Grunstein, M. (2004). Mapping global histone acetylation patterns to gene expression. *Cell* *117*, 721-733.
- Kwon, H., Imbalzano, A.N., Khavari, P.A., Kingston, R.E., and Green, M.R. (1994). Nucleosome disruption and enhancement of activator binding by a human SW1/SNF complex. *Nature* *370*, 477-481.
- Lamkanfi, M., and Dixit, V.M. (2009). Inflammasomes: guardians of cytosolic sanctity. *Immunol Rev* *227*, 95-105.
- Latham, J.A., and Dent, S.Y. (2007). Cross-regulation of histone modifications. *Nature structural & molecular biology* *14*, 1017-1024.
- Lebreton, A., Lakisic, G., Job, V., Fritsch, L., Tham, T.N., Camejo, A., Mattei, P.J., Regnault, B., Nahori, M.A., Cabanes, D., *et al.* (2011). A Bacterial Protein Targets the BAHD1 Chromatin Complex to Stimulate Type III Interferon Response. *Science*.
- Lee, C.H., Murphy, M.R., Lee, J.S., and Chung, J.H. (1999). Targeting a SWI/SNF-related chromatin remodeling complex to the beta-globin promoter in erythroid cells. *Proc Natl Acad Sci U S A* *96*, 12311-12315.
- Lee, K.K., and Workman, J.L. (2007). Histone acetyltransferase complexes: one size doesn't fit all. *Nature reviews Molecular cell biology* *8*, 284-295.
- LeRoy, G., Loyola, A., Lane, W.S., and Reinberg, D. (2000). Purification and characterization of a human factor that assembles and remodels chromatin. *The Journal of biological chemistry* *275*, 14787-14790.
- Li, G., and Reinberg, D. (2011). Chromatin higher-order structures and gene regulation. *Current opinion in genetics & development* *21*, 175-186.

Liou, G.G., Tanny, J.C., Kruger, R.G., Walz, T., and Moazed, D. (2005). Assembly of the SIR complex and its regulation by O-acetyl-ADP-ribose, a product of NAD-dependent histone deacetylation. *Cell* 121, 515-527.

Liu, C.L., Kaplan, T., Kim, M., Buratowski, S., Schreiber, S.L., Friedman, N., and Rando, O.J. (2005). Single-nucleosome mapping of histone modifications in *S. cerevisiae*. *PLoS Biol* 3, e328.

Lohr, D., and Hereford, L. (1979). Yeast chromatin is uniformly digested by DNase-I. *Proceedings of the National Academy of Sciences of the United States of America* 76, 4285-4288.

Lorch, Y., Zhang, M., and Kornberg, R.D. (2001). RSC unravels the nucleosome. *Mol Cell* 7, 89-95.

Loyola, A., and Almouzni, G. (2007). Marking histone H3 variants: how, when and why? *Trends Biochem Sci* 32, 425-433.

Luger, K., Mader, A.W., Richmond, R.K., Sargent, D.F., and Richmond, T.J. (1997). Crystal structure of the nucleosome core particle at 2.8 Å resolution. *Nature* 389, 251-260.

Lusser, A., and Kadonaga, J.T. (2003). Chromatin remodeling by ATP-dependent molecular machines. *Bioessays* 25, 1192-1200.

Madden, J.C., Ruiz, N., and Caparon, M. (2001). Cytolysin-mediated translocation (CMT): a functional equivalent of type III secretion in gram-positive bacteria. *Cell* 104, 143-152.

Manuyakorn, A., Paulus, R., Farrell, J., Dawson, N.A., Tze, S., Cheung-Lau, G., Hines, O.J., Reber, H., Seligson, D.B., Horvath, S., *et al.* (2010). Cellular histone modification patterns predict prognosis and treatment response in resectable pancreatic adenocarcinoma: results from RTOG 9704. *J Clin Oncol* 28, 1358-1365.

Mariathasan, S., Weiss, D.S., Newton, K., McBride, J., O'Rourke, K., Roose-Girma, M., Lee, W.P., Weinrauch, Y., Monack, D.M., and Dixit, V.M. (2006). Cryopyrin activates the inflammasome in response to toxins and ATP. *Nature* 440, 228-232. Epub 2006 Jan 2011.

Marzluff, W.F., Gongidi, P., Woods, K.R., Jin, J., and Maltais, L.J. (2002). The human and mouse replication-dependent histone genes. *Genomics* 80, 487-498.

Matzinger, P. (2002). An innate sense of danger. *Ann N Y Acad Sci* 961, 341-342.

McGourty, K., Thurston, T.L., Matthews, S.A., Pinaud, L., Mota, L.J., and Holden, D.W. (2012). Salmonella inhibits retrograde trafficking of mannose-6-phosphate receptors and lysosome function. *Science* 338, 963-967.

McKinsey, T.A., Zhang, C.L., Lu, J., and Olson, E.N. (2000a). Signal-dependent nuclear export of a histone deacetylase regulates muscle differentiation. *Nature* 408, 106-111.

McKinsey, T.A., Zhang, C.L., and Olson, E.N. (2000b). Activation of the myocyte enhancer factor-2 transcription factor by calcium/calmodulin-dependent protein kinase-stimulated binding of 14-3-3 to histone deacetylase 5. *Proceedings of the National Academy of Sciences of the United States of America* 97, 14400-14405.

McKinsey, T.A., Zhang, C.L., and Olson, E.N. (2001). Identification of a signal-responsive nuclear export sequence in class II histone deacetylases. *Molecular and cellular biology* 21, 6312-6321.

Medzhitov, R., and Janeway, C., Jr. (2000). The Toll receptor family and microbial recognition. *Trends in microbiology* 8, 452-456.

Medzhitov, R., and Janeway, C.A., Jr. (2002). Decoding the patterns of self and nonself by the innate immune system. *Science* 296, 298-300.

Medzhitov, R., Preston-Hurlburt, P., and Janeway, C.A., Jr. (1997). A human homologue of the *Drosophila* Toll protein signals activation of adaptive immunity. *Nature* 388, 394-397.

Mello, J.A., Sillje, H.H., Roche, D.M., Kirschner, D.B., Nigg, E.A., and Almouzni, G. (2002). Human Asf1 and CAF-1 interact and synergize in a repair-coupled nucleosome assembly pathway. *EMBO Rep* 3, 329-334.

Michan, S., and Sinclair, D. (2007). Sirtuins in mammals: insights into their biological function. *The Biochemical journal* 404, 1-13.

Mimuro, H., Suzuki, T., Nagai, S., Rieder, G., Suzuki, M., Nagai, T., Fujita, Y., Nagamatsu, K., Ishijima, N., Koyasu, S., *et al.* (2007). *Helicobacter pylori* dampens gut epithelial self-renewal by inhibiting apoptosis, a bacterial strategy to enhance colonization of the stomach. *Cell host & microbe* 2, 250-263.

Moggs, J.G., Grandi, P., Quivy, J.P., Jonsson, Z.O., Hubscher, U., Becker, P.B., and Almouzni, G. (2000). A CAF-1-PCNA-mediated chromatin assembly pathway triggered by sensing DNA damage. *Mol Cell Biol* 20, 1206-1218.

Mosavi, L.K., Cammett, T.J., Desrosiers, D.C., and Peng, Z.Y. (2004). The ankyrin repeat as molecular architecture for protein recognition. *Protein Sci* 13, 1435-1448.

Mostoslavsky, R., Esteller, M., and Vaquero, A. (2010). At the crossroad of lifespan, calorie restriction, chromatin and disease: meeting on sirtuins. *Cell Cycle* 9, 1907-1912.

Nahas, F., Dryden, S.C., Abrams, J., and Tainsky, M.A. (2007). Mutations in SIRT2 deacetylase which regulate enzymatic activity but not its interaction with HDAC6 and tubulin. *Molecular and cellular biochemistry* 303, 221-230.

- Nakagawa, T., Lomb, D.J., Haigis, M.C., and Guarente, L. (2009). SIRT5 Deacetylates carbamoyl phosphate synthetase 1 and regulates the urea cycle. *Cell* 137, 560-570.
- Noma, K., Allis, C.D., and Grewal, S.I. (2001). Transitions in distinct histone H3 methylation patterns at the heterochromatin domain boundaries. *Science* 293, 1150-1155.
- North, B.J., Marshall, B.L., Borra, M.T., Denu, J.M., and Verdin, E. (2003). The human Sir2 ortholog, SIRT2, is an NAD⁺-dependent tubulin deacetylase. *Mol Cell* 11, 437-444.
- North, B.J., and Verdin, E. (2007a). Interphase nucleo-cytoplasmic shuttling and localization of SIRT2 during mitosis. *PLoS one* 2, e784.
- North, B.J., and Verdin, E. (2007b). Mitotic regulation of SIRT2 by cyclin-dependent kinase 1-dependent phosphorylation. *J Biol Chem* 282, 19546-19555.
- O'Brien, A.D., Rosenstreich, D.L., Scher, I., Campbell, G.H., MacDermott, R.P., and Formal, S.B. (1980). Genetic control of susceptibility to *Salmonella typhimurium* in mice: role of the LPS gene. *Journal of immunology* 124, 20-24.
- Opitz, B., Puschel, A., Beermann, W., Hocke, A.C., Forster, S., Schmeck, B., van Laak, V., Chakraborty, T., Suttorp, N., and Hippenstiel, S. (2006). *Listeria monocytogenes* activated p38 MAPK and induced IL-8 secretion in a nucleotide-binding oligomerization domain 1-dependent manner in endothelial cells. *J Immunol* 176, 484-490.
- Oudet, P., Gross-Bellard, M., and Chambon, P. (1975). Electron microscopic and biochemical evidence that chromatin structure is a repeating unit. *Cell* 4, 281-300.
- Pandithage, R., Lilischkis, R., Harting, K., Wolf, A., Jedamzik, B., Luscher-Firzlaff, J., Vervoorts, J., Lasonder, E., Kremmer, E., Knoll, B., *et al.* (2008). The regulation of SIRT2 function by cyclin-dependent kinases affects cell motility. *The Journal of cell biology* 180, 915-929.
- Park, J., Kim, K.J., Choi, K.S., Grab, D.J., and Dumler, J.S. (2004). *Anaplasma phagocytophilum* AnkA binds to granulocyte DNA and nuclear proteins. *Cell Microbiol* 6, 743-751.
- Paschos, K., and Allday, M.J. (2010). Epigenetic reprogramming of host genes in viral and microbial pathogenesis. *Trends Microbiol* 18, 439-447.
- Pathak, S.K., Basu, S., Bhattacharyya, A., Pathak, S., Banerjee, A., Basu, J., and Kundu, M. (2006). TLR4-dependent NF-kappaB activation and mitogen- and stress-activated protein kinase 1-triggered phosphorylation events are central to *Helicobacter pylori* peptidyl prolyl cis-, trans-isomerase (HP0175)-mediated induction of IL-6 release from macrophages. *J Immunol* 177, 7950-7958.

- Paull, T.T., Rogakou, E.P., Yamazaki, V., Kirchgessner, C.U., Gellert, M., and Bonner, W.M. (2000). A critical role for histone H2AX in recruitment of repair factors to nuclear foci after DNA damage. *Current biology* : CB *10*, 886-895.
- Peng, C., Lu, Z., Xie, Z., Cheng, Z., Chen, Y., Tan, M., Luo, H., Zhang, Y., He, W., Yang, K., *et al.* The first identification of lysine malonylation substrates and its regulatory enzyme. *Mol Cell Proteomics* *10*, M111 012658.
- Pennini, M.E., Perrinet, S., Dautry-Varsat, A., and Subtil, A. (2010). Histone methylation by NUE, a novel nuclear effector of the intracellular pathogen *Chlamydia trachomatis*. *PLoS Pathog* *6*, e1000995.
- Peterson, C.L., and Logie, C. (2000). Recruitment of chromatin remodeling machines. *J Cell Biochem* *78*, 179-185.
- Polo, S.E., and Almouzni, G. (2006). Chromatin assembly: a basic recipe with various flavours. *Curr Opin Genet Dev* *16*, 104-111.
- Poltorak, A., He, X., Smirnova, I., Liu, M.Y., Van Huffel, C., Du, X., Birdwell, D., Alejos, E., Silva, M., Galanos, C., *et al.* (1998). Defective LPS signaling in C3H/HeJ and C57BL/10ScCr mice: mutations in Tlr4 gene. *Science* *282*, 2085-2088.
- Probst, A.V., Dunleavy, E., and Almouzni, G. (2009). Epigenetic inheritance during the cell cycle. *Nature reviews Molecular cell biology* *10*, 192-206.
- Rando, O.J., and Chang, H.Y. (2009). Genome-wide views of chromatin structure. *Annu Rev Biochem* *78*, 245-271.
- Raymond, B., Batsche, E., Boutillon, F., Wu, Y.Z., Leduc, D., Balloy, V., Raoust, E., Muchardt, C., Goossens, P.L., and Touqui, L. (2009). Anthrax lethal toxin impairs IL-8 expression in epithelial cells through inhibition of histone H3 modification. *PLoS Pathog* *5*, e1000359.
- Ribet, D., Hamon, M., Gouin, E., Nahori, M.A., Impens, F., Neyret-Kahn, H., Gevaert, K., Vandekerckhove, J., Dejean, A., and Cossart, P. (2010). *Listeria monocytogenes* impairs SUMOylation for efficient infection. *Nature* *464*, 1192-1195.
- Richardson, E.J., Limaye, B., Inamdar, H., Datta, A., Manjari, K.S., Pullinger, G.D., Thomson, N.R., Joshi, R.R., Watson, M., and Stevens, M.P. Genome sequences of *Salmonella enterica* serovar typhimurium, Choleraesuis, Dublin, and Gallinarum strains of well- defined virulence in food-producing animals. *J Bacteriol* *193*, 3162-3163.
- Riedel, C.G., Downen, R.H., Lourenco, G.F., Kirienko, N.V., Heimbucher, T., West, J.A., Bowman, S.K., Kingston, R.E., Dillin, A., Asara, J.M., *et al.* (2013). DAF-16 employs the chromatin remodeller SWI/SNF to promote stress resistance and longevity. *Nature cell biology*.

Rocheteau, P., Gayraud-Morel, B., Siegl-Cachedenier, I., Blasco, M.A., and Tajbakhsh, S. A subpopulation of adult skeletal muscle stem cells retains all template DNA strands after cell division. *Cell* 148, 112-125.

Roh, T.Y., Ngau, W.C., Cui, K., Landsman, D., and Zhao, K. (2004). High-resolution genome-wide mapping of histone modifications. *Nat Biotechnol* 22, 1013-1016.

Roth, S.Y., Denu, J.M., and Allis, C.D. (2001). Histone acetyltransferases. *Annu Rev Biochem* 70, 81-120.

Rowan, B.G., Weigel, N.L., and O'Malley, B.W. (2000). Phosphorylation of steroid receptor coactivator-1. Identification of the phosphorylation sites and phosphorylation through the mitogen-activated protein kinase pathway. *The Journal of biological chemistry* 275, 4475-4483.

Royet, J. (2004). Infectious non-self recognition in invertebrates: lessons from *Drosophila* and other insect models. *Mol Immunol* 41, 1063-1075.

Royle, M.C., Totemeyer, S., Alldridge, L.C., Maskell, D.J., and Bryant, C.E. (2003). Stimulation of Toll-like receptor 4 by lipopolysaccharide during cellular invasion by live *Salmonella typhimurium* is a critical but not exclusive event leading to macrophage responses. *Journal of immunology* 170, 5445-5454.

Rusche, L.N., Kirchmaier, A.L., and Rine, J. (2003). The establishment, inheritance, and function of silenced chromatin in *Saccharomyces cerevisiae*. *Annual review of biochemistry* 72, 481-516.

Saccani, S., Pantano, S., and Natoli, G. (2002). p38-Dependent marking of inflammatory genes for increased NF-kappa B recruitment. *Nat Immunol* 3, 69-75.

Sansonetti, P.J. (2001). Microbes and microbial toxins: paradigms for microbial-mucosal interactions III. Shigellosis: from symptoms to molecular pathogenesis. *Am J Physiol Gastrointest Liver Physiol* 280, G319-323.

Sansonetti, P.J., Kopecko, D.J., and Formal, S.B. (1982). Involvement of a plasmid in the invasive ability of *Shigella flexneri*. *Infection and immunity* 35, 852-860.

Schmeck, B., Beermann, W., van Laak, V., Zahlten, J., Opitz, B., Witzenrath, M., Hocke, A.C., Chakraborty, T., Kracht, M., Rosseau, S., *et al.* (2005). Intracellular bacteria differentially regulated endothelial cytokine release by MAPK-dependent histone modification. *J Immunol* 175, 2843-2850.

Schmeck, B., Lorenz, J., N'Guessan P, D., Opitz, B., van Laak, V., Zahlten, J., Slevogt, H., Witzenrath, M., Flieger, A., Suttorp, N., *et al.* (2008). Histone acetylation and flagellin are essential for *Legionella pneumophila*-induced cytokine expression. *Journal of immunology* 181, 940-947.

Schnitzler, G., Sif, S., and Kingston, R.E. (1998). Human SWI/SNF interconverts a nucleosome between its base state and a stable remodeled state. *Cell* 94, 17-27.

Schones, D.E., Cui, K., Cuddapah, S., Roh, T.Y., Barski, A., Wang, Z., Wei, G., and Zhao, K. (2008). Dynamic regulation of nucleosome positioning in the human genome. *Cell* 132, 887-898.

Segal, E., Fondufe-Mittendorf, Y., Chen, L., Thastrom, A., Field, Y., Moore, I.K., Wang, J.P., and Widom, J. (2006). A genomic code for nucleosome positioning. *Nature* 442, 772-778.

Seligson, D.B., Horvath, S., McBrien, M.A., Mah, V., Yu, H., Tze, S., Wang, Q., Chia, D., Goodglick, L., and Kurdistani, S.K. (2009). Global levels of histone modifications predict prognosis in different cancers. *The American journal of pathology* 174, 1619-1628.

Shahbazian, M.D., and Grunstein, M. (2007). Functions of site-specific histone acetylation and deacetylation. *Annual Reviews Biochemistry* 76, 75-100.

Shechter, D., Dormann, H.L., Allis, C.D., and Hake, S.B. (2007). Extraction, purification and analysis of histones. *Nat Protoc* 2, 1445-1457.

Shin, H., and Cornelis, G.R. (2007). Type III secretion translocation pores of *Yersinia enterocolitica* trigger maturation and release of pro-inflammatory IL-1beta. *Cellular microbiology* 9, 2893-2902.

Simeone, R., Bottai, D., and Brosch, R. (2009). ESX/type VII secretion systems and their role in host-pathogen interaction. *Current opinion in microbiology* 12, 4-10.

Singh, J., and Klar, A.J. (1992). Active genes in budding yeast display enhanced in vivo accessibility to foreign DNA methylases: a novel in vivo probe for chromatin structure of yeast. *Genes & development* 6, 186-196.

Smith, K.D., Andersen-Nissen, E., Hayashi, F., Strobe, K., Bergman, M.A., Barrett, S.L., Cookson, B.T., and Aderem, A. (2003). Toll-like receptor 5 recognizes a conserved site on flagellin required for protofilament formation and bacterial motility. *Nature immunology* 4, 1247-1253.

Sobel, R.E., Cook, R.G., Perry, C.A., Annunziato, A.T., and Allis, C.D. (1995). Conservation of deposition-related acetylation sites in newly synthesized histones H3 and H4. *Proc Natl Acad Sci U S A* 92, 1237-1241.

Sogo, J.M., Stahl, H., Koller, T., and Knippers, R. (1986). Structure of replicating simian virus 40 minichromosomes. The replication fork, core histone segregation and terminal structures. *J Mol Biol* 189, 189-204.

Spadafora, C., Bellard, M., Compton, J.L., and Chambon, P. (1976). The DNA repeat lengths in chromatins from sea urchin sperm and gastrule cells are markedly different. *FEBS letters* 69, 281-285.

Staes, A., Impens, F., Van Damme, P., Ruttens, B., Goethals, M., Demol, H., Timmerman, E., Vandekerckhove, J., and Gevaert, K. (2011). Selecting protein N-terminal peptides by combined fractional diagonal chromatography. *Nat Protoc* 6, 11.

Sterner, D.E., and Berger, S.L. (2000). Acetylation of histones and transcription-related factors. *Microbiol Mol Biol Rev* 64, 435-459.

Strahl, B.D., and Allis, C.D. (2000). The language of covalent histone modifications. *Nature* 403, 41-45.

Struhl, K. (1999). Fundamentally different logic of gene regulation in eukaryotes and prokaryotes. *Cell* 98, 1-4.

Sudarsanam, P., Iyer, V.R., Brown, P.O., and Winston, F. (2000). Whole-genome expression analysis of *snf/swi* mutants of *Saccharomyces cerevisiae*. *Proc Natl Acad Sci U S A* 97, 3364-3369.

Suka, N., Luo, K., and Grunstein, M. (2002). Sir2p and Sas2p opposingly regulate acetylation of yeast histone H4 lysine16 and spreading of heterochromatin. *Nat Genet* 32, 378-383.

Sun, W., Yu, Y., Dotti, G., Shen, T., Tan, X., Savoldo, B., Pass, A.K., Chu, M., Zhang, D., Lu, X., *et al.* (2009). PPM1A and PPM1B act as IKKbeta phosphatases to terminate TNFalpha-induced IKKbeta-NF-kappaB activation. *Cell Signal* 21, 95-102.

Tagami, H., Ray-Gallet, D., Almouzni, G., and Nakatani, Y. (2004). Histone H3.1 and H3.3 complexes mediate nucleosome assembly pathways dependent or independent of DNA synthesis. *Cell* 116, 51-61.

Theriot, J.A. (1995). The cell biology of infection by intracellular bacterial pathogens. *Annu Rev Cell Dev Biol* 11, 213-239.

Thompson, J.S., Ling, X., and Grunstein, M. (1994). Histone H3 amino terminus is required for telomeric and silent mating locus repression in yeast. *Nature* 369, 245-247.

Tirosh, I., and Barkai, N. (2008). Two strategies for gene regulation by promoter nucleosomes. *Genome Res* 18, 1084-1091.

Turner, B.M. (1993). Decoding the nucleosome. *Cell* 75, 5-8.

Uematsu, S., Jang, M.H., Chevrier, N., Guo, Z., Kumagai, Y., Yamamoto, M., Kato, H., Sougawa, N., Matsui, H., Kuwata, H., *et al.* (2006). Detection of pathogenic intestinal bacteria by Toll-like receptor 5 on intestinal CD11c+ lamina propria cells. *Nature immunology* 7, 868-874.

Van Nhieu, G.T., and Isberg, R.R. (1991). The *Yersinia pseudotuberculosis* invasins protein and human fibronectin bind to mutually exclusive sites on the alpha 5 beta 1 integrin receptor. *The Journal of biological chemistry* 266, 24367-24375.

van Steensel, B. (2011). Chromatin: constructing the big picture. *The EMBO journal* 30, 1885-1895.

Vance, R.E., Isberg, R.R., and Portnoy, D.A. (2009). Patterns of pathogenesis: discrimination of pathogenic and nonpathogenic microbes by the innate immune system. *Cell Host Microbe* 6, 10-21.

Vaquero, A., Scher, M.B., Lee, D.H., Sutton, A., Cheng, H.L., Alt, F.W., Serrano, L., Sternglanz, R., and Reinberg, D. (2006). SirT2 is a histone deacetylase with preference for histone H4 Lys 16 during mitosis. *Genes & development* 20, 1256-1261.

Vazquez-Boland, J.A., Kuhn, M., Berche, P., Chakraborty, T., Dominguez-Bernal, G., Goebel, W., Gonzalez-Zorn, B., Wehland, J., and Kreft, J. (2001). *Listeria* pathogenesis and molecular virulence determinants. *Clinical microbiology reviews* 14, 584-640.

Vazquez-Torres, A., Vallance, B.A., Bergman, M.A., Finlay, B.B., Cookson, B.T., Jones-Carson, J., and Fang, F.C. (2004). Toll-like receptor 4 dependence of innate and adaptive immunity to *Salmonella*: importance of the Kupffer cell network. *Journal of immunology* 172, 6202-6208.

Verdel, A., and Khochbin, S. (1999). Identification of a new family of higher eukaryotic histone deacetylases. Coordinate expression of differentiation-dependent chromatin modifiers. *J Biol Chem* 274, 2440-2445.

Verdin, E., Dequiedt, F., and Kasler, H.G. (2003). Class II histone deacetylases: versatile regulators. *Trends in genetics : TIG* 19, 286-293.

Viboud, G.I., and Bliska, J.B. (2005). *Yersinia* outer proteins: role in modulation of host cell signaling responses and pathogenesis. *Annu Rev Microbiol* 59, 69-89.

Wang, A.H., Kruhlak, M.J., Wu, J., Bertos, N.R., Vezmar, M., Posner, B.I., Bazett-Jones, D.P., and Yang, X.J. (2000). Regulation of histone deacetylase 4 by binding of 14-3-3 proteins. *Molecular and cellular biology* 20, 6904-6912.

Wang, J., Lunyak, V.V., and Jordan, I.K. (2011). Genome-wide prediction and analysis of human chromatin boundary elements. *Nucleic Acids Res* 40, 511-529.

Wang, Y., Curry, H.M., Zwilling, B.S., and Lafuse, W.P. (2005). Mycobacteria inhibition of IFN-gamma induced HLA-DR gene expression by up-regulating histone deacetylation at the promoter region in human THP-1 monocytic cells. *J Immunol* 174, 5687-5694.

Wang, Z., Zang, C., Rosenfeld, J.A., Schones, D.E., Barski, A., Cuddapah, S., Cui, K., Roh, T.Y., Peng, W., Zhang, M.Q., *et al.* (2008). Combinatorial patterns of histone acetylations and methylations in the human genome. *Nature genetics* 40, 897-903.

Weintraub, H., and Groudine, M. (1976). Chromosomal subunits in active genes have an altered conformation. *Science* 193, 848-856.

Wettenhall, J.M., and Smyth, G.K. (2004). limmaGUI: a graphical user interface for linear modeling of microarray data. *Bioinformatics* 20, 3705-3706.

Whitlock, J.P., Jr., and Simpson, R.T. (1977). Localization of the sites along nucleosome DNA which interact with NH₂-terminal histone regions. *J Biol Chem* 252, 6516-6520.

Wines, D.R., Talbert, P.B., Clark, D.V., and Henikoff, S. (1996). Introduction of a DNA methyltransferase into *Drosophila* to probe chromatin structure in vivo. *Chromosoma* 104, 332-340.

Witt, O., Albig, W., and Doenecke, D. (1996). Testis-specific expression of a novel human H3 histone gene. *Exp Cell Res* 229, 301-306.

Xu, F., Zhang, K., and Grunstein, M. (2005). Acetylation in histone H3 globular domain regulates gene expression in yeast. *Cell* 121, 375-385.

Yang, X.J., and Seto, E. (2008). Lysine acetylation: codified crosstalk with other posttranslational modifications. *Mol Cell* 31, 449-461.

Young, J.A., and Collier, R.J. (2007). Anthrax toxin: receptor binding, internalization, pore formation, and translocation. *Annu Rev Biochem* 76, 243-265.

Yu, J., and Kaper, J.B. (1992). Cloning and characterization of the eae gene of enterohaemorrhagic *Escherichia coli* O157:H7. *Molecular microbiology* 6, 411-417.

Yuan, G.C., and Liu, J.S. (2008). Genomic sequence is highly predictive of local nucleosome depletion. *PLoS Comput Biol* 4, e13.

Zhao, Y., Yang, J., Liao, W., Liu, X., Zhang, H., Wang, S., Wang, D., Feng, J., Yu, L., and Zhu, W.G. (2010). Cytosolic FoxO1 is essential for the induction of autophagy and tumour suppressor activity. *Nature cell biology* 12, 665-675.

Zhu, B., Nethery, K.A., Kuriakose, J.A., Wakeel, A., Zhang, X., and McBride, J.W. (2009). Nuclear translocated *Ehrlichia chaffeensis* ankyrin protein interacts with a specific adenine-rich motif of host promoter and intronic Alu elements. *Infect Immun* 77, 4243-4255.

Zuo, T., Liu, T.M., Lan, X., Weng, Y.I., Shen, R., Gu, F., Huang, Y.W., Liyanarachchi, S., Deatherage, D.E., Hsu, P.Y., *et al.* (2011). Epigenetic silencing mediated through activated PI3K/AKT signaling in breast cancer. *Cancer research* 71, 1752-1762.

Zurawski, D.V., Mummy, K.L., Faherty, C.S., McCormick, B.A., and Maurelli, A.T. (2009). *Shigella flexneri* type III secretion system effectors OspB and OspF target the nucleus to downregulate the host inflammatory response via interactions with retinoblastoma protein. *Mol Microbiol* 71, 350-368.

Abstract

Bacterial pathogens dramatically affect host cell transcription programs for their own profit, however the underlying mechanisms in most cases remain elusive. While investigating the effects of *Listeria monocytogenes* on histone modifications, we discovered a new transcription regulatory mechanism by which the expression of genes is repressed, during infection. Upon infection by *L. monocytogenes*, the secreted virulence factor, InlB, binds the c-Met receptor and activates signaling through PI3K/Akt. This signaling platform is necessary for causing the relocalization of the histone deacetylase, SIRT2, to the nucleus and associating to chromatin.

In characterizing the mechanism governing SIRT2 nuclear relocalization during infection, our results have demonstrated that SIRT2 undergoes a post-translational modification. SIRT2 undergoes dephosphorylation at a novel N-terminal phospho-site. SIRT2 is recruited to the transcription start sites of genes repressed during infection leading to H3K18 deacetylation and transcriptional repression.

Finally, my results demonstrate that SIRT2 is hijacked by *L. monocytogenes* and promotes an increase in intracellular bacteria. Together, these data uncover a key role for SIRT2 mediated H3K18 deacetylation during infection and characterize a novel mechanism imposed by a pathogenic bacterium to reprogram the host cell.

Résumé

De nombreuses bactéries pathogènes sont capables d'affecter les programmes transcriptionnels de la cellule hôte pendant l'infection. Cependant, les mécanismes contrôlant ce processus restent largement inconnus. En investiguant les effets de *Listeria monocytogenes* sur les modifications des histones de l'hôte, nous avons mis en évidence un nouveau mécanisme de régulation de transcription nécessaire pour la répression de l'expression de certains gènes, pendant l'infection. Lors de l'infection par *L. monocytogenes*, le facteur de virulence sécrété, InlB, se lie au récepteur c-Met et active la signalisation par les intermédiaires PI3K et Akt. Cette plateforme de signalisation est nécessaire pour la relocalisation de la déacetylase d'histone, SIRT2, au noyau et l'association à la chromatine.

En caractérisant le mécanisme gouvernant la relocalisation nucléaire de SIRT2 lors de l'infection, nous avons démontrés que SIRT2 subit une modification post-traductionnelle. SIRT2 est déphosphorylée à un nouveau site de phosphorylation localisé à la partie N-terminale de la protéine. SIRT2 est recrutée aux sites de démarrage de la transcription des gènes réprimés lors de l'infection menant à la deacetylation de H3K18 et la répression transcriptionnelle.

Nous avons mis en évidence que SIRT2 est détournée par *L. monocytogenes* et provoque une croissance des bactéries intracellulaires. Ces résultats démontrent un rôle clef de SIRT2 en provoquant la deacetylation de H3K18 lors de l'infection et dévoilent un nouveau mécanisme imposé par les bactéries pathogènes dans le but de reprogrammer la cellule hôte.